**AWARD NUMBER:** W81XWH-14-1-0086

**TITLE:** Targeting the S1P Axis and Development of a Novel Therapy for Obesity-Related Triple-Negative Breast Cancer

**PRINCIPAL INVESTIGATOR**: Sarah Spiegel

**CONTRACTING ORGANIZATION**: Virginia Commonwealth University School of Medicine
Richmond, VA 23298-0568

**REPORT DATE:** November 2019

**TYPE OF REPORT:** Final

**PREPARED FOR**: U.S. Army Medical Research and Development Command
Fort Detrick, Maryland 21702-5012

# REPORT DOCUMENTATION PAGE

*Form Approved*
*OMB No. 0704-0188*



| 1. REPORT DATE | 2. REPORT TYPE | 3. DATES COVERED |
|---|---|---|
| Nov 2019 | Final Report | 09/01/2014 - 08/31/2019 |

**4. TITLE AND SUBTITLE**

Targeting the S1P Axis and Development of a Novel Therapy for Obesity-Related Triple-Negative Breast Cancer

**5a. CONTRACT NUMBER**

**5b. GRANT NUMBER**
W81XWH-14-1-0086

**5c. PROGRAM ELEMENT NUMBER**

**6. AUTHOR(S)**
Sarah Spiegel

**5d. PROJECT NUMBER**

**5e. TASK NUMBER**

**5f. WORK UNIT NUMBER**

**7. PERFORMING ORGANIZATION NAME(S) AND ADDRESS(ES)**

Sponsored Programs
800 East Leigh Street, Suite 3200
Box 980568
Richmond, VA 23298-0568

dirospa@vcu.edu
804-828-6772

**8. PERFORMING ORGANIZATION REPORT NUMBER**

**9. SPONSORING / MONITORING AGENCY NAME(S) AND ADDRESS(ES)**

U.S. Army Medical Research and Development Command
Fort Detrick, Maryland 21702-5012

**10. SPONSOR/MONITOR'S ACRONYM(S)**

**11. SPONSOR/MONITOR'S REPORT NUMBER(S)**

**12. DISTRIBUTION / AVAILABILITY STATEMENT**

Approved for Public Release; Distribution Unlimited

**13. SUPPLEMENTARY NOTES**

**14. ABSTRACT**

More than 40,000 women in the US die each year of metastatic breast cancer, for which there are currently no permanent cures. The majority of breast tumors express the estrogen receptor (ER), and anti-estrogens, such as tamoxifen, are the first line of therapy. Unfortunately, half of these patients will ultimately fail therapy due to de novo or acquired resistance, as well as patients with ER, progesterone receptor (PR) and HER2 triple negative breast cancer (TNBC), which is aggressive with high recurrence, metastatic, and mortality rates. Obesity and associated inflammation is now endemic and has been associated with increased risk for lymph node metastasis, endocrine therapy resistance, larger tumors, death, and for presenting with TNBC. However, the links between obesity and breast cancer are not understood and will be investigated here. This proposal will lead to novel therapies that will overcome the overarching challenges of developing safe and effective drugs for treating obesity promoted cancers and TNBC and will identify the bioactive sphingolipid metabolite, sphingosine-1-phosphate (S1P), produced by sphingosine kinases (SphK1 and SphK2), as a critical factor that links obesity and chronic inflammation to drive breast cancer growth and metastasis.

**15. SUBJECT TERMS**
sphingosine-1-phosphate, sphingosine kinase, FTY720 (fingolimod, Gilenya), triple negative breast cancer, ERα, obesity, histone deacetylase, inflammation, tamoxifen resistance

| 16. SECURITY CLASSIFICATION OF: | | | 17. LIMITATION OF ABSTRACT | 18. NUMBER OF PAGES | 19a. NAME OF RESPONSIBLE PERSON |
|---|---|---|---|---|---|
| a. REPORT | b. ABSTRACT | c. THIS PAGE | | | USAMRMC |
| Unclassified | Unclassified | Unclassified | Unclassified | 11 | 19b. TELEPHONE NUMBER *(include area code)* 804-828-9330 |

**Standard Form 298 (Rev. 8-98)**
**Prescribed by ANSI Std. Z39.18**

## Table of Contents

## 1. INTRODUCTION

Approximately 15% of American women will be diagnosed with breast cancer, the 2nd leading cause of cancer death among women. Breast cancer death rates have been dropping due to advances in detection and better treatments, particularly hormonal therapies for the ~70% of breast cancers that express estrogen receptors (ER) and progesterone receptors (PR). Aromatase inhibitors, which prevent the production of estrogen and direct ER antagonists, such as tamoxifen, are especially effective against ER positive tumors and have less side effects than traditional chemo- and radio-therapies. The human epidermal growth factor receptor 2 (HER2), upregulated in 10 to 15% of breast cancers, can also be targeted with an inhibitory monoclonal antibody (Herceptin). However, hormonal therapies are ineffective in the 15 to 20% of tumors that are ER/PR/HER2 negative, termed triple negative breast cancer (TNBC). These tumors are more aggressive and metastatic, leading to significantly worse prognoses. In addition to de novo resistance, acquired resistance to these types of therapies is a major problem. Therefore, it is critical that we understand the other signaling pathways that contribute to breast cancer progression and metastasis in order to develop new approaches for treatment of breast cancer. Our studies have demonstrated that the bioactive sphingolipid metabolite, sphingosine-1-phosphate (S1P), may be an attractive target for TNBC treatment as it regulates numerous physiological and cellular processes that are important for breast cancer progression, including cell proliferation and survival, migration and invasion important for metastasis, inflammation that can paradoxically drive tumorigenesis, and angiogenesis that provides cancer cells with nutrients and oxygen (1). In particular, one of the enzymes that produces S1P, sphingosine kinase 1 (SphK1), is commonly upregulated in breast cancer cells and has been linked to increased cancer progression and poor prognosis, possibly leading to resistance to certain anti-cancer therapies. Moreover, we found that the other sphingosine kinase isoform, SphK2, also plays an important role in breast cancer progression and metastasis. We believe that our studies supported by this grant that are briefly summarized below can lead to novel therapies that will overcome the overarching challenges of developing safe and effective novel drugs for treating obesity-promoted cancers, metastatic breast cancer, as well as TNBC, by identifying the bioactive sphingolipid metabolite, S1P produced by SphK1 and SphK2, as a critical factor that drives breast cancer proliferation and metastasis.

## 2. KEY WORDS

Sphingosine-1-phosphate, sphingosine kinase, FTY720 (fingolimod, Gilenya), triple negative breast cancer, ERα, obesity, histone deacetylase, inflammation, tamoxifen resistance

## 3. ACCOMPLISHMENTS

### 3.1. Major Goals of the Project

Our project had three major aims that were all successfully completed.

**Aim 1.** Determine the role of SphK1 and S1P in obesity promoted chronic inflammation and tumor progression and decipher the molecular links between the SphK1/S1P/S1PR1 axis and persistent NF-kB and STAT3 activation.

**Aim 2.** Target the SphKs/S1P/S1PR1 axis with fingolimod/FTY720 for treatment of obesity-associated breast cancer to suppress the malicious amplification cascade, and reactivate ER expression in ER-negative breast cancer.

**Aim 3.** Examine the association of the SphKs/S1P/S1PR1 axis in human breast cancer and prognosis.

Due to space limitations, only the most important and novel published findings will be briefly described. I am especially pleased that several of the trainees who carried out this work obtained independent positions.

The inability to effectively predict, prevent, and treat metastatic breast cancer is a major problem in breast cancer care. Our proposal provided evidence that the SphKs/S1P/S1PR1 axis is one of the critical factors that drive breast cancer growth and metastasis. We believe that these findings will pave the way for development of new adjuvant therapies targeting this axis as a promising strategy for effective treatment of advanced and refractory breast cancer.

**<u>Aim 1.</u> Role of SphK1 and S1P in obesity promoted breast cancer progression.**

Although obesity with associated inflammation is now recognized as a risk factor for breast cancer and distant metastases, the functional basis for these connections remains poorly understood. Our studies show that in breast cancer patients and in animal breast cancer models, obesity is a sufficient cause for increased expression of S1P, which mediates cancer pathogenesis (1-9). We have completed preclinical studies demonstrating that a high-fat diet accelerated the onset of tumors and increased triple-negative spontaneous breast tumors in MMTV-PyMT transgenic mice (1,6). High-fat diet was also sufficient to upregulate expression of SphK1 along with its receptor S1PR1 in syngeneic and spontaneous breast cancer models (6). We also observed that S1P produced in lung pre-metastatic niches by tumor-induced SphK1 increased macrophage recruitment and induced IL6 and signaling pathways important for metastatic colonization (6). Moreover, overexpression of multidrug resistance transporter ABCC1, but not ABCB1, enhanced S1P secretion, tumor growth, angiogenesis, and lymphangiogenesis, with a concomitant increase in lymph node and lung metastases as well as shorter survival of mice (7). Interestingly, S1P exported via ABCC1 from breast cancer cells upregulated transcription of SphK1, thus promoting additional S1P formation (7). Further support for a key role of S1P in metastasis emerged from a genome-wide in vivo screen that identified novel host regulators of metastatic colonization (10). Our results establish a critical role for circulating S1P produced by tumors and the SphK1/S1P/S1PR1 axis in obesity-related inflammation, formation of lung metastatic niches, and breast cancer metastasis, with potential implications for prevention and treatment (Fig. 1). These findings offer a preclinical proof of concept that signaling by a sphingolipid may be an effective target to prevent obesity-related breast cancer metastasis.

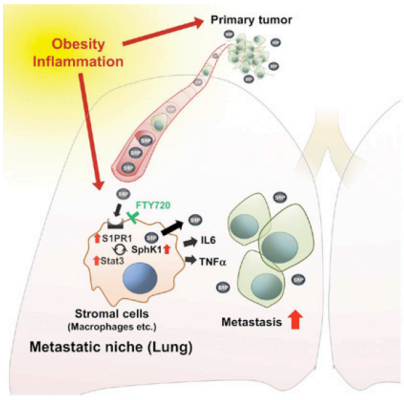


**Figure 1.** Model illustrating the role of SphK1/S1P/S1PR1 axis in the link between obesity, inflammation, breast cancer progression, and lung metastasis. It also indicates targeting of this axis with FTY720 for treatment.

**<u>Aim 2.</u> Target the SphKs/S1P/S1PR1 axis with fingolimod/FTY720 for treatment of obesity-associated breast cancer to suppress the malicious amplification cascade and reactivate ER expression in ER-negative breast cancer**.

Our work supported by this grant also demonstrated that a multi-pronged attack with the multiple sclerosis drug FTY720 (fingolimod, Gilenya) is a novel combination approach for effective treatment of both conventional hormonal therapy-resistant breast cancer and TNBC (1-8). We found that oral administration of clinically relevant doses of FTY720 suppressed development, progression and aggressiveness of spontaneous breast tumors in these mice (2). In ERα-negative human and murine breast cancer cells, FTY720 reactivated expression of silenced ERα and sensitized them to tamoxifen. We also observed that the active phosphorylated form of FTY720 acts not only as a functional antagonist of S1PR1, but is also a potent histone deacetylase inhibitor that reactivates ERα expression and thus enhances hormonal therapy for breast cancer (2). FTY720 also greatly reduced tumor growth in the syngeneic orthotopic 4T1-luc2 metastatic mouse breast cancer model used in our lab (9), accompanied by reduced levels of S1P and dihydro-S1P (ligands for S1PR1) in tumor interstitial fluid (4,5). While these observations further support our proposal that S1P may have an important role within the tumor microenvironment, they also provide important insight into an additional mechanism of action of FTY720 on cancer progression due to reduction of S1P via suppression of SphK1 activity. Importantly, in tumor-bearing mice, FTY720 treatment reduced pro-inflammatory cytokines, macrophage infiltration, S1P-mediated signaling, and tumor progression and metastasis induced by obesity, thereby prolonging survival (6). Thus, our results establish a critical role for circulating S1P produced by tumors and the SphK/S1P/S1PR1 axis in breast cancer progression, inflammation, formation of lung metastatic niches, and metastasis, with potential implications for prevention and treatment of TNBC with FTY720.

In a recent study, we demonstrated in TNBC cells, which lack the canonical estrogen receptor, ERα66 but express the novel splice variant ERα36, that ERα36 is the receptor responsible for E2-induced activation of SphK1 and formation and secretion of S1P (11). Tamoxifen, the first-line endocrine therapy for breast cancer, is an antagonist of ERα66, but an agonist of ERα36, and, like E2, activates SphK1 and increases secretion of S1P. A major problem with tamoxifen therapy is development of acquired resistance. We found that tamoxifen resistance correlated with increased SphK1 and ERα36 expression in tamoxifen-resistant breast cancer cells, in patient-derived xenografts, and in endocrine-resistant breast cancer patients (11). Our data further indicate that targeting the SphK1 axis may be a therapeutic option to circumvent endocrine resistance and improve patient outcome. Taken together, these findings offer preclinical proof of concept that the SphK/S1P/S1PR1 axis plays an important role in breast cancer progression and metastasis.

**Aim 3. Examine the association of the SphKs/S1P/S1PR1 axis in human breast cancer and prognosis.** Consistent with our observation that a HFD upregulates expression of SphK1, the enzyme that produces S1P, along with its receptor S1PR1 in syngeneic and spontaneous breast tumors (6), we found that the activated phosphorylated SphK1 was highly expressed in TNBC and particularly prevalent in larger tumors (higher T stage) and in tumors from patients with lymph node metastases (higher TNM stage) (7). In addition, patients with breast tumors that had higher expression of phosphorylated SphK1 ($P$ = 0.011) or SphK1 ($P$ = 0.0014) had worse disease-free survival (7). In addition, using novel methods for sphingolipid analyses developed in our lab (3), we found that S1P levels were higher in human breast tumor tissue interstitial fluid than in the normal breast tissue (4). Moreover, patients with breast cancers that express both activated SphK1 and ABCC1 have significantly shorter disease-free survival. These findings suggest that export of S1P via ABCC1 functions in a malicious feed-forward manner to amplify the S1P axis involved in breast cancer progression and metastasis, which has important implications for prognosis of breast cancer patients and for potential therapeutic targets. Taken together, these studies suggest that activation of SphK1 in breast cancer worsens patient survival by export of S1P to the tumor microenvironment to enhance key processes involved in cancer progression.

### 3.3. Opportunities for Training and Professional Development

This project was not designed to provide training and professional development opportunities. However, we should note that the VCU School of Medicine has developed several new programs to enhance the training and professional development of graduate students and postdoctoral fellows. These vital programs provide these trainees, who are critical to the scientific endeavor, with career and mentoring resources based on the FASEB Individual Development Plan, including web-based tools for an Individual Development Plan, job opportunities in BioCareers, career resources from AAAS, CV/resume writing samples from UCSF Office of Career and Professional Development, and other career development websites. For graduate students these functions reside within the Office of Graduate Education, for Postdoctoral trainees, these reside in the Office of Research and Innovation. While no trainees were included in the original proposal, I am actively involved in training graduate students and mentoring junior investigators. I have been advising Melissa Maczis on career development. Using the “Individual Development Plan” website, she created an Individual Development Plan (IDP) and has been using it to record the immediate and long-term objectives of her research and her career path plan. She has been making outstanding progress toward accomplishing her career goals and based on her accomplishments successfully applied for and received a predoctoral fellowship from NIH (F31 CA220798).

### 3.4. How were the results disseminated to communities of interest?

I presented several research lectures on this project to the cancer research community at the Massey Cancer Center Retreat and in the regular meetings of the Massey Cancer Center Cancer Cell Signaling Program that I direct together with Dr. Andrew Larner. I also presented this work to the international scientific community in several Keynote lectures (See below). Melissa Maczis also presented her work in seminars to VCU graduate students.

## 4. IMPACT

### 4.1. The impact on the development of the principal discipline of the project

The work supported by this grant strongly supports the idea that a multi-pronged attack with FTY720 is a novel combination approach for effective treatment of conventional hormonal therapy-resistant breast cancer and triple-negative breast cancer. We previously found that the active phosphorylated form of FTY720 is a potent histone deacetylase inhibitor that reactivates ERalpha expression and enhances hormonal therapy for breast cancer (2). FTY720 has several advantages over available HDAC inhibitors as potential treatments for breast cancer patients: it is an orally bio-available pro-drug; it has already been approved for human use; it regulates expression of only a limited number of genes compared to other HDAC inhibitors; it has good pharmacokinetics and a long half life; it suppresses several survival and proliferative pathways; and it is much less toxic, it accumulates in tumor tissues, and both the phosphorylated and unphosphorylated forms target important pathways in breast cancer. We also found that FTY720, which targets the SphK1/S1P/S1PR1 axis, prevents the amplification cascade and mitigates obesity-promoted metastatic niche formation and breast cancer metastasis (6,7). Hence, we believe that our studies will pave the way for exploration of new clinical trials using FTY720 as a prototype of new adjuvant treatment strategies for hormonal resistant breast cancer. This might be particularly relevant in view of the increase in obesity that is now endemic and in de novo and acquired resistance to hormonal therapy. In an unrelated project, we found that treatment of mice with FTY720 targeted S1PR1 and blocked and reversed neuropathic pain induced by bortezomib (Stockstill et al., J. Exp. Med. 215:1301-1313, 2018) (reviewed in 12). The development of chemotherapy-induced painful peripheral neuropathy is a major dose-limiting side effect of many chemotherapeutics. Thus, in addition to synergizing with chemotherapy, FTY720 also might suppress chemotherapy-induced neuropathic pain. As FTY720 also shows promising anticancer potential and is FDA approved, rapid clinical translation of our findings is anticipated.

### 4.2. The Impact on Other Disciplines

Although this work may not have a direct impact on other disciplines it might contribute to them, particularly in the treatment of cognitive impairment. HDAC inhibitors have shown promise as a treatment to combat the cognitive decline associated with aging and neurodegenerative disease, as well as to ameliorate the symptoms of depression and posttraumatic stress disorder, among others. Due to its unique features described above and its high brain penetration, FTY720 might be more effective than other HDAC inhibitors as an adjuvant therapy for erasing aversive memories (2). This might also be relevant to suppression of cognitive impairment and neuropathic pain associated with chemotherapy. Moreover, our recent work shows that targeting the S1P/S1PR1 axis by treatment with FTY720 greatly reduces cancer-induced bone pain and neuroinflammation (Grenald et al., Pain. 158:1733-1742, 2017) (reviewed in 12) and supports potential fast-track clinical application of the FDA-approved drug, FTY720, as a therapeutic avenue for preventing “chemo brain”, i.e. chemotherapy-related cognitive impairment or cognitive dysfunction.

### 4.3. The Impact on Technology Transfer

Nothing to report

### 4.4. The impact on Society Beyond Science and Technology

Nothing to report

## 5. CHANGES/PROBLEMS

There were no significant changes in the project or its direction.

## 6. PRODUCTS

### Publications supported by DoD Award W81XWH-14-1-0086


**1.** Maczis, M., S. Milstien, and **S. Spiegel.** Sphingosine-1-phosphate and estrogen signaling in breast cancer. Adv Biol Regul 60: 160-165, 2016 http://www.ncbi.nlm.nih.gov/pubmed/26601898. PMCID: in progress

**2.** Hait, N. C., D. Avni, A. Yamada, M. Nagahashi, T. Aoyagi, H. Aoki, C. I. Dumur, Z. Zelenko, E. J. Gallagher, D. Leroith, S. Milstien, K. Takabe, and **S. Spiegel**. The phosphorylated prodrug FTY720 is a histone deacetylase inhibitor that reactivates ERalpha expression and enhances hormonal therapy for breast cancer. Oncogenesis 4: e156, 2015 https://www.ncbi.nlm.nih.gov/pubmed/26053034. PMC4753524

**3.** Newton, J., S. Lima, M. Maceyka, and **S. Spiegel**. Revisiting the sphingolipid rheostat: Evolving concepts in cancer therapy. Exp Cell Res 333: 195-200, 2015 http://www.ncbi.nlm.nih.gov/entrez/query.fcgi?cmd=Retrieve&db=PubMed&dopt=Citation&list_uids=25770011. PMC4415605

**4.** Nagahashi, M., A. Yamada, T. Aoyagi, J. Allegood, T. Wakai, **S. Spiegel**, and K. Takabe. Sphingosine-1-phosphate in the lymphatic fluid determined by novel methods. Heliyon 2: e00219, 2016 https://www.ncbi.nlm.nih.gov/pubmed/28054036. PMC5198727

**5.** Nagahashi, M., A. Yamada, H. Miyazaki, J. C. Allegood, J. Tsuchida, T. Aoyagi, W. C. Huang, K. P. Terracina, B. J. Adams, O. M. Rashid, S. Milstien, T. Wakai, **S. Spiegel**, and K. Takabe. Interstitial Fluid Sphingosine-1-Phosphate in Murine Mammary Gland and Cancer and Human Breast Tissue and Cancer Determined by Novel Methods. J Mammary Gland Biol Neoplasia 21: 9-17, 2016 http://www.ncbi.nlm.nih.gov/pubmed/27194029. PMC4947521

**6.** Nagahashi, M., A. Yamada, E. Katsuta, T. Aoyagi, W. C. Huang, K. P. Terracina, N. C. Hait, J. C. Allegood, J. Tsuchida, K. Yuza, M. Nakajima, M. Abe, K. Sakimura, S. Milstien, T. Wakai, **S. Spiegel**, and K. Takabe. Targeting the SphK1/S1P/S1PR1 Axis That Links Obesity, Chronic Inflammation, and Breast Cancer Metastasis. Cancer Res 78: 1713-1725, 2018 https://www.ncbi.nlm.nih.gov/pubmed/29351902.

**7.** Yamada, A., M. Nagahashi, T. Aoyagi, W. C. Huang, S. Lima, N. C. Hait, A. Maiti, K. Kida, K. P. Terracina, H. Miyazaki, T. Ishikawa, I. Endo, M. R. Waters, Q. Qi, L. Yan, S. Milstien, **S. Spiegel,** and K. Takabe. ABCC1-Exported Sphingosine-1-phosphate, Produced by Sphingosine Kinase 1, Shortens Survival of Mice and Patients with Breast Cancer. Mol Cancer Res 16: 1059-1070, 2018 https://www.ncbi.nlm.nih.gov/pubmed/29523764. PMC6071310

**8.** Geffken, K., and **S. Spiegel.** Sphingosine kinase 1 in breast cancer. Adv Biol Regul 67: 59-65, 2018 https://www.ncbi.nlm.nih.gov/pubmed/29055687. PMC5807162

**9.** Katsuta, E., S. C. DeMasi, K. P. Terracina, **S. Spiegel,** G. Q. Phan, H. D. Bear, and K. Takabe. Modified breast cancer model for preclinical immunotherapy studies. J Surg Res 204: 467-474, 2016 http://www.ncbi.nlm.nih.gov/pubmed/27565084. PMC5002312

**10.** van der Weyden, L., M. J. Arends, A. D. Campbell, T. Bald, H. Wardle-Jones, N. Griggs, M. D. Velasco-Herrera, T. Tuting, O. J. Sansom, N. A. Karp, S. Clare, D. Gleeson, E. Ryder, A. Galli, E. Tuck, E. L. Cambridge, T. Voet, I. C. Macaulay, K. Wong, P. Sanger Mouse Genetics, **S. Spiegel**, A. O. Speak, and D. J. Adams. Genome-wide in vivo screen identifies novel host regulators of metastatic colonization. Nature 541: 233-236, 2017 https://www.ncbi.nlm.nih.gov/pubmed/28052056. PMC5603286

**11.** Maczis, M. A., M. Maceyka, M. R. Waters, J. Newton, M. Singh, M. F. Rigsby, T. H. Turner, M. A. Alzubi, J. C. Harrell, S. Milstien, and **S. Spiegel**. Sphingosine kinase 1 activation by estrogen receptor alpha36 contributes to tamoxifen resistance in breast cancer. J Lipid Res 59: 2297-2307, 2018 https://www.ncbi.nlm.nih.gov/pubmed/30315000. PMC6277156

**12.** Singh, S. and **S. Spiegel**. Targeting the sphingosine-1-phosphate axis with FTY720/Fingolimod as a novel therapy for triple-negative breast cancer and chemotherapy-induced neuropathic pain. Adv Biol Regul in press, 2019.

**Abstracts**

1. Hait NC, Avni D, Yamada A, Milstien S, Takabe K, **Spiegel S**. FTY720-P is a potent inhibitor of class I histone deacetylases that enhances histone acetylation, reactivates ERα expression, and increases hormonal therapeutic sensitivity of breast cancer. AACR abstract, April 18-22, 2015, Philadelphia, PA. Cancer Research, Abstract 112, DOI: 10.1158/1538-7445.
2. Hait NC, Avni D, Yamada A, Nagahashi M, Aoyagi T, Milstien S, Takabe K, **Spiegel S**. FTY720 Administration Reduces Breast Cancer Progression. Southeastern Regional Lipid Conference (SERLC) 49th Annual Conference. November 5-7, 2015. Cashiers, NC.
3. Maczis AM, Hait NC, Milstien S, **Spiegel S**. Role of Sphingosine-1-Phosphate in Non-Genomic Effects of ERα36 in Breast Cancer. SERLC, Cashiers, NC, November 5-7, 2015.
4. Maczis AM, Hait NC, Milstien S, **Spiegel S**. Role of ERα36 in Sphingosine-1-Phosphate/Sphingosine Kinase 1 Axis in Breast Cancer. Graduate Symposium, Richmond, VA, April 19, 2016.
5. Maczis AM, Hait NC, Milstien S, **Spiegel S**. Role of ERα36 in Sphingosine-1-Phosphate/Sphingosine Kinase 1 Axis in Breast Cancer. 12th Annual Women's Health Research Day, Richmond, VA, April 27, 2016. (Award: Basic Science Research Award)
6. Maczis AM, Hait NC, Milstien S, **Spiegel S**. Sphingosine-1-Phosphate/Sphingosine Kinase 1 Axis Activated by 17β-Estradiol Through Estrogen Receptor alpha splice variant, ERα36, in Breast Cancer. CRR, Richmond, VA, June 17, 2016. (Award: 3rd Place Poster Presentation).
7. **Spiegel S.** Sphingosine-1-Phosphate: A Bridge From Bench To Clinic. April 2016, FASEB Journal vol. 30 no. 1 Supplement 243.1
8. Takabe K, Nagahashi M, **Spiegel S**. Sphingosine-1-phosphate Signaling Targeted by FTY720 Suppresses Obesity-Related Breast Cancer Progression, Metastasis, and Improves Survival. Society of Surgical Oncology 69th Annual Cancer Symposium, Boston, MA, March 2-5, 2016.
9. Aoki H, Aoki M, Mukhopadhyay P, Katsuta E, DeMasi S, Terracina KP, **Spiegel S,** Takabe K. How Fast Can the Immune Response Eliminate Murine Cancer Cells from a Different Background? Society of Surgical Oncology 69th Annual Cancer Symposium, Boston, MA, March 2-5, 2016.
10. Maczis MA, Milstien S, **Spiegel S**. Role of sphingosine-1-phosphate in non-genomic effects of estrogen in triple negative breast cancer. 34th Daniel T. Watts Research Poster Symposium, VCU, October 26, 2017
11. Maczis MA, Lynch KR, Santo WL, Milstien S, **Spiegel S.** The Sphingosine-1-Phosphate Gradient Regulates Breast Cancer Metastasis, FASEB Lysophospholipid and Related Mediators-from Bench to Clinic, New Orleans, 2017
12. Maczis MA, Milstien S, **Spiegel S**. Role of sphingosine-1-phosphate in non-genomic effects of estrogen in triple negative breast cancer. FASEB Lysophospholipid and Related Mediators-from Bench to Clinic, New Orleans, 2017
13. Maczis MA, Milstien S, **Spiegel S**. Non-genomic effects of estrogen Stimulated Sphingosine-1-Phosphate Signaling in triple negative breast cancer expressing only estrogen receptor alpha 36. Massey Cancer Research Retreat, June 16, 2017
16. Maczis MA, Lynch KR, Santo WL, Milstien S, **Spiegel S**. The Sphingosine-1-Phosphate Gradient regulates Breast cancer Metastasis. 34th Daniel T. Watts Research Poster Symposium, VCU, October 26, 2017
17. Maczis MA, Maceyka M, Waters MR, Singh M, Turner TH, Alzubi M, Harrell JC, Milstien S, **Spiegel S**. Key Role of Sphingosine-1-phosphate in de novo and acquired tamoxifen resistant breast cancer. Massey Cancer Research Retreat, June 8, 2018
18. Maczis MA Lynch KR, Santo SL, Milstien S, **Spiegel S**. Importance of sphingosine kinase 2 and spinster 2 in breast cancer progression and metastasis. Massey Cancer Research Retreat, June 8, 2018
19. Maczis MA, Milstien S, **Spiegel S**. Role of ERalpha36 and sphingosine-1-phosphate in de novo and acquired tamoxifen resistant breast cancer, 4th International meeting on Molecular Medicine of Sphingolipids, Monday, October 28, 2019
20. Singh, S, Spiegel S. Targeting the sphingosine-1-phosphate axis with FTY720/fingolimod as a

novel therapy for triple-negative breast cancer and neuropathic pain. Sixtieth International Symposium on Biological Regulation and Enzyme Activity in Normal and Neoplastic tissues. September, 2019, University of Bologna, Italy.

**Presentations**

Dr. Hait presented: The Phosphorylated Pro-drug FTY70, a Histone Deacetylase Inhibitor, Reactivates ERα Expression and Enhances Hormonal Therapy of ERα-Negative Breast Cancer. MCC, Richmond, VA. February 20, 2015.

Dr. Spiegel presented: Sphingosine-1-phosphate, from insipid lipid to key regulator of lymphocyte trafficking and the link between inflammation and cancer. Sackler Lectureships, Tel-Aviv University, Tel Aviv, Israel. March 15, 2015

Dr. Spiegel presented: Novel actions of sphingosine-1-phosphate and the multiple sclerosis pro-drug FTY720/fingolimod: Implications for cancer. Sackler Lectureship, Tel-Aviv University, Israel. March 18, 2015.

Dr. Spiegel presented: Women in Science. Cell Biology of Animal Lectins. The Weizmann Institute of Science, Rehovot, Israel. June 21-25, 2015.

Dr. Spiegel presented: Active Phosphorylated FTY720/Fingolimod is a Potent Inhibitor of Class I Histone Deacetylases that Reactivates Estrogen Receptor Expression and Increases Hormonal Therapeutic Sensitivity of Breast Cancer. International Ceramide Conference Sphingolipid Club Joint Meeting, Cesme, Izmir, Turkey. May 6-10, 2015.

Dr. Spiegel presented a Keynote Address as a JLR Special Lecture: Sphingosine1phosphate from Bench to Clinic: Evolving concepts. FASEB Science Research Conference - Lysophospholipids and related mediators - From bench to clinic. Banff, Alberta, Canada. August 23-28, 2015.

Dr. Spiegel presented: Sphingosine-1-phosphate and estrogen signaling in breast cancer. 56th ABR Symposium, Bologna, Italy. October 5-6, 2015.

Dr. Spiegel presented: Role of the sphingosine-1-phosphate axis in the tumor microenvironment and development of a novel therapy for obesity-related triple-negative breast cancer. Frontiers in Basic Cancer Research Conference, Philadelphia, PA. October 23-26, 2015

Dr. Spiegel presented: The road from Wilchek to sphingosine-1-phosphate. Affinity and Biorecognition. Meir Wilchek's 80th Birthday Symposium. Weizmann Institute of Science, Rehovot, Israel. October 27-30, 2015

Dr. Spiegel presented: The key role of sphingosine-1-phosphate in the link between inflammation and cancer. The 49th Annual Miami Winter Symposium on Inflammation. Miami, FL. January 24-27, 2016

Dr. Spiegel presented: Sphingosine-1-phosphate: A Bridge from Bench to Clinic. ASBMB 2016 Annual Meeting, San Diego, CA. April 2-6, 2016

Dr. Spiegel presented: Sphingosine-1-phosphate: From bench to Translational Medicine. Lipid Mediators In Health and Disease II, La Jolla, CA. May 19-20, 2016

Dr. Spiegel presented: New aspects of sphingosine-1-phosphate in inflammation and cancer, 2017 FASEB Conference on Lysophospholipid and Related Mediators: from Bench to Clinic, New Orleans, LA, August 20-25, 2017

Dr. Spiegel presented: New aspects of sphingosine-1-phosphate in inflammation and cancer, Keynote Lecture, 12th Sphingolipid Club Meeting, Trabia, Sicily, Italy, September 6-10, 2017

Dr. Spiegel presented: S1P gradient and Spns2 transporter in lymphocyte trafficking and breast cancer metastasis, The FEBS Congress 2017, Jerusalem, Israel, September 10-14, 2017

Dr. Spiegel presented: S1P in breast cancer metastasis, Fifty-Eighth International Symposium on Biological Regulation and Enzyme Activity in Normal and Neoplastic Tissues University of Bologna, Italy October 2-3, 2017

Dr. Spiegel presented: Sphingosine-1-Phosphate In Breast Cancer Metastasis, 3rd Meeting of the GRK Sphingolipids in health and diseases, Essen, Germany, December 6-8, 2017

Dr. Spiegel presented: Sphingosine Kinase 1 in Endocytic Membrane Trafficking and p53-Dependent Autophagic Cell Death, Gordon Research Conference on Glyco and Sphingolipid Biology,

Galveston, Texas, February 11 - 16, 2018

Dr. Spiegel presented: Infection, Inflammation and Immunity in Cancer, 4th International meeting on Molecular Medicine of Sphingolipids, Monday, October 28, 2019

Dr. Spiegel presented: Targeting the sphingosine-1-phosphate axis with FTY720/fingolimod as a novel therapy for triple-negative breast cancer and neuropathic pain. 16th International Conference on Bioactive Lipids in Cancer and Related Diseases. October, 2019. St. Peters

## 7. PARTICIPANTS & OTHER COLLABORATING ORGANIZATIONS

Individuals who have worked on the project

Name: Sarah Spiegel
Project Role: PI – No change

Name: Sheldon Milstien
Project Role: Co-Investigator – No change

Name: Kazuaki Takabe
Project Role: Co-Investigator – Left VCU June 2016, now at Roswell Park, Clinical Chief of Breast Surgery and Breast Disease Site Leader. We successfully were able to continue our long-standing collaboration with him.

Name: Nita Hait
Project Role: Collaborator, left VCU in May 2016 to obtain an independent position. I am very pleased that he was able to obtain this based on his work with me.

Name: Andreia Leopoldino
Project Role: Visiting Scientist from Brazil for 6 months in my lab during 2015.

Name: Melissa Maczis
Project Role: Graduate Student
An outstanding graduate student working on the project. She was able to obtain an individual F31 fellowship that started July 1, 2017.

**Has there been a change in the active other support of the PD/PI(s) or senior/key personnel since the last reporting period?** No changes from the last reporting period.

**What other organizations were involved as partners?**
Nothing to Report

Advances in Biological Regulation 60 (2016) 160–165

Contents lists available at ScienceDirect

Advances in Biological Regulation

journal homepage: www.elsevier.com/locate/jbior

# Sphingosine-1-phosphate and estrogen signaling in breast cancer

Melissa Maczis, Sheldon Milstien, Sarah Spiegel*

*Department of Biochemistry and Molecular Biology and the Massey Cancer Center, Virginia Commonwealth University School of Medicine, Richmond, VA 23298, USA*

ARTICLE INFO

*Article history:*
Received 23 September 2015
Received in revised form 28 September 2015
Accepted 28 September 2015
Available online 19 October 2015

*Keywords:*
Sphingosine-1-phosphate
Sphingosine kinase
Estradiol
Breast cancer
FTY720/Fingolimod

ABSTRACT

Breast cancer remains the most common malignant disease in women. The estrogen receptor-α (ERα) and its ligand 17β-estradiol ($E_2$) play important roles in breast cancer. $E_2$ elicits cellular effects by binding to ERα in the cytosol followed by receptor dimerization and translocation to the nucleus where it regulates gene expression by binding to ERE response elements. However, it has become apparent that $E_2$ also exerts rapid non-genomic effects through membrane-associated receptors. There is emerging evidence that this induces formation of the bioactive sphingolipid metabolite sphingosine-1-phosphate (S1P). S1P in turn has been implicated in many processes important in breast cancer progression. One of the enzymes that produce S1P, sphingosine kinase 1 (SphK1), is upregulated in breast cancer and its expression has been correlated with poor prognosis. This review is focused on the role of the SphK/S1P axis in estrogen signaling and breast cancer progression and will discuss new therapeutic approaches targeting this axis for breast cancer treatment.



**Contents**



*Abbreviations:* ERα, estrogen receptor α; EGFR, epidermal growth factor receptor; ERE, estrogen response element; ERK, extracellular signal regulated kinase; $E_2$, 17β-estradiol; HDAC, histone deacetylase; HER2, human epidermal growth factor receptor 2; MAPK, mitogen activated protein kinase; PHB2, prohibitin 2; SphK, sphingosine kinase; S1P, sphingosine-1-phosphate; S1PR, S1P receptor; TNBC, triple negative breast cancer; TRAF2, TNF receptor-associate factor 2.

* Corresponding author.
*E-mail address:* sarah.spiegel@vcuhealth.org (S. Spiegel).

http://dx.doi.org/10.1016/j.jbior.2015.09.006
2212-4926/

## 1. Introduction

The estrogen receptor-α (ERα) and its ligand 17β-estradiol ($E_2$) play important roles in breast cancer. Most of the canonical genomic effects of binding of $E_2$ to ERα are mediated by nuclear transcriptional regulation. However, $E_2$ also exerts rapid non-genomic signaling through membrane-associated receptors many of them resulting from increased formation of the bioactive sphingolipid metabolite sphingosine-1-phosphate (S1P). S1P and sphingosine kinases (SphKs) that produce it have been implicated in many processes important in breast cancer progression. In this review, we discuss the role of the SphK/S1P axis in estrogen signaling and breast cancer progression and also some new therapeutic approaches to potentially target this axis for breast cancer treatment.

### *1.1. Formation and metabolism of S1P*

It has long been known that sphingolipid metabolism generates metabolites with important functions. The best characterized are ceramide, the backbone of all sphingolipids, its breakdown product sphingosine, and S1P. S1P metabolism has been discussed in many reviews (Hannun and Obeid, 2008; Maceyka and Spiegel, 2014; Shamseddine et al., 2015) and is only briefly outlined here. Two sphingosine kinases, known as SphK1 and SphK2, catalyze the phosphorylation of sphingosine to S1P, which is irreversibly cleaved by S1P lyase to phosphoethanolamine and a fatty aldehyde or dephosphorylated back to sphingosine by several phosphatases which then can be reutilized for ceramide and sphingolipid formation. Tissue levels of S1P are thus determined by the balance between activity of SphKs and S1P lyase and phosphatases.

### *1.2. S1P signaling*

#### *1.2.1. S1P and its receptors*

S1P has important roles in regulation of a wide variety of complex biological processes important for breast cancer progression (Carroll et al., 2015; Maceyka and Spiegel, 2014). Most of these actions are mediated by binding to a family of five specific cell surface receptors (S1PR1-5) (Maceyka and Spiegel, 2014). Numerous stimuli, including hormones such as estradiol ($E_2$), rapidly activate SphK1 and/or SphK2 to transiently increase intracellular S1P levels in specific pools. S1P produced mainly by activated SphK1 can then be secreted by Spns2, a member of the major facilitator superfamily of non-ATP-dependent transporters or by ABC transporters ABCA1, ABCC1, and ABCG2 (Nishi et al., 2014; Takabe and Spiegel, 2014). S1P in turn activates its receptors in an autocrine or paracrine manner known as 'inside-out' signaling of S1P (Hobson et al., 2001; Takabe et al., 2008). Physiological responses regulated by S1P depend on the spectrum of ubiquitously but differentially expressed S1PRs and the variety of G proteins they are coupled to. Thus, many signaling pathways downstream of S1PRs that have been linked to cancer progression have been shown to be activated depending on the cell type, including MAPKs, phospholipase C, adenylate cyclase, and Rac/PI3K/Akt, to name a few (Pyne et al., 2014; Takabe et al., 2008). Moreover, various types of cancer cells differentially express different sets of S1PRs, thus providing S1P with the ability to regulate numerous cellular processes important for breast cancer, including growth, survival, migration, invasion, inflammation, angiogenesis, and lymphangiogenesis (Nagahashi et al., 2014).

#### *1.2.2. Intracellular actions of S1P*

While it has long been suspected that S1P also has intracellular actions that are independent of S1PRs, only recently have several intracellular targets been identified that are likely to be important in the context of cancer. We found that S1P, but not dihydro-S1P, produced by SphK1 activated by TNF directly binds to and activates the E3 ubiquitin ligase activity of TNF receptor-associate factor 2 (TRAF2), an important component in NF-κB signaling (Alvarez et al., 2010). NF-κB regulates transcription of pro-survival or anti-apoptosis genes, thus identifying one of the mechanisms for the pro-survival actions of S1P in cancer progression. Interestingly, in contrast to SphK1, which is localized to the cytosol, SphK2 is mainly in the nucleus of most types of cells. We showed that nuclear S1P produced by ERK/MAPK-dependent activation of SphK2 is an endogenous inhibitor of histone deacetylases (HDACs) (Hait et al., 2009). Since SphK2 is present in repressor complexes together with HDACs in the nucleus of breast cancer cells (Hait et al., 2009), the S1P it produces inhibits HDAC activity resulting in enhanced transcription of specific target genes. This was the first indication that nuclear sphingolipid metabolism is involved in epigenetic regulation. Another link between nuclear S1P and gene expression was recently reported by Ogretmen and colleagues who discovered that S1P binds to hTERT and stabilizes telomerase at the nuclear periphery by allosterically mimicking hTERT phosphorylation. In murine xenografts, inhibitors of SphK2 decreased tumor growth and overexpression of wild-type hTERT in cancer cells, but not a hTERT mutant that was unable to bind S1P, restored tumor growth (Panneer Selvam et al., 2015). Their results suggest that S1P promotes telomerase stability and telomere maintenance important for cancer cell proliferation and tumor growth. In the mitochondria, SphK2 produces S1P that binds to prohibitin 2 (PHB2), a protein that regulates mitochondria assembly and function. Deleting SphK2 or PHB2 induced a mitochondrial respiration defect through cytochrome c oxidase (Strub et al., 2011) and may be important for the well-known Warburg metabolism of cancer cells. In this regard, it was suggested that SphK1, but not SphK2, functions to maintain the Warburg effect and cell survival (Watson et al., 2013).

### 1.3. Role of estrogen in breast cancer

Breast cancer is the most common cancer among women worldwide and occurs in about 1 in 8 women in the US (http://www.cancer.org, last accessed June 10, 2015). The estrogen receptor-α (ERα) plays an important role in breast cancer pathogenesis and progression (McDonnell and Norris, 2002). Patients with tumors that express ERα are termed "ERα-positive" and those lacking ERα are termed "ERα-negative". The majority of human breast cancers start out as estrogen-dependent because they are derived from cells that express ERα (Saha Roy and Vadlamudi, 2012). The steroid hormone, $E_2$, interacts directly with estrogen-specific cytoplasmic/nuclear receptors, ERα66 and ERα46 (Marino et al., 2006). ERα66 is the main ERα responsible for ERα-positive breast cancer responses to $E_2$. ERα46 is a 46 kDa splice variant that also functions in association with ERα66. The canonical pathway by which $E_2$ elicits cellular effects is initiated by binding to ERα in the cytosol followed by homo- or hetero-dimerization and translocation to the nucleus. In the nucleus, ERα dimers function as transcription factors by binding to specific response elements (ERE) on DNA, and either activating or repressing transcription (Mangelsdorf et al., 1995). These genomic responses are slow and take days to induce effects through translational events. $E_2$ also initiates rapid non-genomic responses, taking minutes to cause an effect through a membrane-associated 36 kDa splice variant (ERα36) of ERα66 (Marino et al., 2006), or through a G protein-coupled receptor (GPR30) (Filardo et al., 2007). Ample evidence has accumulated suggesting an important role for S1P in $E_2$-mediated signaling (Sukocheva and Wadham, 2014).

### 1.4. Role of the SphK1/S1P axis in ER signaling

Our initial demonstration that overexpression of SphK1 in human breast cancer cells promoted tumorigenesis and neovascularization when implanted in nude mice (Nava et al., 2002) was followed by numerous reports confirming the importance of SphK1 and formation of S1P as anti-apoptotic and growth-promoting factors in breast cancer (Carroll et al., 2015; Newton et al., 2015; Pyne et al., 2014; Sukocheva and Wadham, 2014; Truman et al., 2014). Moreover, expression of SphK1 has been shown to correlate with poor prognosis in breast cancer patients (Pyne et al., 2014; Ruckhaberle et al., 2008).

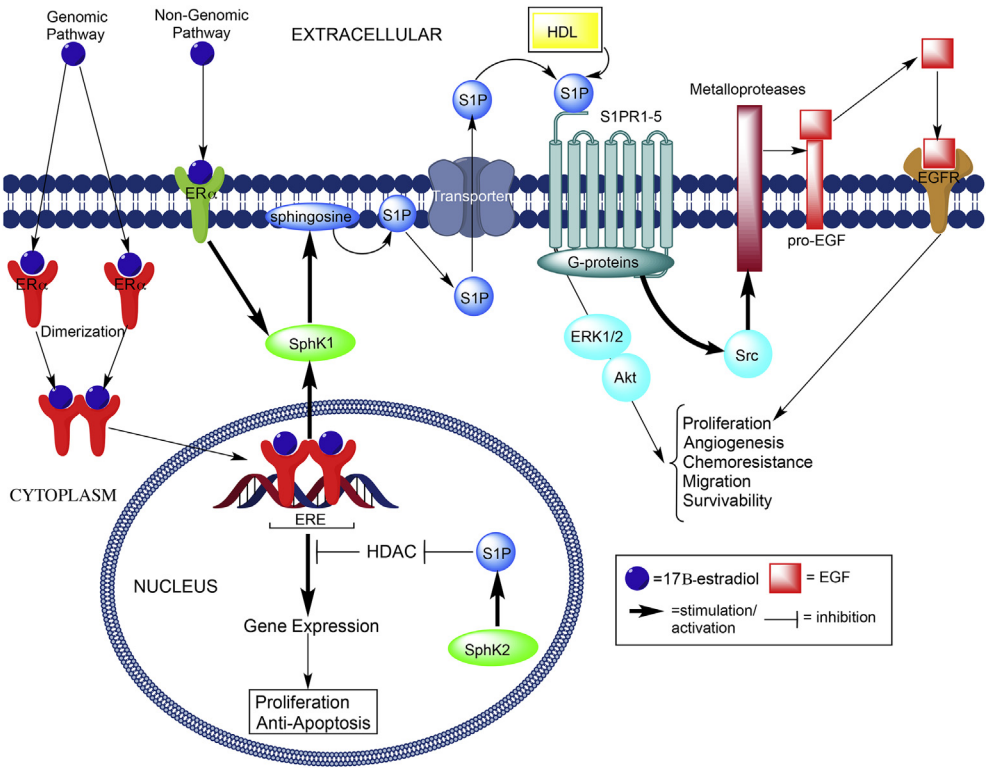


**Fig. 1.** Role of the SphK/S1P axis in signaling pathways initiated by $E_2$. Binding of E2 to cytosolic ERα induces its dimerization and translocation to the nucleus where it associates with estrogen response elements (ERE) to regulate gene expression. $E_2$ can also signal through cell surface $E_2$ receptors to initiate rapid non-genomic effects that include activation of SphK1 and production of S1P. After export of this S1P by transporters, it activates S1PRs (such as S1PR3) leading to downstream signaling that regulates many processes important for breast cancer progression including processing of pro-EGFR by metalloproteinases. EGF then stimulates EGFR-mediated signaling important for cell growth (Sukocheva et al., 2013). S1P produced in the nucleus by SphK2 is an endogenous inhibitor of HDACs (Hait et al., 2009).

$E_2$ activates SphK1 in breast cancer cells and increases formation and export of S1P (Sukocheva and Wadham, 2014; Takabe and Spiegel, 2014). Increased SphK1 activity correlates with enhanced cell growth, and also is required for $E_2$-dependent activation of MAPK and intracellular $Ca^{2+}$ mobilization in ERα-positive MCF-7 breast cancer cells (Sukocheva et al., 2006).

Anti-estrogen therapy with tamoxifen or aromatase inhibitors is the treatment of choice for ERα-positive breast cancer. Unfortunately, loss of ERα expression leading to resistance to hormonal therapies is common and hormonal therapies are not effective in ERα-negative breast cancers. One of the mechanisms by which breast cancer cells become resistant is a switch to growth factor-dependent growth. Intriguingly, activation of ERα by $E_2$ activates EGFR by a "criss-cross" transactivation process important for $E_2$-dependent growth that requires ERα, activation of SphK1, production and secretion of S1P that activates S1PR3, leading to enhanced processing of pro-EGFR and activation of EGFR (Sukocheva et al., 2006) (Fig. 1). This also caused increased localization of EGFR in endosomes to delay its degradation and direct it for recycling for continuous proliferative signaling (Sukocheva et al., 2009). Interestingly, SphK1 mRNA is also increased after $E_2$ treatment, suggesting that SphK1 is transcriptionally regulated by ERα66. Transactivation to EGFR was also detected in T47D ERα-positive cells in response to $E_2$ treatment, but not in ERα-negative SK-BR-3; whereas, S1P was able to transactivate the EGFR in both ERα-positive and ERα-negative cells (Sukocheva et al., 2013). This suggests that both $E_2$ and S1P are critical components in the transactivation of EGFR in the transition from $E_2$-dependent growth to growth-factor-dependent growth. Moreover, SphK1 was required for EGF-induced breast cancer migration, proliferation, and cell survival and both ERα and GPR30 have been implicated in initiation of this signaling (Sukocheva and Wadham, 2014). However, only $E_2$ and not EGF stimulated export of S1P via ABCC1 and/or ABCG2 from breast cancer cells in an ERα-dependent manner (Takabe et al., 2010). Although Spns2, another bona fide S1P transporter, has been shown to export S1P from cells (Nishi et al., 2014; Takabe and Spiegel, 2014) and to be important in inflammatory and autoimmune diseases in mouse models (Donoviel et al., 2015), its involvement in breast cancer has not yet been investigated.

### 1.5. S1P in development of tamoxifen resistance

Tamoxifen is an anti-estrogen drug that binds to ERα, preventing estrogen binding, thereby causing cell growth arrest in breast cancer cells that are estrogen-dependent. Previous studies have shown that when patients with ERα-positive breast cancer are treated with tamoxifen for 5 years, the rate of cancer recurrence is reduced by 39 percent and breast cancer mortality is decreased by about one-third throughout the first 15 years (Davies et al., 2011). Unfortunately, half of these patients will ultimately fail therapy due to acquired resistance. Moreover, breast cancer in patients whose tumors do not express ERα, progesterone receptor, and human epidermal growth factor receptor 2 (HER2, also known as ErbB-2), termed triple-negative breast cancer (TNBC), is aggressive with high recurrence, metastatic, and mortality rates (Bayraktar and Gluck, 2013). These patients do not respond to hormonal therapy due to *de novo* (intrinsic) resistance and have limited treatment options.

The SphK1/S1P/S1PRs axis has been implicated in the development of tamoxifen resistance or acquired (extrinsic) chemoresistance. SphK1 expression and activity were shown to be elevated in acquired-tamoxifen resistant ERα-positive MCF7 cells, and SphK1 inhibition or downregulation restored the anti-proliferative and pro-apoptotic effects of tamoxifen (Sukocheva et al., 2009; Watson et al., 2010). In a cohort of 304 ERα-positive breast cancer patients, SphK1 expression correlated with tamoxifen resistance (Pyne et al., 2012). Moreover, high SphK1 and ERK1/2 expression in tumors of ERα-positive breast cancer patients, high S1PR1, but not S1PR2, expression, and higher expression of S1PR1/3 and ERK1/2 were all found to be associated with shorter time to recurrence on tamoxifen (Watson et al., 2010). These correlations suggest that the SphK1/S1P/S1PR1/3 axis and ERK1/2 may cooperate to promote ERα-positive breast cancer progression and resistance to anti-estrogen therapies.

### 1.6. Inhibition of the ER/S1P axis

Inhibitors that effectively target the ERα/S1P axis could also potentially be useful as new therapies for breast cancer. Numerous studies have shown the inhibitors of SphK1 decrease cancer cell growth and survival and also sensitize them to chemotherapeutics. For example, the non-selective SphK1/2 inhibitor, SKI-II, has been shown to abrogate ERα signaling, likely acting both as a SphK inhibitor and in a similar manner as tamoxifen by directly binding to the ERα and blocking binding of $E_2$ (Antoon et al., 2011a). Moreover, SphK1 inhibition by siRNA knockdown or treatment with SKI-5C sensitizes TNBC cells to chemotherapeutic drugs (Datta et al., 2014). However, fewer studies have shown the utility of SphK1 inhibitors *in vivo*. We found that treatment mice bearing syngeneic breast tumors with the specific SphK1 inhibitor SK1-I not only suppressed S1P levels in the tumor and circulation, but importantly reduced tumor burden and metastases to lymph nodes and lungs (Nagahashi et al., 2012). Growth of MDA-MB-468 xenograft tumors in mice was significantly inhibited by the SphK1/2 inhibitor SKI-II and the tyrosine kinase inhibitor gefitinib when used in combination, but not as single agents (Martin et al., 2014). Although inhibition of SphK2 has also been reported to reduce tumorigenesis (Antoon et al., 2011b; Liu et al., 2013), further studies are needed to insure that these effects are solely dependent on inhibition of SphK2 activity.

We and others found that the multiple sclerosis pro-drug FTY720/fingolimod, a sphingosine analog that is phosphorylated mainly by SphK2 to a S1P mimetic *in vivo*, has pleiotropic anti-cancer actions in breast cancer cells and in animal models. First, FTY720 has anti-proliferative actions in many types of cancer cells without affecting normal cells (Romero Rosales et al., 2011). Moreover, FTY720 is a substrate and thus a competitive inhibitor of SphK1 and SphK2, decreasing levels of pro-

survival S1P and increasing levels of pro-apoptotic sphingosine (Pyne et al., 2014). Phosphorylated FTY720 (FTY720-P) is also a functional antagonist of and downregulates S1PR1, which interferes with activation of NF-κB and STAT3, and inhibits neovascularization in B cell-derived tumors (Deng et al., 2012; Lee et al., 2010; Liu et al., 2012) and colorectal cancer (Liang et al., 2013; Nagahashi et al., 2014). Furthermore, in breast cancer cells, FTY720-P produced in the nucleus by nuclear SphK2 is a potent inhibitor of class 1 HDACs that enhances histone acetylations and regulates expression of a restricted set of genes important for cancer progression, independently of its known effects on canonical signaling through S1PR1 (Hait et al., 2015). Importantly, in ERα-negative human and murine breast cancer cells and in ERα-negative syngeneic breast tumors, FTY720 activated re-expression of silenced ERα, which restored the ability of the anti-estrogen drug tamoxifen to block breast cancer proliferation and enhance apoptosis (Hait et al., 2015). Because a high fat diet and associated obesity are now endemic and associated with worse prognosis in breast cancer, we also investigated the effect of FTY720 administration on increased tumorigenesis in high fat diet fed mice. FTY720 significantly impaired development, progression and aggressiveness of spontaneous breast tumors in MMTV-PyMT transgenic mice and also reduced HDAC activity and restored expression of estrogen and progesterone receptors induced by the high fat diet (Hait et al., 2015). Taken together, these results provide further support the notion that FTY720 deserves consideration as a new therapeutic for treatment of both hormonal therapy-resistant breast cancer and triple-negative breast cancer.

## Conflicts of interest

The authors declare no competing financial interests.

## Acknowledgments

This work was supported by grants from Department of Defense BCRP Program Award W81XWH-14-1-0086 (S. Spiegel).

## References

Alvarez, S.E., Harikumar, K.B., Hait, N.C., Allegood, J., Strub, G.M., Kim, E.Y., et al., 2010. Sphingosine-1-phosphate is a missing cofactor for the E3 ubiquitin ligase TRAF2. Nature 465, 1084–1088.
Antoon, J.W., Meacham, W.D., Bratton, M.R., Slaughter, E.M., Rhodes, L.V., Ashe, H.B., et al., 2011a. Pharmacological inhibition of sphingosine kinase isoforms alters estrogen receptor signaling in human breast cancer. J. Mol. Endocrinol. 46, 205–216.
Antoon, J.W., White, M.D., Slaughter, E.M., Driver, J.L., Khalili, H.S., Elliott, S., et al., 2011b. Targeting NFkB mediated breast cancer chemoresistance through selective inhibition of sphingosine kinase-2. Cancer Biol. Ther. 11, 678–689.
Bayraktar, S., Gluck, S., 2013. Molecularly targeted therapies for metastatic triple-negative breast cancer. Breast Cancer Res. Treat. 138, 21–35.
Carroll, B., Donaldson, J.C., Obeid, L., 2015. Sphingolipids in the DNA damage response. Adv. Biol. Regul. 58, 38–52.
Datta, A., Loo, S.Y., Huang, B., Wong, L., Tan, S.S., Tan, T.Z., et al., 2014. SPHK1 regulates proliferation and survival responses in triple-negative breast cancer. Oncotarget 5, 5920–5933.
Davies, C., Godwin, J., Gray, R., Clarke, M., Cutter, D., Darby, S., et al., 2011. Relevance of breast cancer hormone receptors and other factors to the efficacy of adjuvant tamoxifen: patient-level meta-analysis of randomised trials. Lancet 378, 771–784.
Deng, J., Liu, Y., Lee, H., Herrmann, A., Zhang, W., Zhang, C., et al., 2012. S1PR1-STAT3 signaling is crucial for myeloid cell colonization at future metastatic sites. Cancer Cell 21, 642–654.
Donoviel, M.S., Hait, N.C., Ramachandran, S., Maceyka, M., Takabe, K., Milstien, S., et al., 2015. Spinster 2, a sphingosine-1-phosphate transporter, plays a critical role in inflammatory and autoimmune diseases. FASEB J. (in press).
Filardo, E., Quinn, J., Pang, Y., Graeber, C., Shaw, S., Dong, J., et al., 2007. Activation of the novel estrogen receptor G protein-coupled receptor 30 (GPR30) at the plasma membrane. Endocrinology 148, 3236–3245.
Hait, N.C., Allegood, J., Maceyka, M., Strub, G.M., Harikumar, K.B., Singh, S.K., et al., 2009. Regulation of histone acetylation in the nucleus by sphingosine-1-phosphate. Science 325, 1254–1257.
Hait, N.C., Avni, D., Yamada, A., Nagahashi, M., Aoyagi, T., Aoki, H., et al., 2015. The phosphorylated prodrug FTY720 is a histone deacetylase inhibitor that reactivates ERalpha expression and enhances hormonal therapy for breast cancer. Oncogenesis 4, e156.
Hannun, Y.A., Obeid, L.M., 2008. Principles of bioactive lipid signalling: lessons from sphingolipids. Nat. Rev. Mol. Cell Biol. 9, 139–150.
Hobson, J.P., Rosenfeldt, H.M., Barak, L.S., Olivera, A., Poulton, S., Caron, M.G., et al., 2001. Role of the sphingosine-1-phosphate receptor EDG-1 in PDGF-induced cell motility. Science 291, 1800–1803.
Lee, H., Deng, J., Kujawski, M., Yang, C., Liu, Y., Herrmann, A., et al., 2010. STAT3-induced S1PR1 expression is crucial for persistent STAT3 activation in tumors. Nat. Med. 16, 1421–1428.
Liang, J., Nagahashi, M., Kim, E.Y., Harikumar, K.B., Yamada, A., Huang, W.C., et al., 2013. Sphingosine-1-phosphate links persistent STAT3 activation, chronic intestinal inflammation, and development of colitis-associated cancer. Cancer Cell 23, 107–120.
Liu, K., Guo, T.L., Hait, N.C., Allegood, J., Parikh, H.I., Xu, W., et al., 2013. Biological characterization of 3-(2-amino-ethyl)-5-[3-(4-butoxyl-phenyl)-propylidene]-thiazolidine-2,4-dione (K145) as a selective sphingosine Kinase-2 inhibitor and anticancer Agent. Plos One 8, e56471.
Liu, Y., Deng, J., Wang, L., Lee, H., Armstrong, B., Scuto, A., et al., 2012. S1PR1 is an effective target to block STAT3 signaling in activated B cell-like diffuse large B-cell lymphoma. Blood 120, 1458–1465.
Maceyka, M., Spiegel, S., 2014. Sphingolipid metabolites in inflammatory disease. Nature 510, 58–67.
Mangelsdorf, D.J., Thummel, C., Beato, M., Herrlich, P., Schutz, G., Umesono, K., et al., 1995. The nuclear receptor superfamily: the second decade. Cell 83, 835–839.
Marino, M., Galluzzo, P., Ascenzi, P., 2006. Estrogen signaling multiple pathways to impact gene transcription. Curr. Genomics 7, 497–508.
Martin, J.L., de Silva, H.C., Lin, M.Z., Scott, C.D., Baxter, R.C., 2014. Inhibition of insulin-like growth factor-binding protein-3 signaling through sphingosine kinase-1 sensitizes triple-negative breast cancer cells to EGF receptor blockade. Mol. Cancer Ther. 13, 316–328.
McDonnell, D.P., Norris, J.D., 2002. Connections and regulation of the human estrogen receptor. Science 296, 1642–1644.
Nagahashi, M., Hait, N.C., Maceyka, M., Avni, D., Takabe, K., Milstien, S., et al., 2014. Sphingosine-1-phosphate in chronic intestinal inflammation and cancer. Adv. Biol. Regul. 54C, 112–120.
Nagahashi, M., Ramachandran, S., Kim, E.Y., Allegood, J.C., Rashid, O.M., Yamada, A., et al., 2012. Sphingosine-1-phosphate produced by sphingosine kinase 1 promotes breast cancer progression by stimulating angiogenesis and lymphangiogenesis. Cancer Res. 72, 726–735.

Nava, V.E., Hobson, J.P., Murthy, S., Milstien, S., Spiegel, S., 2002. Sphingosine kinase type 1 promotes estrogen-dependent tumorigenesis of breast cancer MCF-7 cells. Exp. Cell Res. 281, 115–127.
Newton, J., Lima, S., Maceyka, M., Spiegel, S., 2015. Revisiting the sphingolipid rheostat: evolving concepts in cancer therapy. Exp. Cell Res. 333, 195–200.
Nishi, T., Kobayashi, N., Hisano, Y., Kawahara, A., Yamaguchi, A., 2014. Molecular and physiological functions of sphingosine 1-phosphate transporters. Biochim. Biophys. Acta 841, 759–765.
Panneer Selvam, S., De Palma, R.M., Oaks, J.J., Oleinik, N., Peterson, Y.K., Stahelin, R.V., et al., 2015. Binding of the sphingolipid S1P to hTERT stabilizes telomerase at the nuclear periphery by allosterically mimicking protein phosphorylation. Sci. Signal. 8, ra58.
Pyne, N.J., Ohotski, J., Bittman, R., Pyne, S., 2014. The role of sphingosine 1-phosphate in inflammation and cancer. Adv. Biol. Regul. 54, 121–129.
Pyne, N.J., Tonelli, F., Lim, K.G., Long, J.S., Edwards, J., Pyne, S., 2012. Sphingosine 1-phosphate signalling in cancer. Biochem. Soc. Trans. 40, 94–100.
Romero Rosales, K., Singh, G., Wu, K., Chen, J., Janes, M.R., Lilly, M.B., et al., 2011. Sphingolipid-based drugs selectively kill cancer cells by down-regulating nutrient transporter proteins. Biochem. J. 439, 299–311.
Ruckhaberle, E., Rody, A., Engels, K., Gaetje, R., von Minckwitz, G., Schiffmann, S., et al., 2008. Microarray analysis of altered sphingolipid metabolism reveals prognostic significance of sphingosine kinase 1 in breast cancer. Breast Cancer Res. Treat. 112, 41–52.
Saha Roy, S., Vadlamudi, R.K., 2012. Role of estrogen receptor signaling in breast cancer metastasis. Int. J. Breast Cancer 2012, 654698.
Shamseddine, A.A., Airola, M.V., Hannun, Y.A., 2015. Roles and regulation of neutral sphingomyelinase-2 in cellular and pathological processes. Adv. Biol. Regul. 57, 24–41.
Strub, G.M., Paillard, M., Liang, J., Gomez, L., Allegood, J.C., Hait, N.C., et al., 2011. Sphingosine-1-phosphate produced by sphingosine kinase 2 in mitochondria interacts with prohibitin 2 to regulate complex IV assembly and respiration. FASEB J. 25, 600–612.
Sukocheva, O., Wadham, C., 2014. Role of sphingolipids in oestrogen signalling in breast cancer cells: an update. J. Endocrinol. 220, R25–R35.
Sukocheva, O., Wadham, C., Holmes, A., Albanese, N., Verrier, E., Feng, F., et al., 2006. Estrogen transactivates EGFR via the sphingosine 1-phosphate receptor Edg-3: the role of sphingosine kinase-1. J. Cell Biol. 173, 301–310.
Sukocheva, O., Wadham, C., Xia, P., 2013. Estrogen defines the dynamics and destination of transactivated EGF receptor in breast cancer cells: role of S1P(3) receptor and Cdc42. Exp. Cell Res. 319, 455–465.
Sukocheva, O., Wang, L., Verrier, E., Vadas, M.A., Xia, P., 2009. Restoring endocrine response in breast cancer cells by inhibition of the sphingosine kinase-1 signaling pathway. Endocrinology 150, 4484–4492.
Takabe, K., Kim, R.H., Allegood, J.C., Mitra, P., Ramachandran, S., Nagahashi, M., et al., 2010. Estradiol induces export of sphingosine 1-phosphate from breast cancer cells via ABCC1 and ABCG2. J. Biol. Chem. 285, 10477–10486.
Takabe, K., Paugh, S.W., Milstien, S., Spiegel, S., 2008. "Inside-out" signaling of sphingosine-1-phosphate: therapeutic targets. Pharmacol. Rev. 60, 181–195.
Takabe, K., Spiegel, S., 2014. Export of sphingosine-1-phosphate and cancer progression. J. Lipid Res. 9, 1839–1846.
Truman, J.P., Garcia-Barros, M., Obeid, L.M., Hannun, Y.A., 2014. Evolving concepts in cancer therapy through targeting sphingolipid metabolism. Biochim. Biophys. Acta 1841, 1174–1188.
Watson, C., Long, J.S., Orange, C., Tannahill, C.L., Mallon, E., McGlynn, L.M., et al., 2010. High expression of sphingosine 1-phosphate receptors, S1P1 and S1P3, sphingosine kinase 1, and extracellular signal-regulated kinase-1/2 is associated with development of tamoxifen resistance in estrogen receptor-positive breast cancer patients. Am. J. Pathol. 177, 2205–2215.
Watson, D.G., Tonelli, F., Alossaimi, M., Williamson, L., Chan, E., Gorshkova, I., et al., 2013. The roles of sphingosine kinases 1 and 2 in regulating the Warburg effect in prostate cancer cells. Cell Signal. 25, 1011–1017.

OPEN

Citation: Oncogenesis (2015) **4**, e156; doi:10.1038/oncsis.2015.16

www.nature.com/oncsis

ORIGINAL ARTICLE

# The phosphorylated prodrug FTY720 is a histone deacetylase inhibitor that reactivates ERα expression and enhances hormonal therapy for breast cancer

NC Hait[1], D Avni[1], A Yamada[2], M Nagahashi[2], T Aoyagi[2], H Aoki[2], CI Dumur[3], Z Zelenko[4], EJ Gallagher[4], D Leroith[4], S Milstien[1], K Takabe[2] and S Spiegel[1]

Estrogen receptor-α (ERα)-negative breast cancer is clinically aggressive and does not respond to conventional hormonal therapies. Strategies that lead to re-expression of ERα could sensitize ERα-negative breast cancers to selective ER modulators. FTY720 (fingolimod, Gilenya), a sphingosine analog, is the Food and Drug Administration (FDA)-approved prodrug for treatment of multiple sclerosis that also has anticancer actions that are not yet well understood. We found that FTY720 is phosphorylated in breast cancer cells by nuclear sphingosine kinase 2 and accumulates there. Nuclear FTY720-P is a potent inhibitor of class I histone deacetylases (HDACs) that enhances histone acetylations and regulates expression of a restricted set of genes independently of its known effects on canonical signaling through sphingosine-1-phosphate receptors. High-fat diet (HFD) and obesity, which is now endemic, increase breast cancer risk and have been associated with worse prognosis. HFD accelerated the onset of tumors with more advanced lesions and increased triple-negative spontaneous breast tumors and HDAC activity in MMTV-PyMT transgenic mice. Oral administration of clinically relevant doses of FTY720 suppressed development, progression and aggressiveness of spontaneous breast tumors in these mice, reduced HDAC activity and strikingly reversed HFD-induced loss of estrogen and progesterone receptors in advanced carcinoma. In ERα-negative human and murine breast cancer cells, FTY720 reactivated expression of silenced ERα and sensitized them to tamoxifen. Moreover, treatment with FTY720 also re-expressed ERα and increased therapeutic sensitivity of ERα-negative syngeneic breast tumors to tamoxifen *in vivo* more potently than a known HDAC inhibitor. Our work suggests that a multipronged attack with FTY720 is a novel combination approach for effective treatment of both conventional hormonal therapy-resistant breast cancer and triple-negative breast cancer.

*Oncogenesis* (2015) **4,** e156; doi:10.1038/oncsis.2015.16; published online 8 June 2015

## INTRODUCTION

The majority of breast tumors express the estrogen receptor-α (ERα) that plays important roles in breast cancer pathogenesis and progression, and hormonal therapies such as tamoxifen (TAM) are the first line of adjuvant therapy.[1,2] Unfortunately, 30% of these patients will ultimately fail therapy because of *de novo* or acquired resistance. Moreover, patients with ER, progesterone receptor (PR) and human epidermal growth factor receptor 2 (also known as ErbB-2) triple-negative breast cancer, which is aggressive with high recurrence, metastatic and mortality rates,[3] do not respond to hormonal therapies and have limited treatment options. Epidemiological and clinical studies indicate that obesity, which is now endemic, increases breast cancer risk and is associated with worse prognosis[4] that may be due in part to the high frequency of triple-negative breast cancer and ineffectual hormonal therapy.[5] As hormonal therapy is so effective with relatively few side effects, the possibility of reversing hormonal unresponsiveness is an appealing treatment approach. Histone deacetylases (HDACs) are negative regulators of ERα transcription, and HDAC inhibitors, including suberoylanilide hydroxamic acid (SAHA, vorinostat) and trichostatin A, have been shown to reactivate ERα expression in ERα – negative breast cancer cells and reverse TAM resistance in preclinical studies.[6–8] Encouragingly, in phase II clinical trials, the combination of vorinostat and TAM showed promising activity in reversing hormone resistance.[9]

FTY720 (fingolimod), the Food and Drug Administration (FDA) approved prodrug for the treatment of multiple sclerosis, is phosphorylated *in vivo* by sphingosine kinase 2 (SphK2) to its active form FTY720-phosphate (FTY720-P), a mimetic of sphingosine-1-phosphate (S1P) and an agonist of four S1P receptors (S1PRs) that interferes with immune cell trafficking by inducing internalization and degradation of S1PR1.[10] However, FTY720 has strong anticancer effects *in vitro* and *in vivo* in various types of cancers including breast[11,12] that are not well understood independently of its effects on immune cell trafficking.[13] Although some of its actions have been attributed to FTY720-P acting as a functional antagonist of S1PR1, reducing persistent activation of the transcription factor STAT3 (signal transducer and activator of transcription 3) important in malignant progression,[14–16] others have shown that the unphosphorylated FTY720 is an activator of protein phosphatase 2A, a tumor suppressor that is inactivated in many cancers.[17,18] However, our recent study suggests that

[1]Department of Biochemistry and Molecular Biology, Virginia Commonwealth University School of Medicine, Richmond, VA, USA; [2]Department of Surgery, Division of Surgical Oncology, Virginia Commonwealth University School of Medicine, Richmond, VA, USA; [3]Department of Pathology, and Massey Cancer Center, Virginia Commonwealth University School of Medicine, Richmond, VA, USA and [4]Division of Endocrinology, Diabetes and Bone Diseases, Icahn School of Medicine at Mt Sinai, New York, NY, USA. Correspondence: Dr S Spiegel or Dr NC Hait, Department of Biochemistry and Molecular Biology, VCU School of Medicine, P.O. Box 980614, 1101 East Marshall Street, Richmond, VA 23298-0614, USA. E-mail: sspiegel@vcu.edu, nchait@vcu.edu

Received 10 April 2015; accepted 28 April 2015

FTY720-P and not FTY720 binds and inhibits recombinant class I HDACs.[19] Because it is generally believed that FTY720 in cancer cells is phosphorylated at the plasma membrane by SphK2 to form FTY720-P that acts via S1PRs, we asked where FTY720 is phosphorylated in breast cancer cells and whether FTY720-P also inhibits HDACs in these cells and in tumors to regulate histone acetylation and gene expression, and can be used to re-express ERα in ER-negative aggressive breast carcinoma for hormonal therapies.

## RESULTS

### SphK2 produces FTY720-P in the nucleus of breast cancer cells that inhibits class I HDACs

Following treatment with FTY720, an analog of sphingosine, FTY720-P is produced and accumulates over time in the nucleus of human and murine breast cancer cells in agreement with the predominant nuclear localization of SphK2 in these cells (Figures 1a, c, and f). Nuclear S1P levels were concomitantly decreased by almost twofold in these cell lines after FTY720 treatment because of decreased phosphorylation of the endogenous substrate sphingosine (Figures 1a and c). Interestingly, although it is generally assumed that most of the actions of the phosphorylated active form of FTY720 are at the plasma membrane to modulate S1PR signaling,[10] much more FTY720-P was present in cells than secreted into the media where it can interact with S1PRs (Figures 1b and d). Overexpression of SphK2 robustly increased the formation of nuclear FTY720-P by $>20$-fold in MDA-MB-231 cells (Figure 1e) and 100-fold in MCF7 cells (Figure 1g), whereas catalytically inactive SphK2$^{G212E}$ had no significant effect on phosphorylation of FTY720 or formation of nuclear S1P. In agreement with our previous results showing that FTY720-P inhibits recombinant class I HDACs,[19] we observed that FTY720-P but not FTY720 itself inhibited endogenous class I HDACs (HDAC1–3 and HDAC8) immunoprecipitated from nuclear extracts with the corresponding antibodies as potently as the pan HDAC inhibitor SAHA (Supplementary Figure S1). However, in contrast to SAHA that inhibited class II HDAC7, FTY720-P did not.

### Phosphorylated FTY720 enhances histone acetylations and regulates gene expression independently of S1PRs

Because the majority of FTY720-P is produced in the nucleus of breast cancer cells where its target HDACs are located, we next examined its effects on histone acetylation. Concomitant with

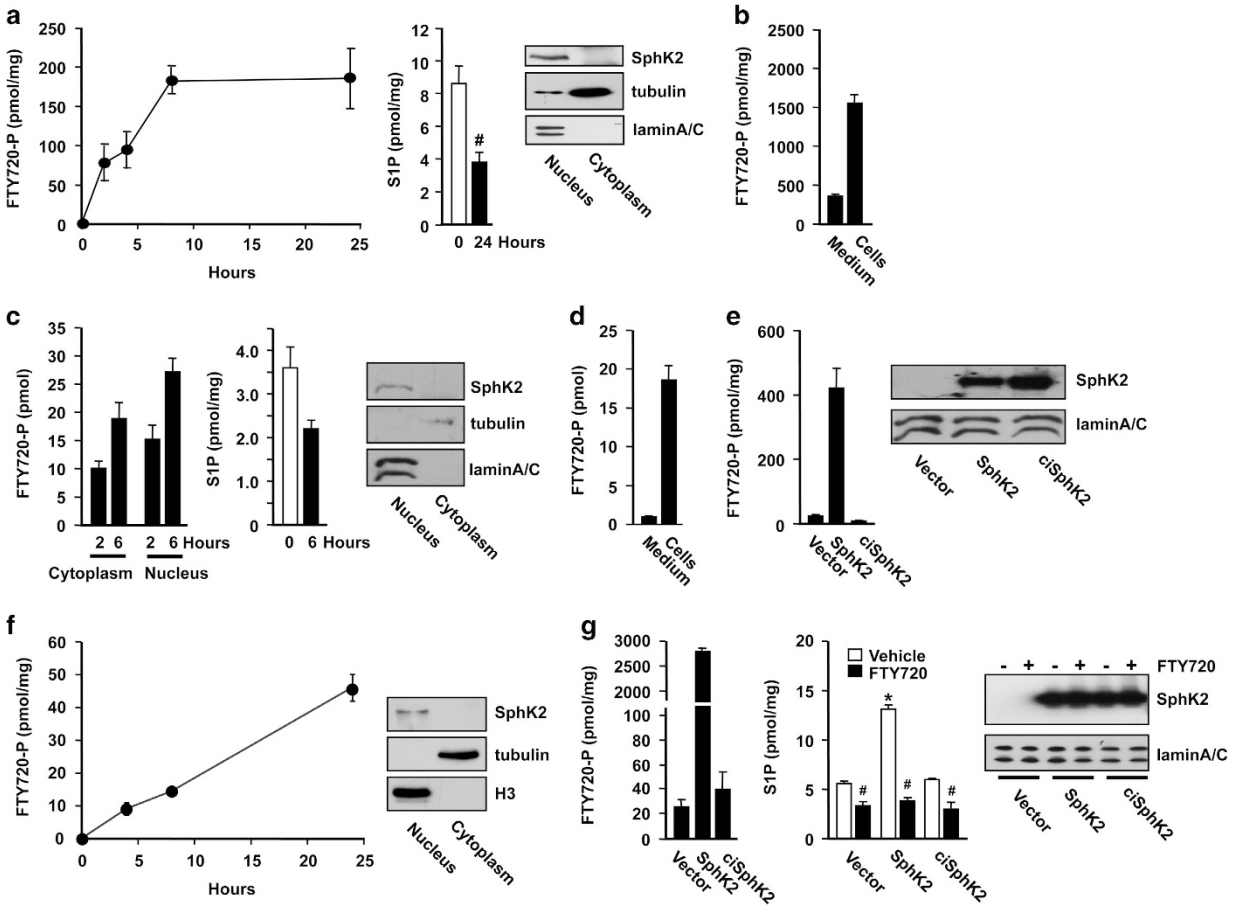


**Figure 1.** FTY720-P is produced in the nucleus of breast cancer cells by SphK2. Breast cancer cell lines, murine 4T1 (**a, b**), human MDA-MB-231 (**c, d**) and human MCF7 (**f**) were treated with 5 μM FTY720. (**a, c**) Nuclear levels of FTY720-P and S1P were determined by liquid chromatography, electrospray ionization/tandem mass spectrometry (LC-ESI-MS/MS) at the indicated times. Equal amounts of protein from nuclear and cytosolic fractions were analyzed by immunoblotting with SphK2 antibody. Antibodies against histone H3 or laminA/C and tubulin were used as nuclear and cytosol markers. (**b**, **d**) Total intracellular and secreted FTY720-P were determined in 4T1 cells after 8 h and MDA-MB-231 cells after 6 h of FTY720 treatment, respectively. MDA-MB-231 cells (**e**) and MCF7 cells (**g**) transfected with vector, SphK2 or catalytically inactive SphK2$^{G212E}$ (ciSphK2) were treated with vehicle or 5 μM FTY720 for 6 and 24 h, respectively. Nuclear levels of FTY720-P and S1P were determined by LC-ESI-MS/MS. Data are mean ± s.d. $^{*}P < 0.005$ compared with vector; $^{\#}P < 0.005$ compared with vehicle. Equal expression of nuclear SphK2 was confirmed by immunoblotting.

increased nuclear FTY720-P (Figure 1), FTY720 increased acetylation of specific lysines of histone H3, H4 and H2B in MCF7 and 4T1 cells (Figures 2a and b). Similar results were found with MDA-MB-231 cells (Supplementary Figure S2a). In order to demonstrate that these effects are because of the intranuclear action of FTY720-P, experiments were carried out with purified MCF7 nuclei devoid of S1PRs. FTY720-P more potently than S1P enhanced histone acetylation in these nuclei (Figure 2c). Treatment of MCF7 cells with the SphK2 inhibitor K145 reduced FTY720-mediated histone acetylation (Supplementary Figure S2b). Importantly, addition of FTY720 itself also increased histone acetylation in these nuclei in a SphK2-dependent manner, as this effect was further enhanced by overexpression of SphK2 (but not catalytically inactive SphK2$^{G212E}$) (Figure 2d) and was prevented by its downregulation (Figure 2f). These effects correlated with the extent of formation of FTY720-P (Figures 2e and g).

To conclusively demonstrate that the effects on histone acetylation are due to direct intranuclear action of FTY720-P on HDAC activity independently of canonical signaling through S1PRs, cells were treated with FTY720-P that activates all S1PRs except S1PR2.[20] Although treatment of cells with FTY720-P, as expected, increased S1PR-mediated phosphorylation of ERK1/2, it did not induce significant changes in histone acetylation or in HDAC activity, in contrast to the significant effects of treatment with FTY720 or SAHA (Figures 2h and i).

Microarray analysis also indicated that the effects of FTY720 on gene expression in breast cancer cells are clearly distinguished from S1P receptor occupancy (Figure 3a). Unsupervised cluster analysis on 22 277 probe sets as well as supervised hierarchical cluster analyses demonstrated that there were no major differences in the clustering of the gene expression profiles between the naive, vehicle-treated and S1P-treated groups, whereas significant differences were observed in gene clustering between them and the FTY720- and SAHA-treated groups (Figure 3a). Although activation of S1PRs did not significantly alter gene expression, FTY720 treatment significantly changed the profiles of 713 genes. In comparison, SAHA significantly altered expression of 3166 genes, of which 276 were common to FTY720 (Figure 3b). The gene ontology analysis revealed that the majority of the commonly affected genes were related to transcription followed by lipid and steroid biosynthesis, transport and metabolic processes (Figure 3c). In addition, regulation of cell growth and angiogenesis genes was also prominent. Together, these results indicate that breast cancer cells take up FTY720 and that FTY720-P produced in the nucleus by SphK2 inhibits class I HDACs and increases specific histone acetylations and regulates expression of a restricted subset of gene programs independently of S1PRs.

## FTY720 treatment suppresses development and progression of spontaneous breast tumors in HFD-fed MMTV-PyMT transgenic mice

Aberrant expression of class I HDACs and dysregulation of global histone acetylations has been found in a many cancers, including breast, and HDACs are promising targets in cancer therapeutics

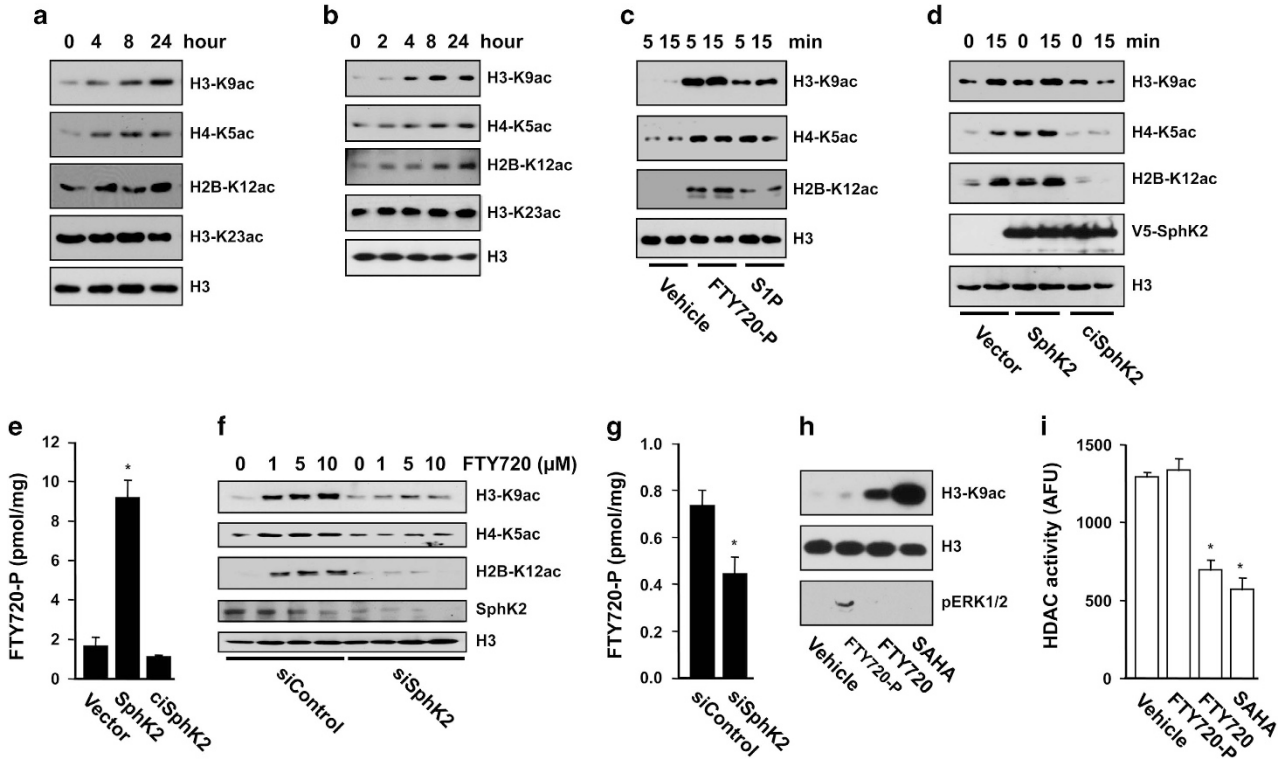


**Figure 2.** Nuclear FTY720-P enhances specific histone acetylations in breast cancer cells. MCF7 cells (**a**) and 4T1 cells (**b**) were treated with FTY720 (5 μM) for the indicated times. Histone acetylations in nuclear extracts were detected by immunoblotting with antibodies to specific histone acetylation sites. (**c**) Purified nuclei from naive MCF7 cells were incubated for the indicated times with vehicle, S1P (1 μM) or FTY720-P (1 μM) and histone acetylations determined. (**d**, **e**) Purified nuclei were isolated from MCF7 cells transfected with vector, SphK2 or ciSphK2 and treated with FTY720 (1 μM) for 15 min. (**f**, **g**) Purified nuclei were isolated from MCF7 cells transfected with siControl or siSphK2 and incubated with the indicated concentrations of FTY720 for 15 min. Histone acetylations were determined by immunoblotting (**d**, **f**) and levels of FTY720-P by liquid chromatography, electrospray ionization/tandem mass spectrometry (LC-ESI-MS/MS) (**e**, **g**). *$P < 0.05$. (**h, i**) Naive MCF7 cells were treated with vehicle, FTY720-P (100 nM), FTY720 (1 μM) or SAHA (2 μM) for 2 h, nuclear extracts were analyzed by western blotting with the indicated antibodies (**h**) and HDAC activity measured and expressed as arbitrary fluorescence units (AFU) (**i**). *$P < 0.001$.

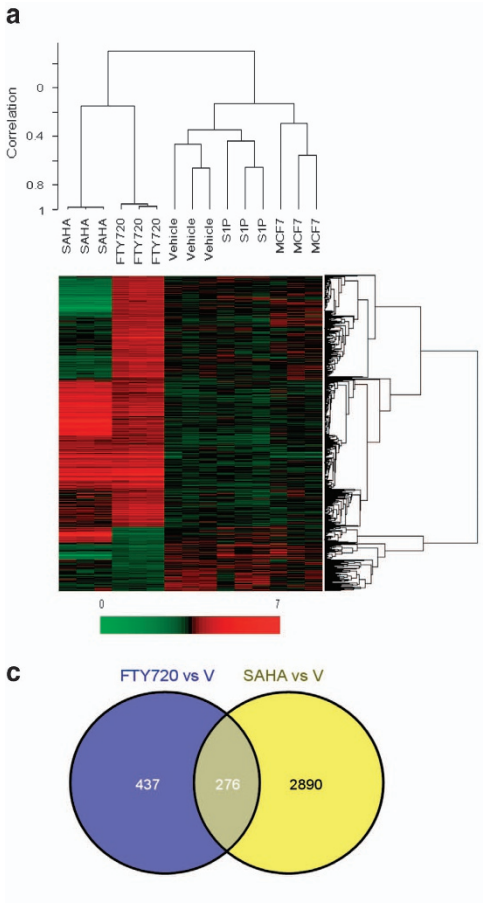


b

| GO Biological Process (Proportion on the 276 common probe sets) | n | Proportion |
|---|---|---|
| Unknown | 51 | 18.48% |
| transcription | 29 | 10.51% |
| lipid and steroid metabolic processes | 27 | 9.78% |
| transport | 11 | 3.99% |
| negative regulation of transcription from RNA polymerase II promoter | 8 | 2.90% |
| metabolic process | 7 | 2.54% |
| angiogenesis | 6 | 2.17% |
| protein amino acid phosphorylation | 5 | 1.81% |
| regulation of cell growth | 5 | 1.81% |
| regulation of cyclin-dependent protein kinase activity | 5 | 1.81% |
| cellular aromatic compound metabolic process | 4 | 1.45% |
| cellular component movement | 4 | 1.45% |
| response to hypoxia | 4 | 1.45% |
| apoptosis | 3 | 1.09% |
| autophagy | 3 | 1.09% |
| citrate metabolic process | 3 | 1.09% |
| endocytosis | 3 | 1.09% |
| mRNA processing | 3 | 1.09% |
| nucleobase, nucleoside, nucleotide and nucleic acid metabolic process | 3 | 1.09% |
| protein complex assembly | 3 | 1.09% |
| protein folding | 3 | 1.09% |
| regulation of transcription, DNA-dependent | 3 | 1.09% |
| regulation of translation | 3 | 1.09% |
| skeletal system development | 3 | 1.09% |
| carbohydrate metabolic process | 2 | 0.72% |
| cell cycle | 2 | 0.72% |
| cell cycle checkpoint | 2 | 0.72% |
| cytoskeleton organization | 2 | 0.72% |
| DNA damage checkpoint | 2 | 0.72% |
| DNA repair | 2 | 0.72% |
| liver development | 2 | 0.72% |
| MAPKKK cascade | 2 | 0.72% |
| nucleosome assembly | 2 | 0.72% |
| protein targeting to Golgi | 2 | 0.72% |
| proteolysis | 2 | 0.72% |
| ribosome biogenesis | 2 | 0.72% |
| signal transduction | 2 | 0.72% |
| somatic cell DNA recombination | 2 | 0.72% |
| de novo pyrimidine base biosynthetic process | 1 | 0.36% |
| activation of MAPK activity | 1 | 0.36% |

**Figure 3.** Microarray analysis of genes regulated by FTY720 and SAHA. Gene expression in naive MCF7 cells or MCF7 cells treated with vehicle, S1P (100 nM), FTY720 (1 μM) or SAHA (1 μM) for 24 h was determined by microarray analyses. (**a**) Heatmap showing supervised hierarchical clustering of 713 genes differentially expressed in FTY720-treated cells compared with naive. Expression level of a given gene is indicated by red (high) and green (low). Note that not all of the genes differentially regulated by SAHA are shown. (**b**) Venn diagram of genes differentially regulated by FTY720 and SAHA. (**c**) The gene ontology (GO) Biological Process analyses of 276 common probe sets regulated by SAHA and FTY720 treatment ranked for biological processes.

(reviewed in refs 21–24). Therefore, it was of interest to examine whether the HDAC inhibitory activity of FTY720-P could mitigate breast cancer development in a mouse model. Because diet, particularly fat intake, contributes to the development and progression of breast cancer and has been associated with worse prognosis,[4,5,25] MMTV-PyMT transgenic mice, which spontaneously develop breast cancer that closely mimics progression of the human disease,[26,27] were fed a high-fat diet (HFD). Female PyMT transgenic mice on a normal chow diet spontaneously developed palpable mammary tumors by 7.5 weeks (Figure 4a). In agreement with others,[28,29] feeding a HFD accelerated the onset of tumors that were palpable by 6 weeks (Figure 4a) and increased tumor multiplicity and size (Figures 4a and b). Although FTY720 administration decreased tumor burden without affecting onset in mice on normal diet (Figure 4a), it significantly increased the latency for appearance of palpable tumors to 7.5 weeks and dramatically suppressed tumor development in mice on HFD (Figures 4a–c). In addition, HFD-fed PyMT mice exhibited more advanced mammary carcinogenic lesions with poorly differentiated malignant cells of dissimilar cell shape and size (Figure 4d). These changes were all mitigated by FTY720 treatment. Consistent with the profound effect on tumor size, there was a significant increase in proliferation determined by Ki67 staining in the mice fed HFD compared with normal diet, which was decreased by FTY720 (Figures 4d and e). Conversely, TUNEL (terminal deoxynucleotidyl transferase dUTP nick end labeling) staining revealed a large increase in apoptotic cells in tumors from FTY720-treated MMTV-PyMT transgenic mice (Figures 4d and e).

### FTY720 treatment reverses HFD-induced HDAC activity and loss of estrogen and progesterone receptors in advanced carcinoma

In agreement with the advanced carcinoma observed in animals fed with HFD and consistent with a previous report,[29] expression of cyclin D1 was elevated (Figures 4d and 5a) and immunohistochemistry revealed high intensity of cyclin D1-positive clusters within these tumors (Figure 4d). In contrast, ERα protein and mRNA as well as PR mRNA were significantly reduced (Figure 5a and f), all of which are associated with poor prognosis in human breast cancers.[30] Notably, these characteristics of advanced tumorigenic mammary lesions were reversed by FTY720 administration to the HFD-fed transgenic mice (Figure 5b). Moreover, FTY720 treatment clearly induced nuclear ERα expression (Figure 5b, c, and f). Intriguingly, HFD reduced acetylation of H3-K9, H4-K5 and H2B-K12 in breast tumors that corresponded with increased nuclear HDAC activity (Figures 5a,d). Conversely, FTY720 administration dramatically increased these specific histone acetylations determined by immunoblotting (Figure 5b) and confirmed by immunohistochemical staining of H3-K9ac in mammary tumors (Figure 5c). FTY720 also reduced HDAC activity in breast tumors (Figure 5d), concomitant with marked production

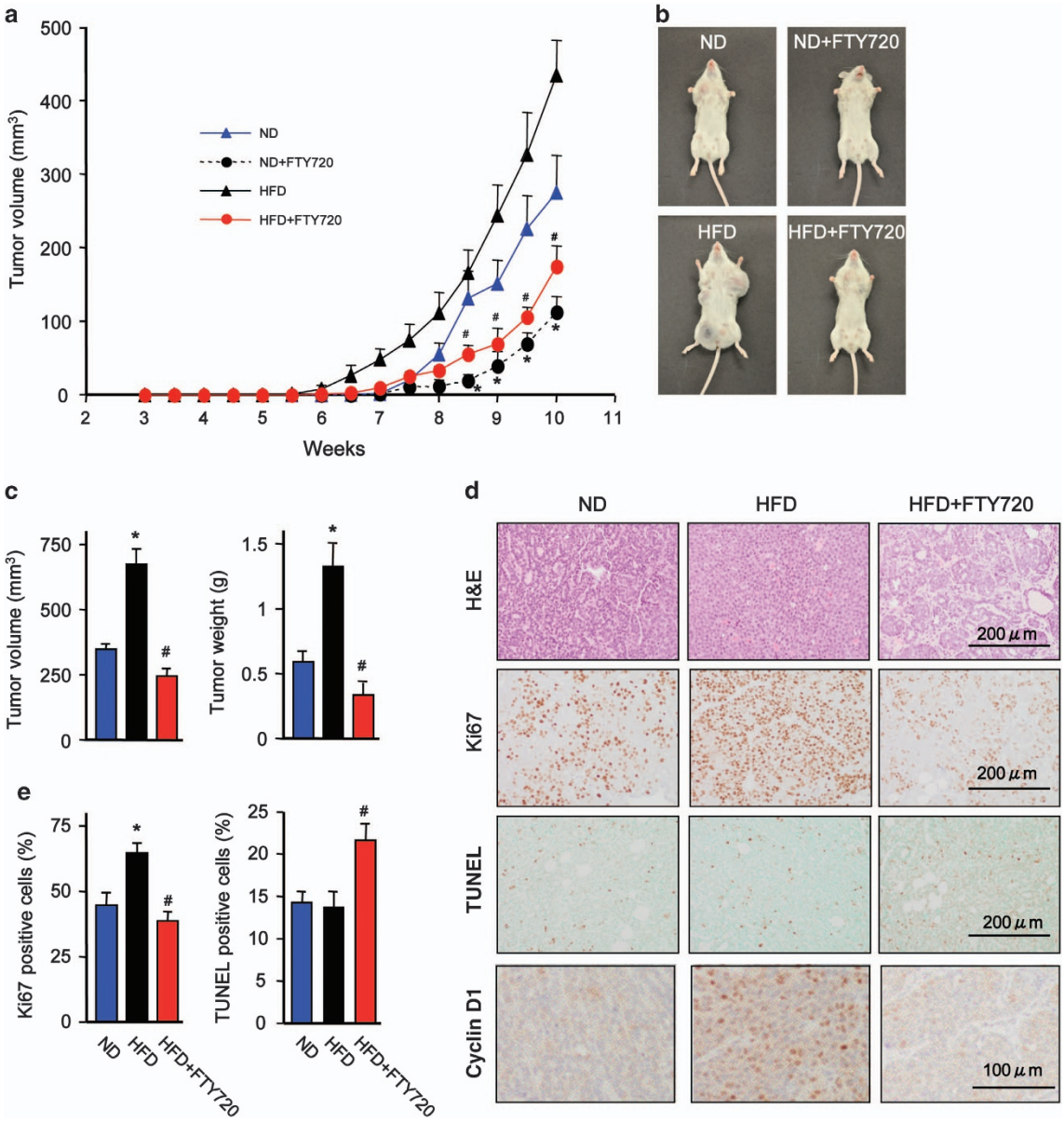


**Figure 4.** FTY720 treatment suppresses advanced tumorigenic mammary lesions in HFD-fed PyMT transgenic mice. Female PyMT transgenic mice were fed with a normal diet (ND) or a Western HFD, and were treated daily with saline or FTY720 (1 mg/kg) by gavage starting after weaning. (**a**) Tumor volumes were determined at the indicated times. (**b**) Representative images of 10-week-old female PyMTTg mice fed with ND or HFD without or with FTY720. Note the difference in the size of the tumors in the mammary pads. (**c**) Tumor volumes and weights were determined at 11 weeks. (**d**, **e**) Tumor sections were stained with hematoxylin and eosin (H&E), proliferation determined by Ki67 staining, apoptosis by TUNEL and cyclin D1 expression determined by immunohistochemistry. Scale bars: 200 μm and 100 μm, as indicated. (**e**) Quantification of Ki67- and TUNEL-positive cells. Data are mean ± s.e.m. $^{\#}P < 0.05$ compared with ND; $^{*}P < 0.05$ compared with HFD.

of nuclear FTY720-P compared with FTY720 (Figure 5e) and increased mRNA levels of ERα and PR, without affecting expression of ErbB2 (Figure 5f). Interestingly, in tumor-free mammary fat pads from MMTV-PyMT transgenic mice or from naive C57BL/6 mice, HFD reduced HDAC activity and increased histone acetylations (Supplementary Figure S3).

### FTY720 sensitizes triple-negative breast cancer cells to TAM by reactivation of silenced ERα expression

HDACs are negative regulators of the ERα transcriptional complex and HDAC inhibitors have been shown to epigenetically restore ERα expression and reverse TAM resistance in hormone-resistant breast cancer cells[6,7,31,32] and in preclinical animal studies.[33,34] As we found that FTY720 is phosphorylated in the nucleus of ERα-negative MDA-MB-231 and 4T1 breast cancer cells by SphK2 (Figure 1) and that FTY720-P is a potent class I HDAC inhibitor, we asked whether it induces ERα re-expression in ERα-negative breast cancer. Although FTY720 alters expression of many fewer genes than SAHA (Figure 3c), FTY720 more potently than SAHA enhanced ERα expression in 4T1 cells (Figure 6a), whereas in MDA-MB-231 cells, it enhanced ERα mRNA and protein expression to the same extent as SAHA (Figures 6b and c). Similar to SAHA, FTY720 also enhanced expression of PR, one of the ERα target genes (Figures 6b and c). As expected, neither SAHA nor FTY720 had a significant effect on expression of ERβ (Figure 6b). Moreover,

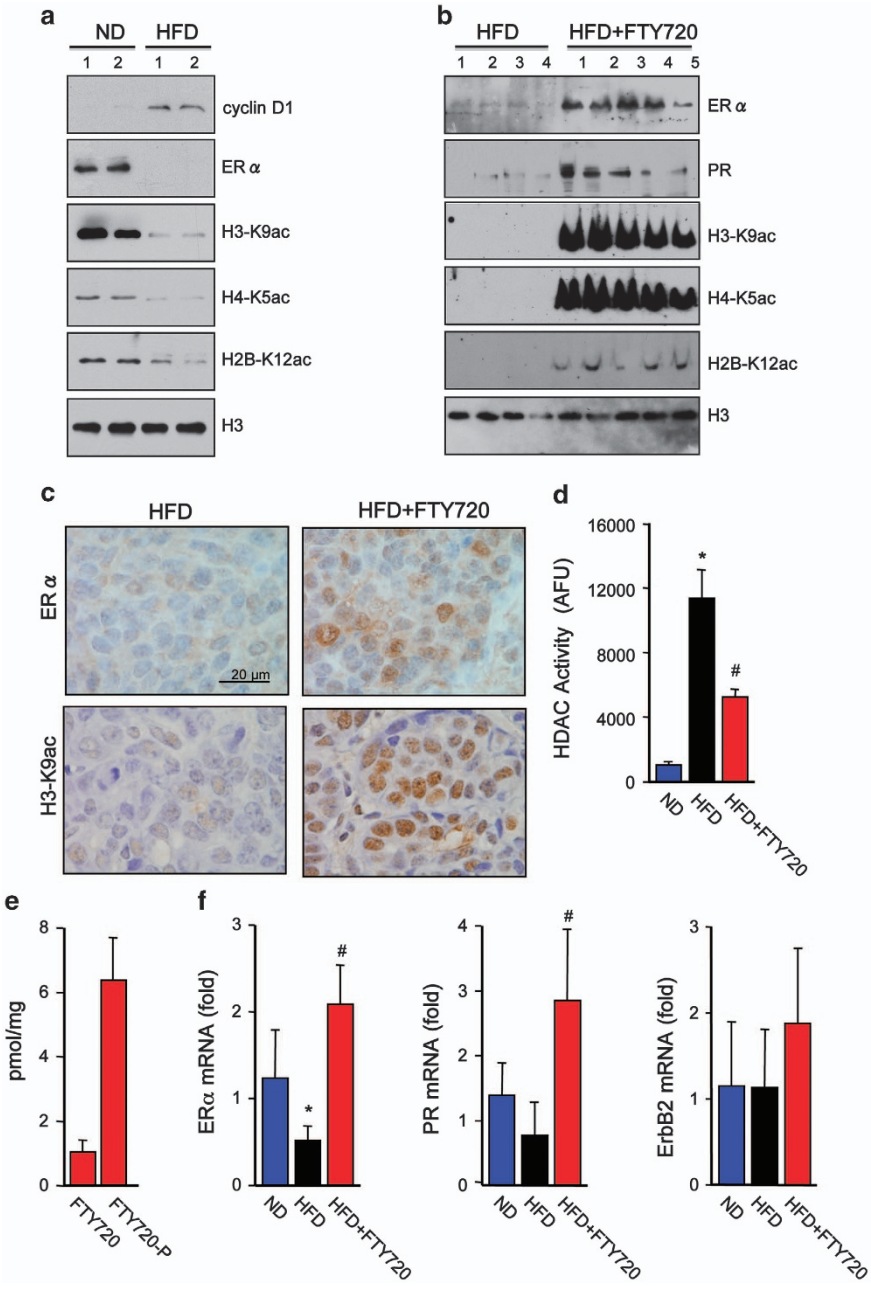


**Figure 5.** FTY720 treatment reverses HFD-induced loss of estrogen and progesterone receptors in PyMT transgenic mice. Female PyMT transgenic mice were fed with a normal diet (ND) or a Western HFD, and were treated daily with saline or FTY720 (1 mg/kg) by gavage starting after weaning ($n = 5$ each), as indicated. (**a**, **b**) Nuclear extracts from tumors were analyzed by western blotting with the indicated antibodies. (**c**) Representative images of tumor sections immunostained with anti-ERα or anti-H3-K9ac antibodies. Scale bars: 20 μm. (**d**) HDAC activity in nuclear extracts of tumors was determined and expressed as arbitrary fluorescence units. (**e**) FTY720 and FTY720-P levels in nuclear extracts of tumors from mice on HFD treated with FTY720 were measured by liquid chromatography, electrospray ionization/tandem mass spectrometry (LC-ESI-MS/MS). (**f**) ERα, PR and ErbB2 mRNA levels in tumors were quantified by quantitative real-time PCR (QPCR) and normalized to *Gapdh*. Data are mean ± s.e.m. $^{*}P < 0.05$ compared with ND; $^{\#}P < 0.05$ compared with HFD.

chromatin immunoprecipitation assays revealed that FTY720, even more potently than SAHA, enhanced association of acetylated histone H3 at the ERα promoter (Figure 6d), indicating that reactivation of ERα expression correlates with ERα promoter hyperacetylation. In agreement, treatment of these ERα-negative cells with E2 enhanced their proliferation only in the presence of FTY720 (Figure 6e). We next examined whether FTY720, which restores ERα expression in ERα-negative breast cancer cells, could also induce sensitivity to TAM, an ERα antagonist. As expected, TAM alone at concentrations up to 10 μM did not inhibit growth of MDA-MB-231 cells (Figure 6f). Like other HDAC inhibitors,[6,31,32] FTY720 reduced growth in a concentration-dependent manner and importantly sensitized the cells to TAM. For example, although a concentration of 2.5 μM TAM or FTY720 alone only reduced growth of MDA-MB-231 cells by 9.3% or 29.3%, respectively, when combined, cell growth was inhibited by >63% (Figure 6f), with a Synergistic Index of 0.23. Similarly, in highly metastatic ERα-negative 4T1 murine mammary carcinoma cells, FTY720 also greatly enhanced the growth inhibitory effect of TAM (Figure 6g), with a Synergistic Index of 0.23.

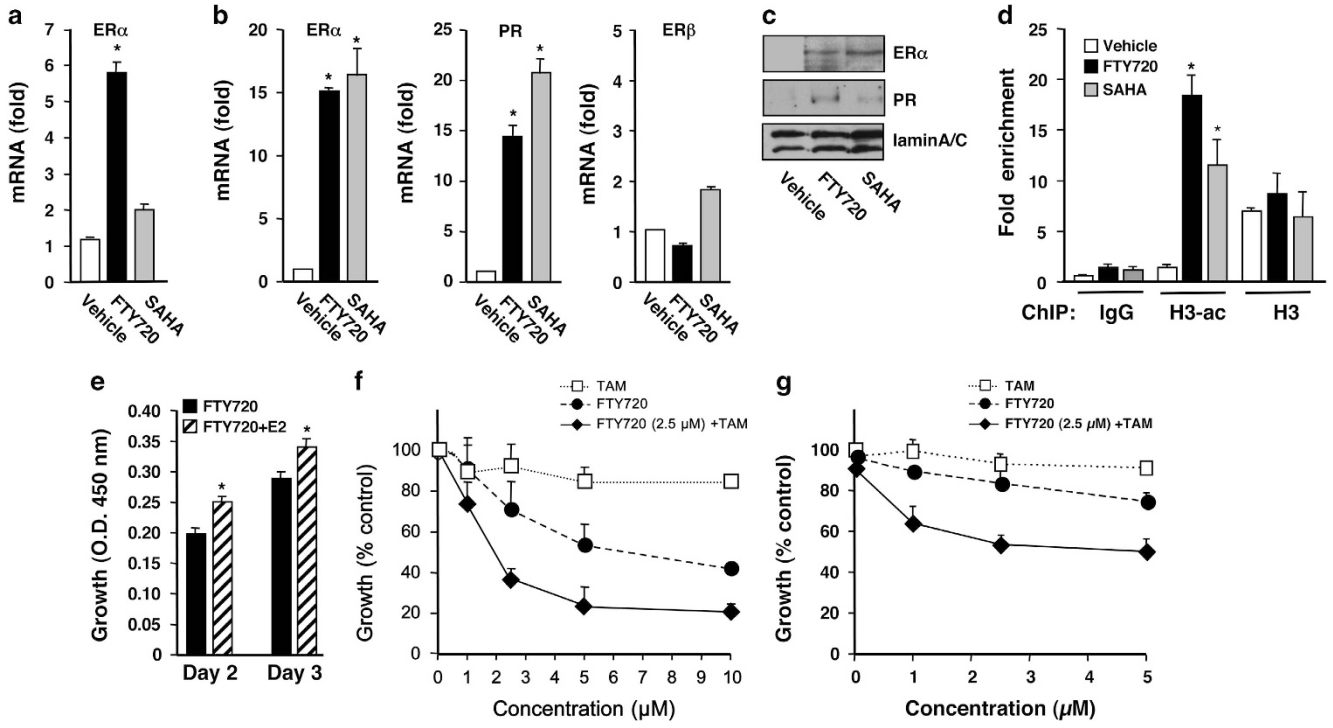


**Figure 6.** FTY720 induces ERα expression in ERα-negative human and murine breast cancer cells and sensitizes them to tamoxifen. 4T1 (**a**) and MDA-MB-231 (**b**) cells were treated with FTY720 (5 μM) or SAHA (1 μM) for 24 h. ERα, PR and ERβ mRNA levels were determined by quantitative real-time PCR (QPCR) and normalized to GAPDH. (**c**) Proteins in MDA-MB-231 nuclear extracts were analyzed by immunoblotting with the indicated antibodies. LaminA/C was used as a loading control. (**d**) MDA-MB-231 cells were subjected to chromatin immunoprecipitation (ChIP) analyses with antibodies to H3-ac, H3 or normal rabbit IgG, as indicated. The precipitated DNA was analyzed by real-time PCR with primers amplifying the core promoter sequence of the ERα gene. Relative binding to the promoter is expressed as fold enrichment compared with input. Data are mean ± s.d. $^*P < 0.003$ compared with vehicle. (**e**) MDA-MB-231 cells were treated with FTY720 (1 nM) without or with 10 nM E2 for the indicated days and cell proliferation was determined by WST assay. (**f**, **g**) MDA-MB-231 cells (**f**) or 4T1 cells (**g**) were treated with the indicated concentrations of TAM or FTY720, or with 2.5 μM FTY720 with increasing concentrations of TAM for 48 h and cell proliferation determined. Data are expressed as % of untreated control.

FTY720 increases therapeutic sensitivity of ERα-negative syngeneic breast tumors to TAM

As we have found that FTY720 treatment induces functional ERα reactivation and sensitizes ERα-negative breast cancer cells to TAM *in vitro*, we sought to determine whether FTY720 also enhances antiestrogen therapy *in vivo*. We utilized a syngeneic mouse metastatic breast cancer model instead of conventional xenografts in immunocompromised nude mice that more accurately mimics human breast cancer.[35,36] ERα-negative 4T1 cells were orthotopically implanted into the second mammary fat pad of immunocompetent mice and randomized to insure similar tumor burdens before treatment. 4T1 cells produced large primary tumors in the chest mammary fat pad that were not significantly reduced by TAM administration (Figure 7a). Orally administered FTY720 reduced tumor growth, an effect that was significantly potentiated by coadministration of TAM (Figures 7a and b). Strikingly, FTY720 enhanced the antitumor efficacy of TAM more than SAHA. TUNEL staining also revealed a large increase in apoptotic cells in tumors from FTY720- plus TAM-treated mice as compared with tumors from mice treated with each separately (Figure 7c). Immunohistochemical analysis revealed that nuclear expression of ERα was increased in tumors from FTY720-treated mice that was more prominent when combined with TAM than even in tumors from mice treated with the combination of SAHA and TAM (Figure 7d). Consistent with the decreased nuclear HDAC activity in tumors from animals treated with FTY720 or SAHA (Figure 7e), acetylation of histone H3-K9, H4-K5 and H2B-K12 was increased in these tumors (Figure 7g), leading to re-expression of ERα (Figures 7f and g). Taken together, these data suggest that FTY720 induces epigenetic ERα reactivation *in vivo* to enhance hormonal therapy of ERα-negative breast cancer.

## DISCUSSION

Hormonal therapies, including selective estrogen receptor modulators and aromatase inhibitors, are the standards of care for treatment of ER-positive breast cancer. However, development of resistance to hormone therapies in advanced breast cancer is a major obstacle. Therefore, epigenetic reactivation of silenced ERα expression by HDAC inhibitors has emerged as an attractive potential mode of therapy for these breast cancer patients.[9] Moreover, treatment of triple-negative breast cancer, which has poor prognosis, remains challenging because the tumors are more aggressive and resistant to hormonal therapy.[30] Epigenetic modifications are responsible for the lack of ERα expression and HDACs 1, 2 and 3 are overexpressed in breast cancer and correlate with more aggressive tumor type.[37] In agreement, we found that consumption of HFD by MMTV-PyMT transgenic mice induced more aggressive, poorly differentiated tumors with increased HDAC activity. In contrast, in mammary pads from naive animals or those without tumors, HFD reduced HDAC activity, supporting the notion that HFD and obesity increase acetylations of histones with changes in the epigenome.[38] Similar to our findings, it was previously reported that HFD-induced HDAC activity plays important roles in epigenetic regulation of tumor suppressor genes involved in colorectal tumor growth and progression,

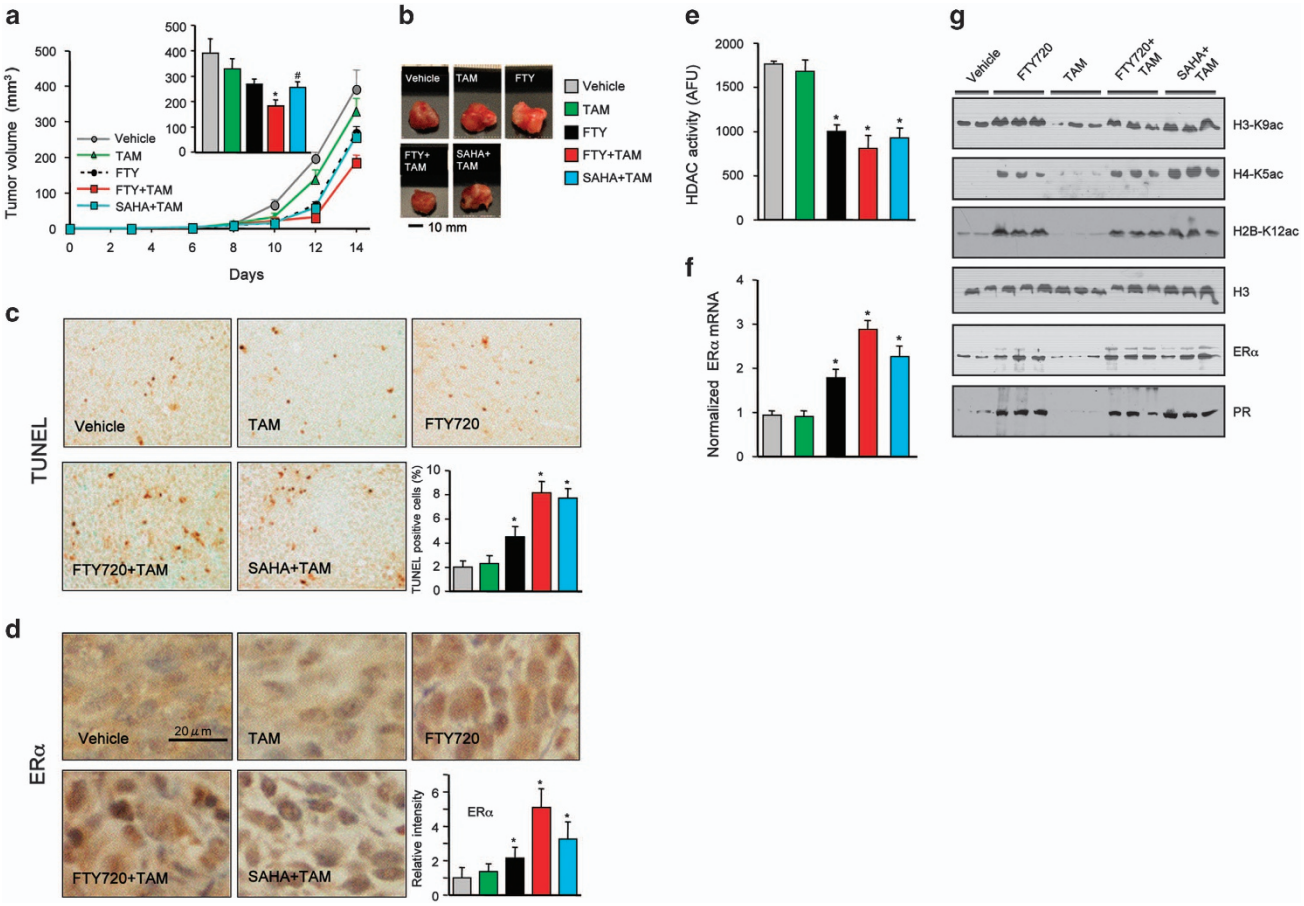


**Figure 7.** FTY720 reduces breast tumor growth and enhances anticancer effectiveness of TAM in ERα-negative 4T1 syngeneic xenografts. 4T1 cells were surgically implanted into the second mammary fat pads under direct vision. Tumor-bearing mice were randomized into five groups 2 days after implantation and then treated with vehicle, FTY720 (1 mg/kg), TAM (25 mg/kg), FTY720 plus TAM or SAHA (intraperitoneal (i.p.) 20 mg/kg) plus TAM by gavage daily till day 15 ($n = 8$). (**a**) Tumor volumes were measured daily. (Insert) Tumor volumes on day 15. (**b**) Representative tumors. $^{*}P < 0.01$, $^{\#}P < 0.05$ compared with vehicle. (**c**, **d**) Immunohistochemical staining of tumor sections for TUNEL (**c**) and ERα (**d**). Scale bar: 20 μm. Quantifications of TUNEL-positive cells and ERα intensity are shown. $^{*}P < 0.05$ compared with vehicle or TAM. (**e**) HDAC activity in nuclear extracts of tumors was determined and expressed as arbitrary fluorescence units. (**f**) Expression of ERα in the tumors was analyzed by quantitative real-time PCR (QPCR) and normalized to *Gapdh*. (**g**) Nuclear extract proteins were analyzed by western blotting with the indicated antibodies. Histone H3 was used as loading control. Data are mean ± s.e.m. $^{*}P < 0.01$ compared with vehicle or TAM.

including increased epithelial–mesenchymal transition and tumor inflammation in a xenograft model.[39]

Several HDAC inhibitors have been developed that restored the efficacy of hormonal therapy in preclinical models[33,34,40] and a few have advanced to clinical trials.[9,41] Combination of the HDAC inhibitor vorinostat with TAM for patients with ER-positive metastatic breast cancer progressing on hormonal therapy showed encouraging reversal of hormone therapy resistance.[9] Similar results were obtained in a phase II clinical trial in postmenopausal women with locally recurrent or metastatic ER-positive breast cancer progressing on treatment with a nonsteroidal aromatase inhibitor when combined with the HDAC inhibitor entinostat,[41] leading to a phase III clinical trial that is currently underway (Clinical-Trials.gov identifier: NCT02115282).

It was originally suggested that the prodrug FTY720 (fingolimod, Gilenya) approved for human use is phosphorylated at the plasma membrane by SphK2 to form FTY720-phosphate that acts via S1P receptors.[10,20] However, in this study we have demonstrated that FTY720 is predominantly phosphorylated to FTY720-P in the nucleus of both ER-positive and ER-negative breast cancer cells. Although it has been suggested that phosphorylation of FTY720 by SphK2 is a requirement for its induction of apoptosis *in vitro* and *in vivo*, the targets for this action have not been identified.[42] We are now showing that the active phosphorylated form of FTY720 is a potent class I HDAC inhibitor. This novel nuclear action of FTY720-P provides a new mechanism to explain the cytotoxic effects of FTY720 in cell culture and its preclinical antitumor efficacy in many xenograft and syngeneic cancer models.[43] Moreover, similar to other HDAC inhibitors, treatment with FTY720 enhances histone acetylation at the ERα promoter leading to its re-expression, and sensitizes ER-negative breast cancer cells to TAM therapy. Interestingly, even in HFD-fed PyMT transgenic mice that developed more advanced, poorly differentiated mammary tumors with increased HDAC activity and decreased expression of ERα and PR, oral administration of FTY720 not only suppressed development and progression of these spontaneous breast tumors, but also reduced HDAC activity in tumors and concomitantly induced expression of ERα and PR. Importantly, FTY720 treatment of breast tumor-bearing mice also induced re-expression of ERα in the tumor and greatly enhanced the anticancer efficacy of TAM, even more potently than a known HDAC inhibitor.

FTY720 has multiple beneficial anticancer activities. First, it has been convincingly shown that the unphosphorylated form is a potent activator of protein phosphatase 2A, a heterotrimeric serine/threonine phosphatase that counteracts the activity of many kinase-driven signaling pathways, including MEK and

AKT.[17,18] In this regard, reduced protein phosphatase 2A activity is a common event in breast cancer that could predict sensitivity to FTY720.[44] Second, unphosphorylated FTY720 also inhibits and induces proteasomal degradation of SphK1,[45] which is upregulated in breast cancer and correlates with poor prognosis and drug resistance.[46–49] High expression of SphK1 and S1PR1 are also associated with development of TAM resistance in ER-positive breast cancer patients.[50] Third, because FTY720-P is a functional antagonist of S1PR1, it can also suppress tumor growth by several S1PR1-dependent mechanisms. It was shown to decrease prosurvival/anti-apoptotic signaling from S1PR1 via suppression of proapoptotic Bim and upregulation of prosurvival Mcl-1 proteins.[51] Targeting S1PR1 with FTY720 also interferes with a major positive feedback loop for persistent STAT3 activation in breast tumor microenvironment critical for malignant progression.[14] Moreover, FTY720 by interfering with the upregulation of SphK1 and S1PR1 curtails the S1P/SphK1/S1PR1 feed-forward amplification loop that leads to nuclear factor-κB and persistent STAT3 activation that play important roles in the link between chronic inflammation and cancer.[16] Finally, in this paper we have uncovered a novel action of FTY720-P as a potent inhibitor of class I HDACs that acts similarly to other HDAC inhibitors to reactivate ERα expression and sensitize breast cancer cells to TAM therapy.

At first glance, the immunosuppressive action of FTY720 would seem to be an undesirable effect in cancer therapy. However, it has been shown that following treatment of tumor-bearing mice with FTY720, there was a significant reduction in accumulation of tumor-associated regulatory T cells and an increase in peripheral blood regulatory T cells, suggesting that FTY720 causes a block in blood-to-tumor regulatory T-cell recruitment that would allow more potent antitumor immunity.[52] Moreover, treatment of mice with FTY720 after tumors were established to block new T-cell trafficking from secondary lymphoid organs still enabled the increase in the capacity of tumor-infiltrating $CD8^+$ T cells to produce IL-2 and to proliferate and subsequent tumor rejection induced by combinatorial immunotherapy with anti-CTLA-4 and anti-PD-L1 monoclonal antibodies.[53]

As HDAC inhibitors are being developed for treatment of breast cancer acting through multiple epigenetic pathways, and numerous clinical trials are underway,[21–24] it is not surprising that FTY720 has such potent anticancer activity. FTY720 has several advantages over available HDAC inhibitors as potential treatments for breast cancer patients: it is an orally bioavailable prodrug; it has already been approved for human use; it regulates expression of only a limited number of genes (a majority related to cholesterol and sphingolipid metabolism) compared with other HDAC inhibitors; it has good pharmacokinetics and a long half-life; it suppresses several survival and proliferative pathways; it is much less toxic, accumulates in tumor tissues, and both the phosphorylated and unphosphorylated forms target important pathways in breast cancer. Hence, we hope that our studies will pave the way for exploration of new clinical trials using FTY720 as a prototype of new adjuvant treatment strategies for hormonal-resistant breast cancer.

## MATERIALS AND METHODS

### Cell culture and transfection

Human breast cancer cells MCF7 and MDA-MB-231 (ATCC, Manassas, VA, USA) and murine 4T1 breast cancer cells (Caliper Life Sciences, Waltham, MA, USA) were cultured and transfected with vector, SphK2 or catalytically inactive $SphK2^{G212E}$ as previously described.[54] SphK2 was downregulated by transfection with ON-TARGETplus SMARTpool siRNA against SphK2, and scrambled siRNA (Dharmacon, Lafayette, CO, USA) was used as control.[54] Cell growth was determined with WST-8 reagent and absorbance was measured at 450 nm.[55]

### Nuclear extracts and immunoblotting

Nuclear extracts from tissues and cells were prepared and protein expression determined by immunoblotting as previously described.[54] Proteins were separated by SDS–polyacrylamide gel electrophoresis, transblotted to nitrocellulose and incubated with primary antibodies as indicated in figure legends, including rabbit polyclonal antibodies to: histone H3-K23ac (1:1000 dilution; EMD Millipore, Billerica, MA, USA); histone H3, H3-K9ac, H4-K5ac and H2B-K12ac (1:1000 dilution; Abcam, Cambridge, MA, USA); laminA/C, tubulin, p-ERK1/2, HDAC3 and HDAC7 (1:1000 dilution; Cell Signaling Technology, Danvers, MA, USA); HDAC1, HDAC2 and HDAC8 (1:1000 dilution; Santa Cruz Biotechnology, Santa Cruz, CA, USA); V5 (1:5000 dilution; Life Technologies, Grand Island, NY, USA); and SphK2 (1:1000 dilution).[54] Immunopositive bands were visualized by enhanced chemiluminescence using secondary antibodies conjugated with horseradish peroxidase (goat anti-rabbit or anti-mouse, 1:5000 dilution; Jackson ImmunoResearch, West Grove, PA, USA) and Super-Signal West Pico chemiluminescent substrate (Pierce Chemical Co., Rockford, IL, USA). Optical densities of bands associated with proteins of interest were quantified using AlphaEaseFC software (Alpha Innotech, Miami, FL, USA) and normalized to the optical densities of their respective tubulin bands.

### Quantification of sphingolipids by mass spectrometry

Sphingolipids were measured by liquid chromatography, electro-spray ionization–tandem mass spectrometry (4000 QTRAP, AB Sciex, Framingham, MA, USA).[54]

### HDAC activity measurements

Enzymatic activities of HDACs immunoprecipitated from nuclear extracts with specific antibodies were measured with fluorometric assay as previously described.[54].

### Quantitative real-time PCR

Total RNA from cells or tumors was isolated with Trizol (life Technologies, Grand Island, NY, USA) and reverse transcribed with the High Capacity cDNA Reverse Transcription Kit and pre-mixed primer probe sets from Applied Biosystems (Foster City, CA, USA). Complementary DNA (cDNA) was amplified with the ABI 7900HT (Applied Biosystems).[54]

### Chromatin immunoprecipitation

Cells were crosslinked with 1% formaldehyde for 10 min at 37 °C and then quenched with glycine, washed with cold phosphate-buffered saline, suspended in SDS buffer, sonicated and centrifuged. Supernatants were pre-cleared with protein G-Sepharose beads (GE Healthcare, Piscataway, NJ, USA) that were blocked with sonicated herring sperm DNA (Promega, San Louis Obispo, CA, USA) in IP buffer (16.7 mM Tris (pH 8), 16.7 mM NaCl, 1.2 mM EDTA, 0.01% SDS, 1.1% Triton X-100, containing 0.05 mg/ml bovine serum albumin). Chromatin was immunoprecipitated with rabbit poly-clonal anti-acetylated H3 or anti-H3 antibodies, or with control rabbit IgG.[54] DNA–protein complexes were pulled down with the protein G-Sepharose beads and then washed with low salt buffer, high salt buffer, LiCl buffer and Tris-EDTA buffer before eluting with 1% SDS in 0.1 M $NaHCO_3$. Crosslinks were reversed by heating at 65 °C overnight in 0.3 M NaCl, followed by proteinase K digestion for 1 h at 55 °C. Input samples were also similarly treated. DNA was purified with QIAquick PCR Purification Kit (Qiagen, Germantown, MD, USA). The ER promoter was analyzed by quantitative real-time PCR using SYBR Green Master Mix (Applied Biosystems) and the following primers: sense, 5′-GAACCGTCCGCAGCT CAAGATC-3′; anti-sense, 5′-GTCTGACCGTAGACCTGCGCGTTG-3′. Results were analyzed relative to input using the ΔCT method. Specific endogenous chromatin immunoprecipitation enrichments were all at least threefold greater than control.

### Animal studies

All animal studies were conducted in the Animal Research Core Facility at VCU School of Medicine in accordance with the institutional guidelines. Animals were bred and maintained in a pathogen-free environment and all procedures were approved by the VCU Institutional Animal Care and Use Committee that is accredited by the Association for Assessment and Accreditation of laboratory Animal Care. All mice were kept on a 12-h light/dark cycle with free access to food.

Male MMTV-PyMT mice on a FVB/N background (Jackson Laboratories, Bar Harbor, MD, USA) were randomly bred with normal FVB/N females to obtain females heterozygous for the PyMT oncogene. Mice were fed a normal diet or HFD (TD.88137; Harlan Laboratories, Indianapolis, IN, USA) containing cholesterol (0.2%), total fat (21% by weight; 42% kcal from fat), saturated fatty acids (>60% of total fatty acids), sucrose (34% by weight), protein (17.3% by weight) and carbohydrate (48.5% by weight). Palpable mammary tumors developed as early as 6 weeks of age. Tumor size was measured with calipers every 3 days and total tumor volume was estimated by the cylinder formula.

For the syngeneic breast cancer model, 4T1 mouse mammary cancer cells were surgically implanted in the upper fat pads of female BALB/c mice (8 to 12 weeks of age, Jackson Laboratories) under direct vision as described previously.[35,36] Tumor-bearing mice were randomized 2 days after implantation into five treatment groups: vehicle, FTY720 (p.o. 1 mg/kg, Cayman Chemical Company, Ann Arbor, MI, USA), TAM (intraperitoneal 25 mg/kg; Sigma-Aldrich, St Louis, MO, USA), FTY720 plus TAM, and SAHA (intraperitoneal 20 mg/kg; Sigma-Aldrich) plus TAM. Tumors were measured regularly and tumor volumes calculated. At the indicated times, animals were killed by exsanguination, blood was collected, tumors excised, weighed, fixed in 10% neutral buffered formalin and embedded in paraffin or frozen in liquid nitrogen for morphological and immunofluorescence analyses.

### Histopathological analysis

Tissue slices (5 μm) were stained with hematoxylin and eosin for morphological analysis. Frozen tissue samples were embedded in Optimal Cutting Medium (OCT 4583; Sakura Finetek, Torrance, CA, USA) for immunofluorescence analysis. Paraffin-embedded slides were deparaffinized, and antigen unmasking was carried out by microwave heating in citrate buffer for 20 min. Slides were incubated with 3% $H_2O_2$ and then with goat or horse serum (DAKO, Carpinteria, CA, USA) for 30 min at room temperature. After washing with phosphate-buffered saline, slides were incubated at 4 °C overnight with the following primary antibodies: ERα (Santa Cruz), H3-K9ac (Abcam), cyclin D1 (Cell Signaling) and Ki67 (Dako). Biotinylated secondary antibodies were added and incubated at room temperature for 20 min. After 5 min with streptavidin-HRP, sections were stained with DAB substrate and counterstained with hematoxylin. Slides were examined with a Zeiss Axioimager A1 (Jena, Germany) and images captured with an AxioCam MRc camera.

### Gene expression microarrays

Total RNA was extracted using the MagMAX-96 for Microarrays Total RNA Isolation Kit (Life Technologies) in an automated manner using the MagMAX Express magnetic particle processor. RNA purity integrity was assessed by spectrophotometry at 260, 270 and 280 nm and by RNA 6000 Nano LabChips with the 2100 Bioanalyzer (Agilent Technologies, Carpenteria, CA, USA).[56] Single-strand cDNA was synthesized from 500 ng total RNA primed with a T7-(dT24) oligonucleotide. Second-strand cDNA synthesis was performed with *Escherichia coli* DNA Polymerase I, and cRNA biotinylated by *in vitro* transcription using the GeneChip 3' *in vitro* transcription Express Kit (Affymetrix, Santa Clara, CA, USA). After incubation at 37 °C for 16 h, labeled cRNA was purified using the GeneChip Sample Cleanup Module. Fragmented cRNA (10 μg) was hybridized on the GeneChip HG-U133A 2.0 array for 16 h at 60 r.p.m. in a 45 °C hybridization oven. Arrays were washed and stained with streptavidin phycoerythrin (Life Technologies) in the Affymetrix fluidics workstation. Every chip was scanned at a high resolution on the Affymetrix GeneChip Scanner 3000 7G and raw intensities for every probe were stored in electronic files by the GeneChip Operating Software v1.4.[36] Overall quality of each array was assessed by monitoring the 3′/5′ ratios for the housekeeping gene, *glyceraldehyde 3-phosphate dehydrogenase* (*GAPDH*), and the percentage of 'Present' genes (%P). Arrays exhibiting *GAPDH* 3′/5′ $< 3.0$ and %$P > 40$% were considered good-quality arrays. For microarray data analyses, background correction, normalization and estimation of probe set expression summaries and filtering and hierarchical cluster analyses were performed using the log-scale Robust Multi-array Analysis method[57] and BRB-ArrayTools v3.1.0 (NCI, Bethesda, MD, USA), respectively. Differentially expressed genes among the classes were identified by *t*-test analyses. To adjust for multiple hypotheses testing, the resulting *P*-values were used to obtain the false discovery rates using the *q*-value method. All analyses were performed on the R environment using functions provided by the BioConductor packages.[58]

### Statistical analysis

Statistical analysis was performed using unpaired two-tailed Student's *t*-test for comparison of two groups. $P < 0.05$ was considered significant. Experiments were repeated at least three times with consistent results. For animal studies, measurements were blind with respect to group assignments.

## CONFLICT OF INTEREST

The authors declare no conflict of interest.

## ACKNOWLEDGEMENTS

This work was supported by grants from Department of Defense BCRP Program Award W81XWH-14-1-0086 (to S Spiegel), NIH R01CA61774, R01GM043880 (to S Spiegel) and in part by NIH R01CA160688 (to K Takabe). D Avni was supported by Department of Defense BCRP Program Postdoctoral Fellowship W81XWH-14-1-0071. We gratefully acknowledge the VCU Lipidomics and Microscopy Cores that are supported in part by funding from the NIH-NCI Cancer Center Support Grant P30CA016059. We thank Dr Jeremy Allegood for skillful sphingolipid analyses and the Anatomic Pathology Research Services (APRS) and Dr Jorge A Almenara for technical assistance with tissue processing, sectioning and staining.

## REFERENCES

1 Clarke R, Leonessa F, Welch JN, Skaar TC. Cellular and molecular pharmacology of antiestrogen action and resistance. *Pharmacol Rev* 2001; **53**: 25–71.
2 McDonnell DP, Norris JD. Connections and regulation of the human estrogen receptor. *Science* 2002; **296**: 1642–1644.
3 Bayraktar S, Gluck S. Molecularly targeted therapies for metastatic triple-negative breast cancer. *Breast Cancer Res Treat* 2013; **138**: 21–35.
4 Phipps AI, Chlebowski RT, Prentice R, McTiernan A, Stefanick ML, Wactawski-Wende J *et al.* Body size, physical activity, and risk of triple-negative and estrogen receptor-positive breast cancer. *Cancer Epidemiol Biomarkers Prev* 2011; **20**: 454–463.
5 Pierobon M, Frankenfeld CL. Obesity as a risk factor for triple-negative breast cancers: a systematic review and meta-analysis. *Breast Cancer Res Treat* 2013; **137**: 307–314.
6 Zhou Q, Atadja P, Davidson NE. Histone deacetylase inhibitor LBH589 reactivates silenced estrogen receptor alpha (ER) gene expression without loss of DNA hypermethylation. *Cancer Biol Ther* 2007; **6**: 64–69.
7 Keen JC, Yan L, Mack KM, Pettit C, Smith D, Sharma D *et al.* A novel histone deacetylase inhibitor, scriptaid, enhances expression of functional estrogen receptor alpha (ER) in ER negative human breast cancer cells in combination with 5-aza 2'-deoxycytidine. *Breast Cancer Res Treat* 2003; **81**: 177–186.
8 Restall C, Doherty J, Liu HB, Genovese R, Paiman L, Byron KA *et al.* A novel histone deacetylase inhibitor augments tamoxifen-mediated attenuation of breast carcinoma growth. *Int J Cancer* 2009; **125**: 483–487.
9 Munster PN, Thurn KT, Thomas S, Raha P, Lacevic M, Miller A *et al.* A phase II study of the histone deacetylase inhibitor vorinostat combined with tamoxifen for the treatment of patients with hormone therapy-resistant breast cancer. *Br J Cancer* 2011; **104**: 1828–1835.
10 Brinkmann V, Billich A, Baumruker T, Heining P, Schmouder R, Francis G *et al.* Fingolimod (FTY720): discovery and development of an oral drug to treat multiple sclerosis. *Nat Rev Drug Discov* 2010; **9**: 883–897.
11 Azuma H, Takahara S, Ichimaru N, Wang JD, Itoh Y, Otsuki Y *et al.* Marked prevention of tumor growth and metastasis by a novel immunosuppressive agent, FTY720, in mouse breast cancer models. *Cancer Res* 2002; **62**: 1410–1419.
12 Mousseau Y, Mollard S, Faucher-Durand K, Richard L, Nizou A, Cook-Moreau J *et al.* Fingolimod potentiates the effects of sunitinib malate in a rat breast cancer model. *Breast Cancer Res Treat* 2012; **134**: 31–40.
13 Pitman MR, Woodcock JM, Lopez AF, Pitson SM. Molecular targets of FTY720 (fingolimod). *Curr Mol Med* 2012; **12**: 1207–1219.
14 Lee H, Deng J, Kujawski M, Yang C, Liu Y, Herrmann A *et al.* STAT3-induced S1PR1 expression is crucial for persistent STAT3 activation in tumors. *Nat Med* 2010; **16**: 1421–1428.
15 Deng J, Liu Y, Lee H, Herrmann A, Zhang W, Zhang C *et al.* S1PR1-STAT3 signaling is crucial for myeloid cell colonization at future metastatic sites. *Cancer Cell* 2012; **21**: 642–654.
16 Liang J, Nagahashi M, Kim EY, Harikumar KB, Yamada A, Huang WC *et al.* Sphingosine-1-phosphate links persistent STAT3 activation, chronic intestinal inflammation, and development of colitis-associated cancer. *Cancer Cell* 2013; **23**: 107–120.

17 Saddoughi SA, Gencer S, Peterson YK, Ward KE, Mukhopadhyay A, Oaks J *et al.* Sphingosine analogue drug FTY720 targets I2PP2A/SET and mediates lung tumour suppression via activation of PP2A-RIPK1-dependent necroptosis. *EMBO Mol Med* 2013; **5**: 105–121.
18 Perrotti D, Neviani P. Protein phosphatase 2A: a target for anticancer therapy. *Lancet Oncol* 2013; **14**: e229–e238.
19 Hait NC, Wise LE, Allegood JC, O'Brien M, Avni D, Reeves TM *et al.* Active, phosphorylated fingolimod inhibits histone deacetylases and facilitates fear extinction memory. *Nat Neurosci* 2014; **17**: 971–980.
20 Mandala S, Hajdu R, Bergstrom J, Quackenbush E, Xie J, Milligan J *et al.* Alteration of lymphocyte trafficking by sphingosine-1-phosphate receptor agonists. *Science* 2002; **296**: 346–349.
21 Glozak MA, Seto E. Histone deacetylases and cancer. *Oncogene* 2007; **26**: 5420–5432.
22 Barneda-Zahonero B, Parra M. Histone deacetylases and cancer. *Mol Oncol* 2012; **6**: 579–589.
23 Spiegel S, Milstien S, Grant S. Endogenous modulators and pharmacological inhibitors of histone deacetylases in cancer therapy. *Oncogene* 2012; **31**: 537–551.
24 Delcuve GP, Khan DH, Davie JR. Targeting class I histone deacetylases in cancer therapy. *Expert Opin Ther Targets* 2013; **17**: 29–41.
25 Sieri S, Chiodini P, Agnoli C, Pala V, Berrino F, Trichopoulou A *et al.* Dietary fat intake and development of specific breast cancer subtypes. *J Natl Cancer Inst* 2014; **106**: dju068 doi: 10.1093/jnci/dju068.
26 Maglione JE, Moghanaki D, Young LJ, Manner CK, Ellies LG, Joseph SO *et al.* Transgenic polyoma middle-T mice model premalignant mammary disease. *Cancer Res* 2001; **61**: 8298–8305.
27 Lin EY, Jones JG, Li P, Zhu L, Whitney KD, Muller WJ *et al.* Progression to malignancy in the polyoma middle T oncoprotein mouse breast cancer model provides a reliable model for human diseases. *Am J Pathol* 2003; **163**: 2113–2126.
28 La Merrill M, Gordon RR, Hunter KW, Threadgill DW, Pomp D. Dietary fat alters pulmonary metastasis of mammary cancers through cancer autonomous and non-autonomous changes in gene expression. *Clin Exp Metastasis* 2010; **27**: 107–116.
29 Llaverias G, Danilo C, Mercier I, Daumer K, Capozza F, Williams TM *et al.* Role of cholesterol in the development and progression of breast cancer. *Am J Pathol* 2011; **178**: 402–412.
30 Foulkes WD, Smith IE, Reis-Filho JS. Triple-negative breast cancer. *N Engl J Med* 2010; **363**: 1938–1948.
31 Jang ER, Lim SJ, Lee ES, Jeong G, Kim TY, Bang YJ *et al.* The histone deacetylase inhibitor trichostatin A sensitizes estrogen receptor alpha-negative breast cancer cells to tamoxifen. *Oncogene* 2004; **23**: 1724–1736.
32 Huang Y, Vasilatos SN, Boric L, Shaw PG, Davidson NE. Inhibitors of histone demethylation and histone deacetylation cooperate in regulating gene expression and inhibiting growth in human breast cancer cells. *Breast Cancer Res Treat* 2012; **131**: 777–789.
33 Tate CR, Rhodes LV, Segar HC, Driver JL, Pounder FN, Burow ME *et al.* Targeting triple-negative breast cancer cells with the histone deacetylase inhibitor panobinostat. *Breast Cancer Res* 2012; **14**: R79.
34 Li Y, Meeran SM, Patel SN, Chen H, Hardy TM, Tollefsbol TO. Epigenetic reactivation of estrogen receptor-alpha (ERalpha) by genistein enhances hormonal therapy sensitivity in ERalpha-negative breast cancer. *Mol Cancer* 2013; **12**: 9.
35 Nagahashi M, Ramachandran S, Kim EY, Allegood JC, Rashid OM, Yamada A *et al.* Sphingosine-1-phosphate produced by sphingosine kinase 1 promotes breast cancer progression by stimulating angiogenesis and lymphangiogenesis. *Cancer Res* 2012; **72**: 726–735.
36 Rashid OM, Nagahashi M, Ramachandran S, Dumur C, Schaum J, Yamada A *et al.* An improved syngeneic orthotopic murine model of human breast cancer progression. *Breast Cancer Res Treat* 2014; **147**: 501–512.
37 Muller BM, Jana L, Kasajima A, Lehmann A, Prinzler J, Budczies J *et al.* Differential expression of histone deacetylases HDAC1, 2 and 3 in human breast cancer--overexpression of HDAC2 and HDAC3 is associated with clinicopathological indicators of disease progression. *BMC Cancer* 2013; **13**: 215.
38 Aagaard-Tillery KM, Grove K, Bishop J, Bishop J, Ke X, Fu Q *et al.* Developmental origins of disease and determinants of chromatin structure: maternal diet modifies the primate fetal epigenome. *J Mol Endocrinol* 2008; **41**: 91–102.
39 Tang FY, Pai MH, Chiang EP. Consumption of high-fat diet induces tumor progression and epithelial-mesenchymal transition of colorectal cancer in a mouse xenograft model. *J Nutr Biochem* 2012; **23**: 1302–1313.
40 Sabnis GJ, Goloubeva O, Chumsri S, Nguyen N, Sukumar S, Brodie AM. Functional activation of the estrogen receptor-alpha and aromatase by the HDAC inhibitor entinostat sensitizes ER-negative tumors to letrozole. *Cancer Res* 2011; **71**: 1893–1903.
41 Yardley DA, Ismail-Khan RR, Melichar B, Lichinitser M, Munster PN, Klein PM *et al.* Randomized phase II, double-blind, placebo-controlled study of exemestane with or without entinostat in postmenopausal women with locally recurrent or metastatic estrogen receptor-positive breast cancer progressing on treatment with a nonsteroidal aromatase inhibitor. *J Clin Oncol* 2013; **31**: 2128–2135.
42 Don AS, Martinez-Lamenca C, Webb WR, Proia RL, Roberts E, Rosen H. Essential requirement for sphingosine kinase 2 in a sphingolipid apoptosis pathway activated by FTY720 analogs. *J Biol Chem* 2007; **282**: 15833–15842.
43 Zhang L, Wang HD, Ji XJ, Cong ZX, Zhu JH, Zhou Y. FTY720 for cancer therapy (Review). *Oncol Rep* 2013; **30**: 2571–2578.
44 Baldacchino S, Saliba C, Petroni V, Fenech AG, Borg N, Grech G. Deregulation of the phosphatase, PP2A is a common event in breast cancer, predicting sensitivity to FTY720. *EPMA J* 2014; **5**: 3.
45 Lim KG, Tonelli F, Li Z, Lu X, Bittman R, Pyne S *et al.* FTY720 analogues as sphingosine kinase 1 inhibitors: enzyme inhibition kinetics, allosterism, proteasomal degradation, and actin rearrangment in MCF-7 breast cancer cells. *J Biol Chem* 2011; **286**: 18633–18640.
46 Ruckhaberle E, Rody A, Engels K, Gaetje R, von Minckwitz G, Schiffmann S *et al.* Microarray analysis of altered sphingolipid metabolism reveals prognostic significance of sphingosine kinase 1 in breast cancer. *Breast Cancer Res Treat* 2008; **112**: 41–52.
47 Pyne NJ, Pyne S. Sphingosine 1-phosphate and cancer. *Nat Rev Cancer* 2010; **10**: 489–503.
48 Kunkel GT, Maceyka M, Milstien S, Spiegel S. Targeting the sphingosine-1-phosphate axis in cancer, inflammation and beyond. *Nat Rev Drug Discov* 2013; **12**: 688–702.
49 Datta A, Loo SY, Huang B, Wong L, Tan SS, Tan TZ *et al.* SPHK1 regulates proliferation and survival responses in triple-negative breast cancer. *Oncotarget* 2014; **5**: 5920–5933.
50 Watson C, Long JS, Orange C, Tannahill CL, Mallon E, McGlynn LM *et al.* High expression of sphingosine 1-phosphate receptors, S1P1 and S1P3, sphingosine kinase 1, and extracellular signal-regulated kinase-1/2 is associated with development of tamoxifen resistance in estrogen receptor-positive breast cancer patients. *Am J Pathol* 2010; **177**: 2205–2215.
51 Rutherford C, Childs S, Ohotski J, McGlynn L, Riddick M, Mac F *et al.* Regulation of cell survival by sphingosine-1-phosphate receptor S1P1 via reciprocal ERK-dependent suppression of Bim and PI-3-kinase/protein kinase C-mediated upregulation of Mcl-1. *Cell Death Dis* 2013; **4**: e927.
52 Priceman SJ, Shen S, Wang L, Deng J, Yue C, Kujawski M *et al.* S1PR1 is crucial for accumulation of regulatory T cells in tumors via STAT3. *Cell Rep* 2014; **6**: 992–999.
53 Spranger S, Koblish HK, Horton B, Scherle PA, Newton R, Gajewski TF. Mechanism of tumor rejection with doublets of CTLA-4, PD-1/PD-L1, or IDO blockade involves restored IL-2 production and proliferation of CD8(+) T cells directly within the tumor microenvironment. *J Immunother Cancer* 2014; **2**: 3.
54 Hait NC, Allegood J, Maceyka M, Strub GM, Harikumar KB, Singh SK *et al.* Regulation of histone acetylation in the nucleus by sphingosine-1-phosphate. *Science* 2009; **325**: 1254–1257.
55 Sarkar S, Maceyka M, Hait NC, Paugh SW, Sankala H, Milstien S *et al.* Sphingosine kinase 1 is required for migration, proliferation and survival of MCF-7 human breast cancer cells. *FEBS Lett* 2005; **579**: 5313–5317.
56 Dumur CI, Nasim S, Best AM, Archer KJ, Ladd AC, Mas VR *et al.* Evaluation of quality-control criteria for microarray gene expression analysis. *Clin Chem* 2004; **50**: 1994–2002.
57 Irizarry RA, Bolstad BM, Collin F, Cope LM, Hobbs B, Speed TP. Summaries of Affymetrix GeneChip probe level data. *Nucleic Acids Res* 2003; **31**: e15.
58 Gentleman RC, Carey VJ, Bates DM, Bolstad B, Dettling M, Dudoit S *et al.* Bioconductor: open software development for computational biology and bioinformatics. *Genome Biol* 2004; **5**: R80.



Supplementary Information accompanies this paper on the Oncogenesis website (http://www.nature.com/oncsis).

EXPERIMENTAL CELL RESEARCH 333 (2015) 195–200

Available online at www.sciencedirect.com

ScienceDirect

journal homepage: www.elsevier.com/locate/yexcr

Review Article

# Revisiting the sphingolipid rheostat: Evolving concepts in cancer therapy

*Jason Newton, Santiago Lima, Michael Maceyka, Sarah Spiegel**

*Department of Biochemistry and Molecular Biology, Virginia Commonwealth University School of Medicine and the Massey Cancer Center, Richmond, Virginia 23298, USA*

ARTICLE INFORMATION

*Article Chronology:*
Received 26 February 2015
Accepted 28 February 2015
Available online 11 March 2015

*Keywords:*
Sphingolipid rheostat
Sphingosine-1-phosphate
Sphingosine kinase
Ceramide

## Contents



*Corresponding author.
*E-mail address:* sspiegel@vcu.edu (S. Spiegel).

http://dx.doi.org/10.1016/j.yexcr.2015.02.025

## Introduction

Nearly two decades have passed since it was first proposed that regulation of the interconvertible sphingolipid metabolites, ceramide and sphingosine-1-phosphate (S1P), and their opposing signaling pathways are major determinants of cell fate, a concept referred to as the "sphingolipid rheostat". Since then, many reports have substantiated the role of the sphingolipid rheostat in cell fate determination and in the initiation, progression, and drug sensitivity of cancer. Thus, modulation of the rheostat has emerged as a focus for treatment strategies to battle cancer. S1P regulates numerous processes important for cancer including proliferation, transformation, angiogenesis, metastasis, survival, and drug resistance. Ceramide on the other hand has been linked to cell growth arrest and cell death. With the increased understanding of sphingolipid metabolism and signaling, as well as the present focus on therapies designed to modulate the levels of sphingolipids in cancer, it is an appropriate time to re-examine the sphingolipid rheostat concept and determine how it fits within the current knowledge of sphingolipid signaling in cancer.

## Sphingolipid metabolism

Sphingolipids are essential constituents of all eukaryotic membranes. They contain a sphingoid base, a fatty amino alcohol of typically 18 carbons, in mammalian cells called sphingosine. *De novo* synthesis of the sphingoid base begins with the condensation of palmitate and serine catalyzed by serine palmitoyl transferase, leading to the formation of dihydrosphingosine (sphinganine), which is then amino-acylated with a chain of 14–32 carbons to form various dihydroceramide species by a family of six (dihydro) ceramide synthases. Dihydroceramides are desaturated to form ceramides and complex sphingolipids, such as glycosphingolipids and sphingomyelin that are built by linking different head groups to the primary hydroxyl group of ceramides. During catabolism, both basal and signal-mediated, these head groups are hydrolyzed, re-generating ceramide. Ceramide is a bioactive lipid in its own right, and can be deacylated by ceramidases to yield sphingosine. Sphingosine, which is not an intermediate in the *de novo* biosynthetic pathway, is also a bioactive molecule and can be phosphorylated by sphingosine kinase (SphK) type 1 and 2 to sphingosine-1-phosphate (S1P), again a potent signaling molecule. S1P can be irreversibly degraded by S1P lyase (SPL) or dephosphorylated to sphingosine, which can then be re-acylated back to ceramide. It is the rapid, compartment-specific interconversion of these three metabolites with distinct effects on cell fate that forms the biochemical basis of the so-called "sphingolipid rheostat".

## The sphingolipid rheostat

In 1996, the term "sphingolipid rheostat" was proposed [1] to tie together several seminal findings demonstrating the capacity of S1P and ceramide to differentially regulate cell growth and survival by modulation of opposing signaling pathways [1–3]. This was based on the discoveries that elevation of ceramide induces cell growth arrest and apoptosis [3], whereas S1P production is required for optimal cell proliferation induced by growth factors [4] and suppresses ceramide-mediated apoptosis [1]. Insight that the "sphingolipid rheostat" coordinately regulates the levels of these sphingolipid metabolites to control cell fate emerged from inhibition of SphK leading to decreased S1P and elevated ceramide, and subsequent cell death (Fig. 1). Thus, the sphingolipid rheostat appeared to be a sensing mechanism for cells to regulate their fate in part through the interconversion between S1P and ceramide.

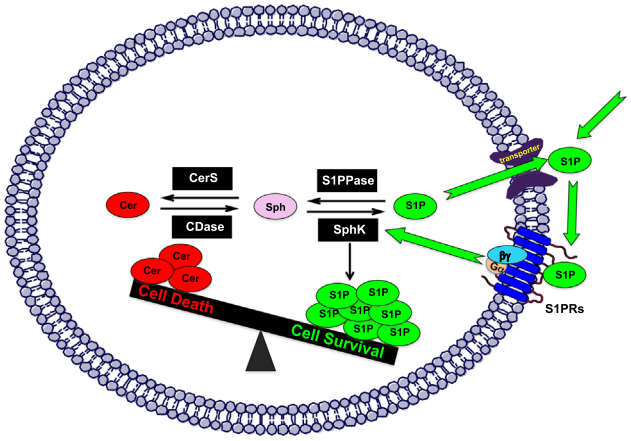


**Fig. 1 – The updated sphingolipid rheostat. This schematic cartoon shows important enzymes that regulate the levels of S1P and ceramide and includes "inside-out" signaling by the S1P/S1PR1 axis that can influence actions of the sphingolipid rheostat. CerS, ceramide synthase; CDase, ceramidase; S1PPase, S1P phosphatase; S1PRs, S1P receptors.**

In the years since, efforts have been made to elucidate the molecular mechanisms and signaling pathways by which these metabolites exert their effects, and to manipulate the S1P/ceramide balance to direct cells down particular paths for the development of therapeutics targeting the sphingolipid rheostat. In the process, these studies have revealed roles that S1P and ceramide play in the etiology of several debilitating human diseases, particularly cancer, and have clarified the enormous complexity of the interplay between S1P, ceramide, and sphingolipid metabolism, and how this affects complex cellular responses and biological programs. In light of these recent findings, we will revisit whether the S1P/ceramide rheostat concept adequately addresses the complex nature by which sphingolipids affect physiological processes and modulate cell fate, and, accordingly, their role in cancer.

## Role of sphingolipid metabolites in cell fate and cancer

### Ceramide

Ceramide is a tumor suppressor, promoting intrinsic and extrinsic apoptotic pathways, autophagic cell death, and the inhibition of cell growth, and thus it is not surprising that enzymes responsible for production of ceramide are often altered in cancer resulting in reduction of ceramide accumulation [5]. Moreover, many chemotherapeutic drugs elevate ceramide, and blocking the increase in ceramide provides drug resistance. While specific molecular species of ceramide have been implicated in some of these

pathways, it is unclear whether the specific species itself is required or is merely a reflection of its compartmental- or enzyme-specific generation. For example, it was shown that in glioblastoma tumors, a metabolic shift favoring S1P at the expense of C18 ceramide may be a major contributor to angiogenesis [6]. Although there are numerous pathways affected by ceramide, only a few direct targets have been convincingly identified. The key players in ceramide regulated signaling in cancer are activation of serine/threonine protein phosphatases, such as PP1, PP2A and PP2C, protein kinase Cζ (PKCζ) and inhibition of AKT (reviewed in Ref. [5]). Formation of ceramide-enriched membrane microdomains is a general mechanism by which ceramide can regulate numerous signaling pathways at the plasma membrane or in the outer mitochondrial membrane important for BAX insertion, oligomerization, pore formation and apoptosis.

### S1P and its receptors

Within two years of the development of the rheostat concept, the first cell surface G-protein coupled receptor for S1P was discovered [7], followed by the identification of the other members of the S1P receptor family, designated S1PR1–5 [8]. Moreover, intracellular S1P generated by activation of SphK can readily be secreted to act in an autocrine or paracrine manner [9], a paradigm that has been coined inside-out signaling by S1P (Fig. 1) [10]. Signaling through S1PR1–5 fits nicely into the rheostat hypothesis as activation of S1PRs has been shown to promote growth, survival, motility angiogenesis, lymphangiogenesis, and metastasis, important for the pro-cancer activities of S1P [11]. For example, several S1PRs activate the pro-survival ERK and Akt signaling pathways, and S1PR3 activation initiates a signaling cascade through the mTOR pathway that counteracts ceramide-mediated autophagy [12]. Moreover, recent studies have shown that the S1P/S1PR1 axis is at the nexus between NF-κB and STAT3 and connects chronic inflammation to colitis-associated cancer [13]. S1P produced by SphK1 is essential for production of the NF-κB-regulated pro-inflammatory cytokines TNF-α and IL-6, leading to activation of the transcription factor STAT3, and consequent upregulation of its target gene S1PR1 [14]. Reciprocally, S1PR1 maintains STAT3 activation in a malicious feed-forward amplification loop important for colon cancer, lymphoma and glioblastoma [14,15].

### S1P transporters

How does S1P, which is made by intracellular SphKs exit cells to activate S1PRs? There is now ample evidence that cells export intercellular S1P into the extracellular environment both through ABC transporters as well as the major facilitator superfamily member, Spinster 2 (Spns2) [10]. The S1P secreted from tumor cells through these transporters can act in an autocrine fashion to promote the growth and motility of the tumors themselves, but more importantly on the tumor microenvironment to enhance angiogenesis and lymphangiogenesis [16], as well as affecting tumor-associated macrophages [14], and may differentially recruit immune cells such as Tregs to block anti-tumor immunity [17].

### S1P intracellular targets

Though the majority of known S1P functions are attributable to its action through cell surface S1PRs, recently several intracellular targets of relevance to cancer have been found. The first of these is TRAF2, an essential component in the TNF- α/NF-κB signaling pathway. TRAF2 is an E3 ubiquitin ligase, and it was found that S1P bound to and stimulated its ubiquitin ligase activity [18]. In addition, SphK1 was shown to be required for the TNF-α-induced ubiquitination of RIP1 and subsequent activation of NF-κB, a pro-growth mediator. Interestingly, another group showed that SphKs were dispensable in bone marrow-derived macrophages for TNF-α-induced activation of NF-κB, though even in wild type macrophages TNF-α did not increase S1P levels, suggesting alternative mechanisms for the stimulation of TRAF2 activity [19]. S1P, produced by SphK2, was shown to bind to and inhibit histone deacetylases 1 and 2, leading to increases in histone acetylation [20]. Further support for this notion that HDACs are intracellular targets of S1P emerged from a recent study in *Drosophila*, which have no identified S1PRs, showing that increased nuclear S1P caused decreased HDAC activity and increased histone acetylation, and importantly suppressed dystrophic muscle degeneration [21]. Furthermore, the pro-drug FTY720 is also phosphorylated in the nucleus by SphK2 and FTY720-phosphate is a potent class I HDAC inhibitor [22], which might explain its potent anti-cancer effects.

## Targeting S1P metabolic enzymes to modulate the sphingolipid rheostat and cancer

Recently several excellent reviews discussed how targeting specific ceramide metabolic enzymes regulates the sphingolipid rheostat to amplify tumor suppressive activities of ceramide and consequently cell fate, and highlights the usefulness of ceramide-based therapeutics for treatment of cancer [5,23]. Therefore, we will mainly focus in this section on effects of targeting S1P metabolism.

### SphK1

In many cancers, elevated levels of SphK1 are an independent predictor of mortality, and strongly correlate with poor prognosis, reduced overall survival, and advanced tumor stages [11,24]. However, no mutations in SphKs have been identified, suggesting that it is the regulation of SphK activity, and hence a potential for S1P "cellular addiction", that is responsible for SphK1's "oncogenic" role [25]. There is some evidence to support this notion: 1) in cell culture, expression of SphK1 and S1P levels dictate resistance to cytotoxic drugs and radiation; 2) in animal models, overexpression of SphK1 and formation of S1P leads to aggressive tumors, and inhibition of SphK1 reverses drug resistance and enhances sensitivity to radiotherapy; 3) SphK1 is overexpressed in many types of cancer and high levels of SphK1 correlate with poor outcomes in patients. Because of these observations, multiple drugs targeting SphK1 have been designed. The "first generation" inhibitors such as N,N-dimethyl-sphingosine and SK1-II, with poor potency and selectivity between SphK isoforms, as well as SK1-I which specifically targets SphK1, though with low potency, showed promise in preclinical animal models. However

studies with the "second generation" of SphK1 inhibitors, such as PF-543, which are much more potent and are highly selective, have limited to no success in inducing apoptosis [26,27], even though in all cases S1P levels were reduced and in two of these studies ceramide levels were concomitantly elevated [6,28]. Why then, if the rheostat postulates that a reduction in S1P and rise in ceramide should increase cell death, are these SphK1 inhibitors ineffective? There are several potential explanations for this: first, reduction of SphK1 levels due to proteasomal degradation may be critical [29]. Second, inhibitors might affect SphK1 activity in different subcellular locations and only those that affect cellular S1P *vs*. sphingosine and ceramide more profoundly are effective compared to those that simply inhibit SphK1. Second generation inhibitors, with their much higher specificity and potency, do not have strong effects on changing the sphingolipid rheostat and only increase ceramide levels at an order of magnitude greater concentration than their $K_i$ values [28]. This further substantiates the notion that the sphingolipid rheostat is a critical component, not only reduction in the levels of S1P. Hence, in light of this, it might be appropriate to consider a more broad-spectrum approach to therapeutics to induce the apoptotic benefits that dictate chemotherapeutic efficiency. Third, as indicated by Abu-husain et al. [6], S1P produced by cancer cells may mainly act in a paracrine manner in the tumor microenvironment that is important for angiogenesis and lymphangiogenesis but does not affect tumor growth itself. It is important to note that all of the studies reported so far with second generation SphK1 inhibitors utilized cultured cancer cells, and therefore it will be important to examine their effects in animal cancer models. As more and more SphK1 drugs are developed with fewer off target effects, establishing how perturbations in S1P/sphingosine balance affects ceramide should become easier. These ventures should also be significantly aided with a variety of SphK1 structures that have been published [30], and with the recent development of a high-throughput assay to screen SphK inhibitors [31].

### SphK2

In contrast to SphK1, the actions of SphK2 remain poorly characterized and much less is known about its biology and roles in cancer and other diseases. However, SphK2 is critical to the function of one of the few FDA approved sphingosine analog drugs, FTY-720, as it phosphorylates it to the "active" form that acts on S1PRs (except S1PR2) [32] and inhibits histone deacetylases [22]. The difficulty in targeting SphK2 in rheostat modulation therapies is that its roles in regulating sphingolipid metabolism are not well understood. SphK2 is present in several subcellular compartments, and there are conflicting data regarding its role in cancer development. Moreover, inhibitors targeting its activity have not been as successfully developed as those for SphK1. Compound ABC294640 (SphK2 $K_i = 9.8\ \mu M$) has shown promise in reducing cancer cell growth *in vitro* and in mouse models of cancer [33,34]. However, this compound has also been linked to potential off target anti-estrogenic effects [35]. In another example, SLR080811 (SphK2 $K_i = 1.3\ \mu M$) showed a reduction of the levels of S1P in cells, though it had no anti-proliferative properties, and when administered to mice, raised blood S1P levels [36], confounding evaluation of its effectiveness as a chemotherapeutic in mice cancer models. Clearly, targeting SphK2 in the treatment of disease is still in its infancy and will require significant efforts to substantially increase the potency and specificity of inhibitors. Unfortunately, unlike SphK1, little is also known of the structure of SphK2 and pharmacophore design for SphK2 is complicated by the necessity to cross secondary subcellular membrane barriers to reach the target.

### S1P lyase and S1P phosphatases

As the terminal step in irreversible catabolism of all sphingolipids, SPL controls levels of S1P and other bioactive sphingolipid metabolites, and is also the link between sphingolipid and phospholipid metabolism. Indeed, deletion of SPL not only increases S1P levels but also sphingosine and ceramide, probably due to reutilization of the sphingosine backbone for ceramide synthesis. Not surprisingly, knockout mice have severely altered lipid homeostasis, aberrant S1P signaling, and inflammatory responses leading to early death [37,38]. SPL levels are downregulated in various human cancers and inversely correlated to clinical outcomes and resistance to treatment, further supporting a role for S1P in cancer development. Several novel findings leading to mechanistic actions of SPL in tumorigenesis and chemoresistance have recently been described. Deletion of intestinal SPL promoted colon carcinogenesis through the S1P/S1PR1 axis and activation of STAT3. STAT3 in turn enhanced expression of specific miRs that target the anti-oncogenes PTEN (a lipid phosphatase that negatively regulates the PI3K/AKT pathway) and cylindromatosis (CYLD; a deubiquitinating enzyme that negatively regulates NF-κB) [39]. Interestingly, upregulation of SPL levels by consumption of sphingadienes, plant-type sphingolipids that cannot be converted to S1P, was able to enhance the metabolism of S1P attenuating STAT3 signaling, cytokine production, and tumorigenesis [39]. SPL deficiency or its inhibition has also been associated with elevated nuclear S1P levels and reduced HDAC activity that in turn induced dysregulation of $Ca^{2+}$ homeostasis [40], and upregulation of several S1P transporters, including multi-drug resistant proteins, contributing to chemoresistance [41].

In addition to SPL, S1P levels are also reversibly regulated by two S1P phosphatases (SGPP1 and SGPP2) that dephosphorylate S1P to sphingosine that can then be used for ceramide formation. This places S1P levels under dual control, with one pathway removing sphingolipids from the signaling pool and the other shifting the rheostat balance from the proliferative effects of S1P to the pro-apoptotic effects of sphingosine and ceramide accumulation. Similar to SPL, there is evidence that S1P phosphatase expression is downregulated in several types of cancer. Closer examinations of these studies reveals that increased S1P content in the tumors was correlated with decreased SGPP2 expression and increased SphK1, supporting the notion of coordinated regulation of sphingolipid metabolism [6].

## Modified rheostat paradigm: addition of the S1P/S1PR axis

The field of cancer research has embraced the concept of the sphingolipid rheostat. As more and more studies involving ceramide and S1P signaling attempt to use the rheostat model to explain their findings, and as the signaling mechanisms by which these sphingolipid metabolites exert their control on cell fate becomes more complex, and additional proteins that regulate sphingolipid metabolism are discovered, the need for a more

nuanced model has become apparent. For example, although initially elevation of ceramide was linked to cell growth inhibition and reduction of tumor growth, more recent studies suggest that ceramides with different fatty acid chain lengths might play distinct functions. *De novo*-generated C18- and C16-ceramides by CerS1 and CerS6 play opposing proapoptotic and prosurvival roles in the regulation of tumor growth, respectively [42]. Whether a specific acyl chain species is required for apoptosis, for example by N-acyl chain-specific binding to effector proteins, or whether the N-acyl chain species generated is merely a reflection of the enzyme- and/or compartment-specific generation of ceramide, has yet to be elucidated.

The molecular roles of S1P in the rheostat have become more complex. It is generally accepted that S1P is a pro-survival factor and many studies have demonstrated that S1P acts through cell surface S1PRs through "inside-out" signaling to promote cancer growth, progression and metastasis [43]. S1P does this through the autocrine promotion of tumor growth and importantly, in a paracrine manner by enhancing angiogenesis, lymphangiogenesis, recruitment of pro-tumor immune cells, and affecting the tumor microenvironment. This suggests that the "sphingolipid rheostat" concept should be modified to include this "inside-out" signaling (Fig. 1). Furthermore, a recent study showed that S1P can also act in a feed-forward, "outside-in" signaling in a paracrine fashion. Namely, S1P acting through S1PRs has been shown to stimulate SphK1 transcription *via* the transcription factor AP-1, which is composed of c-Fos and c-Jun [44]. This positive feedback loop maintains sustained activation of the SphK1-S1P axis and increased fibronectin expression leading to initiation and progression of diabetic nephropathy [44], and could also contribute to the pathogenesis of other diseases including cancer. Moreover, activation of Gq induced plasma membrane translocation of SphK1 and cross-activation of S1PRs [45]. Hence, increased SphK1 activity and increases in S1PR synthesis or their activations, completes this positive feedback amplification loop.

These more recent studies suggest that the enzymes of the rheostat do not just function by directly changing the fate of the sphingoid base (*i.e.* ceramide *vs.* S1P) as initially conceived in the rheostat model, but also by the roles these metabolites have in myriad, often opposing, signaling pathways. While the initial rheostat model was based on the relative intracellular levels of ceramide and S1P determining signaling and cell fate, we now know that the localized production, secretion, and signaling of these metabolites have a profound effect on tumor outcomes. Our new, more nuanced understanding of the sphingolipid rheostat must be taken into consideration as we design, test, and implement new chemotherapeutics targeting this axis for cancer treatment. More work is needed to understand alterations that occur in the complex sphingolipid pathways during cancer development and progression, and their relationship to the Warburg effect and the metabolic shift from oxidative phosphorylation to the synthesis of lipids and biomass essential for increased cellular proliferation [46].

## Acknowledgements

This work was supported by U.S. NIH Grants R01 GM043880 and R01 CA61774 (S.S.), 5T32 HL094290 (J.N.), and 1K22 CA187314 (S. L.) and U.S. Department of Defense W81XWH-14-1-0086 (S.S.)

## REFERENCES

[1] O. Cuvillier, G. Pirianov, B. Kleuser, P.G. Vanek, O.A. Coso, S. Gutkind, S. Spiegel, Suppression of ceramide-mediated programmed cell death by sphingosine-1-phosphate, Nature 381 (1996) 800–803.
[2] H. Zhang, N.N. Desai, A. Olivera, T. Seki, G. Brooker, S. Spiegel, Sphingosine-1-phosphate, a novel lipid, involved in cellular proliferation, J. Cell Biol. 114 (1991) 155–167.
[3] L.M. Obeid, C.M. Lindaric, L.A. Karolak, Y.A. Hannun, Programmed cell death induced by ceramide, Science 259 (1993) 1769–1771.
[4] A. Olivera, S. Spiegel, Sphingosine-1-phosphate as a second messenger in cell proliferation induced by PDGF and FCS mitogens, Nature 365 (1993) 557–560.
[5] S.A. Morad, M.C. Cabot, Ceramide-orchestrated signalling in cancer cells, Nat. Rev. Cancer 13 (2013) 51–65.
[6] H.J. Abuhusain, A. Matin, Q. Qiao, H. Shen, N. Kain, B.W. Day, B.W. Stringer, B. Daniels, M.A. Laaksonen, C. Teo, K.L. McDonald, A.S. Don, A metabolic shift favoring sphingosine 1-phosphate at the expense of ceramide controls glioblastoma angiogenesis, J. Biol. Chem. 288 (2013) 37355–37364.
[7] M.J. Lee, J.R. Van Brocklyn, S. Thangada, C.H. Liu, A.R. Hand, R. Menzeleev, S. Spiegel, T. Hla, Sphingosine-1-phosphate as a ligand for the G protein-coupled receptor EDG-1, Science 279 (1998) 1552–1555.
[8] H. Rosen, R.C. Stevens, M. Hanson, E. Roberts, M.B. Oldstone, Sphingosine-1-phosphate and its receptors: structure, signaling, and influence, Annu. Rev. Biochem. 82 (2013) 637–662.
[9] J.P. Hobson, H.M. Rosenfeldt, L.S. Barak, A. Olivera, S. Poulton, M. G. Caron, S. Milstien, S. Spiegel, Role of the sphingosine-1-phosphate receptor EDG-1 in PDGF-induced cell motility, Science 291 (2001) 1800–1803.
[10] K. Takabe, S. Spiegel, Export of sphingosine-1-phosphate and cancer progression, J. Lipid Res. 55 (2014) 1839–1846.
[11] N.J. Pyne, S. Pyne, Sphingosine 1-phosphate and cancer, Nat. Rev. Cancer 10 (2010) 489–503.
[12] M. Taniguchi, K. Kitatani, T. Kondo, M. Hashimoto-Nishimura, S. Asano, A. Hayashi, S. Mitsutake, Y. Igarashi, H. Umehara, H. Takeya, J. Kigawa, T. Okazaki, Regulation of autophagy and its associated cell death by "sphingolipid rheostat": reciprocal role of ceramide and sphingosine 1-phosphate in the mammalian target of rapamycin pathway, J. Biol. Chem. 287 (2012) 39898–39910.
[13] J. Liang, M. Nagahashi, E.Y. Kim, K.B. Harikumar, A. Yamada, W.C. Huang, N.C. Hait, J.C. Allegood, M.M. Price, D. Avni, K. Takabe, T. Kordula, S. Milstien, S. Spiegel, Sphingosine-1-phosphate links persistent STAT3 activation, chronic intestinal inflammation, and development of colitis-associated cancer, Cancer Cell 23 (2013) 107–120.
[14] J. Deng, Y. Liu, H. Lee, A. Herrmann, W. Zhang, C. Zhang, S. Shen, S.J. Priceman, M. Kujawski, S.K. Pal, A. Raubitschek, D.S. Hoon, S. Forman, R.A. Figlin, J. Liu, R. Jove, H. Yu, S1PR1-STAT3 signaling is crucial for myeloid cell colonization at future metastatic sites, Cancer Cell 21 (2012) 642–654.
[15] Y. Liu, J. Deng, L. Wang, H. Lee, B. Armstrong, A. Scuto, C. Kowolik, L.M. Weiss, S. Forman, H. Yu, S1PR1 is an effective target to block STAT3 signaling in activated B cell-like diffuse large B-cell lymphoma, Blood 120 (2012) 1458–1465.
[16] M. Nagahashi, S. Ramachandran, E.Y. Kim, J.C. Allegood, O.M. Rashid, A. Yamada, R. Zhao, S. Milstien, H. Zhou, S. Spiegel, K. Takabe, Sphingosine-1-phosphate produced by sphingosine kinase 1 promotes breast cancer progression by stimulating angiogenesis and lymphangiogenesis, Cancer Res. 72 (2012) 726–735.
[17] S.J. Priceman, S. Shen, L. Wang, J. Deng, C. Yue, M. Kujawski, H. Yu, S1PR1 is crucial for accumulation of regulatory T cells in tumors via STAT3, Cell Rep. 6 (2014) 992–999.

[18] S.E. Alvarez, K.B. Harikumar, N.C. Hait, J. Allegood, G.M. Strub, E.Y. Kim, M. Maceyka, H. Jiang, C. Luo, T. Kordula, S. Milstien, S. Spiegel, Sphingosine-1-phosphate is a missing cofactor for the E3 ubiquitin ligase TRAF2, Nature 465 (2010) 1084–1088.
[19] Y. Xiong, H.J. Lee, B. Mariko, Y.C. Lu, A.J. Dannenberg, A.S. Haka, F.R. Maxfield, E. Camerer, R.L. Proia, T. Hla, Sphingosine kinases are not required for inflammatory responses in macrophages, J. Biol. Chem. 288 (2013) 32563–32573.
[20] N.C. Hait, J. Allegood, M. Maceyka, G.M. Strub, K.B. Harikumar, S.K. Singh, C. Luo, R. Marmorstein, T. Kordula, S. Milstien, S. Spiegel, Regulation of histone acetylation in the nucleus by sphingosine-1-phosphate, Science 325 (2009) 1254–1257.
[21] D.H. Nguyen-Tran, N.C. Hait, H. Sperber, J. Qi, K. Fischer, N. Ieronimakis, M. Pantoja, A. Hays, J. Allegood, M. Reyes, S. Spiegel, H. Ruohola-Baker, Molecular mechanism of sphingosine-1-phosphate action in Duchenne muscular dystrophy, Dis. Model Mech. 7 (2014) 41–54.
[22] N.C. Hait, L.E. Wise, J.C. Allegood, M. O'Brien, D. Avni, T.M. Reeves, P.E. Knapp, J. Lu, C. Luo, M.F. Miles, S. Milstien, A.H. Lichtman, S. Spiegel, Active, phosphorylated fingolimod inhibits histone deacetylases and facilitates fear extinction memory, Nat. Neurosci. 17 (2014) 971–980.
[23] J.P. Truman, M. Garcia-Barros, L.M. Obeid, Y.A. Hannun, Evolving concepts in cancer therapy through targeting sphingolipid metabolism, Biochim. Biophys. Acta 1841 (2014) 1174–1188.
[24] G.T. Kunkel, M. Maceyka, S. Milstien, S. Spiegel, Targeting the sphingosine-1-phosphate axis in cancer, inflammation and beyond, Nat. Rev. Drug Discov. 12 (2013) 688–702.
[25] M. Vadas, P. Xia, G. McCaughan, J. Gamble, The role of sphingosine kinase 1 in cancer: oncogene or non-oncogene addiction?, Biochim. Biophys. Acta 1781 (2008) 442–447.
[26] K. Rex, S. Jeffries, M.L. Brown, T. Carlson, A. Coxon, F. Fajardo, B. Frank, D. Gustin, A. Kamb, P.D. Kassner, S. Li, Y. Li, K. Morgenstern, M. Plant, K. Quon, A. Ruefli-Brasse, J. Schmidt, E. Swearingen, N. Walker, Z. Wang, J.E. Watson, D. Wickramasinghe, M. Wong, G. Xu, H. Wesche, Sphingosine kinase activity is not required for tumor cell viability, PLoS One 8 (2013) e68328.
[27] M.E. Schnute, M.D. McReynolds, T. Kasten, M. Yates, G. Jerome, J. W. Rains, T. Hall, J. Chrencik, M. Kraus, C.N. Cronin, M. Saabye, M. K. Highkin, R. Broadus, S. Ogawa, K. Cukyne, L.E. Zawadzke, V. Peterkin, K. Iyanar, J.A. Scholten, J. Wendling, H. Fujiwara, O. Nemirovskiy, A.J. Wittwer, M.M. Nagiec, Modulation of cellular S1P levels with a novel, potent and specific inhibitor of sphingosine kinase-1, Biochem. J. 444 (2012) 79–88.
[28] Y. Kharel, T.P. Mathews, A.M. Gellett, J.L. Tomsig, P.C. Kennedy, M. L. Moyer, T.L. Macdonald, K.R. Lynch, Sphingosine kinase type 1 inhibition reveals rapid turnover of circulating sphingosine 1-phosphate, Biochem. J. 440 (2011) 345–353.
[29] C. Loveridge, F. Tonelli, T. Leclercq, K.G. Lim, J.S. Long, E. Berdyshev, R.J. Tate, V. Natarajan, S.M. Pitson, N.J. Pyne, S. Pyne, The sphingosine kinase 1 inhibitor 2-(p-hydroxyanilino)-4-(p-chlorophenyl)thiazole induces proteasomal degradation of sphingosine kinase 1 in mammalian cells, J. Biol. Chem. 285 (2010) 38841–38852.
[30] Z. Wang, X. Min, S.H. Xiao, S. Johnstone, W. Romanow, D. Meininger, H. Xu, J. Liu, J. Dai, S. An, S. Thibault, N. Walker, Molecular basis of sphingosine kinase 1 substrate recognition and catalysis, Structure 21 (2013) 798–809.
[31] S. Lima, S. Milstien, S. Spiegel, A real-time high-throughput fluorescence assay for sphingosine kinases, J. Lipid Res. 55 (2014) 1525–1530.
[32] S. Mandala, R. Hajdu, J. Bergstrom, E. Quackenbush, J. Xie, J. Milligan, R. Thornton, G.J. Shei, D. Card, C. Keohane, M. Rosenbach, J. Hale, C.L. Lynch, K. Rupprecht, W. Parsons, H. Rosen, Alteration of lymphocyte trafficking by sphingosine-1-phosphate receptor agonists, Science 296 (2002) 346–349.
[33] K.J. French, Y. Zhuang, L.W. Maines, P. Gao, W. Wang, V. Beljanski, J.J. Upson, C.L. Green, S.N. Keller, C.D. Smith, Pharmacology and antitumor activity of ABC294640, a selective inhibitor of sphingosine kinase-2, J. Pharmacol. Exp. Ther. 333 (2010) 129–139.
[34] J.K. Venkata, N. An, R. Stuart, L.J. Costa, H. Cai, W. Coker, J.H. Song, K. Gibbs, T. Matson, E. Garrett-Mayer, Z. Wan, B. Ogretmen, C. Smith, Y. Kang, Inhibition of sphingosine kinase 2 downregulates the expression of c-Myc and Mcl-1 and induces apoptosis in multiple myeloma, Blood 124 (2014) 1915–1925.
[35] J.W. Antoon, M.D. White, W.D. Meacham, E.M. Slaughter, S.E. Muir, S. Elliott, L.V. Rhodes, H.B. Ashe, T.E. Wiese, C.D. Smith, M.E. Burow, B.S. Beckman, Antiestrogenic effects of the novel sphingosine kinase-2 inhibitor ABC294640, Endocrinology 151 (2010) 5124–5135.
[36] Y. Kharel, M. Raje, M. Gao, A.M. Gellett, J.L. Tomsig, K.R. Lynch, W.L. Santos, Sphingosine kinase type 2 inhibition elevates circulating sphingosine 1-phosphate, Biochem. J. 447 (2012) 149–157.
[37] M. Bektas, M.L. Allende, B.G. Lee, W. Chen, M.J. Amar, A.T. Remaley, J.D. Saba, R.L. Proia, Sphingosine 1-phosphate lyase deficiency disrupts lipid homeostasis in liver, J. Biol. Chem. 285 (2010) 10880–10889.
[38] A. Aguilar, J.D. Saba, Truth and consequences of sphingosine-1-phosphate lyase, Adv. Biol. Regul. 52 (2012) 17–30.
[39] E. Degagne, A. Pandurangan, P. Bandhuvula, A. Kumar, A. Eltanawy, M. Zhang, Y. Yoshinaga, M. Nefedov, P.J. de Jong, L.G. Fong, S.G. Young, R. Bittman, Y. Ahmedi, J.D. Saba, Sphingosine-1-phosphate lyase downregulation promotes colon carcinogenesis through STAT3-activated microRNAs, J. Clin. Investig. 124 (2014) 536853–536884.
[40] K. Ihlefeld, R.F. Claas, A. Koch, J.M. Pfeilschifter, D. Meyer Zu Heringdorf, Evidence for a link between histone deacetylation and Ca(2)+ homoeostasis in sphingosine-1-phosphate lyase-deficient fibroblasts, Biochem. J. 447 (2012) 457–464.
[41] K. Ihlefeld, H. Vienken, R.F. Claas, K. Blankenbach, A. Rudowski, M. Ter Braak, A. Koch, P.P. Van Veldhoven, J. Pfeilschifter, D. Meyer Zu Heringdorf, Upregulation of ABC transporters contributes to chemoresistance of sphingosine 1-phosphate lyase-deficient fibroblasts, J. Lipid Res. 56 (2015) 60–69.
[42] C.E. Senkal, S. Ponnusamy, J. Bielawski, Y.A. Hannun, B. Ogretmen, Antiapoptotic roles of ceramide-synthase-6-generated C16-ceramide via selective regulation of the ATF6/CHOP arm of ER-stress-response pathways, FASEB J. 24 (2010) 296–308.
[43] S. Milstien, S. Spiegel, Targeting sphingosine-1-phosphate: a novel avenue for cancer therapeutics, Cancer Cell 9 (2006) 148–150.
[44] K. Huang, J. Huang, C. Chen, J. Hao, S. Wang, P. Liu, H. Huang, AP-1 regulates sphingosine kinase 1 expression in a positive feedback manner in glomerular mesangial cells exposed to high glucose, Cell Signal. 26 (2014) 629–638.
[45] M. ter Braak, K. Danneberg, K. Lichte, K. Liphardt, N.T. Ktistakis, S.M. Pitson, T. Hla, K.H. Jakobs, D. Meyer zu Heringdorf, Galpha (q)-mediated plasma membrane translocation of sphingosine kinase-1 and cross-activation of S1P receptors, Biochim. Biophys. Acta 1791 (2009) 357–370.
[46] M.G. Vander Heiden, L.C. Cantley, C.B. Thompson, Understanding the Warburg effect: the metabolic requirements of cell proliferation, Science 324 (2009) 1029–1033.

Heliyon

*Received:*
9 December 2016
*Accepted:*
19 December 2016

Cite as: Masayuki Nagahashi, Akimitsu Yamada, Tomoyoshi Aoyagi, Jeremy Allegood, Toshifumi Wakai, Sarah Spiegel, Kazuaki Takabe . Sphingosine-1-phosphate in the lymphatic fluid determined by novel methods. Heliyon 3 (2017) e00219. doi: 10.1016/j.heliyon.2016.e00219

# Sphingosine-1-phosphate in the lymphatic fluid determined by novel methods

**Masayuki Nagahashi [a,*], Akimitsu Yamada [b], Tomoyoshi Aoyagi [b], Jeremy Allegood [c], Toshifumi Wakai [a], Sarah Spiegel [c], Kazuaki Takabe [d,e,**]**

[a] *Division of Digestive and General Surgery, Niigata University Graduate School of Medical and Dental Sciences, Niigata City, 951-8510, Japan*

[b] *Division of Surgical Oncology, Department of Biochemistry and Molecular Biology, and the Massey Cancer Center, Virginia Commonwealth University School of Medicine, Richmond, Virginia 23298-0011, USA*

[c] *Department of Biochemistry and Molecular Biology, and the Massey Cancer Center, Virginia Commonwealth University School of Medicine, Richmond, Virginia 23298-0011, USA*

[d] *Breast Surgery, Department of Surgical Oncology, Roswell Park Cancer Institute, Buffalo, NY 14263, USA*

[e] *Department of Surgery, University at Buffalo, The State University of New York, Jacobs School of Medicine and Biomedical Sciences, New York*

* Corresponding author at: Division of Digestive and General Surgery, Niigata University Graduate School of Medical and Dental Sciences, 1-757 Asahimachi-dori, Chuo-ku, Niigata City, 951-8510, Japan.

** Corresponding author at: Breast Surgery, Department of Surgical Oncology, Roswell Park Cancer Institute, Elm & Carlton Streets, Buffalo, NY 14263, USA.

E-mail addresses: mnagahashi@med.niigata-u.ac.jp (M. Nagahashi), kazuaki.takabe@roswellpark.org (K. Takabe).

## Abstract

**Background:** Sphingosine-1-phosphate (S1P) is a pleiotropic bioactive lipid mediator that regulates many physiological and pathological processes. It has been suggested that S1P gradient with high concentrations in the blood and lymphatic fluid and low concentrations in the peripheral tissue plays important roles in immune cell trafficking and potentially cancer progression. However, only a few reports have assessed S1P levels in the lymphatic fluid due to lack of an established easy-to-use method. Here, we report a simple technique for collection of lymphatic fluid to determine S1P.

**Materials and methods:** Lymphatic fluid was collected directly with a catheter needle (classical method) or was absorbed onto filter paper after incision of cisterna chyli (new method) in murine models. Blood, lymphatic fluid and

http://dx.doi.org/10.1016/j.heliyon.2016.e00219

mesenteric lymph nodes were corrected from wild type and sphingosine kinase 2 (SphK2) knockout mice to determine S1P levels by mass spectrometry.

**Results:** The volume of lymphatic fluid collected by the new method was at least three times greater than those collected by the classical method. S1P concentrations in lymphatic fluid are lower than in blood and higher than in lymph nodes. Interestingly, S1P levels in lymphatic fluid from SphK2 knockout mice were significantly higher than those in wild type, suggesting an important role of SphK2 and/or SphK1 to regulate S1P levels in lymphatic fluid.

**Conclusions:** In agreement with the previous theory, our results confirm "S1P gradient" among blood, lymphatic fluid and peripheral lymphatic tissues. Convenient methods for collection and measurement of sphingolipids in lymphatic fluid are expected to provide new insights on functions of sphingolipids.

Keywords: Surgery, Biochemistry, Cell biology, Immunology, Oncology, Cancer research

## 1. Introduction

Sphingosine-1-phosphate (S1P) is a pleiotropic bioactive lipid mediator that regulates many physiological and pathological processes including immune cell trafficking, inflammation, angio-/lymphangiogenesis, and cancer progression [1, 2, 3, 4, 5, 6]. We have recently reported that S1P is strongly associated with lymphatic network development [7, 8] and lymphatic metastasis in cancer patients [9, 10, 11]. Further, we have shown that S1P links inflammation and cancer in colitis-associated colon cancer [12, 13]. These many pathological processes are regulated by S1P that is secreted from cells to the extracellular spaces and exerts its functions by binding to five specific G protein–coupled receptors (S1PR1-5) in autocrine and paracrine manners, a process known as "inside-out" signaling [1, 14, 15].

S1P is generated by two sphingosine kinases (SphK1 and SphK2) inside cells, and secreted out of the cell to the extracellular spaces, such as interstitial fluid (IF) and lymphatic fluid [16]. Among the extracellular S1P, the S1P levels in the blood and lymphatic fluid are considered to be high, and those in tissue interstitial fluid are much lower [16]. Previous evidence suggested that the S1P gradient of high S1P concentrations in the circulation (blood and lymphatic fluid) plays an important role in immune cell trafficking [7, 17, 18, 19, 20] and potentially cancer progression. Lymphocytes egress from the secondary lymphatic organs to the blood or lymphatic circulation through S1P-mediated activation of S1PR1 on the cell surface [21, 22]. SphK activity in lymphatic endothelial cells is required for lymphocyte egress from secondary lymphatic organs, and lymphatic endothelial cells have been considered to be a major source of S1P in lymphatic fluid [23, 24].


http://dx.doi.org/10.1016/j.heliyon.2016.e00219

Although S1P levels in blood have been published to be associated with lymphatic metastasis by our group and others [9, 16], only a few reports have assessed its levels due to lack of an established easy-to-use method. Considering the importance of S1P in lymphatic fluid for immune cell trafficking and cancer progression, establishing the easier method to measure it will help researchers to understand disease processes and move the research field forward. Here, we report a simple technique for collection of lymphatic fluid to determine sphingolipids including S1P by high sensitivity liquid chromatography-electrospray ionization tandem mass spectrometry (LC-ESI-MS/MS).

## 2. Material and methods

### 2.1. Reagents

Internal standards were purchased from Avanti Polar Lipids (Alabaster, AL) and added to samples in 20 μl ethanol:methanol:water (7:2:1) as a cocktail of 500 pmol each. The HPLC grade solvents were obtained from VWR (West Chester, PA).

### 2.2. Animals

All animal studies were conducted in the Animal Research Core Facility at VCU School of Medicine in accordance with institutional guidelines. We utilized SphK2 knockout mice as models since they are well characterized, and because we have previously found that SphK2 knockout mice demonstrate compensatory higher expression of SphK1 in the tissues [12]. These knockout mice were kindly given by Dr. Richard L. Proia of National Institute of Diabetes and Digestive and Kidney Diseases [25, 26]. Female C57BL/6 and SphK2 knockout mice and their corresponding wild type (WT) litter mates were used.

### 2.3. Collection of lymphatic fluid from the cisterna chyli

To increase the lymphatic flow in the abdomen, 200 μl of mineral oil was administered by gavage to mice 2 h prior to euthanasia. At that time, the abdomen was opened under anesthesia. Lymphatic flow was confirmed by the white lucent color in the intestinal trunk and the cisterna chyli under stereomicroscopy (Fig. 1). The intestinal trunk is formed by the confluence of the efferent vessels of the cranial mesenteric and celiac nodes, and the single trunk enters into the cisterna chyli located along the abdominal vena cava and aorta on the cranial side of the renal veins [27]. The cisterna chyli was cut with the bevel of a fine needle, and the lymphatic fluid was absorbed with a piece of pre-weighed absorbance paper with a fine and rigid point. The absorbance paper was handled with extreme care in order to avoid contamination from any other intra-peritoneal fluid. This procedure was performed by experienced surgeons, surgical residents, or laboratory technicians.


http://dx.doi.org/10.1016/j.heliyon.2016.e00219

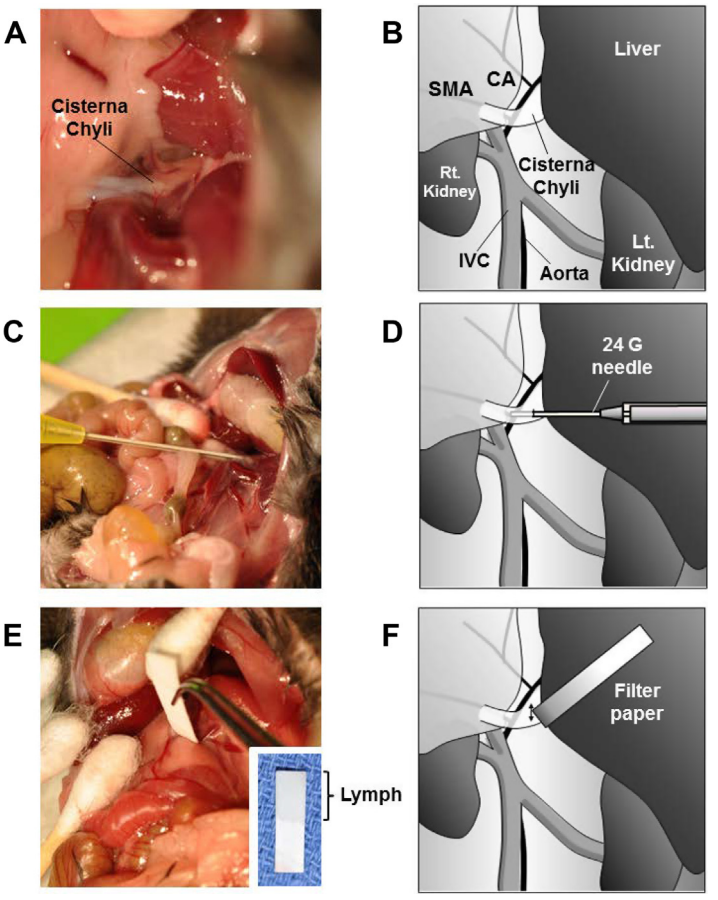


**Fig. 1.** Collection of lymphatic fluid from a mouse. (A) Lymphatic fluid was observed as fluid with white lucent color in the intestinal trunk and the cisterna chyli. (B) Schematic illustration of lymph collection from a mouse. (C and D) Lymphatic fluid was collected directly with a 24 G catheter needle. (E and F) Lymphatic fluid was absorbed onto filter paper after incision of cisterna chyli by needle. CA, celiac artery; SMA, superior mesenteric artery; IVC, inferior vena cava.

The volume of the collected fluid was measured by weight and sphingolipids were analyzed by LC-ESI-MS/MS.

## 2.4. Preparation of blood samples

Whole blood was collected from inferior vena cava (IVC), and 40 μl immediately transferred into 500 μl of methanol in a glass tube for measurement of sphingolipids. The remaining collected blood from the IVC was left undisturbed at room temperature, allowing the blood components to coagulate. Serum was then collected by centrifuging at 2,600 x g for 10 min in a refrigerated centrifuge.


http://dx.doi.org/10.1016/j.heliyon.2016.e00219

## 2.5. Extraction of lipids

Fluid absorbed onto filter paper was placed in 13 × 100 mm borosilicate tubes with a Teflon-lined cap (VWR, West Chester, PA). Methanol (1 ml) and chloroform (0.5 ml) were added along with the internal standard cocktail. The contents were dispersed by sonication at room temperature for 30 s and incubated at 48 °C overnight. KOH (1 M) in methanol (75 μl) was added and, after brief sonication, samples were incubated in a shaking water bath for 2 h at 37 °C to hydrolyze glycerophospholipids. The extract was brought to neutral pH with 6 μl of glacial acetic acid, centrifuged using a table-top centrifuge, and the supernatant was removed and dried in a Speed Vac. The dried residue was reconstituted in 0.5 ml of the starting mobile phase solvent, briefly sonicated and then centrifuged for 5 min in a tabletop centrifuge before transfer of the clear supernatant to the autoinjector vials.

## 2.6. LC-ESI-MS/MS of sphingoid bases, sphingoid base 1-phosphates, and complex sphingolipids

For LC-ESI-MS/MS analyses, a Shimadzu LC-20 AD binary pump system coupled to a SIL-20AC autoinjector and DGU20A3 degasser coupled to an ABI 4000 quadrupole/linear ion trap (QTrap) (Applied Biosystems, Foster City, CA) operating in a triple quadrupole mode was used. Q1 and Q3 were set to pass molecularly distinctive precursor and product ions (or a scan across multiple m/z in Q1 or Q3), using N2 to collisionally induce dissociations in Q2 (which was offset from Q1 by 30–120 eV).

Sphingolipids were separated by reverse phase LC using a Supelco 2.1(i.d.)x50 mm Ascentis C18 column (Sigma, St. Louis, MO) and a binary solvent system at a flow rate of 0.5 ml/min. Prior to injections, the column was equilibrated for 0.5 min with a solvent mixture of 95% mobile phase A1 ($CH_3OH/H_2O$/HCOOH, 58/41/1, v/v/v, with 5 mM ammonium formate) and 5% mobile phase B1 ($CH_3OH$/HCOOH, 99/1, v/v, with 5 mM ammonium formate), and after sample injection (typically 40 μl), the A1/B1 ratio was maintained at 95/5 for 2.25 min, followed by a linear gradient to 100% B1 over 1.5 min, which was held at 100% B1 for 5.5 min, followed by a 0.5 min gradient return to 95/5 A1/B1. The column was re-equilibrated with 95:5 A1/B1 for 0.5 min before the next run.

## 2.7. Statistical analysis

Results were analyzed for statistical significance with a two-tailed Student's t-test, with $P < 0.05$ considered significant. Experiments were repeated at least three times. *In vivo* experiments were repeated three times and each experimental group consisted of at least four mice. Data presented is from one of three representative experiments.


http://dx.doi.org/10.1016/j.heliyon.2016.e00219

## 3. Results

### 3.1. Improved method of lymphatic fluid collection from cisterna chyli

It has been suggested that S1P gradient with high concentrations in the blood and lymphatic fluid and low concentrations in the peripheral tissue plays important roles in immune cell trafficking and potentially cancer progression. However, only a few reports have assessed S1P levels in the lymphatic fluid due to lack of an established easy-to-use method. The classical method for collection of lymphatic fluid require lengthy duration of cannulations. Therefore, we sought to develop a simple method that does not require special equipment and settings. To this end, we compared collection of lymphatic fluid from the cisterna chyli by direct aspiration using a 24-gauge needle (classical method) with a filter paper absorption method after opening the cisterna chyli by incision with the bevel of a needle after adequate exposure of the lymphatic vessel (new method) (Fig. 1). The paper that absorbed lymphatic fluid was colorless indicating that there was little or no contamination with blood (Fig. 1E).

S1P levels were measured by mass spectrometry in the lymphatic fluid collected either by direct aspiration or by paper absorption (Fig. 2A). The volume of the lymphatic fluid collected by the paper absorption method was at least three times greater than that collected by direct aspiration (Fig. 2B). S1P and dihydro-S1P (DHS1P) levels in lymphatic fluid from both paper absorption and direct aspiration methods showed consistent results with minimal variation (Fig. 2C and D). In mice, S1P concentrations in lymphatic fluid were in the range of 0.1 to 0.3 μM (Fig. 2C), compared to more than 0.5 μM in plasma. The level of dihydro-S1P (DHS1P), which is generated by the de novo pathway and is also a ligand for all of the S1P receptors, was about 0.05 μM in lymphatic fluid and almost 0.2 μM in plasma (Fig. 1D). It is important to note that levels of S1P in lymphatic fluid collected by the filter paper method are in excellent agreement with previous reports on lymphatic fluid collected by the cannulation method [23, 28].

### 3.2. S1P gradient between blood, lymphatic fluid, and mesenteric lymph node (MLN)

Next, we tested the theory of S1P gradient among serum, lymphatic fluid, and peripheral tissue such as MLN utilizing our new method to measure S1P in the lymphatic fluid. Levels of Sph, DHSph, S1P, and DHS1P in whole blood, serum, lymph, and MLN from WT mice were determined by LC-ESI-MS/MS (Fig. 3). S1P and DHS1P levels in the lymphatic fluid are significantly lower than those in serum. On the other hand, S1P and DHS1P levels in lymphatic fluid are significantly higher than those in MLN. Of note, both Sph and DHSph levels in


http://dx.doi.org/10.1016/j.heliyon.2016.e00219

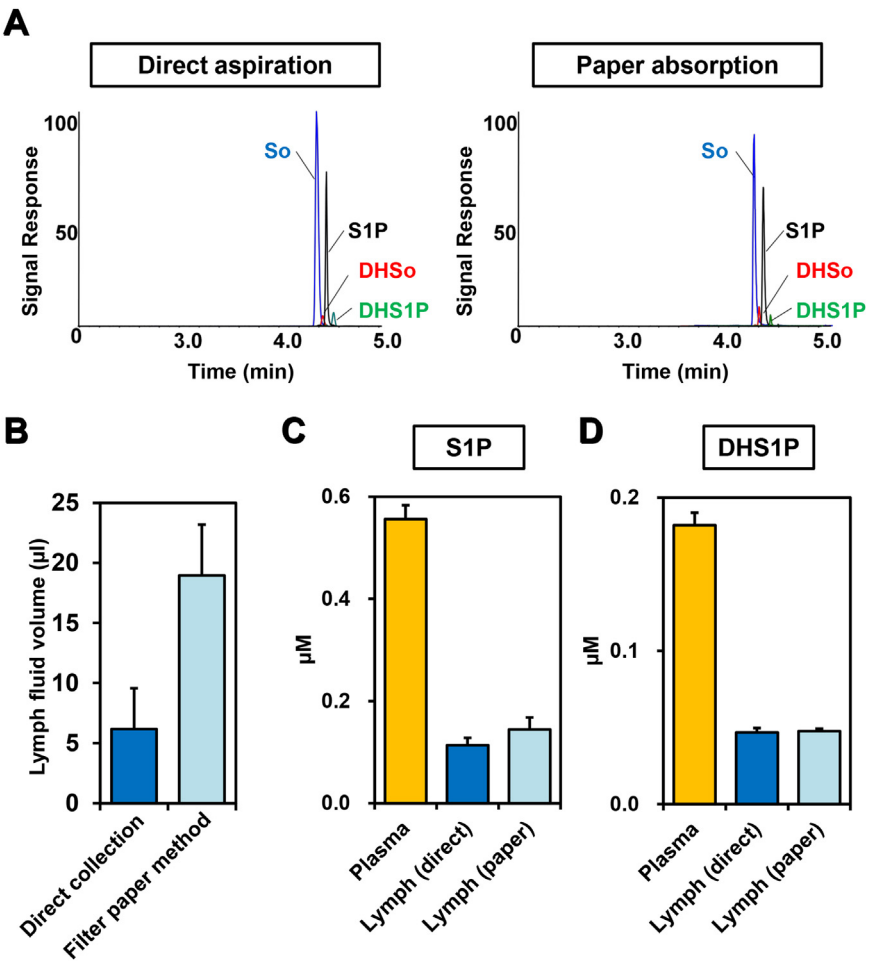


**Fig. 2.** Levels of S1P and dihydro-S1P (DHS1P) in lymphatic fluid measured by mass spectrometry. (A) Detection of sphingoid bases. Extracted ion chromatograms for LC-ESI-MS/MS reverse-phased separation of sphingoid bases in the lymphatic fluid collected by direct aspiration (left) or paper absorption (right) are shown. (B) Volumes of lymphatic fluid collected by the direct method (blue bar) and the filter paper method (light blue bar) are shown. (C and D) Levels of S1P and DHS1P in plasma (yellow bars), or lymphatic fluid collected by the direct method (blue bars) or by the filter paper method (light blue bars) were measured by mass spectrometry. Data shown are mean ± SD (n = 3).

lymph are significantly higher than those in serum (Fig. 3). DHSph, but not Sph, in the MLN showed significantly higher than those in lymphatic fluid (Fig. 3).

## 3.3. Effect of deletion of SphK2 on sphingolipid levels in blood, lymphatic fluid, and MLN

The relative contributions from each of the SphK isoforms to lymphatic fluid and tissue levels of S1P have not been fully elucidated. To this end, we next examined the effects of deletion SphK2. In agreement with previous reports [12, 28], S1P and dihydro-S1P levels in whole blood and serum of SphK2 knockout mice were higher than their WT littermates, most likely due to compensatory up-regulation of


http://dx.doi.org/10.1016/j.heliyon.2016.e00219

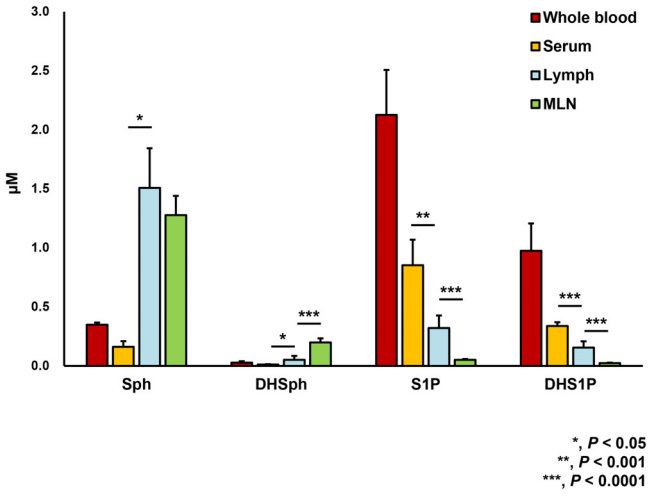


**Fig. 3.** Levels of sphingolipids in whole blood, serum, lymphatic fluid (lymph), and mesenteric lymph node (MLN) from wild type (WT) mice. Levels of sphingosine (Sph), dihydro-Sph (DHSph), S1P, and dihydro-S1P (DHS1P) in whole blood, serum, lymph, and MLN from WT mice were determined by LC-ESI-MS/MS. Mean ± SD (n = 6). *, $P < 0.05$; **, $P < 0.001$; ***, $P < 0.0001$ for serum vs. lymph or lymph vs. MLN.

SphK1 [12] (Fig. 4A and B). Levels of Sph and DHSph in whole blood and serum are much lower than the phosphorylated sphingoid bases in the SphK2 knockout and WT mice, as was previously reported [7, 28, 29, 30, 31]. Interestingly, levels of S1P and dihydro-S1P in the lymphatic fluid as well as mesenteric lymph node were significantly increased in SphK2 mice compared to their littermates (Fig. 3B). These results suggest the roles of SphK2 and/or SphK1 to regulate the levels of S1P and DHS1P in lymphatic fluid and the peripheral tissue.

## 4. Discussion

High levels of S1P in blood and lymphatic fluid are critical for maintenance of tone and integrity of the vascular endothelium. The S1P gradient between high levels in the circulation and the low levels in tissues due to the presence of S1P degrading activity from phosphatases and S1P lyase is important for immune cell trafficking [17, 32]. In this regard, it has been generally assumed that S1P levels in lymphoid tissues are very low so that S1PR1 on lymphocytes can sense the S1P gradient as they exit into the blood or lymphatic fluid. However, only a handful of studies have reported S1P levels in lymphatic fluid [7, 23, 28]. To overcome the hurdles for S1P measurement in the lymphatic fluid, we have established simple and reliable methods to collect adequate amounts of lymphatic fluid to enable the measurement of levels of bioactive sphingolipids by LC-ESI-MS/MS.

The most commonly described technique for lymphatic fluid collection is by cannulation of lymphatic vessels [23, 28, 33, 34]. The cannulation method has


http://dx.doi.org/10.1016/j.heliyon.2016.e00219

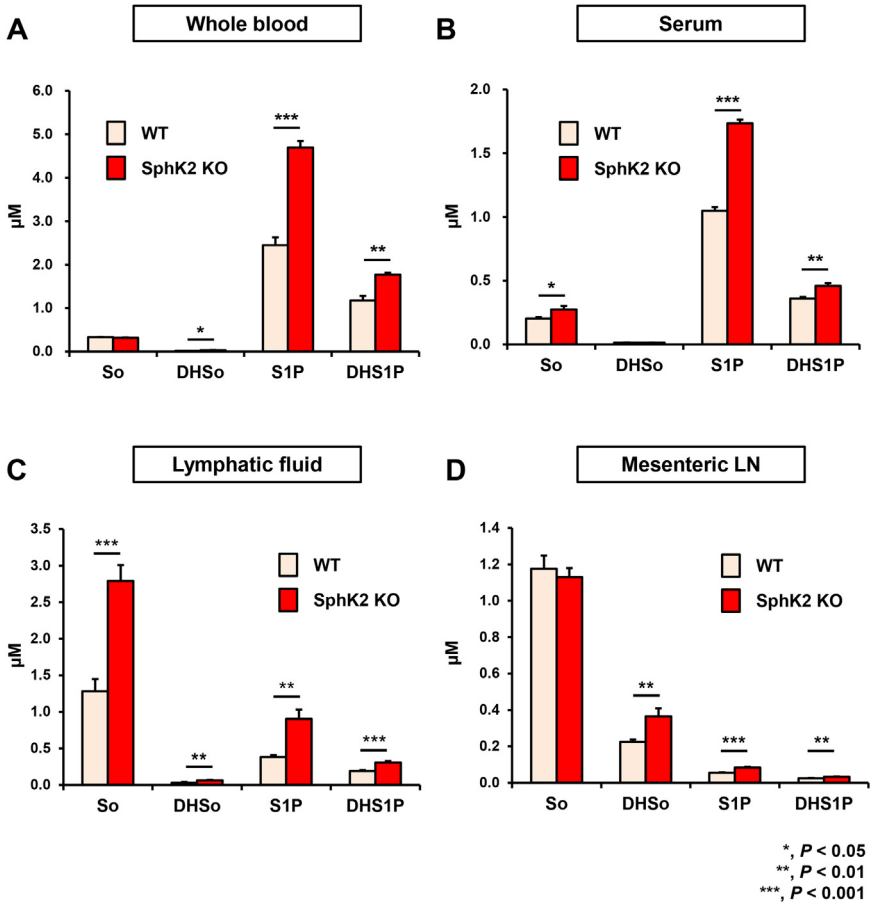


**Fig. 4.** Levels of sphingolipids in lymphatic fluid from SphK2$^{-/-}$ mice and littermate WT mice. Levels of sphingosine (Sph), dihydro-Sph (DHSph), S1P, and dihydro-S1P (DHS1P) in lymphatic fluid in (A) whole blood, (B) serum, (C) lymphatic fluid, (D) mesenteric lymph node from SphK2$^{-/-}$ and their littermate WT were determined by LC-ESI-MS/MS. Mean ± SEM (n = 4). *, $P < 0.05$; **, $P < 0.01$; ***, $P < 0.001$.

several advantages: long-term continuous observation is possible, a higher amount of fluid can be obtained, and importantly, contamination from other body fluids is relatively low. However, this method requires special equipment and is technically challenging in mice and therefore the majority of studies have used larger animals [33, 34]. On the other hand, direct aspiration with a needle is less difficult to perform, but usually collapses the vessel resulting in a lower yield. The challenge of obtaining enough fluid is met by our filter paper absorption method, which does not require special equipment, is relatively easy to perform when adequate exposure of the vessel is obtained, eliminates the effect of irritation from the cannula on the lymphatic vessel wall, and allows for immediate sampling. Since the paper absorption technique is easy to perform, any person who works on animal study can use it. Indeed, not only experienced surgeons, but also surgical residents and technicians were able to perform this technique to collect lymph. It is vital to


http://dx.doi.org/10.1016/j.heliyon.2016.e00219

avoid contamination with blood, which contains high concentrations of S1P. Nevertheless, if it occurs, it can readily be detected by the appearance of the red color of hemoglobin on the filter paper. Contamination with other body fluids could be another concern. However, this is unlikely since the level of S1P in lymphatic fluid collected by the direct filter absorption method is very similar to that obtained by needle aspiration, which has very low possibility of contamination. As a further validation of our method, previous reported S1P levels in lymphatic fluid collected by cannulation [23, 28] are in excellent agreement with the data from the filter paper absorption method. Therefore, we suggest that this paper absorption method is a reliable and simple method for collection of lymphatic fluid from mice. Although this collection method via the cisterna chili is likely only applicable for animal models, it is expected to be a valuable tool for studies to elucidate the functions of S1P in inflammatory diseases, lymphatic vascular disorders, and cancer invasion into the lymphatic system.

SphK1 which is localized mainly in the cytosol and translocated to the plasma membrane upon stimulation by cytokines and growth factors, is important for export of S1P and regulation of its extracellular levels [8, 35]. In contrast, SphK2 is localized to several intracellular organelles including the endoplasmic reticulum, the mitochondria, and the nucleus where it produces S1P that regulates intracellular functions. [36, 37, 38, 39]. Interestingly, knocking out SphK2 increased levels of S1P and dihydro-S1P in both blood and lymphatic fluid. It has been reported that mice lacking both SphK1 and SphK2 in endothelial cells have a loss of S1P in lymphatic fluid while maintaining normal plasma S1P, suggesting that SphKs in lymphatic endothelial cells are the source of S1P in lymphatic fluid [24]. In contrast to lymphatic fluid, serum S1P is derived predominantly from hematopoietic cells, with red blood cells playing a major role [23, 40]. Higher levels of S1P in both serum and lymphatic fluid in SphK2 knockout mice could be explained by upregulation of SphK1 in both hematopoietic cells and endothelial cells. On the other hand, considering that the sources of S1P in serum and lymphatic fluid are different, it is possible that global knockout of SphK2 affects production of S1P in the hematopoietic cells, but induces some compensatory mechanism either in lymphatic endothelial cells or in upstream tissue to maintain S1P level in lymphatic fluid. Further studies are needed with tissue specific knockout of SphK1 and/or SphK2 to explore the mechanisms by which levels of S1P in lymphatic fluid are regulated.

## 5. Conclusions

We determined the levels of S1P in lymphatic fluid, which is lower than blood and higher than lymph nodes. In agreement with the previous theory, our results confirm the “S1P gradient” among blood, lymphatic fluid and the peripheral lymphatic tissues. Convenient methods for collection and measurement of

 http://dx.doi.org/10.1016/j.heliyon.2016.e00219

sphingolipids in lymphatic fluid are expected to provide new insights on functions of sphingolipids.

## Declarations

## Author contribution statement

Masayuki Nagahashi: Conceived and designed the experiments; Performed the experiments; Analyzed and interpreted the data; Wrote the paper.

Akimitsu Yamada, Tomoyoshi Aoyagi: Performed the experiments.

Jeremy Allegood: Performed the experiments; Contributed reagents, materials, analysis tools or data.

Toshifumi Wakai: Analyzed and interpreted the data.

Sarah Spiegel: Analyzed and interpreted the data; Wrote the paper.

Kazuaki Takabe: Conceived and designed the experiments; Analyzed and interpreted the data; Contributed reagents, materials, analysis tools or data; Wrote the paper.

## Funding statement

This work was supported by the Japan Society for the Promotion of Science (JSPS) Grant-in-Aid for Scientific Research Grant Number 15H05676 and 15K15471 for Masayuki Nafahashi, and 15H04927 and 16K15610 for Toshifumi Wakai. Masayuki Nagahashi is also supported by the Uehara Memorial Foundation, Nakayama Cancer Research Institute, Takeda Science Foundation, and Tsukada Medical Foundation. Kazuaki Takabe is supported by NIH/NCI grant R01CA160688 and Susan G. Komen Investigator Initiated Research Grant IIR12222224.

## Competing interest statement

The authors declare no conflict of interest.

## Additional information

No additional information is available for this paper.

## Acknowledgements

The authors would like to acknowledge the VCU Lipidomics Core, the NIH-NCI Cancer Center Support Grant P30 CA016059 to the VCU Massey Cancer Center,


http://dx.doi.org/10.1016/j.heliyon.2016.e00219

as well as a shared resource grant (S10RR031535) from the National Institutes of Health for the mass spectrometric data generated by the VCU Lipidomics Core.

## References

[1] K. Takabe, S.W. Paugh, S. Milstien, S. Spiegel, Inside-out signaling of sphingosine-1-phosphate: therapeutic targets, Pharmacol. Rev. 60 (2008) 181.

[2] S. Spiegel, S. Milstien, Sphingosine-1-phosphate: an enigmatic signalling lipid, Nat. Rev. Mol. Cell Biol. 4 (2003) 397.

[3] G. Daum, A. Grabski, M.A. Reidy, Sphingosine 1-phosphate: a regulator of arterial lesions, Arterioscler. Thromb. Vasc. Biol. 29 (2009) 1439.

[4] N.J. Pyne, S. Pyne, Sphingosine 1-phosphate and cancer, Nat. Rev. Cancer 10 (2010) 489.

[5] M. Nagahashi, S. Ramachandran, O.M. Rashid, K. Takabe, Lymphangiogenesis: a new player in cancer progression, World J. Gastroenterol. 16 (2010) 4003.

[6] M. Nagahashi, Y. Matsuda, K. Moro, J. Tsuchida, D. Soma, et al., DNA damage response and sphingolipid signaling in liver diseases, Surg. Today 46 (2016) 995.

[7] M. Nagahashi, E.Y. Kim, A. Yamada, S. Ramachandran, J.C. Allegood, et al., Spns2, a transporter of phosphorylated sphingoid bases, regulates their blood and lymph levels, and the lymphatic network, FASEB J. 27 (2013) 1001.

[8] M. Nagahashi, K. Takabe, K.P. Terracina, D. Soma, Y. Hirose, et al., Sphingosine-1-phosphate transporters as targets for cancer therapy, Biomed. Res. Int. 2014 (2014) 651727.

[9] M. Nagahashi, S. Ramachandran, E.Y. Kim, J.C. Allegood, O.M. Rashid, et al., Sphingosine-1-phosphate produced by sphingosine kinase 1 promotes breast cancer progression by stimulating angiogenesis and lymphangiogenesis, Cancer Res. 72 (2012) 726.

[10] M. Nagahashi, J. Tsuchida, K. Moro, M. Hasegawa, K. Tatsuda, et al., High levels of sphingolipids in human breast cancer, J. Surg. Res. 204 (2016) 435.

[11] J. Tsuchida, M. Nagahashi, M. Nakajima, K. Moro, K. Tatsuda, et al., Breast cancer sphingosine-1-phosphate is associated with phospho-sphingosine kinase 1 and lymphatic metastasis, J. Surg. Res. 205 (2016) 85.

[12] J. Liang, M. Nagahashi, E.Y. Kim, K.B. Harikumar, A. Yamada, et al., Sphingosine-1-phosphate links persistent STAT3 activation, chronic

 http://dx.doi.org/10.1016/j.heliyon.2016.e00219

intestinal inflammation, and development of colitis-associated cancer, Cancer Cell 23 (2013) 107.

[13] M. Nagahashi, N.C. Hait, M. Maceyka, D. Avni, K. Takabe, et al., Sphingosine-1-phosphate in chronic intestinal inflammation and cancer, Adv. Biol. Regul. 54 (2014) 112.

[14] R.H. Kim, K. Takabe, S. Milstien, S. Spiegel, Export and functions of sphingosine-1-phosphate, Biochim. Biophys. Acta 1791 (2009) 692.

[15] S. Spiegel, S. Milstien, The outs and the ins of sphingosine-1-phosphate in immunity, Nat. Rev. Immunol. 11 (2011) 403.

[16] M. Nagahashi, A. Yamada, H. Miyazaki, J.C. Allegood, J. Tsuchida, et al., Interstitial Fluid Sphingosine-1-Phosphate in Murine Mammary Gland and Cancer and Human Breast Tissue and Cancer Determined by Novel Methods, J. Mammary Gland Biol. Neoplasia 21 (2016) 9.

[17] J.G. Cyster, S.R. Schwab, Sphingosine-1-phosphate and lymphocyte egress from lymphoid organs, Annu. Rev. Immunol. 30 (2012) 69.

[18] A. Ben Shoham, G. Malkinson, S. Krief, Y. Shwartz, Y. Ely, et al., S1P1 inhibits sprouting angiogenesis during vascular development, Development 139 (2012) 3859.

[19] K. Gaengel, C. Niaudet, K. Hagikura, B. Lavina, L. Muhl, et al., The sphingosine-1-phosphate receptor S1PR1 restricts sprouting angiogenesis by regulating the interplay between VE-cadherin and VEGFR2, Dev. Cell 23 (2012) 587.

[20] B. Jung, H. Obinata, S. Galvani, K. Mendelson, B.S. Ding, et al., Flow-regulated endothelial S1P receptor-1 signaling sustains vascular development, Dev. Cell 23 (2012) 600.

[21] M. Matloubian, C.G. Lo, G. Cinamon, M.J. Lesneski, Y. Xu, et al., Lymphocyte egress from thymus and peripheral lymphoid organs is dependent on S1P receptor 1, Nature 427 (2004) 355.

[22] J.G. Cyster, Chemokines, sphingosine-1-phosphate, and cell migration in secondary lymphoid organs, Annu. Rev. Immunol. 23 (2005) 127.

[23] R. Pappu, S.R. Schwab, I. Cornelissen, J.P. Pereira, J.B. Regard, et al., Promotion of lymphocyte egress into blood and lymph by distinct sources of sphingosine-1-phosphate, Science 316 (2007) 295.

[24] T.H. Pham, P. Baluk, Y. Xu, I. Grigorova, A.J. Bankovich, et al., Lymphatic endothelial cell sphingosine kinase activity is required for lymphocyte egress and lymphatic patterning, J. Exp. Med. 207 (2010) 17.

 http://dx.doi.org/10.1016/j.heliyon.2016.e00219

[25] M.L. Allende, T. Sasaki, H. Kawai, A. Olivera, Y. Mi, et al., Mice deficient in sphingosine kinase 1 are rendered lymphopenic by FTY720, J. Biol. Chem. 279 (2004) 52487.

[26] K. Mizugishi, T. Yamashita, A. Olivera, G.F. Miller, S. Spiegel, et al., Essential role for sphingosine kinases in neural and vascular development, Mol. Cell. Biol. 25 (2005) 11113.

[27] Y. Kawashima, M. Sugimura, Y. Hwang, N. Kudo, The lymph system in mice, Jap. J. Vet. Res. 12 (1964) 10.

[28] S.C. Sensken, C. Bode, M. Nagarajan, U. Peest, O. Pabst, et al., Redistribution of sphingosine 1-phosphate by sphingosine kinase 2 contributes to lymphopenia, J. Immunol. 184 (2010) 4133.

[29] S.M. Hammad, J.S. Pierce, F. Soodavar, K.J. Smith, M.M. Al Gadban, et al., Blood sphingolipidomics in healthy humans: impact of sample collection methodology, J. Lipid Res. 51 (2010) 3074.

[30] T. Lan, H. Bi, W. Liu, X. Xie, S. Xu, et al., Simultaneous determination of sphingosine and sphingosine 1-phosphate in biological samples by liquid chromatography-tandem mass spectrometry, J. Chromatogr. B Analyt. Technol. Biomed. Life Sci. 879 (2011) 520.

[31] A.J. Alberg, K. Armeson, J.S. Pierce, J. Bielawski, A. Bielawska, et al., Plasma sphingolipids and lung cancer: a population-based, nested case-control study, Cancer Epidemiol. Biomarkers Prev. 22 (2013) 1374.

[32] W.C. Huang, J. Liang, M. Nagahashi, D. Avni, A. Yamada, et al., Sphingosine-1-phosphate phosphatase 2 promotes disruption of mucosal integrity, and contributes to ulcerative colitis in mice and humans, FASEB J. (2016).

[33] N.L. Trevaskis, S.M. Caliph, G. Nguyen, P. Tso, W.N. Charman, et al., A mouse model to evaluate the impact of species, sex, and lipid load on lymphatic drug transport, Pharm. Res. 30 (2013) 3254.

[34] M. Ionac, T. Laskay, D. Labahn, G. Geisslinger, W. Solbach, Improved technique for cannulation of the murine thoracic duct: a valuable tool for the dissection of immune responses, J. Immunol. Methods 202 (1997) 35.

[35] K. Takabe, R.H. Kim, J.C. Allegood, P. Mitra, S. Ramachandran, et al., Estradiol induces export of sphingosine 1-phosphate from breast cancer cells via ABCC1 and ABCG2, J. Biol. Chem. 285 (2010) 10477.

 http://dx.doi.org/10.1016/j.heliyon.2016.e00219

[36] N.C. Hait, J. Allegood, M. Maceyka, G.M. Strub, K.B. Harikumar, et al., Regulation of histone acetylation in the nucleus by sphingosine-1-phosphate, Science 325 (2009) 1254.

[37] G.M. Strub, M. Paillard, J. Liang, L. Gomez, J.C. Allegood, et al., Sphingosine-1-phosphate produced by sphingosine kinase 2 in mitochondria interacts with prohibitin 2 to regulate complex IV assembly and respiration, FASEB J. 25 (2011) 600.

[38] M. Nagahashi, K. Takabe, R. Liu, K. Peng, X. Wang, et al., Conjugated bile acid-activated S1P receptor 2 is a key regulator of sphingosine kinase 2 and hepatic gene expression, Hepatology 61 (2015) 1216.

[39] M. Nagahashi, K. Yuza, Y. Hirose, M. Nakajima, R. Ramanathan, et al., The roles of bile acids and sphingosine-1-phosphate signaling in the hepato-biliary diseases, J. Lipid Res. (2016).

[40] Y. Yatomi, Plasma sphingosine 1-phosphate metabolism and analysis, Biochim. Biophys. Acta 1780 (2008) 606.

 http://dx.doi.org/10.1016/j.heliyon.2016.e00219

J Mammary Gland Biol Neoplasia (2016) 21:9–17
DOI 10.1007/s10911-016-9354-7

# Interstitial Fluid Sphingosine-1-Phosphate in Murine Mammary Gland and Cancer and Human Breast Tissue and Cancer Determined by Novel Methods

**Masayuki Nagahashi[1,2,3] · Akimitsu Yamada[1,2] · Hiroshi Miyazaki[4] · Jeremy C. Allegood[2] · Junko Tsuchida[3] · Tomoyoshi Aoyagi[1,2] · Wei-Ching Huang[1,2] · Krista P. Terracina[1,2] · Barbara J. Adams[1,2] · Omar M. Rashid[5,6,7] · Sheldon Milstien[2] · Toshifumi Wakai[3] · Sarah Spiegel[2] · Kazuaki Takabe[1,2,8]**

Received: 8 January 2016 / Accepted: 9 May 2016 / Published online: 19 May 2016


**Abstract** The tumor microenvironment is a determining factor for cancer biology and progression. Sphingosine-1-phosphate (S1P), produced by sphingosine kinases (SphKs), is a bioactive lipid mediator that regulates processes important for cancer progression. Despite its critical roles, the levels of S1P in interstitial fluid (IF), an important component of the tumor microenvironment, have never previously been measured due to a lack of efficient methods for collecting and quantifying IF. The purpose of this study is to clarify the levels of S1P in the IF from murine mammary glands and its tumors utilizing our novel methods. We developed an improved centrifugation method to collect IF. Sphingolipids in IF, blood, and tissue samples were measured by mass spectrometry. In mice with a deletion of SphK1, but not SphK2, levels of S1P in IF from the mammary glands were greatly attenuated. Levels of S1P in IF from mammary tumors were reduced when tumor growth was suppressed by oral administration of FTY720/fingolimod. Importantly, sphingosine, dihydrosphingosine, and S1P levels, but not dihydro-S1P, were significantly higher in human breast tumor tissue IF than in the normal breast tissue IF. To our knowledge, this is the first reported S1P IF measurement in murine normal mammary glands and mammary tumors, as well as in human patients with breast cancer. S1P tumor IF measurement illuminates new aspects of the role of S1P in the tumor microenvironment.

**Keywords** Cancer · Endothelial cells · Interstitial fluid · Mass spectrometry · Sphingolipids · Sphingosine-1-phosphate

## Introduction

The tumor microenvironment is a determining factor in cancer biology and progression [1]. Although it has been long known that the lymphatic system is the initial pathway for metastasis in many cancers including mammary cancer, recent findings

✉ Masayuki Nagahashi
mnagahashi@med.niigata-u.ac.jp

✉ Kazuaki Takabe
kazutakabe@gmail.com

[1] Division of Surgical Oncology, Department of Surgery, Virginia Commonwealth University School of Medicine, and Massey Cancer Center, PO Box 980011, West Hospital 7-402, 1200 East Broad Street, Richmond, VA 23298-0011, USA

[2] Department of Biochemistry and Molecular Biology, Virginia Commonwealth University School of Medicine, and the Massey Cancer Center, PO Box 980011, West Hospital 7-402, 1200 East Marshall Street, Richmond, VA 23298, USA

[3] Division of Digestive and General Surgery, Niigata University Graduate School of Medical and Dental Sciences, 1-757 Asahimachi-dori, Chuo-ku, Niigata City, Niigata 951-8510, Japan

[4] Section of General Internal Medicine, Kojin Hospital, 1-710 Shikenya, Moriyama, Nagoya 463-8530, Japan

[5] Holy Cross Hospital Michael and Dianne Bienes Comprehensive Cancer Center, 4725 North Federal Highway, Fort Lauderdale, FL 33308, USA

[6] Massachusetts General Hospital, 55 Fruit St, Boston, MA 02114, USA

[7] University of Miami Miller School of Medicine, 1600 NW 10th Ave, Miami, FL 33136, USA

[8] Breast Surgery, Roswell Park Cancer Institute, Elm & Carlton Streets, Buffalo, NY 14263, USA

suggest new mechanisms for how cancer cells gain access to the lymphatic system and how they manipulate their microenvironment to establish metastasis. An increasing number of proteins in the tumor microenvironment are now known to play important roles in tumor progression [2–4]. Interstitial fluid that bathes the tumor and stromal cells is considered as an important part of the tumor microenvironment not only as the initial route of metastasis, but also as a supplier of factors that promote tumor metastasis.

Sphingosine-1-phosphate (S1P) is a potent bioactive signaling molecule that regulates many physiological and pathological processes involved in immune cell trafficking, inflammation, vascular homeostasis, and cancer progression [5–8]. S1P is generated by sphingosine kinases (SphK1 and SphK2), and is then secreted, exerting its functions by binding to five specific G protein–coupled receptors (S1PR1–5) in autocrine, paracrine, and/or endocrine manners, a process known as "inside-out" signaling [9–11]. "Inside-out" signaling refers to the process by which S1P produced inside cells is secreted by transporters and signals through its receptors on the outside of cells. The "inside-out" signaling of S1P plays important roles in cancer cell pathophysiology [12]. Though we have shown that SphK1 is the significant contributor to extracellular S1P while SphK2 contributed to intracellular S1P of mammary cancer cells [12], to date the relative contribution of each SphK to secreted S1P has never been definitively demonstrated in an in vivo setting.

Recently studies from our laboratory have demonstrated that S1P produced by SphK1 in cancer cells promotes mammary cancer progression by stimulating angiogenesis, lymphangiogenesis, and subsequently lymph node metastasis [13], We have also shown that S1P produced by up-regulation of SphK1 and subsequent activation of the S1PR1 receptor play an essential role in maintaining persistent activation of the important transcription factors NF-kB and Stat3 in a feedforward amplification loop that links chronic inflammation and colitis associated carcinogenesis [14]. Despite this emerging understanding of importance of S1P in cancer cell signaling, the role of S1P in the tumor microenvironment, particularly in the interstitial fluid (IF), remains unclear. This is in part because of difficulties presented by collecting and analyzing IF, a barrier that once surmounted, is expected to provide important insights into the tumor microenvironment and how tumors develop and respond to therapy.

Here we introduce simple and reproducible methods to measure the levels of sphingolipids including S1P in small volume of interstitial fluid from healthy mammary glands and tumor using a modified centrifugation method combined with liquid chromatography-electrospray ionization tandem mass spectrometry (LC-ESI-MS/MS). Using our new method, we are able for the first time to demonstrate the contributions of SphK1 and SphK2 to secreted S1P in vivo, and have been able to provide definitive evidence that S1P is increased in breast tumor interstitial fluid and that this increase is ameliorated by treatment with the prodrug FTY720, concomitantly with suppression of tumor growth.

## Materials and Methods

### Reagents

Internal standards were purchased from Avanti Polar Lipids (Alabaster, AL) and added to samples in 20 μl ethanol:methanol:water (7:2:1) as a cocktail of 500 pmol each. The HPLC grade solvents were obtained from VWR (West Chester, PA). ). FTY720 was from Cayman Chemical Company (Ann Arbor, MI).

### Animals

All animal studies were conducted in the Animal Research Core Facility at VCU School of Medicine in accordance with institutional guidelines. Experiments without breast tumor implantation utilized SphK1$^{-/-}$ and SphK2$^{-/-}$ mice since they are well characterized, and because we have previously found that SphK2$^{-/-}$ mice demonstrate compensatory higher expression of SphK1 in the tissues [14]. These knockout mice were kindly provided by Dr. Richard L. Proia of National Institute of Diabetes and Digestive and Kidney Diseases [15, 16]. We obtained each knockout mouse with littermate WT from heterozygous parents. Experiments with 4T1 breast tumor implantation, used syngeneic Balb/c female mice at 8–10 weeks of age (Harlan, Indianapolis, IN).

### Tumor Growth

4T1-luc2 cells, a mouse mammary gland derived adenocarcinoma cell line that has been engineered to express luciferase (Caliper Life Sciences, Perkin Elmer, Waltham, MA), were cultured in RPMI Medium 1640 with 10 % fetal bovine serum. 4T1-luc2 cells ($1 \times 10^5$ cells in 10 μl RPMI) were implanted in the 2nd chest mammary gland under direct vision as previously described [13, 17]. The tumor burden of 4T1-luc2 cell tumors was determined by measurement of bioluminescence with the IVIS Imaging System (Xenogen, Perkin Elmer). Where indicated, tumor-bearing mice were randomized 2 days after implantation into two treatment groups treated with saline or FTY720 (p.o. 1 mg/kg/day).

### Human Tissue Samples from Patients with Breast Cancer

Breast cancer tissue samples were collected from 7 patients who had invasive tumors larger than 1.5 cm and underwent surgical resection in Niigata University Medical and Dental

Hospital. This study protocol was approved by the Institutional Review Board of Niigata University Medical and Dental Hospital, and informed consent was obtained from all the patients. Cancerous tissue, peri-tumor normal breast tissue and normal breast tissue distant from the cancer were collected from surgical specimens immediately after operation, excised and frozen in liquid nitrogen. Peri-tumor normal breast tissue was defined as tissue within 1 cm from the gross edge of tumor, and distant from tumor was defined as tissue more than 2 cm from the gross edge of tumor. All tissue samples were stored at −80 °C.

### Construction of the IF Collection Tube

Based on the previous "nylon basket" approach to the collection of IF developed by Wiig et al., [3, 18, 19] an IF collection tube was constructed by gluing Spectrum/Mesh nylon filters (20 μM mesh, 55 μM thick, Spectrum Labs. Inc., Rancho Domingguez, CA) to the bottom of Wizard Minicolumn Inserts (Promega, Madison, WI) after removing the original bottom filter. These were then placed on top of the spin columns (Fig. 1).

### Collection of IF from Tissues

Animals were sacrificed by exsanguination, blood was collected, and tissues were harvested for IF collection by an established method [3, 18, 19] with some modifications. Briefly, tissue was excised, blotted gently, and placed in pre-weighed tubes on ice. Tubes were re-weighed to determine tissue weight and the tissue was sectioned several times with scissors. The samples were then transferred into the inserts with nylon mesh, and placed into the pre-weighed centrifuge tubes. The tubes were centrifuged at 106 × g for 10 min at 4 °C and the IF accumulated below the filter. The volume of IF was quantified by weight. PBS containing phosphatase inhibitors (100 μl) was added to the IF and the tubes were centrifuged at 1000 × g for 10 min at 4 °C to remove any contaminating cells (Fig. 1).

### Cell Counting and Immunoblot

Cell numbers were determined in IF without centrifugation, after centrifugation at 106 × g, 1000 × g, 10,000 × g by counting the numbers under microscopy. Protein from lymph node (LN) tissue extracts or from IF were quantified by western blotting with anti-actin antibody and stained with Ponceau S to visualize proteins. Densitometry of the blot was assessed using Image J software, and the relative level of actin was normalized with equal protein amount of LN and IF.

### Quantitation of Sphingolipids by LC-ESI-MS/MS

Lipids were extracted from IF, blood, or tissue samples and sphingolipids were quantified by liquid chromatography, electrospray ionization-tandem mass spectrometry (LC-ESIMS/MS, 4000 QTRAP, ABI) as described previously [12, 20, 21].

### Statistical Analysis

Results were analyzed for statistical significance with a two-tailed Student's t-test, with $P < 0.05$ considered significant. Experiments were repeated at least three times with consistent results.

## Results

### An Improved Method to Collect IF from Tissues

Although it has been suggested that S1P levels are relatively low in IF compared to cells, this has not been verified experimentally [22]. We modified an established method by Wiig et al. [3, 18, 19] and developed a new IF collection tube to enable efficient collection of IF from small tissue samples for sphingolipid measurements (Fig. 1). The recovery of IF was low from tissues weighing less than 200 mg, while the volume of IF collected was proportional to the weight of tissues weighing more than 200 mg (Fig. 2a). To protect S1P from degradation, buffer containing phosphatase inhibitors was added to the IF, and a subsequent centrifugation at 1000 × g was used to remove contaminating cells (Fig. 2b). To examine whether collected IF contained cells or components of broken cells, 10 μg of protein in IF from lymph node tissue and the same amount of protein extracted from lymph node tissue were separated by SDS-PAGE and immunoblotted with an antibody to actin, the major intracellular protein. Actin was barely detectable in the IF (Fig. 2c). Densitometric analysis of the actin band revealed that the IF contained less than 0.3 % of the actin protein as compared to the same amount of protein extracted from lymph node tissue (Fig. 2c). Repeated analyses of IF samples demonstrated minimal variation (i.e. tight error bars), also indicating low contamination.

### Effect of Deletion of SphK1 or SphK2 on Sphingolipid Levels in Blood

As we have an interest in investigating the level and function of S1P in the various fluid compartments of the body, we initially investigated the different contributions of SphK1 and SphK2 to S1P levels in whole blood and serum using knockout mice. In agreement with previous reports [15, 23–25], levels of S1P and dihydro-S1P (DHS1P) in blood as well as in serum of SphK1$^{-/-}$ mice were lower than those

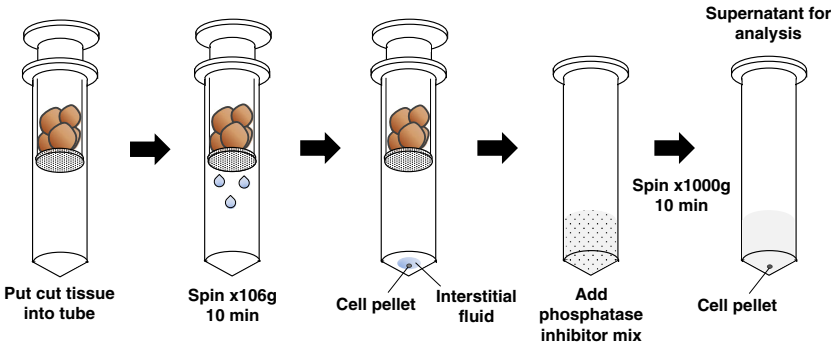


**Fig. 1** Scheme for the isolation of IF from tissues. Excised tissue was placed inside pre-weighed inner tubes with nylon mesh. The tubes were centrifuged at 106 × g for 10 min at 4 °C allowing IF accumulation in the bottom of the tube together with a very small cell pellet. After weighing to determine the volume of IF, phosphatase inhibitor mix was added and the tubes were centrifuged at 1000 × g for 10 min at 4 °C to remove any contaminating cells

found in wild type (WT) littermates (Fig. 3a and 3c). In contrast, and in agreement with others [14, 26], S1P and DHS1P levels in blood as well as serum of SphK2$^{-/-}$ mice were higher than those of their WT littermates, most likely due to compensatory up-regulation of SphK1 that produces S1P and DHS1P in the SphK2$^{-/-}$ animals [14] (Fig. 3b and 3d). Hence, SphK1, rather than SphK2, appears to contribute to the S1P levels in whole blood and serum. Levels of sphingosine (Sph) and dihydro-Sph (DHSph) in blood and serum are much lower than the phosphorylated sphingoid bases in both knockouts and WT mice, as were previously reported [21, 26–29].

## S1P Levels Are Higher in Mammary Gland IF than in Mammary Gland Itself

Next, it was of interest to examine the contribution of SphK1 and SphK2 to levels of bioactive sphingolipids in IF compared to the tissue it was collected from. We examined their levels in IF from mammary gland compared to the tissue itself. S1P and DHS1P levels in mammary glands were much lower than those of Sph and DHSph and there were no major differences in S1P levels between the SphK1 knockouts and their littermate controls (Fig. 4a), yet there were significant decreases in levels of DHS1P and Sph in SphK1$^{-/-}$ mice. S1P levels were slightly increased in SphK2 knockout mice compared to their littermate controls, while levels of Sph were not changed (Fig. 4b). Importantly, substantial concentrations of S1P and DHS1P were found in IF from mammary glands, which were approximately 10-fold higher than those in the tissue. Moreover, deletion of SphK1 greatly reduced levels of both phosphorylated sphingoid bases as well as Sph and DHSph (Fig. 4c). In contrast, deletion of SphK2 did not affect their levels in IF significantly (Fig. 4d).

## Levels of Bioactive Sphingolipids in Breast Tumor IF Correlate with Tumor Growth

We previously showed in a syngeneic mouse breast cancer model in which 4T1-luc2 murine mammary cancer cells were orthotopically implanted into the chest mammary glands of

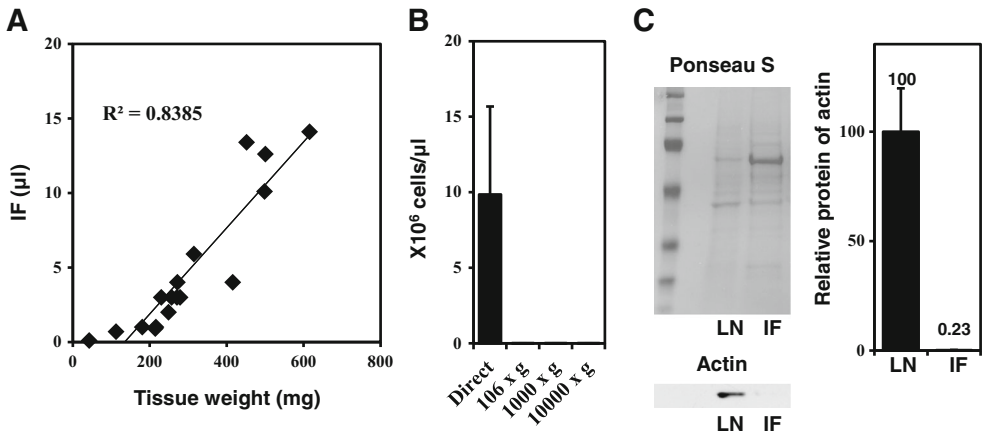


**Fig. 2** Collection of interstitial fluid (IF) from tissues. **a** IF was collected from different amounts of 4T1 breast tumor tissue. Correlation between the tumor tissue weight and the volume of IF collected is shown. **b** Removal of contaminating cells from IF. Cell numbers in IF were determined after centrifugation as indicated. **c** 10 µg of protein from lymph node tissue extracts (LN) or from IF were analyzed by western blotting with anti-actin antibody (lower panel) and stained with Ponceau S to visualize proteins (upper panel). Densitometry of the blot was assessed using Image J software, and the relative level of actin was normalized with equal protein amount of LN and IF

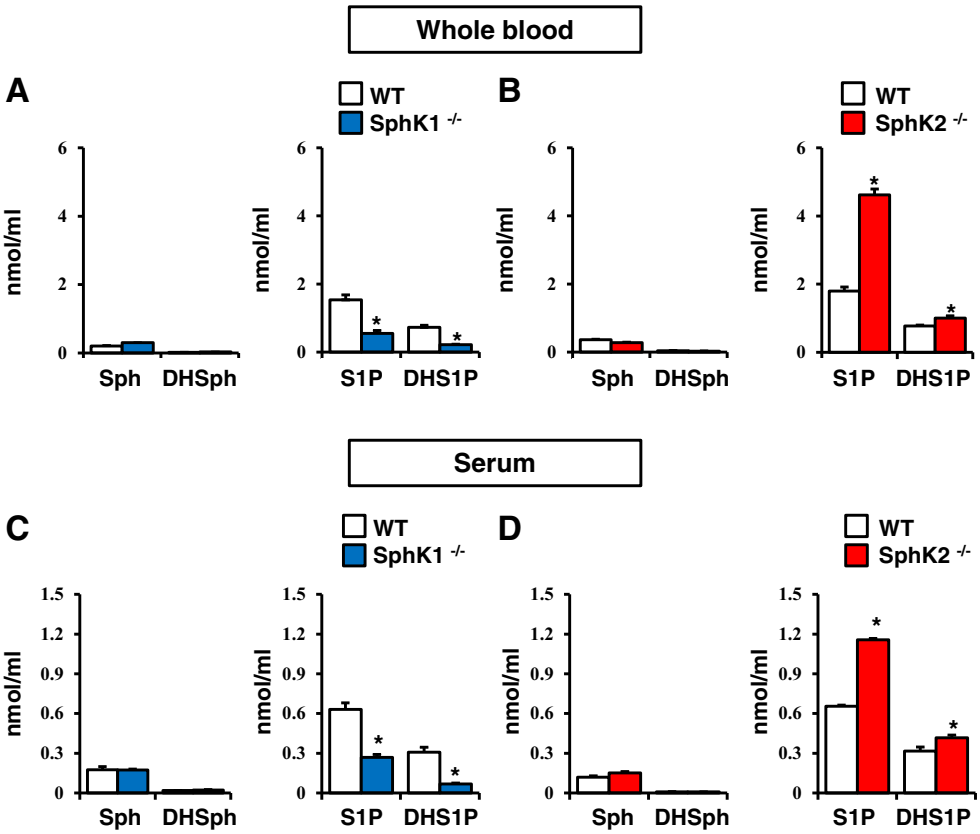


**Fig. 3** Levels of sphingolipids in blood and serum from SphK1$^{-/-}$ and SphK2$^{-/-}$ mice and littermate wild type mice. Levels of sphingosine (Sph), dihydro-Sph (DHSph), S1P, and dihydro-S1P (DHS1P) in blood (**a, b**), and serum (**c, d**) from 2 month old SphK1$^{-/-}$ mice (*blue bars*), SphK2$^{-/-}$ (*red bars*), and their respective WT littermates (*white bars*) were determined by LC-ESI-MS/MS. Mean ± SEM ($n = 4$). *, $P < 0.05$

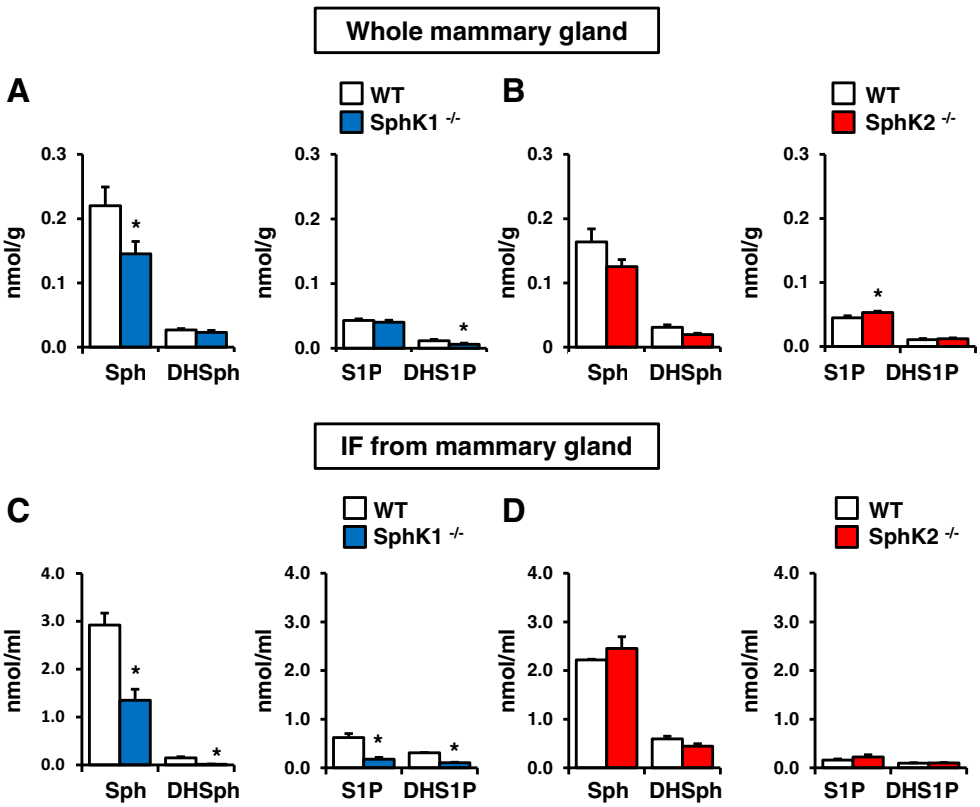


**Fig. 4** Levels of bioactive sphingolipid metabolites in normal mammary glands and mammary gland IF from SphK1$^{-/-}$ and SphK2$^{-/-}$ mice and corresponding littermate wild type (WT) mice. Sphingosine (Sph), dihydro-Sph (DHSph), S1P, and dihydro-S1P (DHS1P) in mammary glands (**a, b**), and IF from the mammary glands (**c, d**) from SphK1$^{-/-}$ mice and WT littermates (**c**), SphK2$^{-/-}$ mice and their WT littermates (**d**) were determined by LC-ESI-MS/MS. Data are mean ± SEM ($n = 4$). *, $P < 0.05$

immunocompetent mice that S1P levels are increased in tumors and correlated with tumor growth [13]. Because we [14] and others [30, 31] have shown that oral administration of FTY720 reduces tumorigenesis, and because of the known effects of FTY720 on S1P signaling, we treated 4T1 tumor bearing mice with FTY720 and examined correlations between tumor burden and levels of bioactive sphingolipids in tumor IF. FTY720 greatly reduced tumor growth, as demonstrated by in vivo bioluminescence and tumor volume measurements (Fig. 5a–c), levels of S1P and DHS1P in tumor IF were significantly decreased compared to saline treated animals (Fig. 5d).

### S1P Levels Are Higher in Breast Cancer IF than in Normal Breast Tissue IF from Human Patients

Next, we examined the levels of sphingolipids in IF from human patients with breast cancer to examine whether the observation seen in animal models is also applicable to the human patients. For this purpose, we obtained IF from breast tumor tissue and normal breast tissue from two different areas (peri-tumoral area and distant area from the tumor) in each patient with breast cancer and determined levels of sphingolipids in the fluid. Importantly, Sph, DHSph, and S1P levels, but not DHS1P, were significantly higher in the breast tumor tissue IF than in the normal breast tissue IF (Fig. 6). There is no significant difference in levels of Sph, DHSph, S1P or DHS1P between IF from normal breast tissue that is distant from tumor and that from peri-tumor normal breast tissue (Fig. 6).

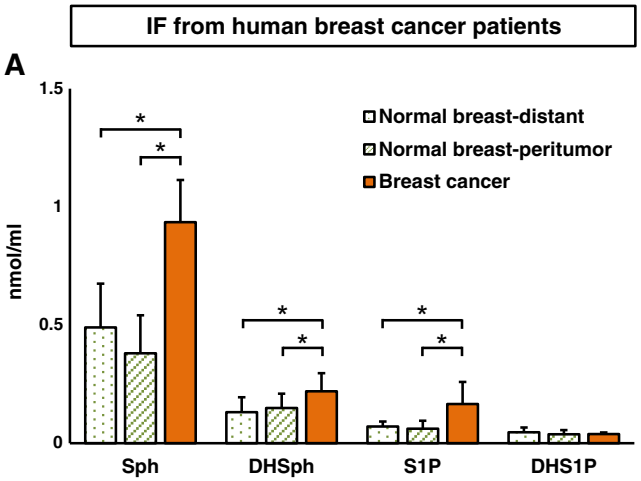


**Fig. 6** Levels of bioactive sphingolipids in IF from breast tumor and normal breast tissue of patients with breast cancer. **a** IF was obtained from breast cancer tissue and normal breast tissue obtained from distant area from tumor and peritumor area. Levels of sphingosine (Sph), dihydro-Sph (DHSph), S1P, and dihydro-S1P (DHS1P) in the IF from tumor and normal breast tissue were determined by mass spectrometry. Data are mean ± SEM. *, $P < 0.05$

## Discussion

High levels of S1P in blood are critical for maintenance of the tone and integrity of the vascular endothelium. The S1P gradient between high levels in the circulation and the low levels in tissues due to the presence of S1P degrading activity from phosphatases and S1P-lyase is important for immune cell trafficking [22]. It has been generally assumed that S1P levels in IF of lymphoid tissues are very low so that S1PR1 on lymphocytes can sense the S1P gradient as they exit into the blood. Previous studies have suggested that S1P secreted by tumor cells plays an important role in tumor progression and metastasis [13]. However, there are no reports on S1P in IF, due in part to the difficulties in collection. To our knowledge, this is the first report of the measurement of S1P and DHS1P in tumor IF in murine normal mammary glands and mammary tumors, as well as in human patients with breast cancer.

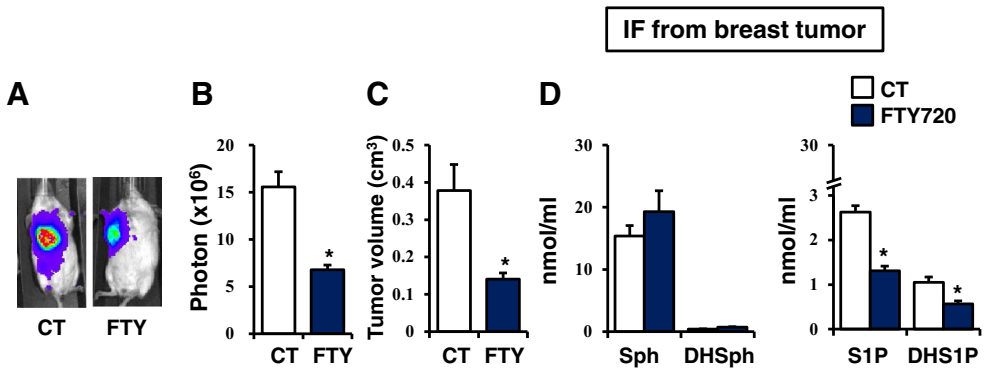


**Fig. 5** Levels of bioactive sphingolipids in breast tumor IF correlate with tumor growth. 4T1-luc2 cells were surgically implanted in mammary glands. Tumor-bearing mice were randomized into 2 groups and treated daily by gavage with saline (*open bars*) or FTY720 (1 mg/kg, *black bars*). **a** Representative IVIS images of 4T1 breast tumors on day 14 after implantation. **b** Tumor burden determined by in vivo bioluminescence. Data are means ± SEM ($n = 5$). *, $P < 0.05$. **c** Tumor size was determined and volume calculated with the cylinder formula. Data are means ± SEM. *, $P < 0.05$. **d** Levels of sphingosine (Sph), dihydro-Sph (DHSph), S1P, and dihydro-S1P (DHS1P) in 4T1 breast tumor IF from saline or FTY720 treated mice were determined by mass spectrometry. Data are mean ± SEM. *, $P < 0.05$

Wiig et al. previously described a method to collect IF without causing cellular damage using low speed centrifugation of tissues on nylon mesh which required a large amount of tissue [3, 18, 19]. In order to collect IF from a smaller amount of tissue, we improved this method by designing a more efficient IF collection tube with a smaller nylon mesh surface area, thereby reducing loss of IF from absorption of the fluid by the mesh. Based on our experience, we recommend the use of at least 400 mg tissue for reproducible collection of IF. Nevertheless, LC-ESI-MS/MS is sufficiently sensitive to accurately measure sphingolipids in a volume of IF of less than 10 μl. As was reported by Wiig et al. [3, 18], we also found negligible contamination of IF with cellular components from contaminating or broken cells as shown by the extremely low amounts of actin.

Using the simple method for collection of IF that we have described, we have been able to validate previous assumptions regarding extracellular S1P as well as discover several new insights into the role of S1P in the tumor microenvironment. Levels of S1P in normal mammary glands are known to be relatively low, much lower than Sph; however, we have found high concentrations of bioactive sphingolipids (reaching 0.6 μM S1P and 0.2 μM DHS1P) to be present in IF from normal mammary glands. Sphingolipid metabolites in mammary gland IF from SphK1$^{-/-}$ mice were significantly decreased, suggesting that it is SphK1 that plays a pivotal role in regulating levels of these metabolites in IF from normal mammary glands. Though in vitro studies have suggested that it is SphK1 and not SphK2 that is the major contributor of secreted S1P, this is the first study to validate this in an in vivo setting.

FTY720 is a pro-drug approved for treatment of multiple sclerosis. It is phosphorylated in vivo to FTY720-phosphate, a S1P mimetic that modulates S1PR functions [32]. However, we [14] and others [30, 31] have shown that FTY720 also potent anti-cancer activities. In agreement, we found that oral administration of FTY720 greatly reduced breast tumor growth in a syngeneic model. Importantly, S1P and DHS1P levels in tumor IF were significantly decreased by FTY720 administration and correlated with the reduction of tumor growth. While this observation further supports the notion that S1P may have an important role within the tumor microenvironment, it also provides an important insight into the possible mechanisms of action of FTY720 on cancer progression. Though FTY720 in its phosphorylated form is known to have its immunosuppressive effects as a functional antagonist of S1PR1, inducing internalization and degradation of S1PR1 and prolonged receptor downregulation, it has also been shown that FTY720 inhibits SphK1 and induces its proteasomal degradation [33, 34]; therefore, the lower levels of S1P in the tumor IF from tumor bearing mice treated with FTY720 compared to saline treated animals could also be due to inhibition or reduction of SphK1 in the breast cancer cells. SphK1 is known to be upregulated in many cancers including breast [35–39] and we have shown that tumor bearing mice have increased systemic S1P [13] and may communicate with the host via the systemic SphK1/S1P axis to regulate lung metastasis/colonization [40]. Our findings suggest the possibility that S1P secreted from tumor cells to IF may be important for metastasis by stimulating S1P signaling important for cancer progression and highlights its important role in the tumor microenvironment. Further studies to investigate the roles of tumor IF in cancer progression is necessary to address this issue.

**Acknowledgments** We gratefully acknowledge the VCU Lipidomics Core, which is supported in part by funding from the NIH-NCI Cancer Center Support Grant P30CA016059.

**Author Contribution** MN and KT conceived the study. MN, AY, TA, WCH, KPT, BA, carried out experiments. HM developed the IF collection tube. JCA performed mass spectrometry analysis. MN and TK wrote the manuscript with assistance from OMR, TW, SS and SM.

**Compliance with Ethical Standards**

**Conflict of Interest** The authors declare no conflict of interest.

**Funding** MN was a Japan Society for the Promotion of Science Postdoctoral Fellow. MN is supported by the Japan Society for the Promotion of Science (JSPS) Grant-in-Aid for Scientific Research Grant Number 15H05676 and 15 K15471, the Uehara Memorial Foundation, Nakayama Cancer Research Institute, Takeda Science Foundation, and Tsukada Medical Foundation. JT is supported by the JSPS Grant-in-Aid for Scientific Research Grant Number 16 K19888. KT is supported by NIH/NCI grant R01CA160688 and Susan G. Komen Investigator Initiated Research Grant IIR12222224. SS is supported by NIH/NCI grant R01CA61774 and in part by the DoD BCRP program under award number W81XWH-14-1-0086. KPT is supported by T32CA085159.

## References

1. Hanahan D, Weinberg RA. Hallmarks of cancer: the next generation. Cell. 2011;144(5):646–74. doi:10.1016/j.cell.2011.02.013.
2. Wiig H, Tenstad O, Iversen PO, Kalluri R, Bjerkvig R. Interstitial fluid: the overlooked component of the tumor microenvironment? Fibrogenesis Tissue Repair. 2010;3:12. doi:10.1186/1755-1536-3-12.
3. Haslene-Hox H, Oveland E, Berg KC, Kolmannskog O, Woie K, Salvesen HB, et al. A new method for isolation of interstitial fluid from human solid tumors applied to proteomic analysis of ovarian carcinoma tissue. PLoS One. 2011;6(4):e19217. doi:10.1371/journal.pone.0019217.
4. Wiig H, Swartz MA. Interstitial fluid and lymph formation and transport: physiological regulation and roles in inflammation and cancer. Physiol Rev. 2012;92(3):1005–60. doi:10.1152/physrev.00037.2011.
5. Takabe K, Spiegel S. Export of sphingosine-1-phosphate and cancer progression. J Lipid Res. 2014. doi:10.1194/jlr.R046656.
6. Spiegel S, Milstien S. Sphingosine-1-phosphate: an enigmatic signalling lipid. Nat Rev Mol Cell Biol. 2003;4(5):397–407. doi:10.1038/nrm1103 nrm1103.

7. Daum G, Grabski A, Reidy MA. Sphingosine 1-phosphate: a regulator of arterial lesions. Arterioscler Thromb Vasc Biol. 2009;29(10):1439–43. doi:10.1161/atvbaha.108.175240.
8. Pyne NJ, Pyne S. Sphingosine 1-phosphate and cancer. Nat Rev Cancer. 2010;10(7):489–503. doi:10.1038/nrc2875.
9. Takabe K, Paugh SW, Milstien S, Spiegel S. "Inside-out" signaling of sphingosine-1-phosphate: therapeutic targets. Pharmacol Rev. 2008;60(2):181–95. doi:10.1124/pr.107.07113.
10. Kim RH, Takabe K, Milstien S, Spiegel S. Export and functions of sphingosine-1-phosphate. Biochim Biophys Acta. 2009;1791(7):692–6. doi:10.1016/j.bbalip.2009.02.011.
11. Spiegel S, Milstien S. The outs and the ins of sphingosine-1-phosphate in immunity. Nat Rev Immunol. 2011;11(6):403–15. doi:10.1038/nri2974.
12. Takabe K, Kim RH, Allegood JC, Mitra P, Ramachandran S, Nagahashi M et al. Estradiol induces export of sphingosine 1-phosphate from breast cancer cells via ABCC1 and ABCG2. J Biol Chem. 2010;285(14):10477–86. doi:10.1074/jbc.M109.064162 .
13. Nagahashi M, Ramachandran S, Kim EY, Allegood JC, Rashid OM, Yamada A, et al. Sphingosine-1-phosphate produced by sphingosine kinase 1 promotes breast cancer progression by stimulating angiogenesis and lymphangiogenesis. Cancer Res. 2012;72(3):726–35. doi:10.1158/0008-5472.can-11-2167.
14. Liang J, Nagahashi M, Kim EY, Harikumar KB, Yamada A, Huang WC, et al. Sphingosine-1-phosphate links persistent STAT3 activation, chronic intestinal inflammation, and development of colitis-associated cancer. Cancer Cell. 2013;23(1):107–20. doi:10.1016/j.ccr.2012.11.013.
15. Allende ML, Sasaki T, Kawai H, Olivera A, Mi Y, van Echten-Deckert G, et al. Mice deficient in sphingosine kinase 1 are rendered lymphopenic by FTY720. J Biol Chem. 2004;279(50):52487–92. doi:10.1074/jbc.M406512200.
16. Mizugishi K, Yamashita T, Olivera A, Miller GF, Spiegel S, Proia RL. Essential role for sphingosine kinases in neural and vascular development. Mol Cell Biol. 2005;25(24):11113–21. doi:10.1128/MCB.25.24.11113-11121.2005.
17. Rashid OM, Nagahashi M, Ramachandran S, Dumur C, Schaum J, Yamada A, et al. An improved syngeneic orthotopic murine model of human breast cancer progression. Breast Cancer Res Treat. 2014;147(3):501–12. doi:10.1007/s10549-014-3118-0.
18. Wiig H, Aukland K, Tenstad O. Isolation of interstitial fluid from rat mammary tumors by a centrifugation method. Am J Phys Heart Circ Phys. 2003;284(1):H416–24. doi:10.1152/ajpheart.00327.2002.
19. Aukland K. Distribution volumes and macromolecular mobility in rat tail tendon interstitium. Am J Phys. 1991;260(2 Pt 2):H409–19.
20. Hait NC, Allegood J, Maceyka M, Strub GM, Harikumar KB, Singh SK, et al. Regulation of histone acetylation in the nucleus by sphingosine-1-phosphate. Science. 2009;325(5945):1254–7. doi:10.1126/science.1176709.
21. Nagahashi M, Kim EY, Yamada A, Ramachandran S, Allegood JC, Hait NC, et al. Spns2, a transporter of phosphorylated sphingoid bases, regulates their blood and lymph levels, and the lymphatic network. FASEB J. 2013;27(3):1001–11. doi:10.1096/fj.12-219618.
22. Cyster JG, Schwab SR. Sphingosine-1-phosphate and lymphocyte egress from lymphoid organs. Annu Rev Immunol. 2012;30:69–94. doi:10.1146/annurev-immunol-020711-075011.
23. Kawamori T, Kaneshiro T, Okumura M, Maalouf S, Uflacker A, Bielawski J, et al. Role for sphingosine kinase 1 in colon carcinogenesis. FASEB J. 2009;23(2):405–14. doi:10.1096/fj.08-117572.
24. Snider AJ, Kawamori T, Bradshaw SG, Orr KA, Gilkeson GS, Hannun YA, et al. A role for sphingosine kinase 1 in dextran sulfate sodium-induced colitis. FASEB J. 2009;23(1):143–52. doi:10.1096/fj.08-118109.
25. Olivera A, Mizugishi K, Tikhonova A, Ciaccia L, Odom S, Proia RL, et al. The sphingosine kinase-sphingosine-1-phosphate axis is a determinant of mast cell function and anaphylaxis. Immunity. 2007;26(3):287–97. doi:10.1016/j.immuni.2007.02.008.
26. Sensken SC, Bode C, Nagarajan M, Peest U, Pabst O, Graler MH. Redistribution of sphingosine 1-phosphate by sphingosine kinase 2 contributes to lymphopenia. J Immunol. 2010;184(8):4133–42. doi:10.4049/jimmunol.0903358.
27. Hammad SM, Pierce JS, Soodavar F, Smith KJ, Al Gadban MM, Rembiesa B, et al. Blood sphingolipidomics in healthy humans: impact of sample collection methodology. J Lipid Res. 2010;51(10):3074–87. doi:10.1194/jlr.D008532.
28. Lan T, Bi H, Liu W, Xie X, Xu S, Huang H. Simultaneous determination of sphingosine and sphingosine 1-phosphate in biological samples by liquid chromatography-tandem mass spectrometry. J Chromatogr B Anal Technol Biomed Life Sci. 2011;879(7–8):520–6. doi:10.1016/j.jchromb.2011.01.015.
29. Alberg AJ, Armeson K, Pierce JS, Bielawski J, Bielawska A, Visvanathan K, et al. Plasma sphingolipids and lung cancer: a population-based, nested case-control study. Cancer Epidemiol Biomark Prev. 2013;22(8):1374–82. doi:10.1158/1055-9965.epi-12-1424.
30. Azuma H, Takahara S, Ichimaru N, Wang JD, Itoh Y, Otsuki Y, et al. Marked prevention of tumor growth and metastasis by a novel immunosuppressive agent, FTY720, in mouse breast cancer models. Cancer Res. 2002;62(5):1410–9.
31. Azuma H, Horie S, Muto S, Otsuki Y, Matsumoto K, Morimoto J, et al. Selective cancer cell apoptosis induced by FTY720; evidence for a Bcl-dependent pathway and impairment in ERK activity. Anticancer Res. 2003;23(4):3183–93.
32. Brinkmann V, Billich A, Baumruker T, Heining P, Schmouder R, Francis G, et al. Fingolimod (FTY720): discovery and development of an oral drug to treat multiple sclerosis. Nat Rev Drug Discov. 2010;9(11):883–97. doi:10.1038/nrd3248.
33. Lim KG, Tonelli F, Li Z, Lu X, Bittman R, Pyne S, et al. FTY720 analogues as sphingosine kinase 1 inhibitors: enzyme inhibition kinetics, allosterism, proteasomal degradation, and actin rearrangement in MCF-7 breast cancer cells. J Biol Chem. 2011;286(21):18633–40. doi:10.1074/jbc.M111.220756.
34. Tonelli F, Lim KG, Loveridge C, Long J, Pitson SM, Tigyi G, et al. FTY720 and (S)-FTY720 vinylphosphonate inhibit sphingosine kinase 1 and promote its proteasomal degradation in human pulmonary artery smooth muscle, breast cancer and androgen-independent prostate cancer cells. Cell Signal. 2010;22(10):1536–42. doi:10.1016/j.cellsig.2010.05.022.
35. Van Brocklyn JR, Jackson CA, Pearl DK, Kotur MS, Snyder PJ, Prior TW. Sphingosine kinase-1 expression correlates with poor survival of patients with glioblastoma multiforme: roles of sphingosine kinase isoforms in growth of glioblastoma cell lines. J Neuropathol Exp Neurol. 2005;64(8):695–705.
36. Ruckhaberle E, Rody A, Engels K, Gaetje R, von Minckwitz G, Schiffmann S, et al. Microarray analysis of altered sphingolipid metabolism reveals prognostic significance of sphingosine kinase 1 in breast cancer. Breast Cancer Res Treat. 2008;112(1):41–52. doi:10.1007/s10549-007-9836-9.
37. Li W, Yu CP, Xia JT, Zhang L, Weng GX, Zheng HQ, et al. Sphingosine kinase 1 is associated with gastric cancer progression and poor survival of patients. Clin Cancer Res. 2009;15(4):1393–9. doi:10.1158/1078-0432.ccr-08-1158.
38. Liu SQ, Su YJ, Qin MB, Mao YB, Huang JA, Tang GD. Sphingosine kinase 1 promotes tumor progression and confers malignancy phenotypes of colon cancer by regulating the focal adhesion kinase pathway and adhesion molecules. Int J Oncol. 2013;42(2):617–26. doi:10.3892/ijo.2012.1733.

39. Pyne S, Edwards J, Ohotski J, Pyne NJ. Sphingosine 1-phosphate receptors and sphingosine kinase 1: novel biomarkers for clinical prognosis in breast, prostate, and hematological cancers. Front Oncol. 2012;2:168. doi:10.3389/fonc.2012.00168.

40. Ponnusamy S, Selvam SP, Mehrotra S, Kawamori T, Snider AJ, Obeid LM, et al. Communication between host organism and cancer cells is transduced by systemic sphingosine kinase 1/sphingosine 1-phosphate signalling to regulate tumour metastasis. EMBO Mol Med. 2012;4(8):761–75. doi:10.1002/emmm.201200244.

Published OnlineFirst January 19, 2018; DOI: 10.1158/0008-5472.CAN-17-1423

Tumor Biology and Immunology

Cancer Research

# Targeting the SphK1/S1P/S1PR1 Axis That Links Obesity, Chronic Inflammation, and Breast Cancer Metastasis

Masayuki Nagahashi[1,2,3], Akimitsu Yamada[2,3,4], Eriko Katsuta[2,5,3], Tomoyoshi Aoyagi[2,3], Wei-Ching Huang[2,3], Krista P. Terracina[2,3], Nitai C. Hait[3,5,6], Jeremy C. Allegood[3], Junko Tsuchida[1], Kizuki Yuza[1], Masato Nakajima[1], Manabu Abe[7], Kenji Sakimura[7], Sheldon Milstien[3], Toshifumi Wakai[1], Sarah Spiegel[3], and Kazuaki Takabe[1,2,3,5,8,9,10]

## Abstract

Although obesity with associated inflammation is now recognized as a risk factor for breast cancer and distant metastases, the functional basis for these connections remain poorly understood. Here, we show that in breast cancer patients and in animal breast cancer models, obesity is a sufficient cause for increased expression of the bioactive sphingolipid mediator sphingosine-1-phosphate (S1P), which mediates cancer pathogenesis. A high-fat diet was sufficient to upregulate expression of sphingosine kinase 1 (SphK1), the enzyme that produces S1P, along with its receptor S1PR1 in syngeneic and spontaneous breast tumors. Targeting the SphK1/S1P/S1PR1 axis with FTY720/fingolimod attenuated key proinflammatory cytokines, macrophage infiltration, and tumor progression induced by obesity. S1P produced in the lung premetastatic niche by tumor-induced SphK1 increased macrophage recruitment into the lung and induced IL6 and signaling pathways important for lung metastatic colonization. Conversely, FTY720 suppressed IL6, macrophage infiltration, and S1P-mediated signaling pathways in the lung induced by a high-fat diet, and it dramatically reduced formation of metastatic foci. In tumor-bearing mice, FTY720 similarly reduced obesity-related inflammation, S1P signaling, and pulmonary metastasis, thereby prolonging survival. Taken together, our results establish a critical role for circulating S1P produced by tumors and the SphK1/S1P/S1PR1 axis in obesity-related inflammation, formation of lung metastatic niches, and breast cancer metastasis, with potential implications for prevention and treatment.

**Significance:** These findings offer a preclinical proof of concept that signaling by a sphingolipid may be an effective target to prevent obesity-related breast cancer metastasis. *Cancer Res; 78(7); 1713–25.* *©2018 AACR.*

[1]Division of Digestive and General Surgery, Niigata University Graduate School of Medical and Dental Sciences, Niigata City, Niigata, Japan. [2]Division of Surgical Oncology, Department of Surgery, Virginia Commonwealth University School of Medicine, Richmond, Virginia. [3]Departments of Biochemistry and Molecular Biology, Virginia Commonwealth University School of Medicine, Richmond, Virginia. [4]Breast and Thyroid Surgery, Yokohama City University Medical Center, Kanagawa, Japan. [5]Division of Breast Surgery, Department of Surgical Oncology, Roswell Park Comprehensive Cancer Center, Buffalo, New York. [6]Department of Molecular and Cellular Biology, Roswell Park Comprehensive Cancer Center, Buffalo, New York. [7]Department of Cellular Neurobiology, Brain Research Institute, Niigata University, Niigata City, Niigata, Japan. [8]Department of Surgery, University at Buffalo Jacobs School of Medicine and Biomedical Sciences, The State University of New York, Buffalo, New York. [9]Department of Breast Surgery and Oncology, Tokyo Medical University, Tokyo, Japan. [10]Department of Surgery, Yokohama City University, Yokohama, Japan.

**Note:** Supplementary data for this article are available at Cancer Research Online (http://cancerres.aacrjournals.org/).

M. Nagahashi and A. Yamada contributed equally to this article.

**Corresponding Authors:** Masayuki Nagahashi, Division of Digestive and General Surgery, Niigata University Graduate School of Medical and Dental Sciences, 1-757 Asahimachi-dori, Chuo-ku, Niigata City 951-8510, Japan. Phone: 812-5227-2228; Fax: 812-5227-0779; E-mail: mnagahashi@med.niigata-u.ac.jp; and Kazuaki Takabe, Breast Surgery, Department of Surgical Oncology, Roswell Park Comprehensive Cancer Center, Buffalo, NY 14263. Phone: 716-845-2918; Fax: 716-845-1668; E-mail: kazuaki.takabe@roswellpark.org

**doi:** 10.1158/0008-5472.CAN-17-1423



## Introduction

Obesity has drastically increased to become one of the leading health concerns in the United States (1), and is now recognized as a risk factor for breast cancer incidence, progression, recurrence, and prognosis (2, 3). Epidemiologic and clinical studies indicate that obesity increases breast cancer risk by approximately 40% in postmenopausal women and is associated with endocrine therapy resistance (2, 4). Obese breast cancer patients are more likely to be diagnosed with larger, higher-grade tumors, have an increased incidence of distant metastases, and elevated risks of recurrence and death (3, 5). However, the mechanisms by which obesity increases breast cancer incidence and worsens prognosis remain ill defined.

High body weight has also been associated with larger and more aggressive tumors in animal models of breast cancer (6–10). Obesity in both humans and rodents is characterized by increased production of insulin and growth factors, low-grade chronic inflammation, and secretion of proinflammatory cytokines that regulate breast cancer development and progression (11–13). Animal models that recapitulate human cancers, such as syngeneic or transgenic murine models with intact immune functions, have provided important clues to the critical roles of the cytokines TNFα and IL6, and have highlighted the key roles played by the master transcription factors NFκB and STAT3 in the link between chronic inflammation and

Published OnlineFirst January 19, 2018; DOI: 10.1158/0008-5472.CAN-17-1423



breast cancer (14–16). Infiltration of macrophages (12) that produce these cytokines into the tumor microenvironment is now recognized as an important enabler of cancer progression, and tumor-associated macrophages (TAM) correlate with increased angiogenesis, metastasis, and decreased survival of breast cancer patients (17). Macrophages have also been shown to be recruited to premetastatic niches, specialized microenvironments in distant organs primed by factors secreted from cancer cells that promote metastatic progression (18–20), but the underlying mechanisms guiding their assembly are largely unknown.

There is growing evidence that sphingosine-1-phosphate (S1P), a pleiotropic bioactive sphingolipid metabolite enriched both in blood and lymphatic fluid is involved in inflammation, obesity, and breast cancer (21). S1P generated by activation of sphingosine kinase 1 (SphK1) is exported out of cells and signals through specific S1P receptors to regulate numerous cellular processes important for breast cancer, including cell growth, survival, invasion, immune cell trafficking, vascular integrity, angiogenesis, and cytokine and chemokine production (22–25). Previous clinical studies have shown that SphK1 is overexpressed in breast cancer and its expression is associated with poor patient outcomes (26, 27). Because it has been suggested that S1P levels are elevated in plasma of obese humans and rodents (28), in this work we explored the role of S1P in obesity promoted breast cancer in patients and in animal models. We uncovered that the SphK1/S1P/S1PR1 axis is a critical factor linking obesity, low-grade chronic inflammation, and breast cancer, identified S1P as an important new factor in metastatic niche formation and demonstrated that targeting the SphK1/S1P/S1PR1 axis is an effective treatment for metastatic breast cancer exacerbated by obesity.

## Materials and Methods

### Cell culture

A C57Bl/6 mouse mammary fat pad–derived adenocarcinoma cell line E0771 was obtained from CH3 BioSystems. A BALB/c mouse mammary fat pad–derived adenocarcinoma cell line 4T1-luc2 that has been engineered to express luciferase was obtained from PerkinElmer. E0771 cells were cultured in DMEM with 10% FBS. 4T1-luc2 cells were cultured in RPMI medium 1640 with 10% FBS. SphK1 was overexpressed by transfection with Lipofectamine Plus (Invitrogen) as described (29). Transfection efficiency was determined by quantitative PCR (qPCR) and Western blot analysis. All these cell lines were used within 10 passages after reception in the current experiments, and have been routinely tested for mycoplasma contamination using the PCR Mycoplasma Detection Kit (ABM) and the last mycoplasma test was performed in August 2017. Mycoplasma-free cell lines were used in all of our experiments.

### Patient samples

Blood was taken prior to operation from 19 breast cancer patients who did not have any complications, and underwent surgery at Niigata University Medical and Dental Hospital. Serum was separated by centrifugation, and preserved at −180°C. All the patients were Japanese, and obesity was defined as body mass index (BMI) 25 kg/m$^2$ among that population. Collection and use of all specimens in this study were approved by the Institutional Review Board of Niigata University. Written informed consent was obtained from all participants and the studies were conducted in accordance with the Declaration of Helsinki.

### Animal models

All animal studies were conducted in the Animal Research Core Facility at VCU School of Medicine in accordance with the institutional guidelines. Animals were bred and maintained in a pathogen-free environment and all procedures were approved by the VCU Institutional Animal Care and Use Committee (IACUC) that is accredited by Association for Assessment and Accreditation of Laboratory Animal Care.

Female C57Bl/6 mice and BALB/c mice were obtained from Jackson Labs. Mice were fed with either normal diet (ND) or high-fat diet (HFD; TD.88137, Harlan Labs) containing cholesterol (0.2%), total fat (21% by weight; 42% kcal from fat), saturated fatty acids (>60% of total fatty acids), sucrose (34% by weight), protein (17.3% by weight), and carbohydrate (48.5% by weight) for 12 weeks prior to implantation of cancer cells. E0771 breast cancer cells ($5 \times 10^4$ cells in 10-μL Matrigel) were surgically implanted in the upper mammary fat pad under direct visualization as described previously (23). Tumor size was measured with calipers every 2 days and total tumor volume was estimated by the cylinder formula. Tumor-bearing mice were randomized 2 days after implantation prior to treatment with saline or FTY720. FTY720 (Cayman Chemicals) was administered by gavage at a dose of 1 mg/kg/day in PBS. Mice were sacrificed by exsanguination, blood was collected, tumors excised, weighed, fixed in formalin, and embedded in paraffin or frozen in liquid nitrogen. For survival studies, mice were euthanized according to a morbidity scale approved by IACUC.

For tumor-conditioned media (TCM) treatments, mice were injected intraperitoneally with TCM (300 μL) from E0771, HeLa, or 4T1-luc2 cells overexpressing *Sphk1* or from vector-transfected cells for 5 days prior to tail vein injections of E0771 cells or 4T1 cells ($1 \times 10^5$/100 μL/mouse), respectively, as described previously (19, 20, 30). Metastatic lesions in the lung were determined histologically, by examining hematoxyin and eosin (H&E)–stained sections.

For the spontaneously developed breast cancer model, male MMTV-PyMT mice on a FVB/N background (Jackson Laboratories) were randomly bred with normal FVB/N females to obtain females heterozygous for the PyMT oncogene. Female heterozygous mice developed palpable mammary tumors as early as 5 weeks of age. Tumor sizes were measured every 3 days by caliper and total tumor volume was estimated by the cylinder formula (31). HFD or ND feeding and FTY720 administration was started at weaning.

### Bioluminescent quantification of tumor burden

D-Luciferin (0.2-mL of 15 mg/mL stock, PerkinElmer) was injected intraperitoneally into mice previously implanted with 4T1-luc2 cells, and Living Image Software (Xenogen) was used to quantify the photons/second emitted by the cells as described previously (23).

### Interstitial fluid collection

Interstitial fluid (IF) from breast and breast tumors was collected as described previously (32, 33). Briefly, tissue was excised and placed in preweighed tubes on ice. Tubes were reweighed to

Published OnlineFirst January 19, 2018; DOI: 10.1158/0008-5472.CAN-17-1423



determine tissue weight and the tissue was sectioned several times with scissors. Samples were then transferred into inserts capped with nylon mesh, and placed into preweighed centrifuge tubes. The tubes were centrifuged at 100 × *g* for 10 minutes at 4°C and the IF accumulated in the bottom. The volume of IF was quantified by weight. PBS containing phosphatase inhibitors (100 μL) was added to the IF and the tubes were centrifuged at 1,000 × *g* for 10 minutes at 4°C to remove any contaminating cells.

### Quantification of S1P and dihydro-S1P by mass spectrometry

Lipids were extracted from blood, tissues, and interstitial fluid, and S1P and dihydro-S1P quantified by liquid chromatography, electrospray ionization-tandem mass spectrometry (LC-ESI-MS/MS, 4000 QTRAP, AB Sciex) as described previously (23, 34, 35).

### Histopathologic analysis

Tissue slices (5 μm) were stained with H&E for morphologic analysis. Paraffin-embedded slides were deparaffinated, and antigen unmasking was carried out by microwave heating in citrate buffer for 20 minutes. Slides were incubated with 3% $H_2O_2$ and then with goat or horse serum (DAKO) for 30 minutes at room temperature. After washing with PBS, slides were incubated at 4°C overnight with the following primary antibodies with indicated dilutions: IL6 (1:200, Abcam), SphK1 (1:100, Abcam), S1PR1 (1:100, Santa Cruz Biotechnology), Ki-67 (1:25, Dako). Biotinylated secondary antibodies (1:200) were added and incubated at room temperature for 20 minutes. After 5 minutes with streptavidin–HRP, sections were stained with DAB substrate and counterstained with hematoxylin. Slides were examined with a Zeiss Axioimager A1 (Jena) and images captured with an AxioCam MRc camera.

### Immunofluorescence analysis

Tumors were also frozen, and embedded in optimal cutting medium (OCT 4583; Sakura Finetek) for immunofluorescence analysis. Sections were fixed in 4% paraformaldehyde, blocked with horse serum containing 2.5% of fraction V for 1 hour, and then stained with primary antibodies at 4°C overnight: anti–IL6 (1:200, Abcam), or anti-F4/80 (1:200, AbD Serotec). After two washes with PBS, sections were stained with Alexa488- and Alexa594-conjugated secondary antibodies (1:500, Invitrogen) for 30 minutes. Nuclei were counterstained with Hoechst 33432 (Invitrogen) for 5 minutes. Slides were mounted and examined with a LSM710 laser-scanning confocal microscope (Zeiss).

### Immunoblotting

Frozen tissue samples were homogenized and sonicated in 300 μL of buffer containing 50 mmol/L HEPES (pH 7.4), 150 mmol/L NaCl, 1 mmol/L EDTA, 1% Triton X-100, 2 mmol/L sodium orthovanadate, 4 mmol/L sodium pyrophosphate, 100 mmol/L NaF, 1:500 protease inhibitor mixture (Sigma). Equal amounts of proteins were separated by SDS-PAGE, transblotted to nitrocellulose, and immunopositive bands visualized by ECL (36).

### Real-time PCR

Total RNA was isolated from tissues and cells using TRIzol (Life Technologies) and reverse transcribed with the High Capacity cDNA Reverse Transcription Kit. Premixed primer-probe sets and TaqMan Universal PCR Master Mix (Applied Biosystems) were employed to examine mRNA levels. cDNAs were diluted 10-fold (for the target genes) or 100-fold (for GAPDH) and amplified using the ABI7900HT cycler. *Gapdh* mRNA was used as an internal control to normalize mRNA expression.

### Statistical analysis

Statistical analysis was performed using unpaired two-tailed Student *t* test for comparison of two groups and ANOVA followed by *post hoc* tests for multiple comparisons (GraphPad Prism). $P < 0.05$ was considered significant. Experiments were repeated at least three times in triplicate with consistent results. *In vivo* experiments were repeated three times and each experimental group consisted of at least six mice.

## Results

### Obesity increases S1P levels in breast cancer patients and in a syngeneic breast cancer model

Because obesity is now recognized as an independent prognostic factor for breast cancer patients (37, 38), and we have shown that S1P levels are elevated in breast tumors (23), it was of interest to examine the effects of obesity on S1P levels in breast cancer patients that did not yet receive therapy. S1P levels in serum from obese breast cancer patients were significantly higher than those from nonobese patients (Fig. 1A). Likewise, serum levels of dihydro-S1P, which also binds to all S1P receptors, were significantly higher in the obese patients (Fig. 1A).

Next, HFD induced obesity in C57Bl/6 mice, a common model because of its similarities to metabolic changes in obese humans, was used to investigate the mechanisms underlying obesity-promoted breast cancer progression. To this end, E0771 mouse breast cancer cells were implanted into mammary fat pad of syngeneic C57Bl/6 mice fed with HFD or ND for 12 weeks (Fig. 1B). As expected, mice fed with HFD developed significantly larger tumors within 30 days than those on ND (Fig. 1C). HFD significantly increased S1P levels in both normal mammary fat pad and breast tumors (Fig. D). HFD also significantly increased S1P levels in the tumor IF, which is a component of the tumor microenvironment and bathes cancer cells in the tumor (Fig. 1D). This is in agreement with our previous finding that tumor generated S1P is secreted into tumor IF (33), and that S1P levels are higher in human breast cancer and its tumor IF compared with those of normal breast tissue (33, 39). Similar to patients, levels of S1P in serum from nontumor-bearing mice and tumor-bearing mice fed with HFD were also significantly increased compared with mice on ND, and the difference between mice fed with ND and those with HFD were larger in the tumor bearing mice than nontumor-bearing mice (Fig. 1D). Moreover, S1P levels in the lung were also increased in the mice fed with HFD regardless of tumor existence (Fig. 1D). Consistent with elevation of S1P in tumors, expression of SphK1, but not SphK2, and S1PR1, albeit to a much lesser extent, was increased in the tumors from mice fed HFD (Fig. 1E).

### The SphK1/S1P/S1PR1 axis connects obesity, chronic inflammation, and breast cancer progression

To investigate the involvement of the S1P/S1PR1 axis in tumor progression in obese animals, we utilized the prodrug FTY720/fingolimod that is phosphorylated *in vivo* to its active form FTY720-P, an S1P mimetic that acts as a functional antagonist of S1PR1 by inducing its internalization and

Published OnlineFirst January 19, 2018; DOI: 10.1158/0008-5472.CAN-17-1423



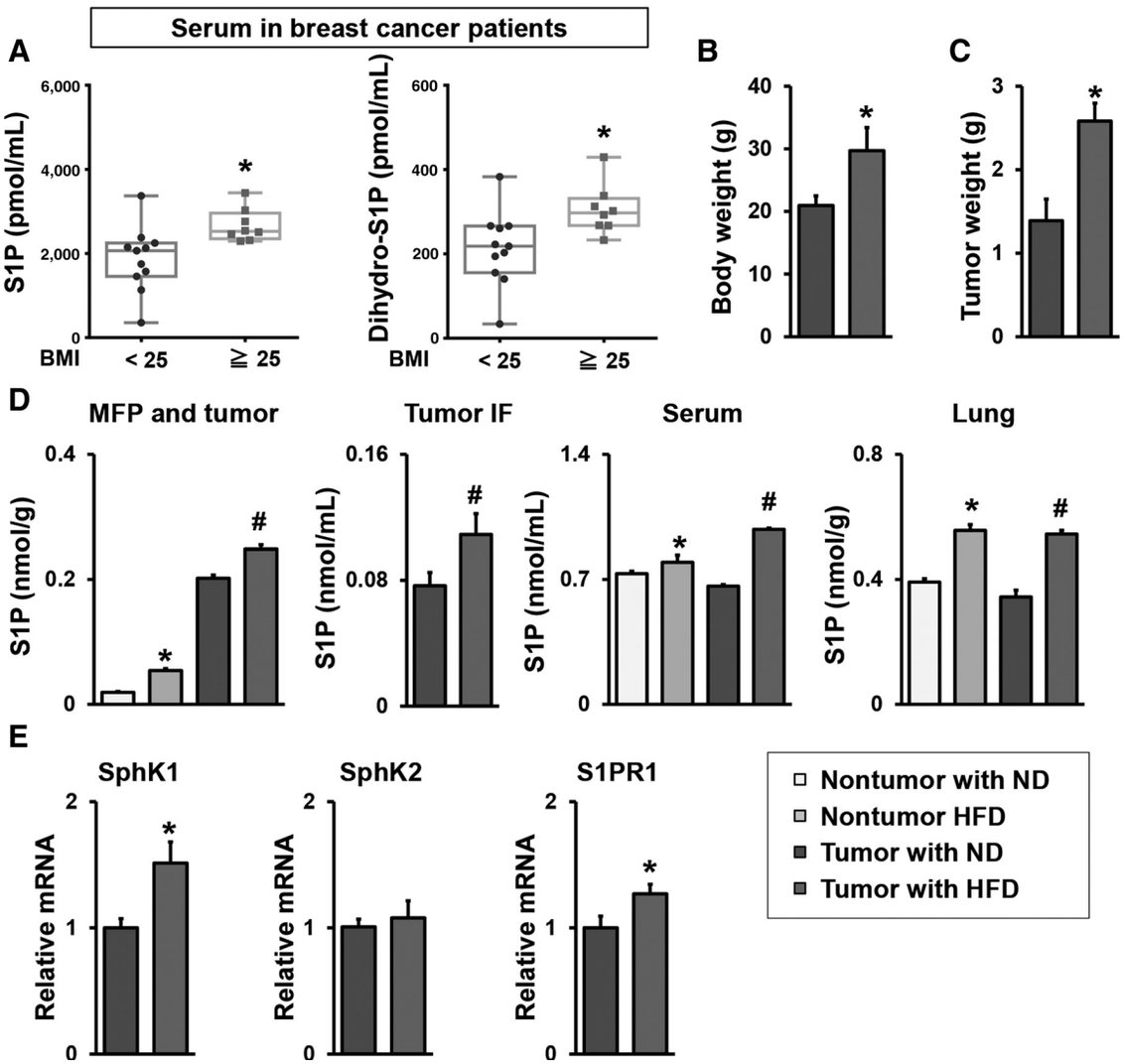


**Figure 1.**

Obesity increased circulating levels of S1P in humans and mice with breast cancer. **A,** S1P and dihydro-S1P levels in serum from preoperative breast cancer patients with BMI < 25 kg/m$^2$ ($n = 11$), or BMI 25 kg/m$^2$ ($n = 8$) were measured by LC-ESI-MS/MS. The S1P and dihydro-S1P levels are shown in the box plot. The central rectangle spans the first quartile to the third quartile. A segment inside the rectangle shows the median and "whiskers" above and below the box shows the value of the minimum and maximum. All data points are also shown as dots. *, $P < 0.05$. **B–E,** The SphK1/S1P/S1PR1 axis in HFD promoted breast cancer progression. **B,** Prior to implantation of E0771 cells into the chest mammary fat pad under direct vision, C57Bl/6 mice were fed ND or HFD for 12 weeks and body weight was measured. **C,** Tumors were harvested 30 days after the implantation, and the tumor weight was measured. Data are means ± SEM. *, $P < 0.05$. **D,** Levels of S1P in mammary fat pad (MFP) and breast tumors, tumor IF, serum without or with breast tumors, and lung without or with breast tumors from mice fed with ND or HFD were measured by LC-ESI-MS/MS. **E,** Expression of *Sphk1*, *Sphk2*, and *S1pr1* in breast tumors was determined by qPCR and normalized to *Gapdh* mRNA. Data are expressed as means ± SEM. *, $P < 0.05$.

degradation (40). When E0771 tumors in syngeneic mice on a HFD reached 5 mm in diameter, mice were treated orally daily with FTY720 (1 mg/kg) or saline. FTY720 significantly suppressed tumor progression determined by decreases of primary tumor volumes and tumor weights in the obese mice (Fig. 2A and B). FTY720 administration, however, did not significantly affect weight gain of HFD-fed mice (Fig. 2C), indicating that FTY720 did not affect diet intake. Treatment with FTY720 also significantly suppressed HFD-induced elevation of S1P in serum, tumors, and IF (Fig. 2D).

The proinflammatory cytokines, IL6 and TNFα, produced by tumor-infiltrating stromal cells, such as TAMs, are known to have important roles in obesity-related cancer progression (12). Indeed, expression of these cytokines was increased in the tumors of HFD-fed mice, compared with those fed ND, which was suppressed by FTY720 treatment (Fig. 2E). Moreover, as expected, HFD increased recruitment of TAMs, as revealed by immunofluorescence with anti-F4/80, (Fig. 2F). Of note, FTY720 dramatically decreased infiltration of TAMs in tumors of HFD-fed mice (Fig. 2F).

Published OnlineFirst January 19, 2018; DOI: 10.1158/0008-5472.CAN-17-1423



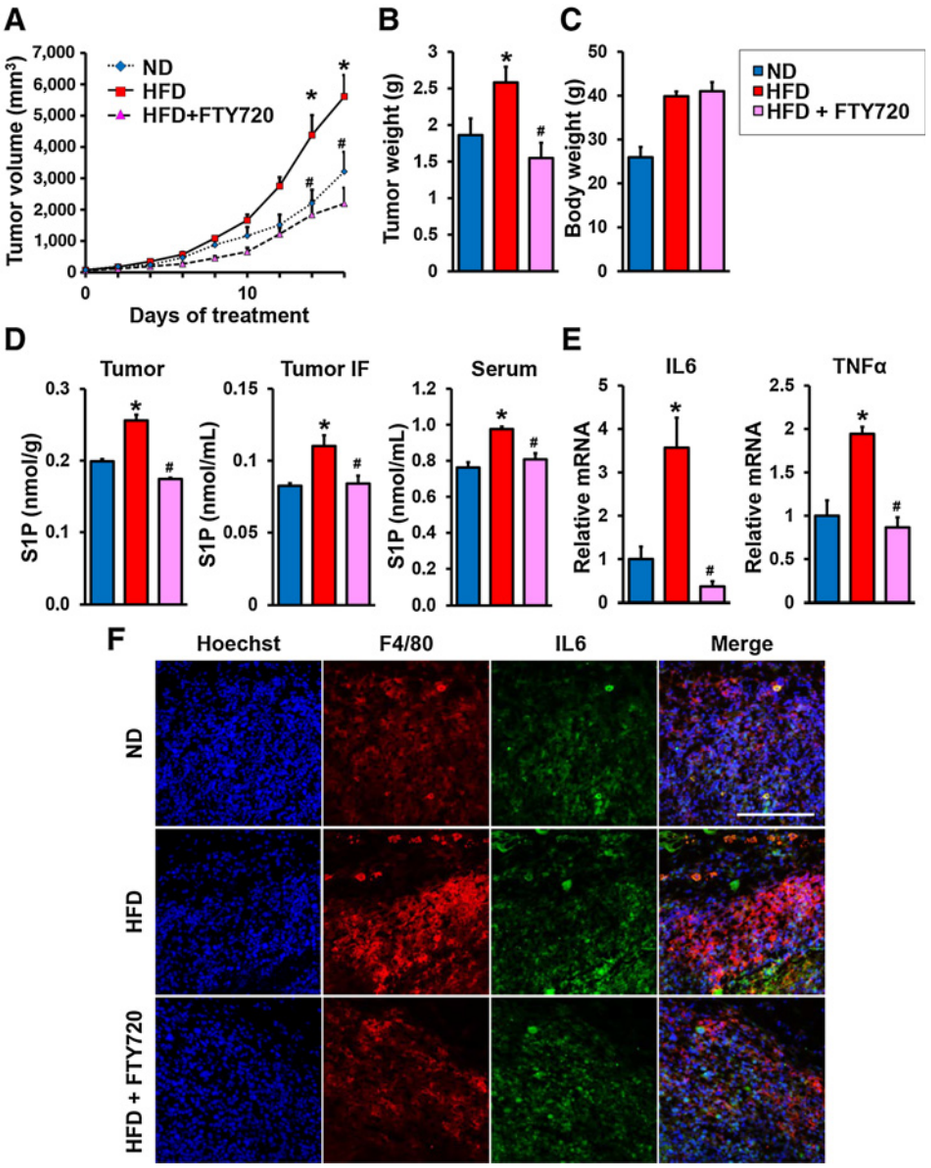


**Figure 2.**

The SphK1/S1P/S1PR1 axis connects obesity, chronic inflammation, and breast cancer progression. **A–E,** Mice were treated as above and when tumors reached 5 mm in diameter, HFD-fed mice were treated by gavage daily with PBS or FTY720 (1 mg/kg). **A,** Tumor volumes were measured on the indicated days. **B–E,** After treatment for 18 days, tumors were harvested and tumor and body weights determined (**B** and **C**). **D,** Levels of S1P in breast tumors, tumor IF, and serum were measured by LC-ESI-MS/MS. **E,** *Tnfα* and *IL6* mRNA levels in tumors were determined by qPCR and normalized to *Gapdh* mRNA. Data are expressed as means ± SEM. *, $P < 0.05$ versus ND; #, $P < 0.05$ versus HFD. **F,** Immunofluorescence analysis of tumors stained for IL6 (green), F4/80 (red), and Hoechst (blue). Scale bar, 100 μm.

**Targeting the SphK1/S1P/S1PR1 axis with FTY720 attenuates obesity-induced tumor progression and inflammation**

An obesogenic HFD has been shown to enhance primary tumorigenesis and metastasis in MMTV-PyMT transgenic mice, which spontaneously develop breast cancer accompanied by recruitment of TAMs and increased tissue inflammation (9, 10). Therefore, we also sought to examine the role of the SphK1/S1P/S1PR1 axis in the link between inflammation and obesity-promoted breast cancer progression in this mouse model that closely mimics progression of the human disease (41). Consistent with previous reports (7–10, 31), HFD increased tumor incidence, multiplicity, and size with a significant increase in proliferation determined by Ki67 staining (Fig. 3A and B). HFD feeding, which increased circulating S1P levels (Fig. 3C), also enhanced mRNA expression of SphK1, but not SphK2, and S1PR1 in tumors, corresponding with increased protein levels determined by IHC (Fig. 3D and E). Because we and others have shown that enhanced S1PR1 expression reciprocally activates STAT3, leading to its persistent activation and upregulation of IL6 expression (36, 42), we also studied the effects of interfering with S1P formation and S1PR1 function and this feed-forward amplification loop with FTY720. Daily administration of FTY720 to HFD-fed MMTV-PyMT transgenic mice not only decreased HFD-induced S1PR1 expression, but also, in agreement with the notion that it is an inhibitor of SphK1 and induces its proteasomal degradation (43, 44), FTY720 almost completely abrogated the increase in SphK1 protein in the tumors (Fig. 3D and E). Concomitantly, FTY720 administration prevented increased levels of circulating S1P (Fig. 3C), prevented activation of Stat3, and increases in IL6 expression, and reduced tumor development of HFD-fed MMTV-PyMT mice (Fig. 3).

Published OnlineFirst January 19, 2018; DOI: 10.1158/0008-5472.CAN-17-1423



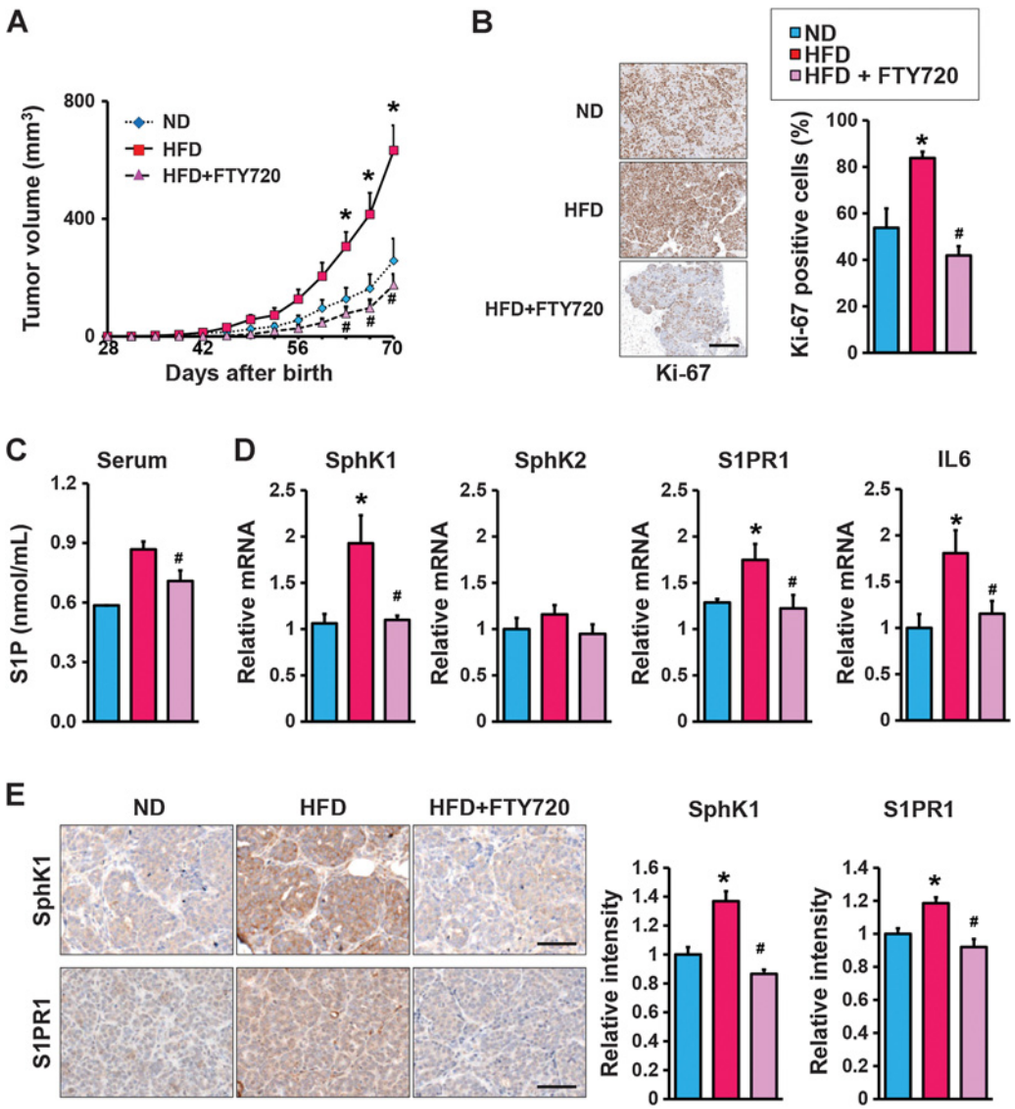


**Figure 3.**

Targeting the SphK1/S1P/S1PR1 axis with FTY720 mitigates HFD-induced inflammation and tumorigenesis in MMTV-PyMT transgenic mice. **A,** Beginning at 3 weeks of age, MMTV-PyMT transgenic mice were fed ND or HFD and treated daily by gavage with PBS or FTY720 (1 mg/kg). **A,** Spontaneous tumor sizes were determined on the indicated days. **B,** Tumor sections were stained with Ki67 antibody and percent Ki67–positive cells determined. Scale bar, 50 μm. **C,** Levels of S1P in serum were measured by LC-ESI-MS/MS. **D,** Expression of *Sphk1, Sphk2, S1pr1,* and *IL6* in breast tumors was determined by qPCR and normalized to *Gapdh* mRNA. **E,** Breast tumors were immunostained with anti-SphK1 or anti-S1PR1. Scale bar, 50 μm. Relative intensity of the immunostaining was quantified. Data are expressed as means ± SEM. *, $P < 0.05$ versus ND; #, $P < 0.05$ versus HFD.

### S1P produced by tumor SphK1 primes distant premetastatic sites

Our results show that S1P is secreted from the primary tumor into the tumor IF that drains into systemic circulation via lymphatic flow. Taken together with a recent study suggesting that S1P transported out of lymph endothelial cells by Spns2 can regulate metastatic colonization (45), it was intriguing to examine whether increased levels of circulating S1P can also promote formation of "premetastatic niches" in distant sites, such as the lung, that assist circulating cancer cells to form metastatic lesions at that location. To this end, prior to tail vein injections of E0771 breast cancer cells (Fig. 4A), mice were treated for 5 days with TCM from control or SphK1-overexpressing E0771 cells that contained increased levels of S1P (Fig. 4A; Supplementary Fig. S1).

Seven days after tumor challenge when there were no significant metastases, H&E staining showed extensive infiltration of inflammatory cells into the lungs of mice receiving TCM containing high levels of S1P (TCM-*Sphk1*) compared with those receiving control TCM (Fig. 4B). Histologic analysis also revealed extensive clusters of macrophages and greater IL6 staining (Fig. 4C). *Sphk1, S1pr1,* and *IL6* mRNA levels were also all significantly higher in those lungs (Fig. 4D). Furthermore, treating mice with TCM

Published OnlineFirst January 19, 2018; DOI: 10.1158/0008-5472.CAN-17-1423



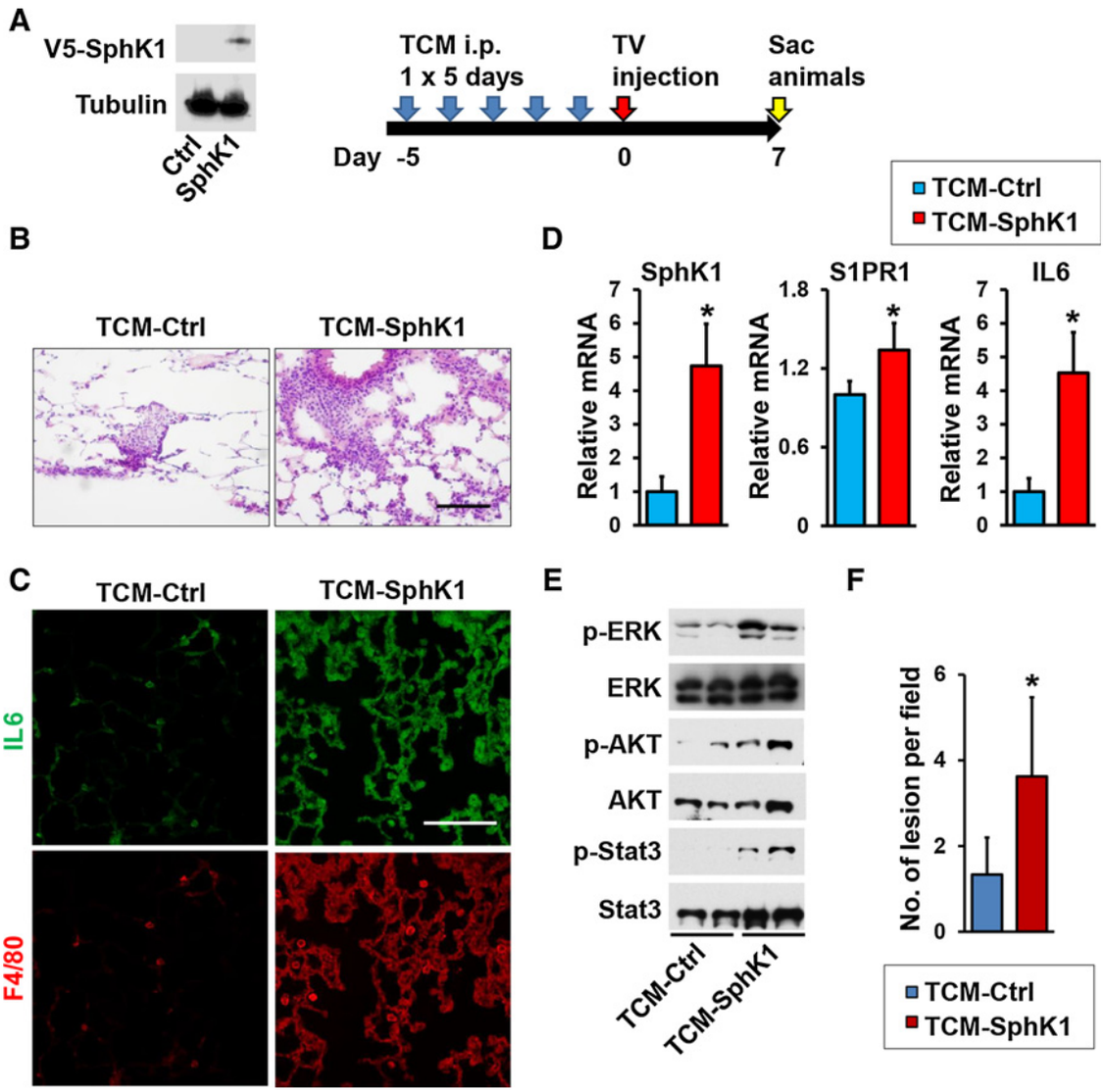


**Figure 4.**

S1P in tumor conditioned medium increased macrophage recruitment and induced factors and signaling pathways important for lung premetastatic niches. **A,** Equal amounts lysates of E0771 cells with SphK1 overexpression or control (Ctrl) analyzed by immunoblotting with the indicated antibodies (left). Schematic overview of regimen for examination of premetastatic niche formation in the lung utilizing TCM (right). **B–E,** Mice were treated with TCM from *Sphk1*-overexpressing E0771 cells (TCM-*Sphk1*) or control E0771 cells (TCM-Ctrl) for 5 days, followed by systemic tumor challenge. Lungs were harvested 7 days later. **B,** H&E staining of lung sections. Scale bar, 100 μm. **C,** Immunofluorescence analysis of lung sections stained for IL6 (green), F4/80 (red), and Hoechst (blue). Scale bar, 100 μm. **D,** Expression of *Sphk1, S1pr1*, and *IL6* mRNA in lungs determined by qPCR and normalized to levels of *Gapdh* mRNA. Data are means ± SEM. *, $P < 0.05$. **E,** Equal amounts of lung lysates analyzed by immunoblotting with the indicated antibodies. **F,** Quantitation of metastatic lesions in the mouse model with TV injection of 4T1-luc2. Data are means ± SD. *, $P < 0.05$ versus TCM-Ctrl.

generated from SphK1-expressing tumor cells, but not TCM derived from control tumor cells, activated ERK, Akt, and STAT3 (Fig. 4E), known survival signaling pathways downstream of S1P/S1PR1, that have been implicated in premetastatic niche formation (19, 36, 42). We confirmed our findings by repeating experiments utilizing tail vein injections of another breast cancer cell line of 4T1-luc2 after 5-day TCM treatment. As expected, histologic analysis revealed that there were increased metastatic foci in the lung in the mice treated with TCM-*Sphk1* compared with those treated with control TCM (Fig. 4F).

### FTY720 inhibits HFD-induced inflammation and lung-seeding ability for breast cancer cells

Because low-grade inflammation is induced by cancer, and obesity may exacerbate that inflammation, obesity has been suggested to increase cancer cell colonization and promote pulmonary breast cancer metastasis (6, 9, 10, 46). We next examined the involvement of the SphK1/S1P/S1PR1 axis in lung seeding ability for breast cancer cells. We performed tail vein injections of 4T1-luc2 cells after 5-day TCM-*Sphk1* treatment, and treated with clinically relevant doses of FTY720

Published OnlineFirst January 19, 2018; DOI: 10.1158/0008-5472.CAN-17-1423



(Fig. 5A), and found that FTY720 significantly decreased the tumor burden detected by IVIS imaging (Fig. 5B). To examine the effect of HFD, mice were fed HFD or ND for 12 weeks prior to treatment with TCM-*Sphk1* and subsequent intravenous injection of E0771 cells (Fig. 5C). The lungs of HFD-fed mice were heavier than those of mice fed ND, suggesting the presence of increased cancer cell–seeding lesions (Fig. 5D). Indeed, histologic analyses showed significantly increased numbers of cancer cell–seeding foci in the lungs of the HFD-fed mice (Fig. 5E). Moreover, HFD-induced obesity also increased recruitment of macrophages (Fig. 5F) that have been shown to mediate inflammatory responses, and increase expression of IL6 (Fig. 5F), which facilitate tumor cell recruitment, extravasation, and colonization into the niche (42, 46). S1P-stimulated signaling including pERK, pAKT, and pStat3, was also enhanced in lungs of mice fed HFD compared with ND (Fig. 5G). Importantly, treatment of mice fed HFD with clinically relevant doses of FTY720 dramatically suppressed HFD-induced formation of cancer cell–seeding foci (Fig. 5D and E), IL6, and macrophage infiltration (Fig. 5F), as well as S1P-mediated signaling pathways (Fig. 5G). Finally, we repeated experiments utilizing tail vein injections of 4T1-luc2 cells after 5-day TCM-*Sphk1* treatment into HFD-fed mice, and treated with FTY720 (Fig. 5H). We found significant decreases of tumor burden in the mice treated with FTY720 compared with control mice (Fig. 5H).

### FTY720 suppresses pulmonary metastasis in MMTV-PyMT transgenic and E0771 syngeneic orthotopic HFD-fed mice

In the metastatic lung colonization assay, cancer cells are injected intravenously and travel directly to the lung rather than from the primary tumor. Accordingly, we next tested the effect of FTY720 on obesity-related cancer metastasis of spontaneous and syngeneic breast tumors where cancer cells metastasize from the breast to the lung, more closely mimicking the pathology of the human disease. HFD enhanced pulmonary metastasis in MMTV-PyMT mice (Fig. 6A), consistent with previous reports (47). FTY720 administration drastically reduced lung metastases (Fig. 6A). Likewise, increased metastasis of breast cancer cells to the lung from E0771 orthotopic breast tumors was observed in mice fed HFD compared with those fed ND (Fig. 6B), with expression of SphK1 and S1PR1 significantly elevated in those lungs (Fig. 6C). Treatment of HFD-fed mice with FTY720 significantly reduced metastasis as well as expression of SphK1 and S1PR1 (Fig. 6B and C), indicating that elevated SphK1/S1P/S1PR1 correlates with HFD increased lung metastasis.

### FTY720 suppresses obesity-related inflammation and S1P signaling and prolongs survival in tumor-bearing mice

The key inflammatory cytokine IL6, which is known to enhance metastatic potentials of tumor cells (46), was elevated in lungs from HFD-fed mice (Fig. 7A) concomitantly with increased S1P levels (Fig. 7B) and activation of key signaling pathways (Fig. 7C). FTY720 suppressed elevation of the proinflammatory cytokines, S1P levels, and stimulation of signaling pathways downstream of S1PR1 as demonstrated by reduction in phosphorylation of ERK, AKT, Stat3, and p65 (Fig. 7A–C). To determine whether FTY720 treatment also affects the survival of mice developing breast cancer lung metastases, we carried out a long-term study of syngeneic mice orthotopically implanted with E0771 cells. In agreement with previous studies in other animal models of breast cancer (48), Kaplan–Meier survival analysis revealed that HFD significantly worsened the survival of these mice compared with those fed ND (Fig. 7D). Daily administration of FTY720 significantly prolonged the survival of HFD-fed mice (Fig. 7D).

## Discussion

Obesity-induced chronic inflammation has decisive roles in the pathogenesis of breast cancer and distal recurrence; however, the underlying mechanisms linking obesity and chronic inflammation to an increased risk of breast cancer and metastasis are poorly understood. In the current study, we identified a novel mechanism involving the SphK1/S1P/S1PR1 axis in a malevolent feed-forward amplification loop that connects obesity, inflammation, and breast cancer progression and metastasis. Targeting this axis with FTY720, which reduced expression of SphK1 and S1PR1 and S1P levels, significantly suppressed breast cancer metastasis and prolonged survival in obese HFD-fed MMTV-PyMT transgenic and E0771 syngeneic orthotopic breast cancer mice. In agreement with the critical role of the SphK1/S1P/S1PR1 axis in persistent activation of NFκB and STAT3 and production of proinflammatory cytokines IL6 and TNFα (19, 36, 42), we found that in animals bearing breast tumors, increased S1P by HFD is essential for the production of IL6, the multifunctional NFκB-regulated cytokine, as well as activation of STAT3 and the upregulation of its target gene *S1pr1* (36). Administration of FTY720 interfered with the SphK1/S1P/S1PR1 axis and prevented STAT3 activation along with decreasing these proinflammatory cytokines and macrophage recruitment, resulting in suppression of obesity-promoted chronic inflammation and breast cancer progression and metastasis.

We have revealed that HFD increases S1P levels in the circulation of not only tumor-bearing animals, but also of nontumor-bearing animals (Fig. 1). Furthermore, S1P levels in the normal mammary fat pad and lung tissue were also increased with HFD without tumor. These findings indicate that obesity itself increase the levels of S1P in the body. Indeed, it has been reported that S1P levels are positively associated with obesity in humans. Plasma levels of S1P were reported to be higher in obese patients than those in nonobese and lean individuals (49). In addition, it was demonstrated that levels of plasma S1P directly correlate with BMI and total body fat percentage (28, 50). Taken together, these findings indicate that the S1P levels in the blood and local organs are increased with obesity most likely in addition to increased S1P secretion from enlarged tumor.

Our data show that HFD-induced obesity increased levels of S1P not only in the primary tumor itself but also in tumor interstitial fluid—a component of the tumor microenvironment, in the systemic circulation, and in distant sites such as the lungs. Similarly, serum S1P levels from obese breast cancer patients are higher than those in normal weight patients. The "seed-and-soil hypothesis," first proposed by Paget, spawned the idea that primary tumors secrete factors that contribute to the development of premetastatic niches, characterized by an abundance of bone marrow–derived cells and stromal cells (30, 51). It has also been shown that even before tumor cells arrive premetastatic niches in distant organs are formed to create a favorable microenvironment for disseminating tumor cell colonization (52). Our data suggest that S1P is one of these

Published OnlineFirst January 19, 2018; DOI: 10.1158/0008-5472.CAN-17-1423



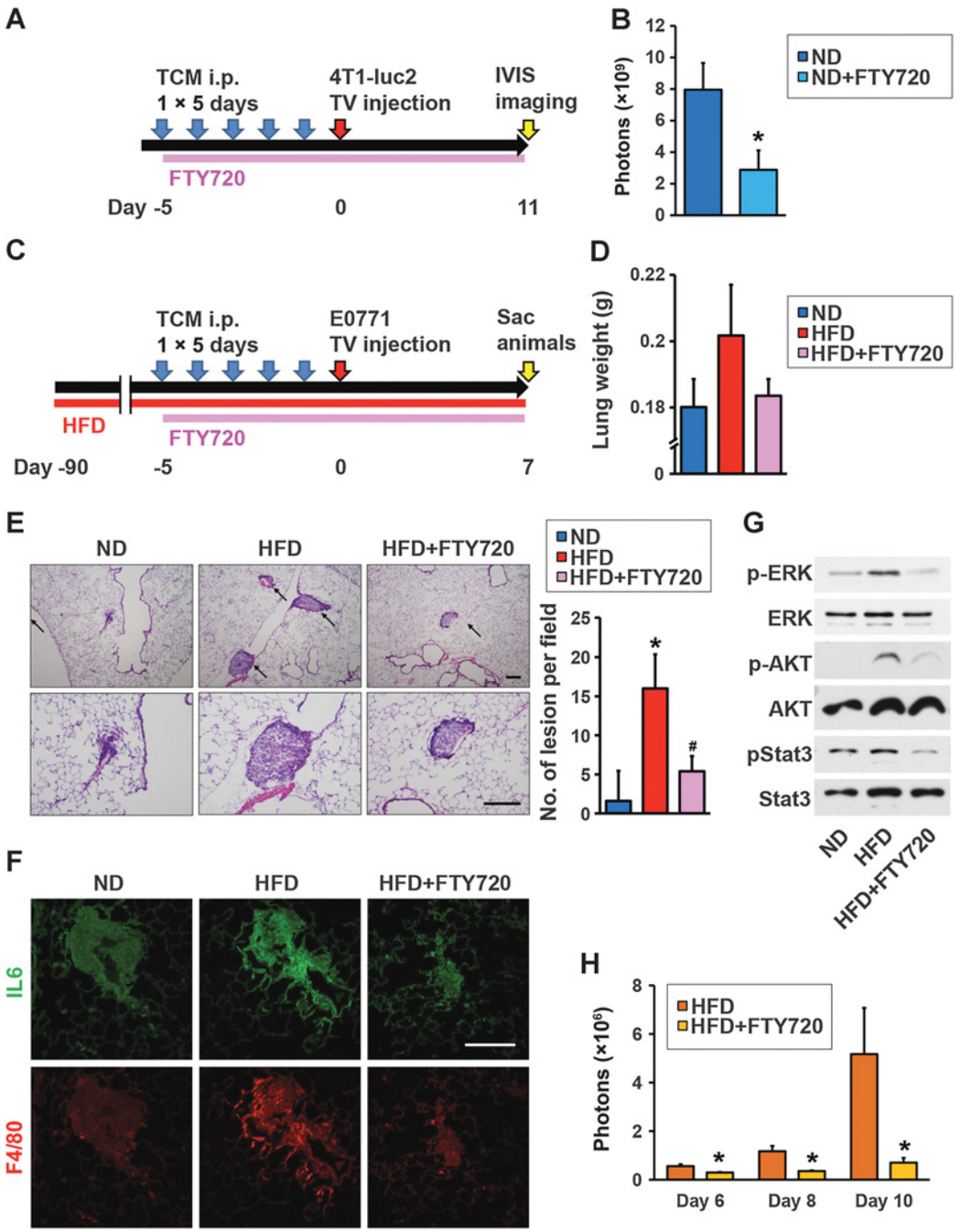


**Figure 5.**

FTY720 suppressed HFD-induced inflammation and lung-seeding ability of breast cancer cells. **A,** Schematic overview of treatment regimen for lung colonization. Mice were fed ND and treated with TCM from *Sphk1*-overexpressing 4T1-luc2 cells (TCM-*Sphk1*) for 5 days and also daily treated orally with PBS or with FTY720 (1 mg/kg) as indicated. At day 6, 4T1 cells were injected intravenously and tumor burden was quantified by *in vivo* bioluminescence on the indicated days. **B,** Tumor burden of mice with tail vein injection of 4T1-luc2 cells treated without or with FTY720 quantified by *in vivo* bioluminescence on day 11. Data are means ± SEM. *, $P < 0.05$ versus ND. **C,** Schematic overview of treatment regimen for lung colonization. Mice were fed ND or HFD for 12 weeks and treated with TCM from *Sphk1*-overexpressing E0771 cells (TCM-*Sphk1*) for 5 days and also daily treated orally with PBS or with FTY720 (1 mg/kg) as indicated. At day 6, E0771 cells were injected intravenously and 7 days later, lungs were harvested. **D,** Lung weights. **E,** H&E staining of lung sections. Top and bottom panels show lower (×40) and higher (×100) magnifications, respectively. Arrows, cancer cell–seeding lesions. Scale bar, 200 μm. Quantitation of cancer cell–seeding lesions. Data are means ± SEM. *, $P < 0.05$ versus ND; #, $P < 0.05$ versus HFD. **F,** Immunofluorescence analysis of lung sections stained for IL6 (green) and F4/80 (red). Scale bar, 100 μm. **G,** Equal amounts of lung lysates analyzed by immunoblotting, with the indicated antibodies. **H,** Tumor burden of HFD-fed mice with tail vein injection of 4T1-luc2 cells treated without or with FTY720 quantified by *in vivo* bioluminescence on the indicated days. Data are means ± SEM. *, $P < 0.05$ versus HFD, respectively.

Published OnlineFirst January 19, 2018; DOI: 10.1158/0008-5472.CAN-17-1423



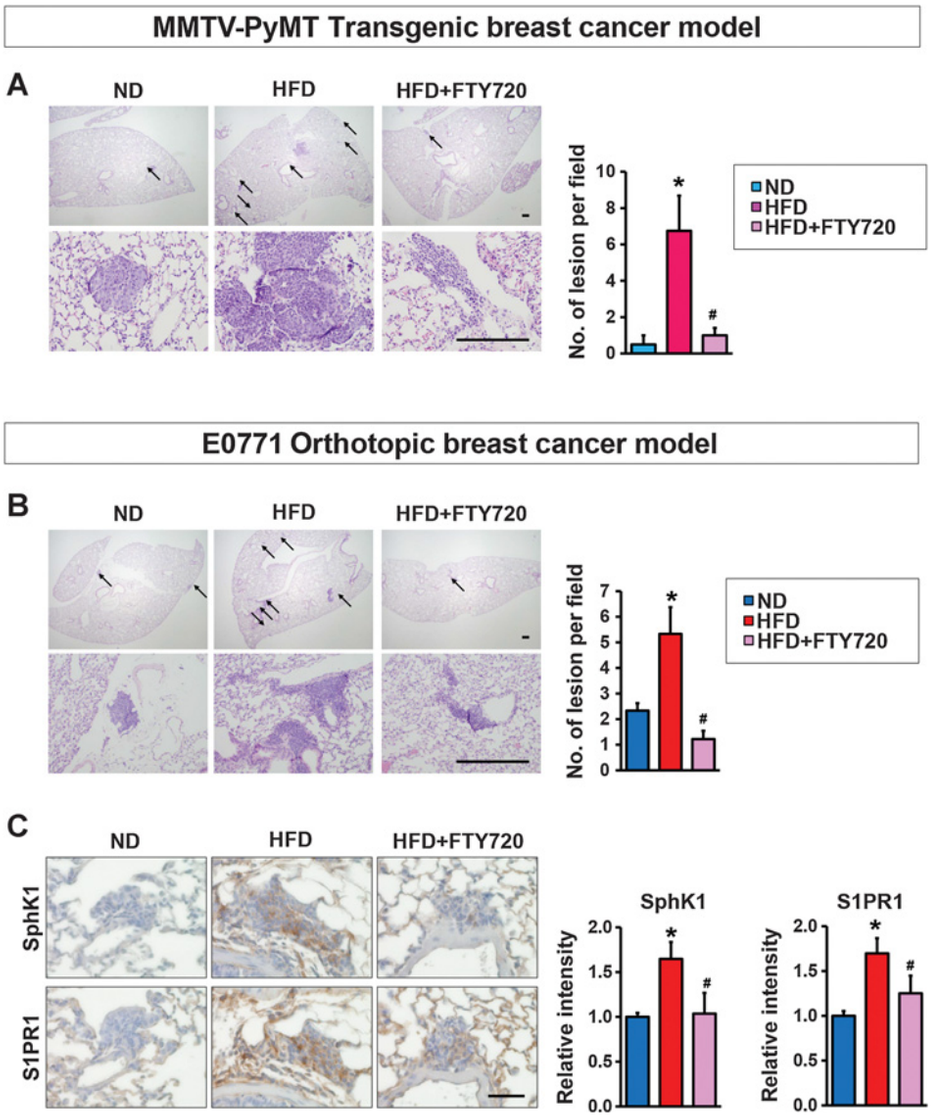


**Figure 6.**

FTY720 suppresses lung metastasis in HFD-fed MMTV-PyMT transgenic and E0771 syngeneic orthotopic breast cancer mice. **A,** MMTV-PyMT transgenic mice were fed with ND or HFD and treated daily by gavage with PBS or FTY720 (1 mg/kg) as indicated. Lungs were harvested when mice were 10 weeks old. **C,** H&E staining of lung sections. Top and bottom panels show lower (×20) and higher (×200) magnifications, respectively. Arrows, metastatic lesions. Scale bar, 100 μm. Quantitation of metastatic lesions. Data are means ± SEM. *, $P < 0.05$ versus ND; #, $P < 0.05$ versus HFD. **B** and **C,** C57Bl/6 mice were fed with ND or HFD for 12 weeks, before E0771 cells were implanted into the chest mammary fat pad under direct vision. When tumor sizes reached 5 mm in diameter, mice fed HFD were randomized into two groups and treated by gavage with PBS or FTY720 (1 mg/kg/day). Lungs were examined 18 days later. **B,** H&E staining of lung sections. Top and bottom panels show lower (×20) and higher (×200) magnifications, respectively. Arrows, metastatic lesions. Scale bar, 100 μm. Quantitation of metastatic lesions. Data are means ± SEM. *, $P < 0.05$ versus ND; #, $P < 0.05$ versus HFD. **C,** Lung sections were immunostained with anti-SphK1 or anti-S1PR1. Scale bar, 50 μm. Relative intensity of immunostaining was quantified. Data are means ± SEM. *, $P < 0.05$ versus PBS; #, $P < 0.05$ versus HFD.

factors secreted by tumor cells due to upregulation of SphK1. We found that TCM from SphK1-overexpressing breast cancer cells, which contains high levels of S1P, promoted metastatic niche formation and lung metastasis. S1PR1 has previously been identified as a key component for persistent activation of STAT3 in both primary tumors and in various cell types including myeloid cells in distant organs, leading to premetastatic niche formation (19, 42). Although in the past it was not clear how S1PR1 was activated, our results suggest that S1P secretion from tumor cells is the primary driver of S1PR1 activation to influence the microenvironment of distant organs such as lung by promoting recruitment of macrophages known to promote tumor cell extravasation, seeding, and persistent growth, and enabling metastasis (Fig. 7E). Consistent with this key role for S1P, a genome-wide screening of 800 mutant mice using an *in vivo* assay for the discovery of new microenvironmental regulators of metastatic colonization identified the S1P transporter Spns2 that regulates levels of S1P in lymph and blood as a critical new player (45).

We also found that in HFD-induced obese animals, SphK1 and S1PR1 expression is increased in metastatic lesions, along with higher levels of proinflammatory cytokines, IL6 and TNFα. Taken together with previous findings, this indicates that upregulation of SphK1, formation of S1P, and subsequent activation of S1PR1 leads to persistent activation of survival signaling and STAT3 in a malicious feed-forward amplification loop critical for breast cancer proliferation, survival, crosstalk with the microenvironment and metastasis.

FTY720, which targets the SphK1/S1P/S1PR1 axis, prevents the amplification cascade and mitigates obesity-promoted metastatic niche formation and breast cancer metastasis. We found that FTY720 decreased S1P levels as well as SphK1 and S1PR1 expression in the breast tumors. It has been reported that FTY720 inhibits SphK1 activity and promotes its proteosomal degradation (53). It has also been reported that FTY720 induces functional antagonism by the rapid polyubiquitylation, endocytosis, and proteasomal degradation of S1PR1 (54). This mechanism may also contribute to FTY720-induced cancer

Published OnlineFirst January 19, 2018; DOI: 10.1158/0008-5472.CAN-17-1423



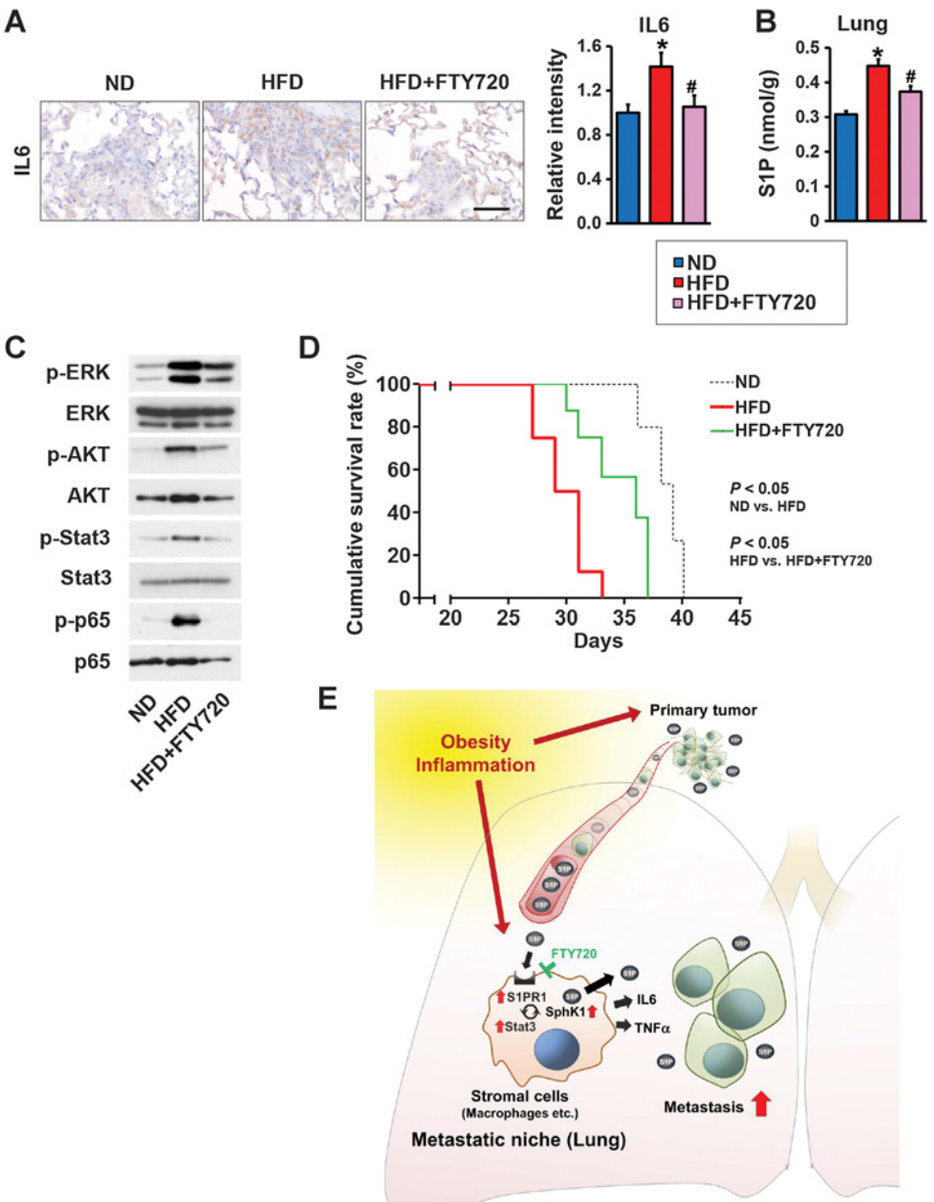


**Figure 7.**

FTY720 mitigates obesity-related lung inflammation and S1P signaling, and prolongs survival of breast cancer–bearing mice. **A–D,** C57Bl/6 mice were fed ND or HFD for 12 weeks. Tumor-bearing mice fed HFD were randomized into two groups 2 days after implantation and then treated by gavage with PBS or FTY720 (1 mg/kg/day) and 18 days later, lungs were examined. **A,** Lung sections were immunostained with anti-IL6. Scale bar, 50 μm. Relative intensity of the immunostaining was quantified. **B,** Levels of S1P in lungs were measured by LC-ESI-MS/MS. Data are means ± SEM. *, $P < 0.05$ versus. ND; #, $P < 0.05$ versus HFD. **C,** Equal amounts of lung lysates were analyzed by Western blotting with the indicated antibodies. **D,** Kaplan–Meier cumulative survival curves for mice fed with ND, HFD, or HFD plus FTY720 treatment. Data from days after E0771 implantation are shown. **E,** Scheme illustrating the role of SphK1/S1P/S1PR1 axis in the link between obesity, inflammation, and breast cancer progression and lung metastasis and targeting this axis with FTY720 for treatment. See text for more details.

cell–selective apoptosis (55) and its inhibition of tumor vascularization and angiogenesis (56). Taken together, these direct effects of FTY720 on sphingolipid metabolism may explain the mechanisms through which FTY720 targets the SphK1/S1P/S1PR1 axis.

It is possible that the reduction of primary tumor size may be at least partly responsible for the decrease of metastatic tumor burden. Although our results of survival data (Fig. 7) showed a benefit from FTY720, the effect was not as dramatic as the results shown in Figs. 4–6. In this case, response to therapy was not linear to the length of survival. While the reduction in disease burden substantiates an important role for the SphK1/S1P/S1PR1 axis, there remained a significant disease burden in treated mice, implying limited efficacy as a single modality therapy. Clinically, it is well known that therapies that reduce metastatic burden often do not result in longer survival in a variety of settings of human patients (57).

Our objective is to elucidate the role of the SphK1/S1P/S1PR1 axis in cancer associated with inflammation and to show the effects of FTY720 in that setting. FTY720 acts by multiple means in addition to its effects on obesity-related inflammation. In agreement with previous reports, we also found that FTY720 inhibited tumor growth in mice treated with ND. In this research, our discovery is that FTY720 is effective on cancer with obesity-associated inflammation. Future development of more specific drugs that target the SphK1/S1P/S1PR1 axis will further aid in elucidating its importance in control of pulmonary metastatic burden and the usefulness of targeting this axis therapeutically for obesity-promoted metastatic breast cancer.

## Disclosure of Potential Conflicts of Interest

No potential conflicts of interest were disclosed.

Published OnlineFirst January 19, 2018; DOI: 10.1158/0008-5472.CAN-17-1423



## Authors' Contributions

**Conception and design:** M. Nagahashi, K. Takabe

**Acquisition of data (provided animals, acquired and managed patients, provided facilities, etc.):** M. Nagahashi, A. Yamada, E. Katsuta, T. Aoyagi, W.-C. Huang, K.P. Terracina, N.C. Hait, J.C. Allegood, J. Tsuchida, K. Yuza, M. Nakajima, M. Abe

**Analysis and interpretation of data (e.g., statistical analysis, biostatistics, computational analysis):** M. Nagahashi, T. Aoyagi, W.-C. Huang, J.C. Allegood, S. Spiegel, K. Takabe

**Writing, review, and/or revision of the manuscript:** M. Nagahashi, K.P. Terracina, S. Milstien, S. Spiegel, K. Takabe

**Administrative, technical, or material support (i.e., reporting or organizing data, constructing databases):** M. Nagahashi, T. Aoyagi, W.-C. Huang, T. Wakai, K. Takabe

**Study supervision:** M. Nagahashi, K. Sakimura, T. Wakai, S. Spiegel, K. Takabe

## Acknowledgments

The VCU Lipidomics and Microscopy Cores are supported in part by funding from the NIH-NCI Cancer Center Support Grant P30 CA016059. M. Nagahashi was a Japan Society for the Promotion of Science Postdoctoral Fellow. M. Nagahashi is supported by the Japan Society for the Promotion of Science (JSPS) Grant-in-Aid for Scientific Research Grant Number 15H05676 and 15K15471, the Uehara Memorial Foundation, Nakayama Cancer Research Institute, Takeda Science Foundation, and Tsukada Medical Foundation. T. Wakai is supported by the JSPS Grant-in-Aid for Scientific Research Grant Number 15H04927 and 16K15610. K. Takabe is supported by NIH/NCI grant R01CA160688 and Susan G. Komen Investigator Initiated Research Grant IIR12222224. S. Spiegel is supported by the Department of Defense BCRP Program Award (W81XWH-14-1-0086). K.P. Terracina was supported by T32CA085159.

The costs of publication of this article were defrayed in part by the payment of page charges. This article must therefore be hereby marked *advertisement* in accordance with 18 U.S.C. Section 1734 solely to indicate this fact.

Received May 14, 2017; revised November 27, 2017; accepted January 16, 2018; published OnlineFirst January 19, 2018.

## References

1. Flegal KM, Carroll MD, Ogden CL, Curtin LR. Prevalence and trends in obesity among US adults, 1999–2008. JAMA 2010;303:235–41.
2. Calle EE, Rodriguez C, Walker-Thurmond K, Thun MJ. Overweight, obesity, and mortality from cancer in a prospectively studied cohort of U.S. adults. N Engl J Med 2003;348:1625–38.
3. Niraula S, Ocana A, Ennis M, Goodwin PJ. Body size and breast cancer prognosis in relation to hormone receptor and menopausal status: a meta-analysis. Breast Cancer Res Treat 2012;134:769–81.
4. Neuhouser ML, Aragaki AK, Prentice RL, Manson JE, Chlebowski R, Carty CL, et al. Overweight, obesity, and postmenopausal invasive breast cancer risk: a secondary analysis of the women's health initiative randomized clinical trials. JAMA Oncol 2015;1:611–21.
5. Demark-Wahnefried W, Platz EA, Ligibel JA, Blair CK, Courneya KS, Meyerhardt JA, et al. The role of obesity in cancer survival and recurrence. Cancer Epidemiol Biomarkers Prev 2012;21:1244–59.
6. Fuentes-Mattei E, Velazquez-Torres G, Phan L, Zhang F, Chou PC, Shin JH, et al. Effects of obesity on transcriptomic changes and cancer hallmarks in estrogen receptor-positive breast cancer. J Natl Cancer Inst 2014;106. doi: 10.1093/jnci/dju158.
7. La Merrill M, Gordon RR, Hunter KW, Threadgill DW, Pomp D. Dietary fat alters pulmonary metastasis of mammary cancers through cancer autonomous and non-autonomous changes in gene expression. Clin Exp Metast 2010;27:107–16.
8. Llaverias G, Danilo C, Mercier I, Daumer K, Capozza F, Williams TM, et al. Role of cholesterol in the development and progression of breast cancer. Am J Pathol 2011;178:402–12.
9. Sundaram S, Yan L. High-fat diet enhances mammary tumorigenesis and pulmonary metastasis and alters inflammatory and angiogenic profiles in MMTV-PyMT mice. Anticancer Res 2016;36:6279–87.
10. Cowen S, McLaughlin SL, Hobbs G, Coad J, Martin KH, Olfert IM, et al. High-fat, high-calorie diet enhances mammary carcinogenesis and local inflammation in MMTV-PyMT mouse model of breast cancer. Cancers 2015;7:1125–42.
11. Maccio A, Madeddu C. Obesity, inflammation, and postmenopausal breast cancer: therapeutic implications. Scientific World Journal 2011;11:2020–36.
12. Khandekar MJ, Cohen P, Spiegelman BM. Molecular mechanisms of cancer development in obesity. Nat Rev Cancer 2011;11:886–95.
13. Antonioli L, Blandizzi C, Pacher P, Hasko G. Immunity, inflammation and cancer: a leading role for adenosine. Nat Rev Cancer 2013;13:842–57.
14. Chang CC, Wu MJ, Yang JY, Camarillo IG, Chang CJ. Leptin-STAT3-G9a signaling promotes obesity-mediated breast cancer progression. Cancer Res 2015;75:2375–86.
15. Donohoe CL, Lysaght J, O'Sullivan J, Reynolds JV. Emerging concepts linking obesity with the hallmarks of cancer. Trends Endocrinol Metab 2017;28:46–62.
16. Feola A, Ricci S, Kouidhi S, Rizzo A, Penon A, Formisano P, et al. Multifaceted breast cancer: the molecular connection with obesity. J Cell Physiol 2017;232:69–77.
17. Sundaram S, Johnson AR, Makowski L. Obesity, metabolism and the microenvironment: Links to cancer. J Carcinogenesis 2013;12:19.
18. Psaila B, Lyden D. The metastatic niche: adapting the foreign soil. Nat Rev Cancer 2009;9:285–93.
19. Deng J, Liu Y, Lee H, Herrmann A, Zhang W, Zhang C, et al. S1PR1-STAT3 signaling is crucial for myeloid cell colonization at future metastatic sites. Cancer Cell 2012;21:642–54.
20. Sceneay J, Chow MT, Chen A, Halse HM, Wong CS, Andrews DM, et al. Primary tumor hypoxia recruits CD11b+/Ly6Cmed/Ly6G+ immune suppressor cells and compromises NK cell cytotoxicity in the premetastatic niche. Cancer Res 2012;72:3906–11.
21. Aoyagi T, Nagahashi M, Yamada A, Takabe K. The role of sphingosine-1-phosphate in breast cancer tumor-induced lymphangiogenesis. Lymphat Res Biol 2012;10:97–106.
22. Pyne NJ, Pyne S. Sphingosine 1-phosphate and cancer. Nat Rev Cancer 2010;10:489–503.
23. Nagahashi M, Ramachandran S, Kim EY, Allegood JC, Rashid OM, Yamada A, et al. Sphingosine-1-phosphate produced by sphingosine kinase 1 promotes breast cancer progression by stimulating angiogenesis and lymphangiogenesis. Cancer Res 2012;72:726–35.
24. Takabe K, Spiegel S. Export of sphingosine-1-phosphate and cancer progression. J Lipid Res 2014;55:1839–46.
25. Nagahashi M, Yuza K, Hirose Y, Nakajima M, Ramanathan R, Hait NC, et al. The roles of bile acids and sphingosine-1-phosphate signaling in the hepatobiliary diseases. J Lipid Res 2016;57:1636–43.
26. Ruckhaberle E, Rody A, Engels K, Gaetje R, von Minckwitz G, Schiffmann S, et al. Microarray analysis of altered sphingolipid metabolism reveals prognostic significance of sphingosine kinase 1 in breast cancer. Breast Cancer Res Treat 2008;112:41–52.
27. Tsuchida J, Nagahashi M, Nakajima M, Moro K, Tatsuda K, Ramanathan R, et al. Breast cancer sphingosine-1-phosphate is associated with phospho-sphingosine kinase 1 and lymphatic metastasis. J Surg Res 2016;205:85–94.
28. Kowalski GM, Carey AL, Selathurai A, Kingwell BA, Bruce CR. Plasma sphingosine-1-phosphate is elevated in obesity. PLoS One 2013;8:e72449.
29. Paugh SW, Paugh BS, Rahmani M, Kapitonov D, Almenara JA, Kordula T, et al. A selective sphingosine kinase 1 inhibitor integrates multiple molecular therapeutic targets in human leukemia. Blood 2008;112:1382–91.

30. Kaplan RN, Riba RD, Zacharoulis S, Bramley AH, Vincent L, Costa C, et al. VEGFR1-positive haematopoietic bone marrow progenitors initiate the pre-metastatic niche. Nature 2005;438:820–7.
31. Hait NC, Avni D, Yamada A, Nagahashi M, Aoyagi T, Aoki H, et al. The phosphorylated prodrug FTY720 is a histone deacetylase inhibitor that reactivates ERalpha expression and enhances hormonal therapy for breast cancer. Oncogenesis 2015;4:e156.
32. Nagahashi M, Kim EY, Yamada A, Ramachandran S, Allegood JC, Hait NC, et al. Spns2, a transporter of phosphorylated sphingoid bases, regulates their blood and lymph levels, and the lymphatic network. FASEB J 2013;27:1001–11.
33. Nagahashi M, Yamada A, Miyazaki H, Allegood JC, Tsuchida J, Aoyagi T, et al. Interstitial fluid sphingosine-1-phosphate in murine mammary gland and cancer and human breast tissue and cancer determined by novel methods. J Mammary Gland Biol Neoplasia 2016;21:9–17.
34. Hait NC, Allegood J, Maceyka M, Strub GM, Harikumar KB, Singh SK, et al. Regulation of histone acetylation in the nucleus by sphingosine-1-phosphate. Science 2009;325:1254–7.
35. Takabe K, Kim RH, Allegood JC, Mitra P, Ramachandran S, Nagahashi M, et al. Estradiol induces export of sphingosine 1-phosphate from breast cancer cells via ABCC1 and ABCG2. J Biol Chem 2010;285:10477–86.
36. Liang J, Nagahashi M, Kim EY, Harikumar KB, Yamada A, Huang WC, et al. Sphingosine-1-phosphate links persistent STAT3 activation, chronic intestinal inflammation, and development of colitis-associated cancer. Cancer Cell 2013;23:107–20.
37. Ewertz M, Gray KP, Regan MM, Ejlertsen B, Price KN, Thurlimann B, et al. Obesity and risk of recurrence or death after adjuvant endocrine therapy with letrozole or tamoxifen in the breast international group 1-98 trial. J Clin Oncol 2012;30:3967–75.
38. Sinicrope FA, Dannenberg AJ. Obesity and breast cancer prognosis: weight of the evidence. J Clin Oncol 2011;29:4–7.
39. Nagahashi M, Tsuchida J, Moro K, Hasegawa M, Tatsuda K, Woelfel IA, et al. High levels of sphingolipids in human breast cancer. J Surg Res 2016;204:435–44.
40. Brinkmann V, Billich A, Baumruker T, Heining P, Schmouder R, Francis G, et al. Fingolimod (FTY720): discovery and development of an oral drug to treat multiple sclerosis. Nat Rev Drug Discov 2010;9:883–97.
41. Maglione JE, Moghanaki D, Young LJ, Manner CK, Ellies LG, Joseph SO, et al. Transgenic Polyoma middle-T mice model premalignant mammary disease. Cancer Res 2001;61:8298–305.
42. Lee H, Deng J, Kujawski M, Yang C, Liu Y, Herrmann A, et al. STAT3-induced S1PR1 expression is crucial for persistent STAT3 activation in tumors. Nat Med 2010;16:1421–8.
43. Lim KG, Tonelli F, Li Z, Lu X, Bittman R, Pyne S, et al. FTY720 analogues as sphingosine kinase 1 inhibitors: enzyme inhibition kinetics, allosterism, proteasomal degradation, and actin rearrangement in MCF-7 breast cancer cells. J Biol Chem 2011;286:18633–40.
44. Tonelli F, Lim KG, Loveridge C, Long J, Pitson SM, Tigyi G, et al. FTY720 and (S)-FTY720 vinylphosphonate inhibit sphingosine kinase 1 and promote its proteasomal degradation in human pulmonary artery smooth muscle, breast cancer and androgen-independent prostate cancer cells. Cell Signal 2010;22:1536–42.
45. van der Weyden L, Arends MJ, Campbell AD, Bald T, Wardle-Jones H, Griggs N, et al. Genome-wide in vivo screen identifies novel host regulators of metastatic colonization. Nature 2017;541:233–6.
46. Liu Y, Cao X. Characteristics and significance of the pre-metastatic Niche. Cancer Cell 2016;30:668–81.
47. Gluschnaider U, Hertz R, Ohayon S, Smeir E, Smets M, Pikarsky E, et al. Long-chain fatty acid analogues suppress breast tumorigenesis and progression. Cancer Res 2014;74:6991–7002.
48. Kim EJ, Choi MR, Park H, Kim M, Hong JE, Lee JY, et al. Dietary fat increases solid tumor growth and metastasis of 4T1 murine mammary carcinoma cells and mortality in obesity-resistant BALB/c mice. Breast Cancer Res 2011;13:R78.
49. Ito S, Iwaki S, Koike K, Yuda Y, Nagasaki A, Ohkawa R, et al. Increased plasma sphingosine-1-phosphate in obese individuals and its capacity to increase the expression of plasminogen activator inhibitor-1 in adipocytes. Coron Artery Dis 2013;24:642–50.
50. Katsuta E, Yan L, Nagahashi M, Raza A, Sturgill JL, Lyon DE, et al. Doxorubicin effect is enhanced by sphingosine-1-phosphate signaling antagonist in breast cancer. J Surg Res 2017;219:202–13.
51. Quail DF, Joyce JA. Microenvironmental regulation of tumor progression and metastasis. Nat Med 2013;19:1423–37.
52. Kaplan RN, Rafii S, Lyden D. Preparing the "soil": the premetastatic niche. Cancer Res 2006;66:11089–93.
53. Valentine WJ, Kiss GN, Liu J, E S, Gotoh M, Murakami-Murofushi K, et al. (S)-FTY720-vinylphosphonate, an analogue of the immunosuppressive agent FTY720, is a pan-antagonist of sphingosine 1-phosphate GPCR signaling and inhibits autotaxin activity. Cell Signal 2010;22:1543–53.
54. Graler MH, Goetzl EJ. The immunosuppressant FTY720 down-regulates sphingosine 1-phosphate G-protein-coupled receptors. FASEB J 2004;18:551–3.
55. Azuma H, Horie S, Muto S, Otsuki Y, Matsumoto K, Morimoto J, et al. Selective cancer cell apoptosis induced by FTY720; evidence for a Bcl-dependent pathway and impairment in ERK activity. Anticancer Res 2003;23:3183–93.
56. LaMontagne K, Littlewood-Evans A, Schnell C, O'Reilly T, Wyder L, Sanchez T, et al. Antagonism of sphingosine-1-phosphate receptors by FTY720 inhibits angiogenesis and tumor vascularization. Cancer Res 2006;66:221–31.
57. Valachis A, Polyzos NP, Patsopoulos NA, Georgoulias V, Mavroudis D, Mauri D. Bevacizumab in metastatic breast cancer: a meta-analysis of randomized controlled trials. Breast Cancer Res Treat 2010;122:1–7.

Published OnlineFirst March 9, 2018; DOI: 10.1158/1541-7786.MCR-17-0353

Tumor Microenvironment

Molecular Cancer Research

# ABCC1-Exported Sphingosine-1-phosphate, Produced by Sphingosine Kinase 1, Shortens Survival of Mice and Patients with Breast Cancer

Akimitsu Yamada[1,2,3,4], Masayuki Nagahashi[1,2,5], Tomoyoshi Aoyagi[1,2], Wei-Ching Huang[1,2,6], Santiago Lima[2], Nitai C. Hait[2,7,8], Aparna Maiti[7], Kumiko Kida[3,4], Krista P. Terracina[1], Hiroshi Miyazaki[9], Takashi Ishikawa[10], Itaru Endo[3], Michael R. Waters[2], Qianya Qi[11], Li Yan[11], Sheldon Milstien[2], Sarah Spiegel[2], and Kazuaki Takabe[1,2,3,5,7,10,12]

## Abstract

Sphingosine-1-phosphate (S1P), a bioactive sphingolipid mediator, has been implicated in regulation of many processes important for breast cancer progression. Previously, we observed that S1P is exported out of human breast cancer cells by ATP-binding cassette (ABC) transporter ABCC1, but not by ABCB1, both known multidrug resistance proteins that efflux chemotherapeutic agents. However, the pathologic consequences of these events to breast cancer progression and metastasis have not been elucidated. Here, it is demonstrated that high expression of ABCC1, but not ABCB1, is associated with poor prognosis in breast cancer patients. Overexpression of ABCC1, but not ABCB1, in human MCF7 and murine 4T1 breast cancer cells enhanced S1P secretion, proliferation, and migration of breast cancer cells. Implantation of breast cancer cells overexpressing ABCC1, but not ABCB1, into the mammary fat pad markedly enhanced tumor growth, angiogenesis, and lymphangiogenesis with a concomitant increase in lymph node and lung metastases as well as shorter survival of mice. Interestingly, S1P exported via ABCC1 from breast cancer cells upregulated transcription of sphingosine kinase 1 (SPHK1), thus promoting more S1P formation. Finally, patients with breast cancers that express both activated SPHK1 and ABCC1 have significantly shorter disease-free survival. These findings suggest that export of S1P via ABCC1 functions in a malicious feed-forward manner to amplify the S1P axis involved in breast cancer progression and metastasis, which has important implications for prognosis of breast cancer patients and for potential therapeutic targets.

**Implication:** Multidrug resistant transporter ABCC1 and activation of SPHK1 in breast cancer worsen patient's survival by export of S1P to the tumor microenvironment to enhance key processes involved in cancer progression. *Mol Cancer Res; 16(6); 1059–70. ©2018 AACR.*

[1]Division of Surgical Oncology, Department of Surgery, Virginia Commonwealth University School of Medicine and the Massey Cancer Center, Richmond, Virginia. [2]Department of Biochemistry and Molecular Biology, Virginia Commonwealth University School of Medicine and the Massey Cancer Center, Richmond, Virginia. [3]Department of Gastroenterological Surgery, Yokohama City University School of Medicine, Kanagawa, Japan. [4]Department of Breast and Thyroid Surgery, Yokohama City University Medical Center, Kanagawa, Japan. [5]Division of Digestive and General Surgery, Niigata University Graduate School of Medical and Dental Sciences, Niigata, Japan. [6]Institute of Stem Cell and Translational Cancer Research, Chang Gung Memorial Hospital, Taoyuan, Taiwan. [7]Division of Breast Surgery, Department of Surgical Oncology, Roswell Park Comprehensive Cancer Center, Buffalo, New York. [8]Department of Molecular & Cellular Biology, Roswell Park Comprehensive Cancer Center, Buffalo, New York. [9]Section of General Internal Medicine, Kojin Hospital, Nagoya, Japan. [10]Department of Breast Surgery, Tokyo Medical University, Tokyo, Japan. [11]Department of Biostatistics & Bioinformatics, Roswell Park Comprehensive Cancer Center, Buffalo, New York. [12]Department of Surgery, University at Buffalo Jacobs School of Medicine and Biomedical Sciences, The State University of New York, Buffalo, New York.

**Note:** Supplementary data for this article are available at Molecular Cancer Research Online (http://mcr.aacrjournals.org/).

**Corresponding Author:** Kazuaki Takabe, Division of Surgical Oncology, Department of Surgery, Roswell Park Comprehensive Cancer Center, Elm & Carlton Streets, Buffalo, NY 14263. Phone: 716-845-5540; Fax: 716-845-1668; E-mail: kazuaki.takabe@roswellpark.org

**doi:** 10.1158/1541-7786.MCR-17-0353



## Introduction

Despite the recent improvement of 5-year survival due to advances in chemotherapy and targeted therapy, close to 40,000 women in the United States continue to succumb to breast cancer every year (1). ATP-binding cassette (ABC) transporters are transmembrane proteins that transport various molecules across cellular membranes including chemotherapeutic agents, functioning as a xenobiotic protective mechanism (2). Some of the ABC transporters, such as ABCB1 (multidrug resistance protein 1: MDR1) and ABCC1 (multidrug resistance associated protein1: MRP1), were originally identified as "multi-drug resistant genes and proteins." Indeed, ABCB1 was demonstrated to export doxorubicin, one of the most frequently used chemotherapeutics for breast cancer that led to development of ABCB1 inhibitors to fight drug resistance (3, 4). Disappointingly, all 12 clinical trials that examined ABCB1-targeted therapy failed to improve survival (5). This suggested to us that other ABC transporters may also drive drug resistance not only because they export drugs, but because they export molecules that biologically aggravate cancer progression and that targeting these transporters may not be sufficient to improve survival.

The bioactive sphingolipid mediator sphingosine-1-phosphate (S1P) is a key regulatory molecule in cancer that promotes cell proliferation, migration, invasion, angiogenesis, and

Published OnlineFirst March 9, 2018; DOI: 10.1158/1541-7786.MCR-17-0353



lymphangiogenesis (6–8). S1P is generated intracellularly by two sphingosine kinases, SphK1 and SphK2, and is exported out of the cells, where it regulates many functions by binding to and signaling through a family of five G protein–coupled receptors (S1PR1–5) in an autocrine, paracrine, and/or endocrine manner, which is known as "inside-out" signaling (9). We previously demonstrated that SphK1, but not SphK2, produces S1P that is exported from MCF7 breast cancer cells stimulated by estradiol (10). We also demonstrated that expression of SphK1 is upregulated in human breast cancers (11) and the level of activated, phosphorylated SphK1 correlates with lymphatic metastasis (12), in agreement with reports by others (13, 14).

It has previously been proposed that ABC transporters such as ABCC1 may function not only as an export mechanism for drugs but also exacerbate cancer progression. However, no candidates for this potential mechanism have yet been uncovered (3, 15). High expression of ABCC1 has also been associated with poor prognosis in several types of human cancers, including breast cancer (5). Based upon our finding that ABCC1 exports S1P (10), it was tempting to suggest that S1P export via ABCC1 contributes to aggressive breast cancers with poor prognosis. Here, we show that export of S1P via ABCC1 functions in a feed-forward manner to amplify the S1P axis involved in breast cancer progression and contributes to shortened survival of mice and humans with breast cancer

## Materials and Methods

### Cell culture

MCF7 human mammary adenocarcinoma cells were obtained from ATCC; a murine mammary adenocarcinoma cell line that overexpresses luciferase 4T1-luc2 was obtained from Perkin Elmer. Human umbilical vein endothelial cells (HUVEC) and human lymphatic endothelial cells (HLEC) were obtained from Angio-Proteomie. Cells were purchased in 2010 to 2012. After purchase, cell lines were expanded and frozen after one to three passages. Cells were expanded and stored according to the manufacturer's instructions. MCF7 and 4T1-luc2 cells were used for no longer than 10 passages, whereas HUVEC and HLEC cells were used for no longer than 3 passages. All cell cultures were routinely tested to rule out mycoplasma infection using Mycoplasma Detection Kit (ABM). MCF7 was cultured in modified IMEM without phenol red supplemented with 10% FBS, 0.22% dextrose, and 2 mmol/L glutamine. 4T1-luc2 was cultured in RPMI 1640 medium with 10% FBS. HUVECs and HLECs were maintained in endothelial cell medium supplemented with 5% FBS and endothelial cell growth supplement (ScienCell Research Laboratories).

Full length *Homo sapiens ABCB1* (NM_000927.4) and *ABCC1* (NM_004996.3) were subcloned into pcDNA3.1 in frame with a C-terminal V5-His tag (Invitrogen) using PCR with the following primers: ABCB1-forward 5′-TAA TAT GGA TCC ATG GAT CTT GAA GGG GAC CG-3′; ABCB1-reverse 5′-TAA TAT GGA TCC ATG GAT CTT GAA GGG GAC CG-3′; ABCC1-forward 5′-TAA TAT TCT AGA TTC TGG CGC TTT GTT CCA GC-3′; ABCC1-reverse 5′-TAA TAA TCT AGA TTC ACC AAG CCG GCG TCT TTG G-3′. Lipofectamine (Invitrogen) and Lipofectamine Plus reagents (Invitrogen) were used to transfect MCF7 and 4T1-luc cells and Geneticin (G418) at 0.8 or 0.1 g/L, respectively, was used to select stably transfected clones.

### *In vitro* assays

Cell proliferation was determined with a WST-8 Kit. Motility was determined by wound healing assays (16). *In vitro* angiogenesis and lymphangiogenesis were determined by tube formation assays as described previously (17, 18). qPCR and western blotting were carried out essentially as described previously (10). Lipids were extracted and sphingolipids quantified by liquid chromatography-electrospray ionization-tandem mass spectrometry (LC-ESI-MS/MS; refs. 10, 19). Cells were fixed for 5 minutes in 4% paraformaldehyde in PBS and blocked by horse serum, and immunocytochemistry was performed using the following primary antibodies: anti-ABCB1 (C219, Abcam), anti-ABCC1 (MRPr1, Monosan), and anti-SphK1 phospho-Ser225 (ECM Biosciences). The specificities of anti-ABCC1 and anti-SphK1 antibodies and anti–phospho-SphK1 specific antibody, phospho-Ser225, were previously confirmed using siRNA knockdown (10, 20). After incubation with biotinylated secondary antibodies, antigens were visualized with 3,30-diaminobenzidine (Dako), and cells were counterstained with hematoxylin.

### Animal studies

All procedures were approved by the VCU Institutional Animal Care and Use Committee that is accredited by the Association for Assessment and Accreditation of Laboratory Animal Care. For mice xenograft experiments, 10- to 18 week-old female BALB/c nu/nu mice (Harlan Laboratories) were ovariectomized via the dorsal approach, and 0.72 mg 17-β-estradiol pellets (Innovative Research) were implanted subcutaneously as described previously (21). MCF7 cells stably expressing ABCB1 (B1), ABCC1 (C1), or vector (V) were orthotopically implanted into the right upper mammary fat pads of nude mice as described previously (18, 22, 23). For syngeneic mice experiments, 4T1-luc2 cells stably expressing ABCB1, ABCC1, or vector were implanted in the same manner in 8- to 12-week-old female BALB/c mice (Harlan Laboratories). Tumor volumes in $mm^3$ were determined by measurements of length and width using calipers every 2 to 3 days. Bioluminescence was used to determine total tumor burden as well as metastases in *ex vivo* in axillary lymph nodes and lungs and was measured and quantified utilizing Xenogen IVIS 200 and Living Image software (Caliper Life Sciences; refs. 24, 25). Tumor interstitial fluid was collected as described previously (26).

For FACS, tumors were minced and digested, and cell suspensions were processed (18). Alexa 488–conjugated LYVE-1 (eBioscience); PE-conjugated podoplanin, PerCP-Cy5.5–conjugated CD45, APC-conjugated CD31, Alexa 700–conjugated TER-119 (BioLegend), or appropriate matched fluorochrome-labeled isotype control mAbs were used for staining. Cells were analyzed by FACS using BD FACSCanto II and BD FACSAria II (BD Biosciences), and data were assessed with BD FACSDiva Software version 6.1.3 (BD Biosciences). The remaining tumor sections were fixed with 10% of neutral-buffered formalin for histopathologic analysis.

### Patient samples

This study was approved by the Institutional Review Board of Yokohama City University (Yokohama, Japan), and the patients provided informed consents before inclusion in the study. The study followed the Declaration of Helsinki and good clinical practice guidelines. Tissues were obtained from 275 patients with stage 1 to 3 breast cancers treated in Yokohama City University Medical Center, Japan, between 2006 and 2008. The clinical

Published OnlineFirst March 9, 2018; DOI: 10.1158/1541-7786.MCR-17-0353



characteristics are presented in Supplementary Table S1. Tissue microarrays were constructed as described previously (27). Because SphK1 is activated by phosphorylation in breast cancer cells, we examined the activation status of SphK1 in breast cancer patients by immunostaining of a tissue microarray from breast cancer patients with a phospho- SphK1–specific antibody. Specificity of the anti-phosphorylated SphK1 antibody was confirmed by immunocytochemistry of MCF7 human breast cancer cells. In agreement with previous studies (10, 28), pSphK1 staining was increased after stimulation of MCF7 cells with estradiol and was absent when SphK1 was downregulated by a specific siRNA (data not shown).

**Histopathologic analyses of mouse and human tumor samples**

Five-micron sections of mouse and human tumors were stained with anti-Ki67 (DAKO), anti-SphK1 (Abcam), anti-SphK1 phospho-Ser225 (ECM Biosciences), anti-CD31 (BD), anti–LYVE-1 (Abcam), or anti-CK8 (Abcam). Sections were examined with a BX-41 light microscope (Olympus) or TCS-SP2 AOBS Confocal Laser Scanning Microscope (Leica), and microvessel density was determined as described previously (29). ABCB1 and ABCC1 staining in the breast tumors was assessed according to the intensity and population of staining. We scored each sample by 0 to 3: 0 = negative, there is no staining in the tumor cells; 1 = weak, more than 10 % of tumor cells stained with weak intensity; 2 = moderate, more than 30% of tumor cells stained with intermediate intensity or less than 30% of tumor cells stained with strong intensity; 3 = strong, more than 30% of tumor cells stained with strong intensity. Negative: 0 and weak: 1 are considered as low expression, whereas moderate: 2 and strong: 3 are considered as high expression as described previously (27).

**Interstitial fluid collection and quantification of sphingolipids by mass spectrometry**

Cells, culture medium, and interstitial fluid from breast tumors were collected as described previously (26). Lipids were extracted from these samples, and sphingolipids were quantified by LC-ESI-MS/MS (4000 QTRAP, AB Sciex) as described previously (26).

**METABRIC data acquisition and preprocessing and survival analysis**

Level 3 *z*-score normalized gene expression data were downloaded from the METABRIC breast cancer study using CBioPortal. All of 2,509 patients with both overall survival data and U133 microarray data from Curtis and colleagues and Pereira and colleagues studies were considered (30, 31). For single gene survival analyses based on expression of SphK1, patients were classified as having high or low expression of the given gene using a gene-specific *z*-score threshold. Patients were labeled as "high" if the expression of the interrogated gene was above the threshold and "low" if below the threshold. To determine the SphK1-specific threshold, *z*-scores of 0, ±0.5, ±1, and ±2 were investigated. For each cutoff, a survival curve was generated. The cutoff that generated the lowest log-rank *P* value was chosen as the SphK1 cutoff. For dual ABCC1 or ABCB1 transporter and SphK1 survival analyses, an inclusive *z*-score threshold of above and below 0 for each gene was used to maximize the size of the study sample. Two patient groups were classified by their patterns of expression of the pair of genes. For all analyses, Kaplan–Meier analysis was performed using GraphPad prism software. Statistical analysis was performed using the Mantel–Cox log-rank test and considered significant at $\alpha = 0.05$ significance level.

**Statistical analysis**

*In vitro* and *in vivo* experiments were repeated at least three times and consistent results are presented. Results were analyzed for statistical significance with the Student *t* test for unpaired samples. Correlations among the clinicopathologic parameters and each transporter or activated SphK1 were evaluated by the Pearson v2 test, the Fisher exact test, and the Mann–Whitney test. Patient outcomes were assessed by disease-free survival, and distributions were estimated by the Kaplan–Meier method using SPSS 19.0 (SPSS Inc.) Differences were compared using the log-rank test. $P < 0.05$ was considered statistically significant.

## Results

**High expression of ABCC1, but not ABCB1, is associated with poor prognosis in breast cancer patients**

To further solidify the association of ABC transporter expression with breast cancer patient prognosis, we extended our previous study, which had a limited number of patients and a short duration (27), utilizing a tumor tissue microarray from a larger cohort of patients, and we analyzed expression of ABC transporters by IHC. Patient and tumor characteristics are summarized in Supplementary Tables S1 and S2. ABCB1 was highly expressed in 32.4% (89/275), whereas ABCC1 was highly expressed in 38.9% (107/275) of the tumors analyzed. Representative images of ABCB1 and ABCC1 stained tissues are shown in Fig. 1A. Patients with high ABCC1 expression had significantly shorter disease-free survival compared with patients with low ABCC1-expressing tumors with the follow-up period up to 8 years ($P = 0.004$; Fig. 1B). In contrast, expression levels of ABCB1 were not associated with disease-free survival despite the extended number of patients and follow-up period (Fig. 1B).

**Overexpression of ABCC1, but not ABCB1, enhances S1P secretion, proliferation, and migration of breast cancer cells and promotes angiogenesis and lymphangiogenesis *in vitro***

To investigate the role of ABC transporters in cancer progression, we generated MCF7 human breast cancer cells and 4T1-luc2 murine breast cancer cells stably overexpressing vector, ABCB1, and ABCC1. Expression of ABCB1 and ABCC1 was confirmed at the mRNA and protein levels by qPCR and Western blotting, respectively, and IHC confirmed that these ABC transporters are expressed on the plasma membrane (Fig. 2A; Supplementary Fig. S1).

Consistent with our previous reports demonstrating that S1P is exported via ABCC1 but not ABCB1 using siRNA (10), and specific inhibitors (20), overexpression of ABCC1, but not ABCB1, significantly increased S1P secretion from human MCF7 and murine 4T1 breast cancer cells, as measured by LC-ESI-MS/MS (Fig. 2B and C). In addition, ABCC1 overexpression increased not only S1P, but also dihydro-S1P (DHS1P; Supplementary Fig. S2A). Moreover, as expected, intracellular S1P was decreased, whereas sphingosine (Sph) was increased (Supplementary Fig. S2B). Although intracellular ceramides and sphingomyelins levels were slightly decreased (Supplementary Figs. S2C, S3A, and S3B), there were no significant changes in intracellular monohexosylceramides (Supplementary Figs. S2C and S3C). Our results imply

Published OnlineFirst March 9, 2018; DOI: 10.1158/1541-7786.MCR-17-0353



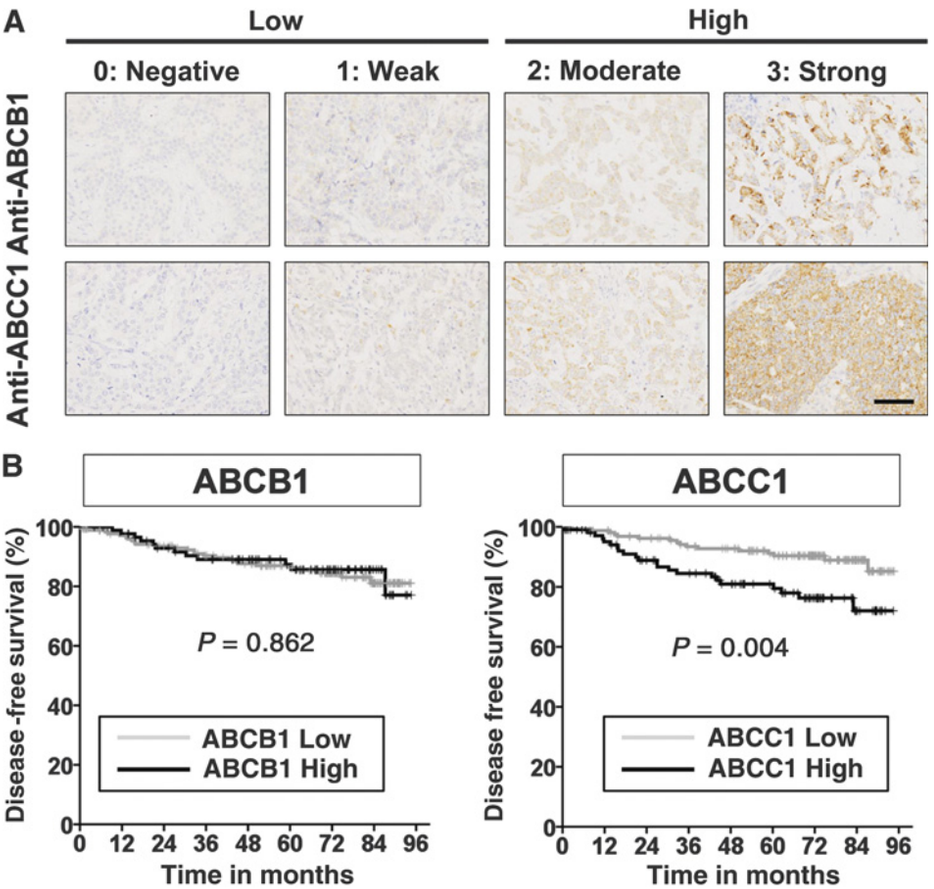


**Figure 1.**
Expression of ABCC1 but not ABCB1 correlates with poor prognosis in human breast cancer patients. Tissue microarrays containing 275 breast tumor tissues were stained with anti-ABCB1 or anti-ABCC1 antibodies. **A,** Expression of ABCB1 and ABCC1 was scored as 0, negative; 1, weak; 2, moderate; or 3, strong. Scores 0 and 1 are considered as low expression, whereas scores 2 and 3 are considered as high expression. Representative images are shown under high magnification for ABCB1 staining (top) and ABCC1 staining (bottom). **B,** Kaplan–Meier disease-free survival curves according to expression of ABCB1 and ABCC1. *P* values were calculated by the log-rank test. Scale bar, 50 μm.

that overexpression of ABCC1 that increases secretion of S1P leads to increased degradation of ceramide to sphingosine to compensate for the loss of intracellular S1P.

We next examined several biological processes important for cancer progression known to be regulated by S1P (7, 8). Overexpression of ABCC1 but not ABCB1 significantly enhanced cell proliferation (Fig. 2D). Moreover, MK571, an ABCC1 inhibitor, not only prevented secretion of S1P, but also suppressed the growth-stimulating effect of ABCC1 overexpression (Fig. 2D). In agreement with previous reports showing that directly adding S1P enhances breast cancer cell proliferation and migration (17, 32), cells expressing ABCC1 also showed significantly enhanced migration in scratch assays that was reduced by treatment with MK571. In contrast, MK571 had no significant effects on migration of vector or ABCB1 transfected cells (Fig. 2E and F). These results suggest that overexpression of ABCC1 increases the export S1P that enhances proliferation and migration of breast cancer cells.

Because S1P is a potent angiogenic and lymphangiogenic factor (18), we next examined whether S1P secreted from cells overexpressing ABC transporters could affect angiogenesis or lymphangiogenesis. Conditioned media from breast cancer cells expressing ABCC1, but not ABCB1 cells, promoted both angiogenesis and lymphangiogenesis of HUVECs and HLECs, respectively (Fig. 2G and H). However, conditioned medium from MCF7 cells expressing ABCC1 that were treated with MK571, an inhibitor of ABCC1 or with SK1-I, a specific inhibitor of SphK1, lost its ability to stimulate *in vitro* angiogenesis and lymphangiogenesis of endothelial and lymph endothelial cells, respectively (Fig. 2G and H). Collectively, these results suggest that S1P produced by SphK1 and secreted from breast cancer cells via ABCC1 transporter could affect not only the cancer cells themselves but also the microenvironment.

### Overexpression of ABCC1, but not ABCB1, markedly enhances tumorigenesis in MCF7 xenografts

We next examined the role of ABCC1 and secreted S1P in breast cancer progression *in vivo* by comparing tumors produced by MCF7 cells stably overexpressing ABCC1 or ABCB1 implanted into ovariectomized athymic nude mice in the presence of estradiol pellets. MCF7 cells were utilized because they readily secrete S1P in response to estradiol (10). Tumors from MCF7 cells overexpressing ABCC1 grew significantly faster and were much larger than tumors from mice implanted with MCF7 cells overexpressing vector or ABCB1 (Fig. 3A). Morphologically, MCF7/C1 tumors appeared more poorly differentiated by H&E staining (Fig. 3B). In agreement, these tumors also had significantly higher mitotic activity than tumors from MCF7 cells overexpressing vector or ABCB1 by Ki67 staining (Fig. 3B and C). Likewise, mice implanted with MCF7 cells overexpressing ABCC1 had significantly higher blood vessel densities detected by CD31

Published OnlineFirst March 9, 2018; DOI: 10.1158/1541-7786.MCR-17-0353



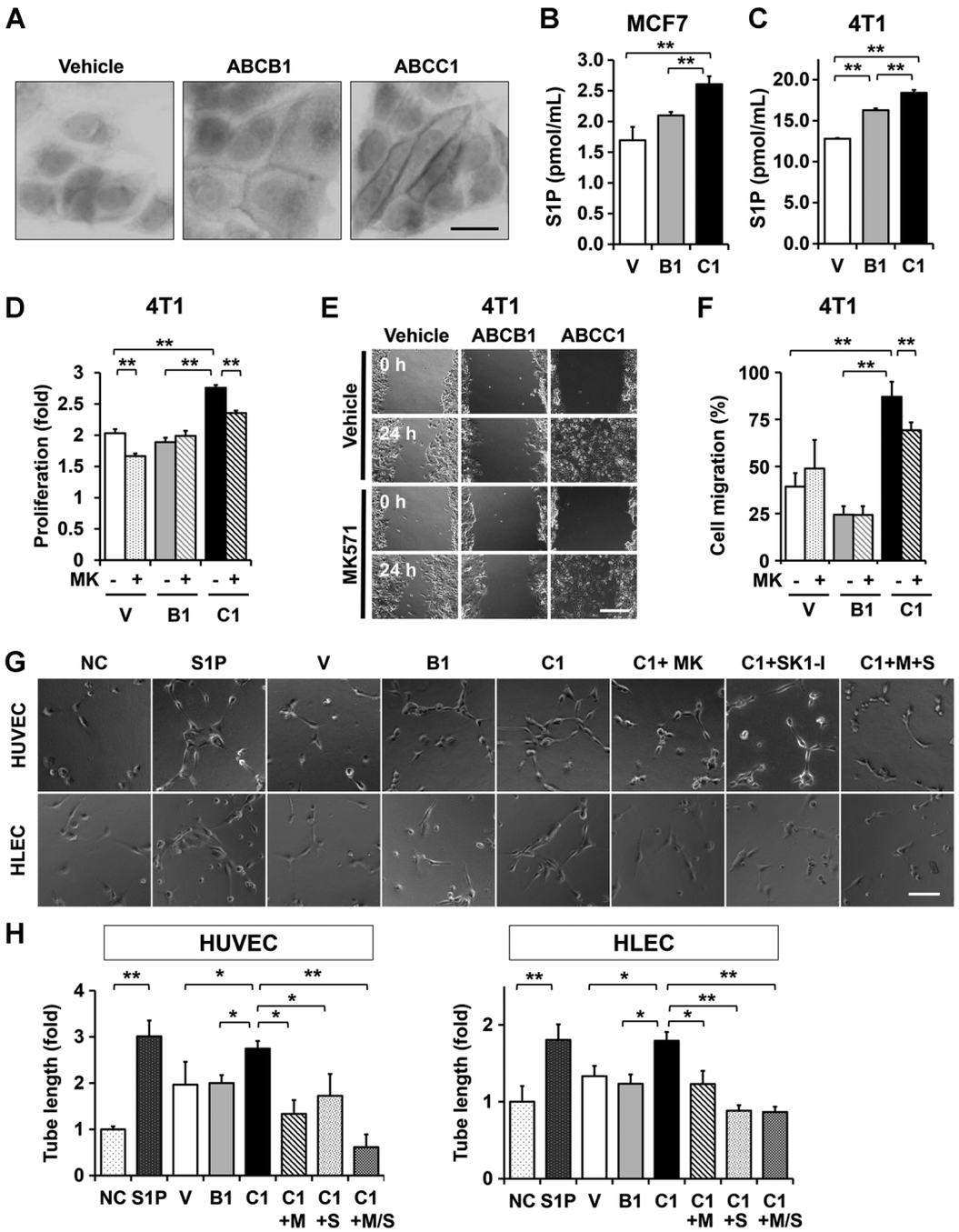


**Figure 2.**

Overexpression of ABCC1, but not ABCB1, enhances proliferation and cell migration of breast cancer cells and promotes S1P secretion–mediated angiogenesis and lymphangiogenesis of endothelial cells. **A–E,** MCF7 or 4T1 breast cancer cells were transfected with vector (V), ABCB1 (B1), or ABCC1 (C1) as indicated. **A,** IHC reveals that expressed ABCB1 and ABCC are localized to the plasma membrane. **B** and **C,** S1P secreted from the indicated breast cancer cells was determined by LC-ESI-MS/MS. **D,** Proliferation of cells treated with vehicle or 20 μmol/L MK571 for 48 hours was determined by WST8 assay. Data are expressed as fold increase compared with 0 time. **E** and **F,** Monolayers of the indicated 4T1 cells treated with vehicle or 20 μmol/L MK57 were wounded and migration of cells into the wounded area was measured 24 hours later. **E,** Representative photographs of wounded areas are shown. **F,** Cell migration was determined as percent of initial wounded area and expressed as means ± SD of 6 determinations. **G** and **H,** HUVECs and HLECs were cultured on reduced growth factor basement membrane matrix-coated 48-well plates and incubated for 6 hours without or with S1P (1 μmol/L) or conditioned medium from MCF cells overexpressing ABCC1 (C1) were pretreated with vehicle (NC, nontreated control) or 20 μmol/L MK571 without or with 10 μmol/L SK1-I for 12 hours and conditioned medium prepared. +M, treated with MK571; +S, treated with SK1-I. Six random fields per condition were photographed (**G**) and total tube length determined (**H**). Scale bars, 20 μm (**A**), 200 μm (**E**), and 100 μm (**G**). *, $P < 0.05$; **, $P < 0.01$ determined by Student $t$ test. Data, means ± SD.

Published OnlineFirst March 9, 2018; DOI: 10.1158/1541-7786.MCR-17-0353



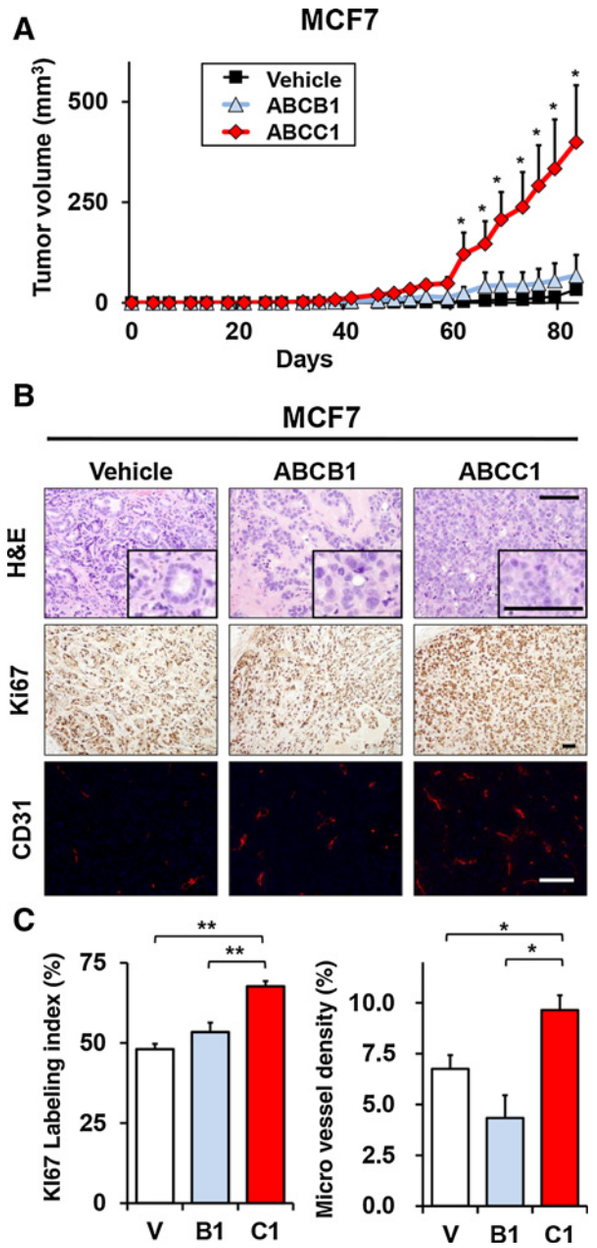


**Figure 3.**

Overexpression of ABCC1, but not ABCB1, enhances MCF7 tumor growth in a mouse xenograft model. **A,** BALB/c nude mice were ovariectomized and estrogen pellets implanted under anesthesia. Tumors were established by surgical implantation of MCF7 cells stably overexpressing vector, ABCB1, or ABCC1 into chest mammary fat pads. Tumor size was measured at the indicated times ($n = 5$ mice/group). **B,** Representative images of H&E and Ki67 staining and confocal immunofluorescent images of stained blood vessels with anti-CD31 (red) and nuclei costained with Hoechst (blue) in tumor sections 83 days after implantation. **C,** Percentage of Ki67-positive cells and microvessel density were determined. Scale bar, 100 μm. *, $P < 0.05$; **, $P < 0.01$ determined by Student $t$ test. Data, means ± SEM.

immunofluorescence (Fig. 3B and C). These results suggest that overexpression of ABCC1 enhances breast cancer progression and angiogenesis.

### Overexpression of ABCC1, but not ABCB1, enhances tumor growth, angiogenesis, and lymphangiogenesis and contributes to poor survival of mice bearing 4T1 syngeneic tumors

Because it is well established that S1P plays critical roles in immune responses and affects the tumor microenvironment, we next examined the role of ABCC1 in an immunocompetent syngeneic breast cancer model. *In vivo* bioluminescence revealed that tumors from 4T1-luc2 cells overexpressing ABCC1 orthotopically implanted in BALB/C mice grew significantly faster and to a much greater size than 4T1-luc2 tumors overexpressing vector or ABCB1 (Fig. 4A). Similar to the xenograft model, tumors of 4T1 cells overexpressing ABCC1 also had high mitotic activity measured by Ki67 staining (Fig. 4B). These tumors also had increased angiogenesis and lymphangiogenesis compared with tumors overexpressing ABCB1 or empty vector, as quantified by microvessel density of blood vessels (MVD) and lymphatic vessels (MLD) determined by immunofluorescence staining for CD31 and Lyve1, respectively (Fig. 4C). These results were further confirmed by flow cytometry of cells from mammary site tumors that quantified blood endothelial cells (BEC) and lymphatic endothelial cells (LEC) using CD31, a marker for both BECs and LECs, and gp38 (podoplanin), a specific marker for LECs (Fig. 4D). Given the significant increase in both angiogenesis and lymphangiogenesis, we then determined lymph node and lung metastasis and survival of the mice. As shown in Fig. 4E, mice implanted with 4T1 cells overexpressing ABCC1 had significantly more metastases not only in lymph nodes but also in the lung, both measured by *ex vivo* bioluminescence, than in mice implanted with 4T1 cells overexpressing ABCB1. Similarly, the numbers of metastatic lesions were significantly greater in the mice bearing ABCC1-expressing tumors, determined by immunofluorescence and H&E staining (Fig. 4F). Furthermore, these mice had significantly shorter survival compared with mice bearing ABCB1-expressing tumors (23 ± 3 days compared with 30 ± 2 days; Fig. 4G). Together, these results suggest that tumors overexpressing ABCC1 are much more aggressive with worse survival, possibly due to enhanced S1P secretion.

### S1P exported via ABCC1 upregulates transcription of SphK1 and enhances its own production of S1P

Previous studies demonstrated that expression of SphK1 is elevated (33, 34) and correlates with poor survival in human breast cancer patients (13) and in mice breast cancer models (18). Therefore, it was of interest to determine expression of SphK1 in breast cancer cells and tumors overexpressing ABC transporters. *SphK1* mRNA levels were significantly increased in both MCF7 and 4T1 cells overexpressing ABCC1 (Fig. 5A; Supplementary Fig. S4). Similarly, IHC revealed increased activated SphK1 determined with a phospho-SphK1–specific antibody (Fig. 5B). Upregulation of *SphK1* mRNA in cells overexpressing ABCC1 was suppressed by MK571, an ABCC1 inhibitor, but had no effects on SphK1 levels in cells overexpressing ABCB1 or vector (Fig. 5C). As these results suggest that S1P secreted through ABCC1 leads to upregulation of SphK1, the kinase that produces it, we next examined whether exogenous S1P can upregulate SphK1 in naïve breast cancer cells. Indeed, *SphK1* mRNA was increased by treatment of 4T1 cells with S1P in a time- and dose-dependent manner (Fig. 5D), supporting the notion that S1P exported by ABCC1 can act in a positive feedback manner to amplify its own production. In agreement with these *in vitro* data, IHC revealed that tumors overexpressing ABCC1 had higher levels of SphK1 and activated

Published OnlineFirst March 9, 2018; DOI: 10.1158/1541-7786.MCR-17-0353



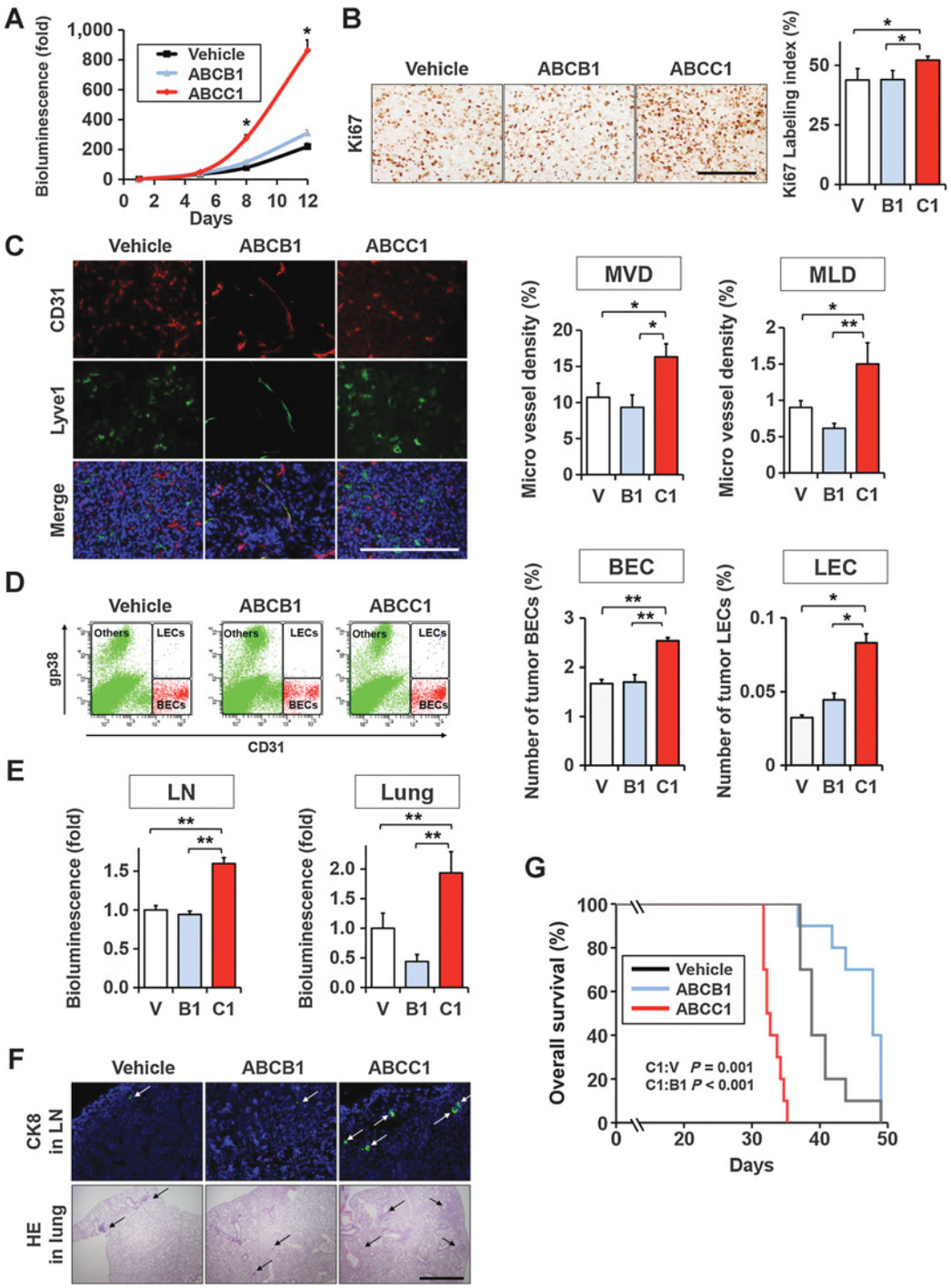


**Figure 4.**

Overexpression of ABCC1, but not ABCB1, enhances 4T1 tumor growth and decreases survival in a syngeneic mouse model. **A–F,** 4T1-luc2 cells transfected with vector, ABCB1, or ABCC1 were implanted into mammary fat pads of BALB/c mice under direct vision (23). **A,** Tumor burden was determined by *in vivo* bioluminescence ($n = 10$ mice/group). **B,** Representative images of Ki67 staining of tumor sections are shown and the percentage of Ki67 positive cells within tumors was enumerated. ($n = 5$) **C,** Confocal immunofluorescent images of tumors stained for blood vessels (anti-CD31, red), lymphatic vessels, (anti-lyve1, green), and nuclei (Hoechst, blue). Microvessel density and lymphatic vessel density were determined. **D,** Tumors were minced, digested with collagenase, and BECs and LECs were quantified by FACS. Representative panels of FACS analysis are shown. **E,** Regional lymph node metastases and lung metastases were determined by *ex vivo* bioluminescence 12 days after implantation. **F,** Confocal immune fluorescent images of lymph nodes stained for adenocarcinoma (anti-CK8, green, white arrows) and nuclei (Hoechst, blue) and H&E-stained lung sections show metastases (black arrow). **G,** Kaplan–Meier survival curves of mice bearing 4T1/V, 4T1/B1, and 4T1/C1 tumors. Days were counted after cancer cell implantation. *P* values were calculated by log-rank test. Scale bar, 100 μm (**B** and **C**); 2 μm (**F**). *, $P < 0.05$; **, $P < 0.01$ based on Student *t* test. Data, means ± SEM.

Published OnlineFirst March 9, 2018; DOI: 10.1158/1541-7786.MCR-17-0353



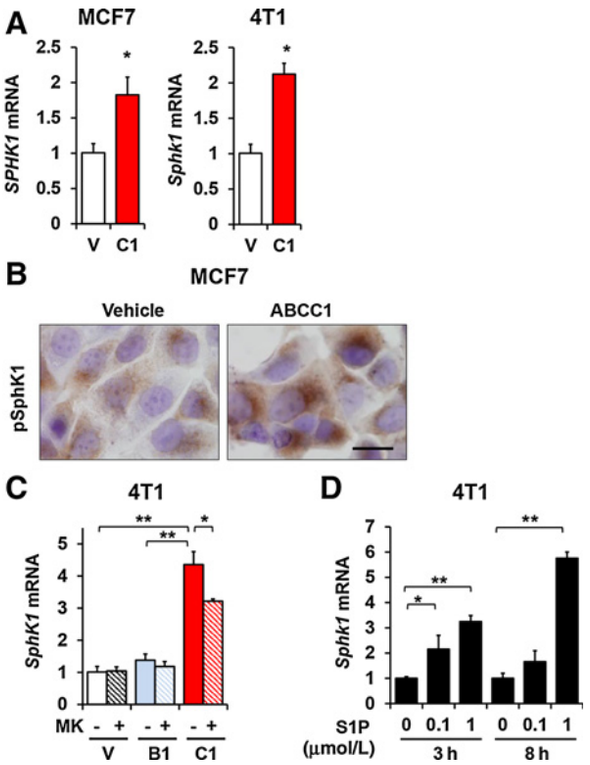


**Figure 5.**

S1P exported via ABCC1 upregulates expression of SphK1. **A,** SphK1 expression in MCF7 and 4T1 cells transfected with vector or ABCC1 was determined by QPCR and normalized to GAPDH. Data, means ± SEM. **B,** Activation of SphK1 in transfected MCF7 cells was determined by immunocytochemistry with pSphK1 antibody. Scale bar, 20 μm. **C,** 4T1 cells transfected as indicated were treated with vehicle or 20 μmol/L MK571 for 24 hours in serum-free medium. Cells were then stimulated in medium containing 10% serum for 3 hours. *SphK1* mRNA levels were determined by qPCR and normalized to *Gapdh*. Data, means ± SD. **D,** Naïve 4T1 cells were starved for 24 hours and treated with 100 nmol/L or 1 μmol/L S1P in 0.4% fatty acid free BSA for 3 or 8 hours as indicated. SphK1 and GAPDH mRNA was determined by qPCR.

SphK1 than those expressing ABCB1 or vector (Fig. 6A–D). Likewise, *SphK*1 mRNA expression was higher in tumors overexpressing ABCC1, as demonstrated by qPCR (Fig. 6E). Consistent with increased SphK1 expression, S1P levels in tumors and in tumor interstitial fluid were significantly higher in tumors overexpressing ABCC1 than tumors overexpressing ABCB1 or vector (Fig. 6F).

### Patients with breast cancers that express both activated SphK1 and ABCC1 have shorter disease-free survival

Because expression of ABCC1 in murine breast tumors upregulates SphK1 and decreases survival, we investigated whether increased expression of SphK1 and ABCC1 in human breast tumors could be a prognosis indicator. To this end, expression of ABCC1 and activated SphK1 in human breast cancer tissues was determined by IHC of human breast tumor microarrays and ER, PgR, and HER2 status was determined by an expert pathologist and tumors divided into 4 subtypes of breast cancer: Luminal [estrogen receptor positive ($ER^+$), $HER2^-$]; Luminal-HER2 ($ER^+$, $HER2^+$); HER2 ($ER^-$, $HER2^+$); and triple-negative breast cancer (TNBC: $ER^-$, $HER2^-$; Supplementary Table S1). Scoring of pSphK1 expression in human breast tumor samples was shown in Fig. 7A. The frequency of strong pSphK1 expression was higher in HER2 overexpressing or TNBC, the more aggressive breast cancer subtypes. pSphK1 was more prevalent and increased in a larger tumors (higher T stage) and in tumors from patients with lymph node metastases (higher TNM stage; Fig. 7B; Supplementary Table S3). Finally, we correlated clinical outcomes with expression of pSphK1 and ABCC1. Importantly, patients with breast tumors that had higher expression of pSphK1 had worse disease-free survival compared with those with weaker pSphK1 levels ($P = 0.011$; Fig. 7C). Strikingly, in patient tumors with high expression of both pSphK1 and ABCC1, disease-free survival was significantly decreased (Fig. 7C). In contrast, there was no significant difference in survival of those expressing high levels of ABCB1 and pSphK1 (Fig. 7C). In agreement with previous studies showing that expression of SphK1 is elevated in patients with breast cancer and correlates with poor prognosis (13), mining of METABRIC breast tumor expression database showed that SphK1 expression significantly correlates with worse survival prognosis (median survival of 124 months with high SphK1 expression compared with 163 months for patients with low SphK1 expression, $P = 0.0014$; Fig. 7D). Furthermore, those with high levels of both SphK1 and ABCC1 had much worse prognosis with median survival of 114 months ($P < 0.0068$, Fig. 7D). Such correlations were not observed with ABCB1 expression (Fig. 7D).

Together, these findings support the notion that breast cancer patients with tumors that have high ABCC1 expression have poorer survival, at least in part, due to enhanced expression of SphK1 and secretion of S1P into the tumor microenvironment.

## Discussion

Among the many known ABC transporters, ABCB1 and ABCC1 are two multidrug resistant proteins that are upregulated in breast cancer in response to chemotherapy and contribute to chemoresistance (2). ABCB1 is the most well studied as it effluxes the commonly used anticancer drugs, anthracyclines and taxanes. However, clinical trials with agents targeting ABCB1 have all failed (35). Recent reports suggest that the functions of ABC transporters are not limited merely to the efflux of drugs as they also transport other types of molecules including lipids (36). Lipid-derived signaling molecules, such as leukotrienes and prostaglandins, conjugated organic anions, and S1P, have also been identified as substrates of multitasking ABCC1 transporter (37). Among them, the bioactive sphingolipid mediator S1P is now recognized as a critical regulator of many physiologic processes important for breast cancer progression (38). S1P is generated inside cancer cells by SphK1, and then exported outside of the cell into the tumor microenvironment where it can bind to five G protein–coupled receptors whose downstream signaling is responsible for most of the action of S1P. This "inside-out" signaling by S1P plays a pivotal role in cancer cells and in the tumor microenvironment by regulating inflammatory cells recruitment and stimulating angiogenesis and lymphangiogenesis (39). SphK1 levels are upregulated in many malignant tumors, including lung (40), kidney (33), colon (41), breast (13, 18), prostate (42), stomach (43), liver (44), brain (45), in non-Hodgkin lymphoma (46), and chronic myeloid leukemia (47), and has been reported to be associated with poor prognosis in several types of cancer, including esophageal (48), bladder

Published OnlineFirst March 9, 2018; DOI: 10.1158/1541-7786.MCR-17-0353



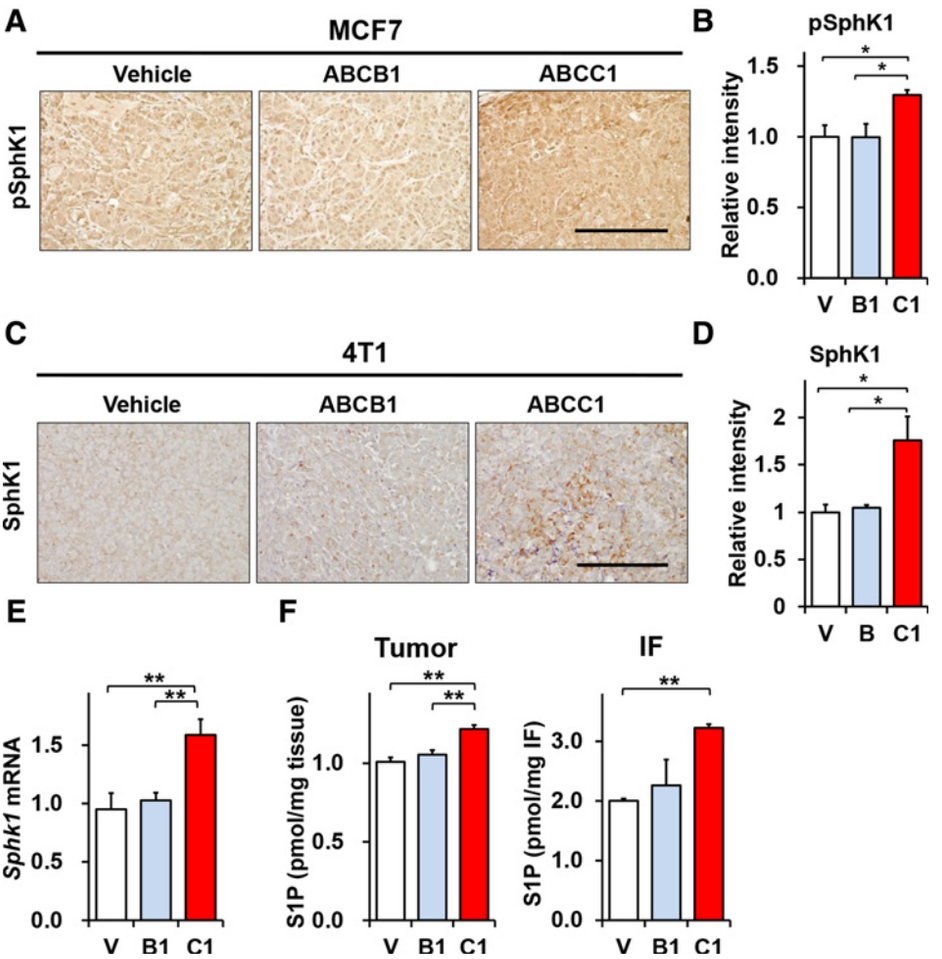


**Figure 6.**
Overexpression of ABCC1 in breast tumors enhances expression of SphK1 and increases S1P in tumor interstitial fluid. **A** and **B,** MCF7 cells transfected with vector, ABCB1, or ABCC1 were implanted into chest mammary fat pads of ovariectomized BALB/c nude mice. pSphK1 in tumors determined by IHC on day 32. **C–E,** 4T1-luc2 cells transfected with vector, ABCB1, or ABCC1 were implanted into mammary fat pads of BALB/c mice and tumors analyzed on day 12. SphK1 expression in 4T1 tumors was examined by staining with anti-SphK1 antibody. **B** and **D,** Relative intensity of immunostaining was quantified by NIH ImageJ. Scale bar, 200 μm. **E,** *Sphk1* mRNA level in tumors were determined by qPCR and normalized to *Gapdh*. **F,** S1P levels in tumors ($n = 10$) and in tumor interstitial fluid ($n = 5$) were determined by LC-ESI-MS/MS. Data, means ± SEM. *, $P < 0.05$; **, $P < 0.01$.

(49), prostate (50), and breast (13, 51). In agreement, we found that expression of SphK1 correlates with breast cancer staging. We also demonstrated for the first time that activated SphK1, determined with a phospho-SphK1–specific antibody, which is a direct reflection of S1P production, is associated with poor survival in human breast cancer. Interestingly, patients whose breast tumor had high expression of both activated SphK1 and ABCC1 had significantly shorter disease-free survival, whereas no associations were observed with expression of ABCB1. These findings are consistent with the view that increased production of S1P by higher levels of pSphK1 and its increased efflux of S1P by ABCC1 combine to shorten survival.

It is now recognized that tumors display another level of complexity by regulating the tumor microenvironment (52). We demonstrated previously that S1P is increased in breast tumors and in their interstitial fluid that fills the space of the tumor microenvironment (26) and that S1P can enhance breast cancer–induced angiogenesis and lymphangiogenesis (18, 53). In the current study, we have shown that S1P levels in tumor and interstitial fluid are higher in breast tumors that overexpress ABCC1. Furthermore, export of S1P by ABCC1 not only affected the cancer cells themselves and markedly enhanced tumor growth, it also influenced the tumor microenvironment, increasing angiogenesis, and lymphangiogenesis. It is thus not surprising that these rapidly growing tumors aggressively metastasized to lymph nodes or distant organs and shortened survival of mice bearing these tumors. In sharp contrast, overexpression of ABCB1 could result in a slightly increased level of S1P around breast cancer cells that have very high endogenous SphK1, but the effects of small increases in S1P levels on physiologic functions, such as tumor progression and metastasis, would not be expected to be significant. Our results suggest that export of S1P by ABCC1 is as important as production of S1P by SphK1 in cancer progression and in the tumor microenvironment.

Another unexpected and important finding in this study was that S1P exported via ABCC1 from breast cancer cells upregulated their expression of SphK1, leading to further increased production of S1P that in turn acts on the tumor cells themselves and on the tumor microenvironment. Hence, exported S1P acts in a malicious feed-forward amplification loop to amplify the S1P axis that drives tumorigenesis and metastasis. Although not examined in the current study, the results of many previous studies suggest that these effects of S1P are mediated by binding to S1P receptors present on the cancer cells or on cells in the microenvironment, including endothelial and lymphendothelial cells (8). Similar to the shorter survival of mice bearing tumors overexpressing ABCC1 (that upregulates SphK1), patients with tumors that overexpress both SphK1 and ABCC1 have poor prognosis. Taken together, our

Published OnlineFirst March 9, 2018; DOI: 10.1158/1541-7786.MCR-17-0353



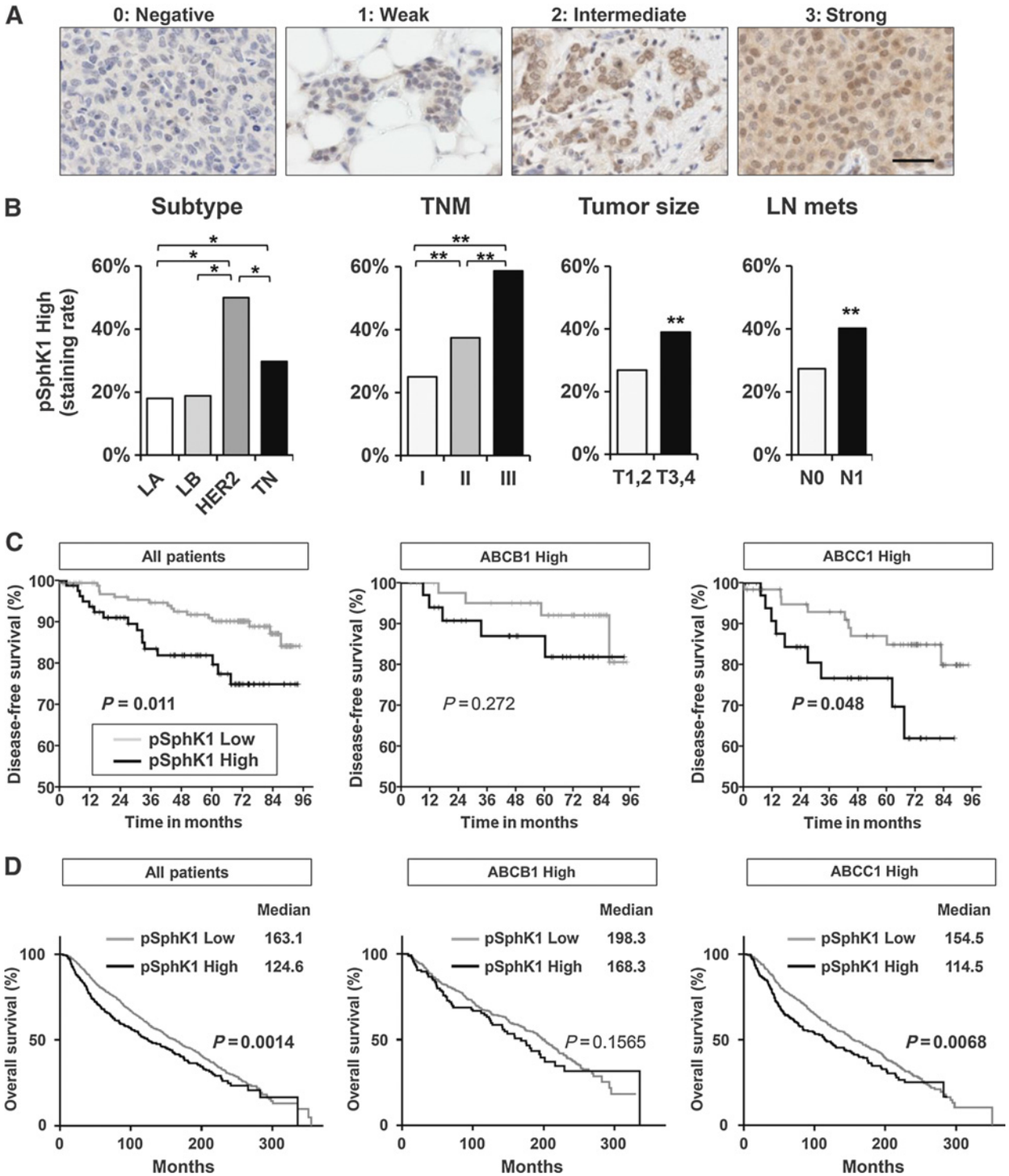


**Figure 7.**

Patients with breast cancers that express both activated SphK1 and ABCC1 have shorter disease-free survival. pSphK1 in 275 human breast tumors examined by IHC. **A,** Scoring of pSphK1 expression in human breast tumor samples. **B,** Frequency of high pSphK1 expression in human breast tumors correlated with clinicopathologic factors, tumor size, and lymph node metastasis status and TNM stage. *, $P < 0.05$; **, $P < 0.01$. **C,** Kaplan–Meier disease-free survival curves according to expression of pSphK1, co-expression of pSphK1 with ABCB1, and coexpression of pSphK1 with ABCC1. *P* values were calculated by the log-rank test. **D,** Kaplan–Meier survival analysis of breast cancer patients from the METABRIC database. Data were obtained from patients with clinical and expression information. Median survival is tabulated along with a log-rank *P* value representing the significance of high gene expression of SphK1 among all patients, among ABCB1 high patients, or among ABCC1 high patients on patient survival.

results suggest that combined therapies that target SphK1 (S1P production) and ABCC1 (S1P secretion) should be more beneficial than targeting each of them alone or then inhibitors of ABCB1. Our study might also explain the failure of previous clinical trials targeting ABCB1. We suggest that ABCC1, not ABCB1, contributes to worse prognosis through the export of the potent lipid mediator, S1P, independently of its effects on efflux chemotherapeutic drugs. This represents a new concept of action of ABCC1 and a significant advancement in understanding of the role of ABC transporters in breast cancer, with the potential for applicability in other malignancies.

## Disclosure of Potential Conflicts of Interest

No potential conflicts of interest were disclosed.

## Authors' Contributions

**Conception and design:** A. Yamada, S. Spiegel, K. Takabe
**Development of methodology:** W.-C. Huang
**Acquisition of data (provided animals, acquired and managed patients, provided facilities, etc.):** A. Yamada, M. Nagahashi, T. Aoyagi, W.-C. Huang, S. Lima, N.C. Hait, A. Maiti, K. Kida, K.P. Terracina, H. Miyazaki, T. Ishikawa
**Analysis and interpretation of data (e.g., statistical analysis, biostatistics, computational analysis):** A. Yamada, W.-C. Huang, M.R. Waters, Q. Qi, L. Yan, S. Spiegel, K. Takabe
**Writing, review, and/or revision of the manuscript:** A. Yamada, K.P. Terracina, S. Milstien, S. Spiegel, K. Takabe
**Administrative, technical, or material support (i.e., reporting or organizing data, constructing databases):** T. Ishikawa, I. Endo, K. Takabe
**Study supervision:** K. Takabe

## Acknowledgments

This work was supported by NIH grants (R01CA160688 to K. Takabe and R01CA61774 to S. Spiegel), Susan G. Komen Foundation Investigator Initiated Research Grant (IIR12222224; to K. Takabe), Department of Defense BCRP Program Award (W81XWH-14-1-0086 to S. Spiegel), and Grants-in-Aid for Scientific Research from the Japan Society for the Promotion of Science (JSPS; 16K19055 to A. Yamada, and 15H05676 and 15 K15471 to M. Nagahashi). The VCU Lipidomics and Microscopy Cores are supported in part by funding from the NIH, NCI Cancer Center Support Grant P30 CA016059.

The authors thank Dr. Jeremy Allegood for the lipidomics analyses. We thank Dr. Jorge A. Almenara, Director of the Anatomic Pathology Research Services (APRS), and the Tissue and Data Acquisition and Analysis Core (TDAAC) of VCU for technical assistance with tissue processing, sectioning and staining.

The costs of publication of this article were defrayed in part by the payment of page charges. This article must therefore be hereby marked *advertisement* in accordance with 18 U.S.C. Section 1734 solely to indicate this fact.

Received July 6, 2017; revised December 16, 2017; accepted February 9, 2018; published first March 9, 2018.

## References

1. DeSantis CE, Fedewa SA, Goding Sauer A, Kramer JL, Smith RA, Jemal A. Breast cancer statistics, 2015: convergence of incidence rates between black and white women. CA Cancer J Clin 2016;66:31–42.
2. Szakacs G, Annereau JP, Lababidi S, Shankavaram U, Arciello A, Bussey KJ, et al. Predicting drug sensitivity and resistance: profiling ABC transporter genes in cancer cells. Cancer Cell 2004;6:129–37.
3. Fletcher JI, Haber M, Henderson MJ, Norris MD. ABC transporters in cancer: more than just drug efflux pumps. Nat Rev Cancer 2010;10:147–56.
4. Chen Z, Shi T, Zhang L, Zhu P, Deng M, Huang C, et al. Mammalian drug efflux transporters of the ATP binding cassette (ABC) family in multidrug resistance: a review of the past decade. Cancer Lett 2016;370:153–64.
5. Leonessa F, Clarke R. ATP binding cassette transporters and drug resistance in breast cancer. Endocr Relat Cancer 2003;10:43–73.
6. Takabe K, Spiegel S. Export of sphingosine-1-phosphate and cancer progression. J Lipid Res 2014;55:1839–46.
7. Pyne NJ, Pyne S. Sphingosine 1-phosphate and cancer. Nat Rev Cancer 2010;10:489–503.
8. Kunkel GT, Maceyka M, Milstien S, Spiegel S. Targeting the sphingosine-1-phosphate axis in cancer, inflammation and beyond. Nat Rev Drug Discov 2013;12:688–702.
9. Takabe K, Paugh SW, Milstien S, Spiegel S. "Inside-out" signaling of sphingosine-1-phosphate: therapeutic targets. Pharmacol Rev 2008;60:181–95.
10. Takabe K, Kim RH, Allegood JC, Mitra P, Ramachandran S, Nagahashi M, et al. Estradiol induces export of sphingosine 1-phosphate from breast cancer cells via ABCC1 and ABCG2. J Biol Chem 2010;285:10477–86.
11. Nagahashi M, Tsuchida J, Moro K, Hasegawa M, Tatsuda K, Woelfel IA, et al. High levels of sphingolipids in human breast cancer. J Surg Res 2016;204:435–44.
12. Tsuchida J, Nagahashi M, Nakajima M, Moro K, Tatsuda K, Ramanathan R, et al. Breast cancer sphingosine-1-phosphate is associated with phosphosphingosine kinase 1 and lymphatic metastasis. J Surg Res 2016;205:85–94.
13. Ruckhaberle E, Rody A, Engels K, Gaetje R, von Minckwitz G, Schiffmann S, et al. Microarray analysis of altered sphingolipid metabolism reveals prognostic significance of sphingosine kinase 1 in breast cancer. Breast Cancer Res Treat 2008;112:41–52.
14. Watson C, Long JS, Orange C, Tannahill CL, Mallon E, McGlynn LM, et al. High expression of sphingosine 1-phosphate receptors, S1P1 and S1P3, sphingosine kinase 1, and extracellular signal-regulated kinase-1/2 is associated with development of tamoxifen resistance in estrogen receptor-positive breast cancer patients. Am J Pathol 2010;177:2205–15.
15. Katoh SY, Ueno M, Takakura N. Involvement of MDR1 function in proliferation of tumour cells. J Biochem 2008;143:517–24.
16. Shida D, Fang X, Kordula T, Takabe K, Lepine S, Alvarez SE, et al. Cross-talk between LPA1 and epidermal growth factor receptors mediates up-regulation of sphingosine kinase 1 to promote gastric cancer cell motility and invasion. Cancer Res 2008;68:6569–77.
17. Wang F, Van Brocklyn JR, Hobson JP, Movafagh S, Zukowska-Grojec Z, Milstien S, et al. Sphingosine 1-phosphate stimulates cell migration through a G(i)-coupled cell surface receptor. Potential involvement in angiogenesis. J Biol Chem 1999;274:35343–50.
18. Nagahashi M, Ramachandran S, Kim EY, Allegood JC, Rashid OM, Yamada A, et al. Sphingosine-1-phosphate produced by sphingosine kinase 1 promotes breast cancer progression by stimulating angiogenesis and lymphangiogenesis. Cancer Res 2012;72:726–35.
19. Hait NC, Allegood J, Maceyka M, Strub GM, Harikumar KB, Singh SK, et al. Regulation of histone acetylation in the nucleus by sphingosine-1-phosphate. Science 2009;325:1254–7.
20. Mitra P, Oskeritzian CA, Payne SG, Beaven MA, Milstien S, Spiegel S. Role of ABCC1 in export of sphingosine-1-phosphate from mast cells. Proc Natl Acad Sci U S A 2006;103:16394–9.
21. Ingberg E, Theodorsson A, Theodorsson E, Strom JO. Methods for long-term 17beta-estradiol administration to mice. Gen Comp Endocrinol 2012;175:188–93.
22. Rashid OM, Nagahashi M, Ramachandran S, Dumur C, Schaum J, Yamada A, et al. An improved syngeneic orthotopic murine model of human breast cancer progression. Breast Cancer Res Treat 2014;147:501–12.
23. Rashid OM, Nagahashi M, Ramachandran S, Graham L, Yamada A, Spiegel S, et al. Resection of the primary tumor improves survival in metastatic breast cancer by reducing overall tumor burden. Surgery 2013;153:771–8.
24. Katsuta E, DeMasi SC, Terracina KP, Spiegel S, Phan GQ, Bear HD, et al. Modified breast cancer model for preclinical immunotherapy studies. J Surg Res 2016;204:467–74.
25. Terracina KP, Aoyagi T, Huang WC, Nagahashi M, Yamada A, Aoki K, et al. Development of a metastatic murine colon cancer model. J Surg Res 2015;199:106–14.
26. Nagahashi M, Yamada A, Miyazaki H, Allegood JC, Tsuchida J, Aoyagi T, et al. Interstitial fluid sphingosine-1-phosphate in murine mammary gland

Published OnlineFirst March 9, 2018; DOI: 10.1158/1541-7786.MCR-17-0353



and cancer and human breast tissue and cancer determined by novel methods. J Mammary Gland Biol Neoplasia 2016;21:9–17.
27. Yamada A, Ishikawa T, Ota I, Kimura M, Shimizu D, Tanabe M, et al. High expression of ATP-binding cassette transporter ABCC11 in breast tumors is associated with aggressive subtypes and low disease-free survival. Breast Cancer Res Treat 2013;137:773–82.
28. Sukocheva O, Wadham C, Holmes A, Albanese N, Verrier E, Feng F, et al. Estrogen transactivates EGFR via the sphingosine 1-phosphate receptor Edg-3: the role of sphingosine kinase-1. J Cell Biol 2006;173: 301–10.
29. Nagahashi M, Shirai Y, Wakai T, Sakata J, Ajioka Y, Hatakeyama K. Perimuscular connective tissue contains more and larger lymphatic vessels than the shallower layers in human gallbladders. World J Gastroenterol 2007;13:4480–3.
30. Curtis C, Shah SP, Chin SF, Turashvili G, Rueda OM, Dunning MJ, et al. The genomic and transcriptomic architecture of 2,000 breast tumours reveals novel subgroups. Nature 2012;486:346–52.
31. Pereira B, Chin SF, Rueda OM, Vollan HK, Provenzano E, Bardwell HA, et al. The somatic mutation profiles of 2,433 breast cancers refines their genomic and transcriptomic landscapes. Nat Commun 2016;7:11479.
32. Goetzl EJ, Dolezalova H, Kong Y, Zeng L. Dual mechanisms for lysophospholipid induction of proliferation of human breast carcinoma cells. Cancer Res 1999;59:4732–7.
33. French KJ, Schrecengost RS, Lee BD, Zhuang Y, Smith SN, Eberly JL, et al. Discovery and evaluation of inhibitors of human sphingosine kinase. Cancer Res 2003;63:5962–9.
34. Shida D, Takabe K, Kapitonov D, Milstien S, Spiegel S. Targeting SphK1 as a new strategy against cancer. Curr Drug Targets 2008;9:662–73.
35. Dean M. ABC transporters, drug resistance, and cancer stem cells. J Mammary Gland Biol Neoplasia 2009;14:3–9.
36. Quazi F, Molday RS. Lipid transport by mammalian ABC proteins. Essays Biochem 2011;50:265–90.
37. Cole SP. Multidrug resistance protein 1 (MRP1, ABCC1), a "multitasking" ATP-binding cassette (ABC) transporter. J Biol Chem 2014;289: 30880–8.
38. Maceyka M, Harikumar KB, Milstien S, Spiegel S. Sphingosine-1-phosphate signaling and its role in disease. Trends Cell Biol 2012;22:50–60.
39. Nagahashi M, Takabe K, Terracina KP, Soma D, Hirose Y, Kobayashi T, et al. Sphingosine-1-phosphate transporters as targets for cancer therapy. BioMed Res Int 2014;2014:651727.
40. Song L, Xiong H, Li J, Liao W, Wang L, Wu J, et al. Sphingosine kinase-1 enhances resistance to apoptosis through activation of PI3K/Akt/NF-kappaB pathway in human non-small cell lung cancer. Clin Cancer Res 2011;17:1839–49.
41. Kawamori T, Osta W, Johnson KR, Pettus BJ, Bielawski J, Tanaka T, et al. Sphingosine kinase 1 is up-regulated in colon carcinogenesis. FASEB J 2006;20:386–8.
42. Malavaud B, Pchejetski D, Mazerolles C, de Paiva GR, Calvet C, Doumerc N, et al. Sphingosine kinase-1 activity and expression in human prostate cancer resection specimens. Eur J Cancer 2010;46:3417–24.
43. Li W, Yu CP, Xia JT, Zhang L, Weng GX, Zheng HQ, et al. Sphingosine kinase 1 is associated with gastric cancer progression and poor survival of patients. Clin Cancer Res 2009;15:1393–9.
44. Shi J, He YY, Sun JX, Guo WX, Li N, Xue J, et al. The impact of sphingosine kinase 1 on the prognosis of hepatocellular carcinoma patients with portal vein tumor thrombus. Ann Hepatol 2015;14:198–206.
45. Li J, Guan HY, Gong LY, Song LB, Zhang N, Wu J, et al. Clinical significance of sphingosine kinase-1 expression in human astrocytomas progression and overall patient survival. Clin Cancer Res 2008;14:6996–7003.
46. Bayerl MG, Bruggeman RD, Conroy EJ, Hengst JA, King TS, Jimenez M, et al. Sphingosine kinase 1 protein and mRNA are overexpressed in non-Hodgkin lymphomas and are attractive targets for novel pharmacological interventions. Leuk Lymphoma 2008;49:948–54.
47. Marfe G, Di Stefano C, Gambacurta A, Ottone T, Martini V, Abruzzese E, et al. Sphingosine kinase 1 overexpression is regulated by signaling through PI3K, AKT2, and mTOR in imatinib-resistant chronic myeloid leukemia cells. Exp Hematol 2011;39:653–65.
48. Pan J, Tao YF, Zhou Z, Cao BR, Wu SY, Zhang YL, et al. An novel role of sphingosine kinase-1 (SPHK1) in the invasion and metastasis of esophageal carcinoma. J Transl Med 2011;9:157.
49. Meng XD, Zhou ZS, Qiu JH, Shen WH, Wu Q, Xiao J. Increased SPHK1 expression is associated with poor prognosis in bladder cancer. Tumour Biol 2014;35:2075–80.
50. Pchejetski D, Bohler T, Stebbing J, Waxman J. Therapeutic potential of targeting sphingosine kinase 1 in prostate cancer. Nat Rev Urol 2011; 8:569–678.
51. Pyne S, Edwards J, Ohotski J, Pyne NJ. Sphingosine 1-phosphate receptors and sphingosine kinase 1: novel biomarkers for clinical prognosis in breast, prostate, and hematological cancers. Front Oncol 2012;2:168.
52. Hanahan D, Weinberg RA. Hallmarks of cancer: the next generation. Cell 2011;144:646–74.
53. Aoyagi T, Nagahashi M, Yamada A, Takabe K. The role of sphingosine-1-phosphate in breast cancer tumor-induced lymphangiogenesis. Lymphat Res Biol 2012;10:97–106.

Advances in Biological Regulation 67 (2018) 59–65

Contents lists available at ScienceDirect

Advances in Biological Regulation

journal homepage: www.elsevier.com/locate/jbior

# Sphingosine kinase 1 in breast cancer

Kurt Geffken, Sarah Spiegel*

*Department of Biochemistry and Molecular Biology and the Massey Cancer Center, Virginia Commonwealth University School of Medicine, Richmond, VA 23298 USA*

ARTICLE INFO

*Keywords:*
Sphingosine-1-phosphate
Sphingosine kinase
Estradiol
Breast cancer
FTY720/Fingolimod

ABSTRACT

Breast cancer affects 1 out of 8 women in the US and is the second highest cause of death from cancer for women, leading to considerable research examining the causes, progression, and treatment of breast cancer. Over the last two decades, sphingosine-1-phosphate (S1P), a potent sphingolipid metabolite, has been implicated in many processes important for breast cancer including growth, progression, transformation and metastasis, and is the focus of this review. In particular, one of the kinases that produces S1P, sphingosine kinase 1 (SphK1), has come under increasing scrutiny as it is commonly upregulated in breast cancer cells and has been linked with poorer prognosis and progression, possibly leading to resistance to certain anti-cancer therapies. In this review, we will also discuss preclinical studies of both estrogen receptor (ER) positive as well as triple-negative breast cancer mouse models with inhibitors of SphK1 and other compounds that target the S1P axis and have shown good promise in reducing tumor growth and metastasis. It is hoped that in the future this will lead to development of novel combination approaches for effective treatment of both conventional hormonal therapy-resistant breast cancer and triple-negative breast cancer.

## 1. Introduction

Breast cancer affects nearly 1 out of every 8 women over their lifetime and is the second leading cancer cause of death for women behind lung cancer in the US. Fortunately, over the last 30 years, breast cancer death rates have been dropping due to increased awareness of the disease, advances in detection, and better treatments. A large factor in these better treatments has been development of hormonal therapies to directly target specific receptors in the cancer cells such as estrogen (ER) and progesterone receptors (PR) that are present in roughly 70% of breast cancers. ER positive tumors in particular can be treated with estrogen antagonists such as tamoxifen to great effect with less side effects than traditional chemotherapy. The human epidermal growth factor receptor 2 (HER2), that is upregulated in 10–15% of breast cancers tumors can also be treated with a monoclonal antibody. However, there are still 15–20% of tumors that are ER/PR/HER2 negative, termed triple negative breast cancer (TNBC), which are usually more aggressive and metastatic with significantly worse prognosis. Therefore, current cancer research is also focused on deeper understanding of novel signaling pathways that can contribute to breast cancer growth and metastasis. In the last 20 years, it has become apparent that the bioactive sphingolipid metabolite, sphingosine-1-phosphate (S1P), regulates processes important for breast cancer including inflammation that can drive tumorigenesis, angiogenesis, which provides cancer cells with nutrients and oxygen, cell growth and

*Abbreviations:* BCSCs, breast cancer stem cells; ER, estrogen receptor; EGFR, epidermal growth factor receptor; ERK, extracellular signal regulated kinase; E2, 17β-estradiol; HDAC, histone deacetylase; HER2, human epidermal growth factor receptor 2; MAPK, mitogen activated protein kinase; PKC, protein kinase C; RTK, receptor tyrosine kinase; SphK, sphingosine kinase; S1P, sphingosine-1-phosphate; S1PR, S1P receptor; TNBC, triple-negative breast cancer

* Corresponding author.
*E-mail address:* sarah.spiegel@vcuhealth.org (S. Spiegel).

http://dx.doi.org/10.1016/j.jbior.2017.10.005
Received 21 September 2017; Received in revised form 13 October 2017; Accepted 13 October 2017
Available online 16 October 2017

survival, as well as migration and invasion important for metastasis (Espaillat et al., 2017; Maczis et al., 2016; Nagahashi et al., 2014; Newton et al., 2015; Pyne et al., 2014, 2016; Pyne and Pyne, 2010). In this review, we will summarize current research findings on S1P in breast cancer and examine the roles of the S1P/sphingosine kinase 1 (SphK1) axis in breast cancer signaling, prognosis, progression and as a possible target for future treatments, especially for TNBC and tumors that show resistance to typical first line treatments.

## 2. Formation of sphingosine-1-phosphate

Sphingolipids are important membrane constituents of all eukaryotic cells that also generate bioactive metabolites, such as S1P. The formation of S1P from sphingosine, produced by degradation of sphingolipids, begins with the activation of one of two enzymes, SphK1 or SphK2, resulting in the former case in its translocation from the cytosolic compartment to the plasma membrane where its substrate sphingosine resides (Hannun and Obeid, 2008). Numerous growth factors such as EGF, hormones, such as estradiol (E2), and pro-inflammatory cytokines such as IL-1 and IL-6 activate SphK1 (Gao et al., 2015; Maceyka et al., 2012; Maceyka and Spiegel, 2014; Maczis et al., 2016). In many cases, it has been shown that this is due to stimulation of extracellular signal-regulated kinases 1/2 (ERK1/2) that in turn phosphorylate SphK1 on Ser225 allowing for its specific targeting to the plasma membrane (Pitson et al., 2003). This is in contrast to SphK2 that also resides in intracellular compartments, including the nucleus, and produces S1P there (Hait et al., 2009). As with other potent mediators, S1P is rapidly turned over either by dephosphorylation back to sphingosine by phosphatases or irreversibly cleaved by S1P lyase to ethanolamine phosphate and hexadecenal (Aguilar and Saba, 2012; Hannun and Obeid, 2008; Maceyka and Spiegel, 2014).

## 3. Sphingosine-1-phosphate signaling in breast cancer

Following activation of SphK1 and restricted formation of S1P, the majority of the effects mediated by S1P occur after its export from the cell by the specific transporter called spinster 2 (Spns2) or by ATP-binding cassette transporters ABCA1, ABCC1, and ABCG2. S1P then can bind to one of five specific G protein-coupled cell surface S1P receptors (S1PR1-5) in an autocrine/paracrine manner, termed “inside-out” signaling. This leads to stimulation of downstream signaling mediated by overlapping G-proteins (Maceyka et al., 2012; Maczis et al., 2016; Takabe et al., 2008) (Fig. 1). A complete description of all of the interconnected signaling pathways that are activated by S1P is beyond the scope of this review, and this area has been extensively reviewed (Kihara et al., 2014; Pyne et al., 2016). Therefore, we will mainly focus on S1PR1 and S1PR3, two receptors that have been linked to breast cancer progression.

Intriguingly, S1PR1 has been linked to persistent activation of signal transducer and activator of transcription 3 (STAT3). STAT3

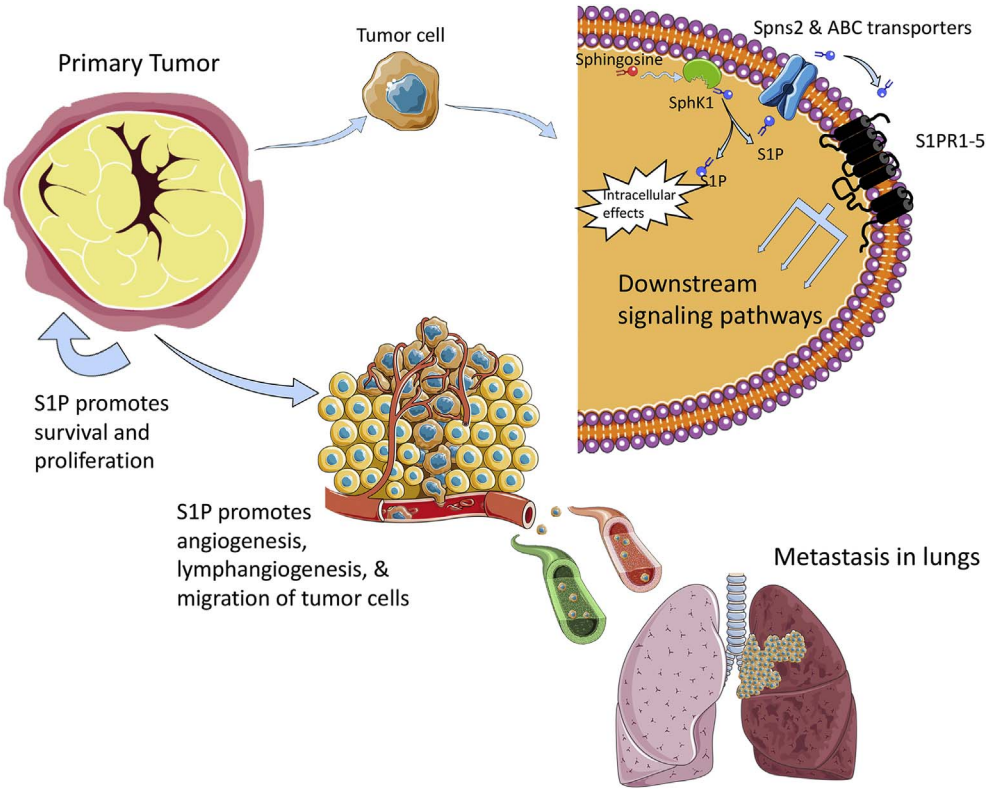


**Fig. 1.** Role of the SphK1/S1P axis in breast tumor progression and metastasis.

has been shown to be involved in many aspects of tumor growth and metastasis by activating a wide range of pathways promoting proliferation, survival, inflammation, invasion, and angiogenesis (Yu et al., 2014). STAT3 also enhances transcription of S1PR1 and activation of S1PR1 by S1P reciprocally activates STAT3 (Alshaker et al., 2014, 2015; Espaillat et al., 2017; Lee et al., 2010; Liang et al., 2013; Nagahashi et al., 2014). In breast cancer in particular, persistent STAT3 activation seems to be mainly due to upregulation of the pro-inflammatory cytokine IL-6 and S1PR1 (Alshaker et al., 2014, 2015; Lee et al., 2010). Moreover, IL-6 can activate SphK1 leading to a strong feed-forward mechanism promoting cancer cell progression (Lee et al., 2010). This signaling pathway is further complicated in ER negative breast cancer cells. as the adipokine leptin, a product of adipocytes, has also been shown to upregulate STAT3 and SphK1. SphK1 in turn induces production of IL-6, which then activates STAT3 (Alshaker et al., 2014, 2015). Pharmacological and molecular approaches further demonstrated that leptin-induced SphK1 activity and expression are mediated by activation of ERK1/2 and Src family kinase pathways, but not by the major pathways downstream of the leptin receptor, janus kinase 2 (JAK2) (Alshaker et al., 2015). As obesity is a risk factor for breast cancer and related to poorer prognosis, these studies could have implications for ER-negative breast cancer.

Binding of S1P to S1PR1 has also been shown to activate various receptor tyrosine kinases (RTKs) important for angiogenesis and proliferation such as VEGFR, EGFR, and PDGFR. This can result in “criss-cross” pathway activations as the growth factors that activate these RTKs can also activate SphK1. For example, EGF activation of SphK1 plays an important role in the migration of breast cancer cells towards EGF along with increased cell growth (Sarkar et al., 2005). S1P also potentiates the EGFR signaling pathway by insulin-like growth factor binding protein 3 (IGFBP-3), a growth promoter associated with poorer prognosis, suggesting that inhibition of both EGFR and SphK1 could have beneficial therapeutic effects in TNBC (Martin et al., 2014). Moreover, VEGF-mediated activation of SphK1 plays an essential role in regulating angiogenesis and lymphangiogenesis (Anelli et al., 2010; Nagahashi et al., 2012).

As for S1PR3, its activation via S1P was linked to the activation of the Notch signaling pathway along with p38MAPK in breast cancer stem cells (BCSCs) leading to proliferation and tumorigenicity (Hirata et al., 2014). BCSCs can also be activated by carcinogens, such as benzyl butyl phthalate, which has been shown to increase SphK1 expression leading to S1PR3 activation, implying that S1PR3 is a determinant of pollutant-driven breast cancer metastasis (Wang et al., 2016).

Most of S1PR3's cancer promoting and pro-survival effects can be attributed to sustained activation of ERK1/2 and AKT/PI3K pathways, key regulators of cell cycle progression, survival, and proliferation mechanisms in breast cancer cells (Datta et al., 2014; Wang et al., 2016; Watson et al., 2010). In triple-negative MDA-MB-231 breast cancer cells, early and sustained phosphorylation of both ERK1/2 and AKT/PI3K was inhibited by a SphK1 inhibitor while only sustained activation was inhibited by pertussis toxin, a potent G protein inhibitor, suggesting that S1PRs are crucial only for sustained activation (Datta et al., 2014). Aside from activating its own downstream signaling cascade, the AKT/PI3K pathway is involved in crosstalk with several other pathways, including RAS/RAF/MEK and ER, further strengthening the interconnecting pro-survival and progression pathways (Maiti et al., 2017). Another study in TNBC cells substantiated a link between sphingosine, SphK1, and the protein kinase C (PKC) serine/threonine kinase family, important regulators of cell proliferation and survival (Kotelevets et al., 2012). This study also showed that targeting SphK1 in triple-negative MDA-MB-231 breast cancer cells decreased proliferation and survival by compromising PKC activity and cytokinesis (Kotelevets et al., 2012). While the exact mechanisms of these pathways have not been elucidated, they support the significance of SphK1 as a target for cancer therapy. A recent study with MDA-MB-231 cells looked at how S1P signaling affected adhesion and invasion via the tumor cell microenvironment. It was reported that extracellular matrix rigidity-dependent S1P secretion regulates metastatic cancer cell invasion and adhesion (Ko et al., 2016). These results suggest that alterations in the mechanical environment of the extracellular matrix surrounding the tumor cells actively regulate secretion of S1P, which in turn, may contribute to cancer progression. In summary, many of the pathways modulated by the SphK1/S1P/S1PR axis in breast cancer cells are overlapping, promoting their growth, survival, proliferation, and metastasis (Fig. 1).

In addition to the very well-known functions of S1P as a ligand for S1PRs, recent studies suggest that S1P also has important intracellular actions (Maceyka et al., 2012). Especially relevant is the observation that SphK2 is present in the nucleus of many breast cancer cell lines (Hait et al., 2009; Igarashi et al., 2003; Sankala et al., 2007) where it produces S1P that inhibits class I histone deacetylases (HDACs) (Hait et al., 2009). Thus, it was suggested that HDACs are direct intracellular targets of S1P and link nuclear sphingolipid metabolism and S1P to epigenetic regulation of expression of specific genes (Hait et al., 2009). Recently, we found that FTY720 is also phosphorylated in breast cancer cells by nuclear SphK2 and accumulates there. Moreover, like S1P, nuclear FTY720-P is also a potent inhibitor of class I HDACs. Furthermore, we observed that high fat diet increased triple-negative spontaneous breast tumors and HDAC activity in MMTV-PyMT transgenic mice that was suppressed by oral administration of FTY720. Interestingly, this treatment not only inhibited HDACs, it also reversed high fat diet-induced loss of ER and PR in advanced carcinoma (Hait et al., 2015). Furthermore, treatment with FTY720 also re-expressed ER and increased therapeutic sensitivity of TNBC syngeneic breast tumors to tamoxifen in vivo more potently than a known HDAC inhibitor. This work suggests that in combination, FTY720 could be an effective treatment of both conventional hormonal therapy-resistant breast cancer and triple-negative breast cancer (Hait et al., 2015).

## 4. Sphingosine kinase 1 and estrogen receptor signaling

Nearly 80% of breast cancers are ER positive, meaning they are dependent on estrogens such as 17β-estradiol (E2) to signal growth, proliferation and metastasis. E2 normally binds to ER in the cytoplasm and after dimerization, translocates to the nucleus. In the nucleus, the ER dimers bind to estrogen response elements and act as transcription factors to activate or repress gene transcription (Klinge, 2001). E2 can also induce rapid, non-genomic cellular changes through membrane ERs that are still ill defined, including the

splice variant ER36 and the G protein-coupled receptor GPR30 (Wang and Yin, 2015; Zhou et al., 2016). These membrane ERs have been shown to activate SphK1, producing S1P and activate signaling pathways downstream of S1PRs leading to increased cell growth, higher microvessel density in tumors, and enhanced resistance to anti-cancer drugs in response to hormonal therapies (Maczis et al., 2016; Sukocheva et al., 2006, 2013; Takabe et al., 2010). GPR30 was suggested to activate SphK1 as its downregulation by anti-sense oligonucleotides inhibited E2-mediated activation of SphK1 in MCF-7 breast cancer cells (Sukocheva et al., 2006). However, the identity of the responsible receptor has not yet been conclusively established. E2-mediated formation of S1P led to rapid release of S1P from breast cancer cells via the ABCC1 and the ABCG2 transporters (Takabe et al., 2010) and “inside out” signaling by S1P (Maczis et al., 2016; Sukocheva et al., 2006, 2013). Furthermore, inhibiting these transporters blocked E2-induced activation of ERK1/2 (Takabe et al., 2010). It was convincingly demonstrated that activation of S1PR3 by S1P transactivated EGFR through a pathway mediated by Src and matrix metalloproteases. This switch from E2/ER-mediated growth to SphK1/EGFR activation has also been thought to contribute to resistance to hormonal therapies such as tamoxifen (Maczis et al., 2016; Sukocheva and Wadham, 2014; Sukocheva et al., 2006).

SphK1 activity has also been linked to the effects of several microRNAs that are regulated by ER. miR-515-5P, a tumor suppresser, was shown to reduce SphK1 activity and loss of miR-515-5P resulted in increased oncogenic SphK1 activity. In addition, E2 treatment downregulated miR-515-5P levels, and miR-515-5p is downregulated in ER-positive compared to ER-negative breast cancers (Pinho et al., 2013).

## 5. Sphingosine kinase 1 and breast cancer prognosis

Over the last few years, new evidence from several studies has illuminated the multi-factorial role of the SphK1/S1P axis in breast cancer and its link with worse prognosis and overall outcomes (Maczis et al., 2016; Ruckhaberle et al., 2008). It also usually corresponds with upregulation of associated S1PRs and chemotherapeutic resistance (Gao et al., 2015). In one study, 62.5% of tumors analyzed (20 out of 32) had at least a 2-fold increase in SphK1 mRNA expression compared to surrounding normal breast tissue (Datta et al., 2014). Furthermore, ER negative tumors had higher SphK1 levels than ER-positive tumors and the deadlier, triple-negative tumors had the highest levels of SphK1 expression of all tumor types examined. Overall, the analysis revealed an inverse correlation between SphK1 levels and survival of breast cancer patients. One of the possible causes investigated in this study was resistance to doxorubicin and docetaxel-based chemotherapies, mainstays for treatment of ER positive breast cancer, and it was found that non-responders to treatment had significantly higher SphK1 mRNA levels. This infers that SphK1 does not just promote progression and growth of tumors but also impacts survival through its effects on drug resistance (Datta et al., 2014). Patients with high levels of cytoplasmic Sphk1 compared to low SphK1 had a nearly 8-years shorter mean time to recurrence on tamoxifen (12.61 years with low SphK1 and 4.65 years with high SphK1 expression). Further investigations examined expression of S1PR1 and S1PR3 in particular and it was noted that patients with high membrane S1PR1 had a roughly 3 years shorter mean time to recurrence on tamoxifen and just over 8 years shorter disease-specific survival. It has been speculated that these differences in recurrence and survival could be due to E2 activation of SphK1 leading to the activation of the ERK1/2 pathways downstream of S1PR3 (Watson et al., 2010). Similar observations were made in another study (Ohotski et al., 2013).

Interestingly, S1P levels in breast cancer patients with lymph node metastasis that correlate with poor prognosis were significantly higher than those with negative lymph nodes, consistent with the notion that S1P plays an important role in angiogenesis, lymphangiogenesis, and metastasis (Tsuchida et al., 2016). Another interesting finding was that SphK1 levels determined by immunohistochemistry in deadlier TNBC tumors were lower, in contrast with some earlier studies. However, the S1P levels were higher, possibly suggesting the tumor microenvironment is responsible for the increase in S1P, not the tumor itself. This agreed with their observation of higher levels of S1P in patients with increased white blood cells, and suggested that since TNBCs are more immunogenic and immune cells express SphK1 and secrete S1P, they could increase S1P levels in the microenvironment (Tsuchida et al., 2016).

In sum, high levels of SphK1 expression and resulting high levels of S1P are most likely related to poorer prognosis for most patients. This could be due to the ability of the SphK1/S1P axis to promote cancer cell growth, proliferation, survival, and drug resistance. Thus, decreasing SphK1 expression and activity and S1P production could represent a new approach to improve prognosis of breast cancer.

## 6. Sphingosine kinase 1 in animal models of breast cancer progression and metastasis

Most of the data on SphK1 and its relationship to breast cancer in humans have come from analysis of tumor samples combined with patient follow-up data. An increasing number of studies have used mouse models to examine the role of the SphK1/S1P axis in breast cancer progression. The first observation was that breast cancer cells stably overexpressing SphK1 formed more and larger tumors in mice than vector transfectants with higher microvessel density in their periphery (Nava et al., 2002). Similar results were obtained by orthotopically implanting 4T1-luc2 murine breast cancer cells into the mammary fat pads of immune competent female mice (Nagahashi et al., 2012). The 4T1-luc2 tumors are rapidly growing and metastasize first to the lymph nodes and then the lungs, reminiscent to human breast cancer progression. Interestingly, circulating levels of S1P in tumor bearing mice were also significantly increased. Treatment of these mice with the specific SphK1 inhibitor SKI-1 decreased plasma S1P levels concomitantly with significant reductions in tumor volume, weight, and mitotic activity as well as lymph node and lung metastsis (Nagahashi et al., 2012). Moreover, cancer stem cells overexpressing SphK1 had increased ability to develop tumors in nude mice. Tumorigenicity of these cancer stem cells was inhibited by S1PR3 knockdown or a S1PR3 antagonist indicating that S1P promotes expansion of cancer stem

cells via S1PR3 by a ligand-independent Notch activation (Hirata et al., 2014).

Growth of tumors to beyond a certain size requires the formation of new blood vessels, termed angiogenesis, to continue to feed the rapidly growing and dividing cells (Nagahashi et al., 2012). To further spread throughout the body, the tumor cells usually extravasate and travel through the lymph system while also promoting formation of new lymph vessels through lymphangiogenesis. Both tumor size and metastasis are crucial in determining the staging and prognosis of a cancer (Nagahashi et al., 2016). There are also many cellular factors that contribute to angiogenesis and lymphangiogenesis, and perhaps others still to be discovered. However, it is becoming clear that S1P plays an important role in these processes. The angiogenic and lymphangiogenic actions of S1P are likely mediated via activation of S1PR1 on endothelial cells (Anelli et al., 2010; Nagahashi et al., 2012). As discussed above, S1P is commonly elevated in cancer tissues and in the circulation and also in lymph interstitial fluid from human breast cancer tumors (Nagahashi et al., 2016).

## 7. SphK1/S1P/S1P receptor axis as a therapeutic target for breast cancer

With such strong connections between SphK1/S1P/S1PR axis and the growth and progression of breast cancer cells, SphK1 and S1PR offer new and novel targets for possible future treatment avenues aimed at treating breast cancer, especially TNBC. Several preclinical studies have used mouse breast cancer models to investigate the effects of SphK1 inhibiters or S1PR modulators on tumor growth. A combination of the non-specific SphK inhibitor SKI-II with gefitinib, an EGFR inhibitor, significantly inhibited growth of xenograft MDA-MB-468 TNBC tumors whereas neither SKI-II or gefitinib alone had any effects (Martin et al., 2014). Another SphK1 inhibitor, SKI-5C, also significantly reduced growth of tumors from another TNBC cell line, MDA-MB-231, in xenografted SCID mice (Datta et al., 2014). Using an improved syngeneic breast cancer cell implantation method that mimics human breast cancer biology better than conventional xenograft subcutaneous implantation, treatment with the specific SphK1 inhibitor SK1-I suppressed tumor growth of murine 4T1 breast cancer cells and S1P levels and reduced metastases to lymph nodes and lungs (Nagahashi et al., 2012).

Lastly, one of the most promising possible future avenues for breast cancer treatments that target the S1P axis is Fingolimod (FTY720), a sphingosine analog pro-drug currently used to treat multiple sclerosis that has long been known to have beneficial effects in many preclinical breast cancer models (Azuma et al., 2002; Deng et al., 2012; Hait et al., 2015; Rincon et al., 2015). FTY720 effects are not limited only to suppressing the development and progression of breast tumors on its own but also is an effective adjuvant therapy. Treatment with FTY720 potentiated the anti-cancer effects of doxorubicin in MDA-MB-231 xenograft tumors and particularly in MDA-MB-231 cells that acquired resistance to doxorubicin (Rincon et al., 2015). FTY720 has been shown to synergize with the effect of tumor necrosis factor-related apoptosis-inducing ligand (TRAIL) reducing tumor volume and inducing apoptosis in xenograft breast cancer models without affecting normal cells (Woo et al., 2015). FTY720 has several anti-cancer targets that contribute to its multi-potent effectiveness. When phosphorylated by SphK2, FTY720-P is a S1P mimetic that acts as a functional antagonist of S1PR1, reducing the persistent activation of STAT3 (Deng et al., 2012) and thus diminishes accumulation of regulatory T cells in tumors (Priceman et al., 2014).

We found that FTY720 is phosphorylated by nuclear SphK2 in breast cancer cells. FTY720-P accumulates in the nucleus and potently inhibits class I histone deacetylases (HDACs) leading to increased histone acetylations and expression of a restricted set of genes independently of its known effects on S1PRs. We also observed that feeding a high-fat diet accelerated formation of tumors and increased triple-negative spontaneous breast tumors in MMTV-PyMT transgenic mice and that oral treatment with FTY720 inhibited development and aggressiveness of spontaneous breast tumors in these mice, reduced HDAC activity and dramatically reversed high-fat diet-induced loss of ER and PR in advanced carcinoma. Like other HDAC inhibitors, treatment of ER-negative breast cancer cells with FTY720 reactivated expression of silenced ER and sensitized them to tamoxifen. Furthermore, treatment with FTY720 also re-expressed ER and increased therapeutic sensitivity of ER-negative syngeneic breast tumors to tamoxifen in vivo more strongly than a pan HDAC inhibitor.

Unphosphorylated FTY720 also has anti-cancer actions. It inhibits SphK1 by binding to an allosteric site that exerts auto-inhibition on the catalytic site. It also induces proteasomal degradation of SphK1 and thus inhibits actions of S1P (Lim et al., 2011). Moreover, part of the effectiveness of FTY720 in tumor suppression can be attributed to its ability to activate the tumor suppressor PP2A (Perrotti and Neviani, 2013; Saddoughi et al., 2013), which is commonly inhibited in breast cancer and is crucial for maintaining tumor cell properties (Rincon et al., 2015).

Overall these studies show that FTY720 is a multi-faceted drug with the potential to work as an effective anti-cancer drug by itself and also as an adjuvant to hormonal therapies, traditional chemotherapies, and even radiation therapies to treat not only ER-positive tumors but also the more difficult TNBCs and tumors that develop resistance to chemotherapeutic agents. As FTY720 is already an FDA approved drug for treating humans, it is hoped that it can re-purposed for use as a cancer treatment.

## Acknowledgements

This work was supported by grants from Department of Defense BCRP Program Award W81XWH-14-1-0086 and NIGMS grant R01GM043880 (S. Spiegel).

## Competing interests statement

The authors declare no competing financial interests.

## References


Aguilar, A., Saba, J.D., 2012. Truth and consequences of sphingosine-1-phosphate lyase. Adv. Biol. Regul. 52 (1), 17–30.

Alshaker, H., Krell, J., Frampton, A.E., Waxman, J., Blyuss, O., Zaikin, A., Winkler, M., Stebbing, J., Yague, E., Pchejetski, D., 2014. Leptin induces upregulation of sphingosine kinase 1 in oestrogen receptor-negative breast cancer via Src family kinase-mediated, janus kinase 2-independent pathway. Breast Cancer Res. Treat. 16 (5), 426.

Alshaker, H., Wang, Q., Frampton, A.E., Krell, J., Waxman, J., Winkler, M., Stebbing, J., Cooper, C., Yague, E., Pchejetski, D., 2015. Sphingosine kinase 1 contributes to leptin-induced STAT3 phosphorylation through IL-6/gp130 transactivation in oestrogen receptor-negative breast cancer. Breast Cancer Res. Treat. 149 (1), 59–67.

Anelli, V., Gault, C.R., Snider, A.J., Obeid, L.M., 2010. Role of sphingosine kinase-1 in paracrine/transcellular angiogenesis and lymphangiogenesis in vitro. FASEB J. 24 (8), 2727–2738.

Azuma, H., Takahara, S., Ichimaru, N., Wang, J.D., Itoh, Y., Otsuki, Y., Morimoto, J., Fukui, R., Hoshiga, M., Ishihara, T., Nonomura, N., Suzuki, S., Okuyama, A., Katsuoka, Y., 2002. Marked prevention of tumor growth and metastasis by a novel immunosuppressive agent, FTY720, in mouse breast cancer models. Cancer Res. 62 (5), 1410–1419.

Datta, A., Loo, S.Y., Huang, B., Wong, L., Tan, S.S., Tan, T.Z., Lee, S.C., Thiery, J.P., Lim, Y.C., Yong, W.P., Lam, Y., Kumar, A.P., Yap, C.T., 2014. SPHK1 regulates proliferation and survival responses in triple-negative breast cancer. Oncotarget 5 (15), 5920–5933.

Deng, J., Liu, Y., Lee, H., Herrmann, A., Zhang, W., Zhang, C., Shen, S., Priceman, S.J., Kujawski, M., Pal, S.K., Raubitschek, A., Hoon, D.S., Forman, S., Figlin, R.A., Liu, J., Jove, R., Yu, H., 2012. S1PR1-STAT3 signaling is crucial for myeloid cell colonization at future metastatic sites. Cancer Cell 21 (5), 642–654.

Espaillat, M.P., Kew, R.R., Obeid, L.M., 2017. Sphingolipids in neutrophil function and inflammatory responses: mechanisms and implications for intestinal immunity and inflammation in ulcerative colitis. Adv. Biol. Regul. 63, 140–155.

Gao, Y., Gao, F., Chen, K., Tian, M.L., Zhao, D.L., 2015. Sphingosine kinase 1 as an anticancer therapeutic target. Drug Des. Devel. Ther. 9, 3239–3245.

Hait, N.C., Allegood, J., Maceyka, M., Strub, G.M., Harikumar, K.B., Singh, S.K., Luo, C., Marmorstein, R., Kordula, T., Milstien, S., Spiegel, S., 2009. Regulation of histone acetylation in the nucleus by sphingosine-1-phosphate. Science 325 (5945), 1254–1257.

Hait, N.C., Avni, D., Yamada, A., Nagahashi, M., Aoyagi, T., Aoki, H., Dumur, C.I., Zelenko, Z., Gallagher, E.J., Leroith, D., Milstien, S., Takabe, K., Spiegel, S., 2015. The phosphorylated prodrug FTY720 is a histone deacetylase inhibitor that reactivates ERalpha expression and enhances hormonal therapy for breast cancer. Oncogenesis 4, e156.

Hannun, Y.A., Obeid, L.M., 2008. Principles of bioactive lipid signalling: lessons from sphingolipids. Nat. Rev. Mol. Cell Biol. 9 (2), 139–150.

Hirata, N., Yamada, S., Shoda, T., Kurihara, M., Sekino, Y., Kanda, Y., 2014. Sphingosine-1-phosphate promotes expansion of cancer stem cells via S1PR3 by a ligand-independent Notch activation. Nat. Commun. 5, 4806.

Igarashi, N., Okada, T., Hayashi, S., Fujita, T., Jahangeer, S., Nakamura, S.I., 2003. Sphingosine kinase 2 is a nuclear protein and inhibits DNA synthesis. J. Biol. Chem. 278 (47), 46832–46839.

Kihara, Y., Maceyka, M., Spiegel, S., Chun, J., 2014. Lysophospholipid receptor nomenclature review: IUPHAR Review 8. Br. J. Pharmacol. 171 (15), 3575–3594.

Klinge, C.M., 2001. Estrogen receptor interaction with estrogen response elements. Nucleic Acids Res. 29 (14), 2905–2919.

Ko, P., Kim, D., You, E., Jung, J., Oh, S., Kim, J., Lee, K.H., Rhee, S., 2016. Extracellular matrix rigidity-dependent sphingosine-1-phosphate secretion regulates metastatic cancer cell invasion and adhesion. Sci. Rep. 6, 21564.

Kotelevets, N., Fabbro, D., Huwiler, A., Zangemeister-Wittke, U., 2012. Targeting sphingosine kinase 1 in carcinoma cells decreases proliferation and survival by compromising PKC activity and cytokinesis. PLoS One 7 (6), e39209.

Lee, H., Deng, J., Kujawski, M., Yang, C., Liu, Y., Herrmann, A., Kortylewski, M., Horne, D., Somlo, G., Forman, S., Jove, R., Yu, H., 2010. STAT3-induced S1PR1 expression is crucial for persistent STAT3 activation in tumors. Nat. Med. 16 (12), 1421–1428.

Liang, J., Nagahashi, M., Kim, E.Y., Harikumar, K.B., Yamada, A., Huang, W.C., Hait, N.C., Allegood, J.C., Price, M.M., Avni, D., Takabe, K., Kordula, T., Milstien, S., Spiegel, S., 2013. Sphingosine-1-phosphate links persistent STAT3 activation, chronic intestinal inflammation, and development of colitis-associated cancer. Cancer Cell 23 (1), 107–120.

Lim, K.G., Tonelli, F., Li, Z., Lu, X., Bittman, R., Pyne, S., Pyne, N.J., 2011. FTY720 analogues as sphingosine kinase 1 inhibitors: enzyme inhibition kinetics, allosterism, proteasomal degradation, and actin rearrangment in MCF-7 breast cancer cells. J. Biol. Chem. 286 (21), 18633–18640.

Maceyka, M., Harikumar, K.B., Milstien, S., Spiegel, S., 2012. Sphingosine-1-phosphate signaling and its role in disease. Trends Cell Biol. 22 (1), 50–60.

Maceyka, M., Spiegel, S., 2014. Sphingolipid metabolites in inflammatory disease. Nature 510 (7503), 58–67.

Maczis, M., Milstien, S., Spiegel, S., 2016. Sphingosine-1-phosphate and estrogen signaling in breast cancer. Adv. Biol. Regul. 60, 160–165.

Maiti, A., Takabe, K., Hait, N.C., 2017. Metastatic triple-negative breast cancer is dependent on SphKs/S1P signaling for growth and survival. Cell Signal 32, 85–92.

Martin, J.L., de Silva, H.C., Lin, M.Z., Scott, C.D., Baxter, R.C., 2014. Inhibition of insulin-like growth factor-binding protein-3 signaling through sphingosine kinase-1 sensitizes triple-negative breast cancer cells to EGF receptor blockade. Mol. Cancer Ther. 13 (2) 3163–3128.

Nagahashi, M., Hait, N.C., Maceyka, M., Avni, D., Takabe, K., Milstien, S., Spiegel, S., 2014. Sphingosine-1-phosphate in chronic intestinal inflammation and cancer. Adv. Biol. Regul. 54C, 112–120.

Nagahashi, M., Ramachandran, S., Kim, E.Y., Allegood, J.C., Rashid, O.M., Yamada, A., Zhao, R., Milstien, S., Zhou, H., Spiegel, S., Takabe, K., 2012. Sphingosine-1-phosphate produced by sphingosine kinase 1 promotes breast cancer progression by stimulating angiogenesis and lymphangiogenesis. Cancer Res. 72 (3), 726–735.

Nagahashi, M., Yamada, A., Miyazaki, H., Allegood, J.C., Tsuchida, J., Aoyagi, T., Huang, W.C., Terracina, K.P., Adams, B.J., Rashid, O.M., Milstien, S., Wakai, T., Spiegel, S., Takabe, K., 2016. Interstitial fluid sphingosine-1-phosphate in murine mammary gland and cancer and human breast tissue and cancer determined by novel methods. J. Mammary Gland. Biol. Neoplasia 21 (1–2), 9–17.

Nava, V.E., Hobson, J.P., Murthy, S., Milstien, S., Spiegel, S., 2002. Sphingosine kinase type 1 promotes estrogen-dependent tumorigenesis of breast cancer MCF-7 cells. Exp. Cell Res. 281 (1), 115–127.

Newton, J., Lima, S., Maceyka, M., Spiegel, S., 2015. Revisiting the sphingolipid rheostat: evolving concepts in cancer therapy. Exp. Cell Res. 333 (2), 195–200.

Ohotski, J., Edwards, J., Elsberger, B., Watson, C., Orange, C., Mallon, E., Pyne, S., Pyne, N.J., 2013. Identification of novel functional and spatial associations between sphingosine kinase 1, sphingosine 1-phosphate receptors and other signaling proteins that affect prognostic outcome in estrogen receptor-positive breast cancer. Int. J. Cancer 132 (3), 605–616.

Perrotti, D., Neviani, P., 2013. Protein phosphatase 2A: a target for anticancer therapy. Lancet Oncol. 14 (6), e229–238.

Pinho, F.G., Frampton, A.E., Nunes, J., Krell, J., Alshaker, H., Jacob, J., Pellegrino, L., Roca-Alonso, L., de Giorgio, A., Harding, V., Waxman, J., Stebbing, J., Pchejetski, D., Castellano, L., 2013. Downregulation of microRNA-515-5p by the estrogen receptor modulates sphingosine kinase 1 and breast cancer cell proliferation. Cancer Res. 73 (19), 5936–5948.

Pitson, S.M., Moretti, P.A., Zebol, J.R., Lynn, H.E., Xia, P., Vadas, M.A., Wattenberg, B.W., 2003. Activation of sphingosine kinase 1 by ERK1/2-mediated phosphorylation. EMBO J. 22 (20), 5491–5500.

Priceman, S.J., Shen, S., Wang, L., Deng, J., Yue, C., Kujawski, M., Yu, H., 2014. S1PR1 is crucial for accumulation of regulatory T cells in tumors via STAT3. Cell Rep. 6 (6), 992–999.

Pyne, N.J., McNaughton, M., Boomkamp, S., MacRitchie, N., Evangelisti, C., Martelli, A.M., Jiang, H.R., Ubhi, S., Pyne, S., 2016. Role of sphingosine 1-phosphate receptors, sphingosine kinases and sphingosine in cancer and inflammation. Adv. Biol. Regul. 60, 151–159.

Pyne, N.J., Ohotski, J., Bittman, R., Pyne, S., 2014. The role of sphingosine 1-phosphate in inflammation and cancer. Adv. Biol. Regul. 54, 121–129.

Pyne, N.J., Pyne, S., 2010. Sphingosine 1-phosphate and cancer. Nat. Rev. Cancer 10 (7), 489–503.

Rincon, R., Cristobal, I., Zazo, S., Arpi, O., Menendez, S., Manso, R., Lluch, A., Eroles, P., Rovira, A., Albanell, J., Garcia-Foncillas, J., Madoz-Gurpide, J., Rojo, F., 2015. PP2A inhibition determines poor outcome and doxorubicin resistance in early breast cancer and its activation shows promising therapeutic effects. Oncotarget 6 (6), 4299–4314.

Ruckhaberle, E., Rody, A., Engels, K., Gaetje, R., von Minckwitz, G., Schiffmann, S., Grosch, S., Geisslinger, G., Holtrich, U., Karn, T., Kaufmann, M., 2008. Microarray

analysis of altered sphingolipid metabolism reveals prognostic significance of sphingosine kinase 1 in breast cancer. Breast Cancer Res. Treat. 112 (1), 41–52.
Saddoughi, S.A., Gencer, S., Peterson, Y.K., Ward, K.E., Mukhopadhyay, A., Oaks, J., Bielawski, J., Szulc, Z.M., Thomas, R.J., Selvam, S.P., Senkal, C.E., Garrett-Mayer, E., De Palma, R.M., Fedarovich, D., Liu, A., Habib, A.A., Stahelin, R.V., Perrotti, D., Ogretmen, B., 2013. Sphingosine analogue drug FTY720 targets I2PP2A/SET and mediates lung tumour suppression via activation of PP2A-RIPK1-dependent necroptosis. EMBO Mol. Med. 5 (1), 105–121.
Sankala, H.M., Hait, N.C., Paugh, S.W., Shida, D., Lepine, S., Elmore, L.W., Dent, P., Milstien, S., Spiegel, S., 2007. Involvement of sphingosine kinase 2 in p53-independent induction of p21 by the chemotherapeutic drug doxorubicin. Cancer Res. 67 (21), 10466–10474.
Sarkar, S., Maceyka, M., Hait, N.C., Paugh, S.W., Sankala, H., Milstien, S., Spiegel, S., 2005. Sphingosine kinase 1 is required for migration, proliferation and survival of MCF-7 human breast cancer cells. FEBS Lett. 579 (24), 5313–5317.
Sukocheva, O., Wadham, C., 2014. Role of sphingolipids in oestrogen signalling in breast cancer cells: an update. J. Endocrinol. 220 (3), R25–R35.
Sukocheva, O., Wadham, C., Holmes, A., Albanese, N., Verrier, E., Feng, F., Bernal, A., Derian, C.K., Ullrich, A., Vadas, M.A., Xia, P., 2006. Estrogen transactivates EGFR via the sphingosine 1-phosphate receptor Edg-3: the role of sphingosine kinase-1. J. Cell Biol. 173 (2), 301–310.
Sukocheva, O., Wadham, C., Xia, P., 2013. Estrogen defines the dynamics and destination of transactivated EGF receptor in breast cancer cells: role of S1P(3) receptor and Cdc42. Exp. Cell Res. 319 (4), 455–465.
Takabe, K., Kim, R.H., Allegood, J.C., Mitra, P., Ramachandran, S., Nagahashi, M., Harikumar, K.B., Hait, N.C., Milstien, S., Spiegel, S., 2010. Estradiol induces export of sphingosine 1-phosphate from breast cancer cells via ABCC1 and ABCG2. J. Biol. Chem. 285 (14), 10477–10486.
Takabe, K., Paugh, S.W., Milstien, S., Spiegel, S., 2008. "Inside-out" signaling of sphingosine-1-phosphate: therapeutic targets. Pharmacol. Rev. 60 (2), 181–195.
Tsuchida, J., Nagahashi, M., Nakajima, M., Moro, K., Tatsuda, K., Ramanathan, R., Takabe, K., Wakai, T., 2016. Breast cancer sphingosine-1-phosphate is associated with phospho-sphingosine kinase 1 and lymphatic metastasis. J. Surg. Res. 205 (1), 85–94.
Wang, Y.C., Tsai, C.F., Chuang, H.L., Chang, Y.C., Chen, H.S., Lee, J.N., Tsai, E.M., 2016. Benzyl butyl phthalate promotes breast cancer stem cell expansion via SPHK1/S1P/S1PR3 signaling. Oncotarget 7 (20), 29563–29576.
Wang, Z.Y., Yin, L., 2015. Estrogen receptor alpha-36 (ER-alpha36): a new player in human breast cancer. Mol. Cell Endocrinol. 418 (Pt 3), 193–206.
Watson, C., Long, J.S., Orange, C., Tannahill, C.L., Mallon, E., McGlynn, L.M., Pyne, S., Pyne, N.J., Edwards, J., 2010. High expression of sphingosine 1-phosphate receptors, S1P1 and S1P3, sphingosine kinase 1, and extracellular signal-regulated kinase-1/2 is associated with development of tamoxifen resistance in estrogen receptor-positive breast cancer patients. Am. J. Pathol. 177 (5), 2205–2215.
Woo, S.M., Seo, B.R., Min, K.J., Kwon, T.K., 2015. FTY720 enhances TRAIL-mediated apoptosis by up-regulating DR5 and down-regulating Mcl-1 in cancer cells. Oncotarget 6 (13), 11614–11626.
Yu, H., Lee, H., Herrmann, A., Buettner, R., Jove, R., 2014. Revisiting STAT3 signalling in cancer: new and unexpected biological functions. Nat. Rev. Cancer 14 (11), 736–746.
Zhou, K., Sun, P., Zhang, Y., You, X., Li, P., Wang, T., 2016. Estrogen stimulated migration and invasion of estrogen receptor-negative breast cancer cells involves an ezrin-dependent crosstalk between G protein-coupled receptor 30 and estrogen receptor beta signaling. Steroids 111, 113–120.

Available online at www.sciencedirect.com

ScienceDirect

journal homepage: www.JournalofSurgicalResearch.com

Association for Academic Surgery

# Modified breast cancer model for preclinical immunotherapy studies

*Eriko Katsuta, MD, PhD,*[a,b,c] *Stephanie C. DeMasi, BS,*[a,b] *Krista P. Terracina, MD,*[a,b] *Sarah Spiegel, PhD,*[b] *Giao Q. Phan, MD,*[a] *Harry D. Bear, MD, PhD,*[a] *and Kazuaki Takabe, MD, PhD, FACS*[a,b,c,*]

[a] *Division of Surgical Oncology, Department of Surgery, Virginia Commonwealth University School of Medicine and The Massey Cancer Center, Richmond, Virginia*

[b] *Department of Biochemistry and Molecular Biology, Virginia Commonwealth University School of Medicine and The Massey Cancer Center, Richmond, Virginia*

[c] *Breast Surgery, Department of Surgical Oncology, Roswell Park Cancer Institute, Buffalo, New York*

ARTICLE INFO

*Article history:*
Received 4 February 2016
Received in revised form
13 April 2016
Accepted 1 June 2016
Available online 8 June 2016

*Keywords:*
Breast cancer
Syngeneic model
Preclinical
Immunotherapy

ABSTRACT

*Background:* Interest in immunotherapy for breast cancer is rapidly emerging, and applicable animal models that mimic human cancer are urgently needed for preclinical studies. This study aimed to improve a technique for orthotopic inoculation of syngeneic breast cancer cells to be used as a preclinical animal model for immunotherapy.

*Materials and methods:* We used our previously reported murine model of orthotopic cancer cell inoculation under direct vision and compared the efficiency of tumorigenesis with tumor cells suspended in either phosphate-buffered saline or Matrigel containing varying numbers of cells. As a model for immune rejection, murine BALB/c–derived 4T1-*luc2* breast cancer cells were inoculated orthotopically into both BALB/c and C57BL/6 mice.

*Results:* Matrigel-suspended cells formed larger tumors with higher efficiency than phosphate-buffered saline-suspended cells. The maximum volume of Matrigel that could be inoculated without spillage was 20 μL and 30 μL in the #2 and #4 mammary fat pads, respectively. Tumor take rates increased as the injected cell number increased. In this immune rejection model, there were no significant differences in tumor weight between the strains up to day 7, after which tumor weight decreased in C57BL/6 mice. Bioluminescence in C57BL/6 mice was also significantly less than that in BALB/c mice and increased up to day 7, then swiftly decreased thereafter.

*Conclusions:* This improved technique of innoculating murine breast cancer cells using bioluminescence technology may be useful in evaluating the efficacy of tumor regression mediated by immune responses, as shown by an allogeneic response in C57BL/6 mice.



* *Corresponding author.* Breast Surgery, Department of Surgical Oncology, Roswell Park Cancer Institute, Elm & Carlton Streets, Buffalo, NY 14263. Tel.: +1 858 945 5405; fax: +1 804 828 4808.
E-mail address: kazuaki.takabe@roswellpark.org (K. Takabe).

0022-4804/$ – see front matter © 2016 Elsevier Inc. All rights reserved.
http://dx.doi.org/10.1016/j.jss.2016.06.003

## Introduction

Immunotherapy, including checkpoint inhibitors, cancer vaccines, adoptive cell immunotherapy, and strategies that exploit chimeric antigen receptor–engineered T cells, is rapidly emerging as a promising modality for different types of cancers.[1] The early success of immune checkpoint inhibition, such as targeted therapy against cytotoxic T-lymphocyte–associated protein 4 (CTLA-4), along with programmed death-1 (PD-1)[2,3] and the PD-1 ligand, PD-L1,[4] has drawn much attention.[5]

One of the most commonly used animal models for oncologic preclinical studies is xenografts of human cancer cells or patient-derived cancer tissue into immune-deficient mice.[6,7] However, these models are not suitable to evaluate immune responses or the effects of immunotherapy because the host animal lacks a fully functioning immune system. Spontaneous tumorigenic models using transgenic mice or carcinogens have been developed in animals with an intact immune system, but these models may require a long waiting time for the development of cancer, which limits their practicality.[8,9] Furthermore, these models usually require expensive equipment, such as mouse-specific imaging scanners (computed tomography, magnetic resonance imaging, or positron emission tomography), to detect and measure tumors. Even with such state-of-the-art diagnostic imaging equipment, the evaluation of immunotherapy responses remains challenging. Tumor size may not necessarily reflect the amount of cancer cells, as tumors may initially enlarge on imaging studies due to accumulated infiltrating immune cells when immunotherapy is actually effective. Recently, patient-derived "humanized" xenograft models have been developed using patient tumors implanted into immune-deficient mice that are engineered to have intact human immune cells.[10-12] However, the cost of these animals and other limitations, including take rate, viral contamination and selection pressure, hinder this approach,[10] and even these modern models cannot escape from the challenges of assessing tumor responses to immunotherapy.[12] Thus, orthotopic inoculation of syngeneic murine tumor cells tagged with a bioluminescent reporter into immune intact mice is the most straightforward, fast, and affordable model to study the effect of immunotherapy at this point.

We have previously reported the establishment of a murine syngeneic breast cancer model using cell inoculation into chest mammary fat pads under direct vision, which can mimic human cancer progression.[13-15] In this study, we report the establishment of an improved orthotopic inoculation technique of murine breast cancer cells using *luciferase*-tagged 4T1-*luc2* murine cancer cells suspended in Matrigel and demonstrate that this model is useful to assess immune-mediated regression of breast tumors.

## Materials and methods

### Cell culture

4T1-*luc2* cells, a mouse mammary adenocarcinoma cell line derived from BALB/c mice that has been engineered to express luciferase was purchased from Caliper Life Sciences/PerkinElmer (Hopkinton, MA). 4T1-*luc2* cells were cultured in RPMI Medium 1640 with 10% fetal bovine serum. E0771 cells, a C57BL/6 mouse mammary fat pad–derived adenocarcinoma cell line, were cultured in Dulbecco's Modified Eagle Medium with 10% fetal bovine serum.

### Animal models

Approval from the Virginia Commonwealth University Institutional Animal Care and Use Committee was obtained for all experiments. Female BALB/c and C57BL/6 mice were obtained from Jackson Laboratory. All cell inoculations into #2 (chest) and #4 (abdomen) mammary fat pads under direct vision were carried out as previously described.[13] All procedures were performed using sterile technique under isoflurane anesthesia, and the animals were prepped and draped in a sterile manner. In brief, a 10-mm incision was made medial to the nipple, and a cotton swab was used to expose the mammary gland. A syringe with a 26-G needle was used to inject the cell suspension directly into the mammary gland under direct vision, and the wound was closed with a suture. To maximize the take rate, cell inoculations were conducted within 1 h from preparation of cell suspensions. Tumor growth was monitored by caliper measurement, and animals were weighed every other day.

#### *Preparation of Matrigel and phosphate-buffered saline cell suspensions*

$1 \times 10^4$ of 4T1-*luc2* cells were suspended in 20 μL of either phosphate-buffered saline (PBS) or Matrigel. Cells were inoculated into #2 and #4 mammary fat pads of BALB/c mice ($n = 8$). Fourteen days after inoculation, tumors were assessed by palpation, then harvested, and weighed.

#### *Determination of the optimum amount of Matrigel for injection into mammary fat pads*

To determine the amount of Matrigel a mammary fat pad can hold, 10 μL of Matrigel stained with 10% Trypan blue was injected incrementally into the #2 and #4 mammary fat pads ($n = 12$, each group). Spillage of Matrigel out of the fat pad was assessed visually after each injection.

#### *Tumorigenesis with different numbers of cells inoculated*

4T1-luc2 cells ($5 \times 10^2$, $1 \times 10^3$, $5 \times 10^3$, $1 \times 10^4$) or E0771 cells ($5 \times 10^4$, $1 \times 10^5$, $5 \times 10^5$, $1 \times 10^6$) were suspended in 20 μL of Matrigel, then inoculated into the #2 and #4 mammary fat pads of C57BL/6 or BALB/c mice, respectively ($n = 8$, each group). Formation of tumors was determined by palpation. Larger numbers of E0771 cells were inoculated because of the slower growth rate of this tumor in the appropriate syngeneic mouse strain.

#### *4T1-luc2 tumors in C57BL/6 mice (immune rejection model)*

$1 \times 10^4$ of 4T1-*luc2* cells, derived from BALB/c mice, suspended in Matrigel were implanted into the right #2 fat pad of C57BL/6 mice or BALB/c mice as a control. Tumor growth was monitored every other day by bioluminescence (IVIS)

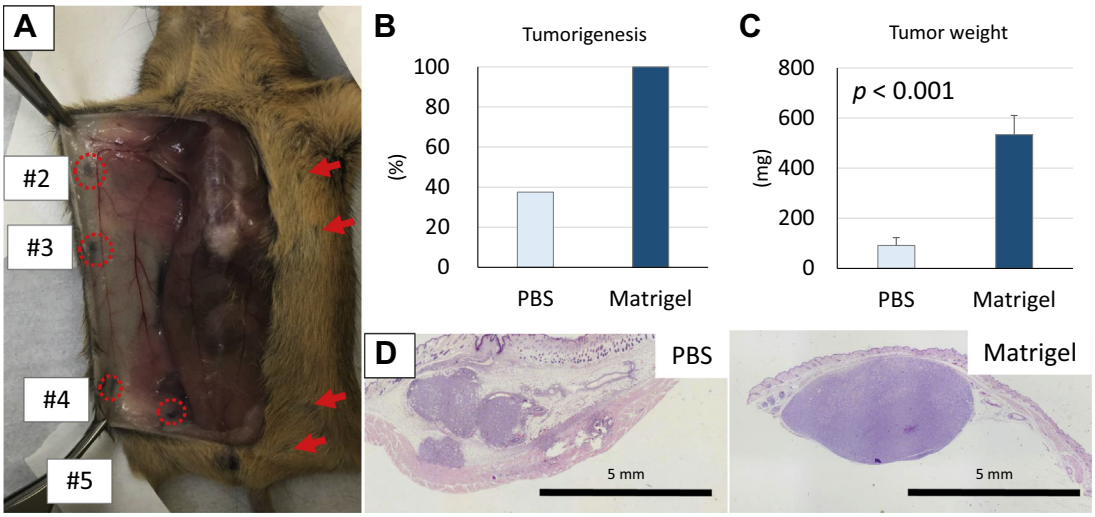


**Fig. 1 – Location of mouse mammary fat pads and the difference in tumorigenesis of cancer cells suspended in Matrigel or PBS. (A) The locations of mouse mammary fat pads (#2-5) were identified after midline incision (red circles and arrows). This representative image depicts the ease to access #2 and #4 mammary fat pads for inoculation under direct vision. Note, #1 pads cannot be seen, and #3 pads are too small, and #5 pads are too deep at the base of the legs for accurate inoculation. (B) Tumorigenesis 2 wk after inoculation of $1 \times 10^4$ 4T1-*luc2* cells. (C) Tumor weights were significantly greater in the tumors from Matrigel-suspended cells, than from the PBS-suspended cells ($n = 8$). (D) Histologic examination showed that inoculation of PBS-suspended cells resulted in scattering of cancer cells in the mammary fat pad, and cancer cells were also seen in secondary tumors outside the mammary fat pad, whereas Matrigel-suspended cells formed single tumors confined to the mammary fat pad. (Color version of figure is available online.)**

imaging ($n = 4$). For tumor weight analysis, cells were inoculated into bilateral #2 and #4 fat pad, and tumors were harvested and weighed on days 3, 7, and 9 ($n = 8$, each). Pathologic analyses were performed after formalin fixation of the tumors. Tumor sections were prepared and stained with hematoxylin and eosin by Virginia Commonwealth University Health System Anatomic Pathology Research Services.

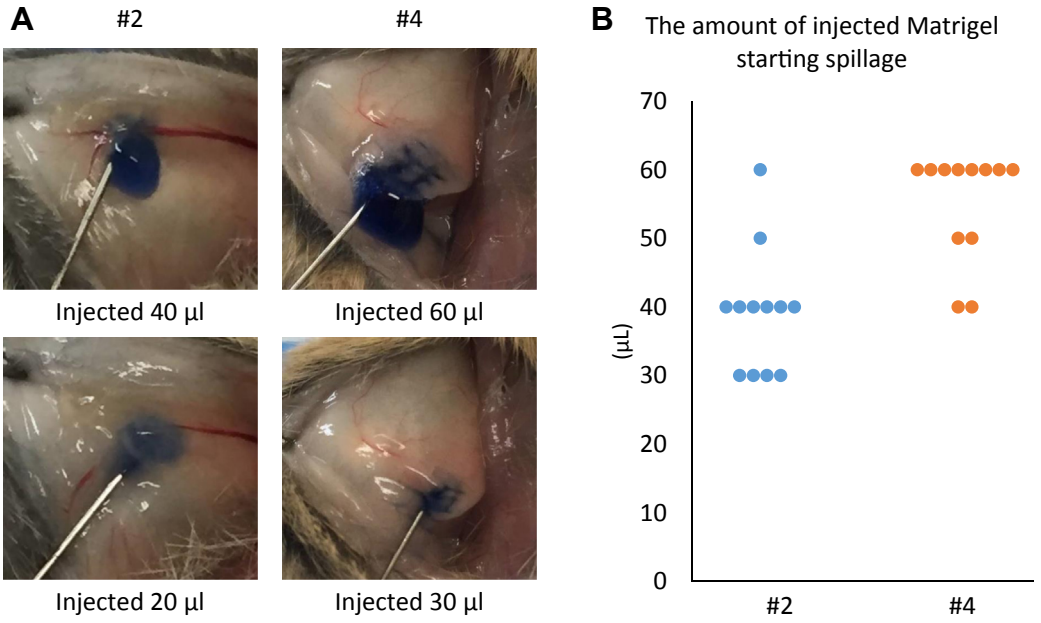


**Fig. 2 – The amount of Matrigel a mammary fat pad can hold without spillage. Trypan blue–stained Matrigel was injected into mammary fat pads in 10-µL increments, and spillage was detected visually. (A) Representative images of Trypan blue–stained Matrigel inoculation. Spillage out of the mammary fat pads is observed in the 20-µL injection in #2 (left) and 30-µL injection in #4 (right) mammary fat pads. (B) The amount of Matrigel that began to spill out of the pads when inoculated to either #2 or #4 mammary fat pads. (Color version of figure is available online.)**

### *Bioluminescent quantification of tumor burden*

Xenogen IVIS-200 and Living Image software (Caliper Life Sciences/PerkinElmer) were used to quantify the photons per second emitted by 4T1-*luc2* cells. D-Luciferin (150 mg/kg; PerkinElmer) was injected intraperitoneally into mice previously implanted with 4T1-*luc2* cells. Bioluminescence was measured and quantified at 5-min intervals up to photocount peak. Bioluminescence was then determined by the peak number of photons per second calculated over this time frame.[15]

### *Statistical analyses*

Statistical analyses were performed by the chi-square test or Fisher exact test with a single degree of freedom, and the Student's *t*-test was used to analyze the differences between two groups. *P* values $<0.05$ were considered to have statistical significance. All statistical analyses were performed using SPSS version 23.0 (SPSS, Chicago, IL).

## Results

### *Comparison of tumorigenesis after inoculation of cell suspensions in Matrigel or PBS*

The locations of mouse mammary fat pads are illustrated in Figure 1A after injection of 10% Trypan blue dye through the skin close to the nipple. The image shows the relative ease of access to #2 and #4 mammary fat pads for inoculation under direct vision from exposure through a midline incision. Notable in Figure 1A, #1 pads are not visible despite wide exposure, #3 pads are too small to access, and #5 pads are too deep at the base of the legs for accurate inoculation. Therefore, #2 and #4 mammary fat pads were used for orthotopic inoculation of breast cancer cells in subsequent experiments.

In our previous study, we found that inoculation of cell suspensions in PBS resulted in spillage out of the mammary fat pads, with scatter of cells outside the pads.[13] Therefore, the volume injected was minimized, which limited the number of cells that could be inoculated. We now have compared the efficiency of generating 4T1-*luc2* tumors from cells suspended in Matrigel with that of PBS-suspended cells in our orthotopic inoculation under direct vision model. Only 3 of 8 mice (37.5%) developed palpable tumors from cells injected in PBS, whereas all mice (8 of 8, 100%) developed tumors after inoculation of tumor cells suspended in Matrigel by 2 wk (Fig. 1B). Tumors generated from Matrigel-suspended cells weighed significantly more than those generated from cells suspended in PBS ($P < 0.001$; Fig. 1C). In agreement with our previous observations,[13] inoculation of PBS-suspended cells resulted in cancer cells forming tumors not only in the mammary fat pad but also in subcutaneous tissue outside of the mammary fat pad (Fig. 1D left panel) In contrast, Matrigel-suspended cells formed single tumors confined to the mammary fat pad (Fig. 1D right panel). These results demonstrate that cells suspended in Matrigel are more efficient at generating a discrete primary breast tumor in our orthotopic model.

### *Determination of the amount of Matrigel a mammary fat pad can hold*

We then investigated the amount of Matrigel that the #2 or #4 mammary fat pads can hold without spillage. The amount of injectate (Trypan blue–stained Matrigel) was incrementally increased by 10 μL until spillage occurred. As shown in Figure 2A and B, spillage was observed when more than 20 μL or 30 μL of Matrigel was injected into the #2 or #4 mammary fat pads, respectively. Therefore, 20 μL and 30 μL of Matrigel were identified to be the most suitable amounts to inject into #2 or #4 fat pads, respectively.

### *Dependence of tumor formation on number of cells inoculated*

To examine the relationship between inoculated cell number and generation of tumors, increasing numbers of cells were inoculated into the #2 or #4 mammary fat pads and tumorigenesis monitored. We used the two most commonly used syngeneic breast cancer models, 4T1-luc2 cells into BALB/c

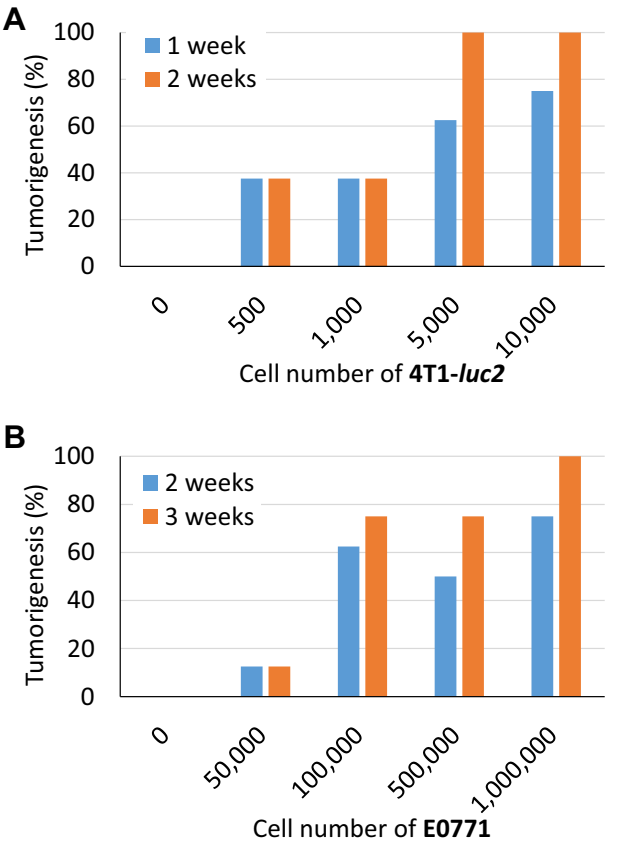


**Fig. 3 – Number of cells in Matrigel inoculates required to generate palpable tumors in two syngeneic breast cancer models. Shown on the X axes are the numbers of 4T1-luc2 cells inoculated into mammary fat pads of BALB/c mice ($n = 8$; A) and E0771 cells inoculated into C57BL/6 mice ($n = 8$; B). The proportion of mice with palpable tumors (tumorigenesis) was assessed at 1 and 2 wk after inoculation for 4T1-luc2 and 2 and 3 weeks for E0771. (Color version of figure is available online.)**

mice and E0771 cells into C57BL/6 mice. We found that tumorigenesis increased as the inoculated cell number increased for both cell lines, where all animals developed a tumor with $5 \times 10^3$ 4T1-luc2 cells, and $1 \times 10^6$ E0771 cells (Fig. 3A and B).

### *Tumor growth in different background mice*

To investigate whether our model is appropriate to assess immune-mediated regression of breast tumors, we examined the growth of 4T1-*luc2* cells, inoculated in Matrigel, in an environment where the cells will be rejected by an allogeneic immune response. 4T1-*luc2* cells were orthotopically inoculated into either syngeneic (BALB/c) or allogeneic (C57BL/6) mice. Thus, the tumors growing in C57BL/6 mice would be expected to be destroyed by the native immune system. The number of viable cancer cells and tumor burden were monitored *in vivo* by bioluminescence (Fig. 4A). Two-fold increases in tumor growth measured by bioluminescence imaging were nearly identical in both backgrounds 24 h after inoculation. By 7 d after inoculation, 4T1-*luc2* cells in C57BL/6 mice grew approximately 160 fold their inoculated amount, whereas the tumors in BALB/c mice grew 1200 fold their inoculated amount (Fig. 4B). The BALB/c tumors continued to grow rapidly to reach an almost 10,000-fold increase in bioluminescence signal, whereas the C57BL/6 mice tumors swiftly decreased the signal from day 7, and the viable cancer cells were eliminated by day 14. We further analyzed the time after injection of luciferin required to reach a peak photocount, which is

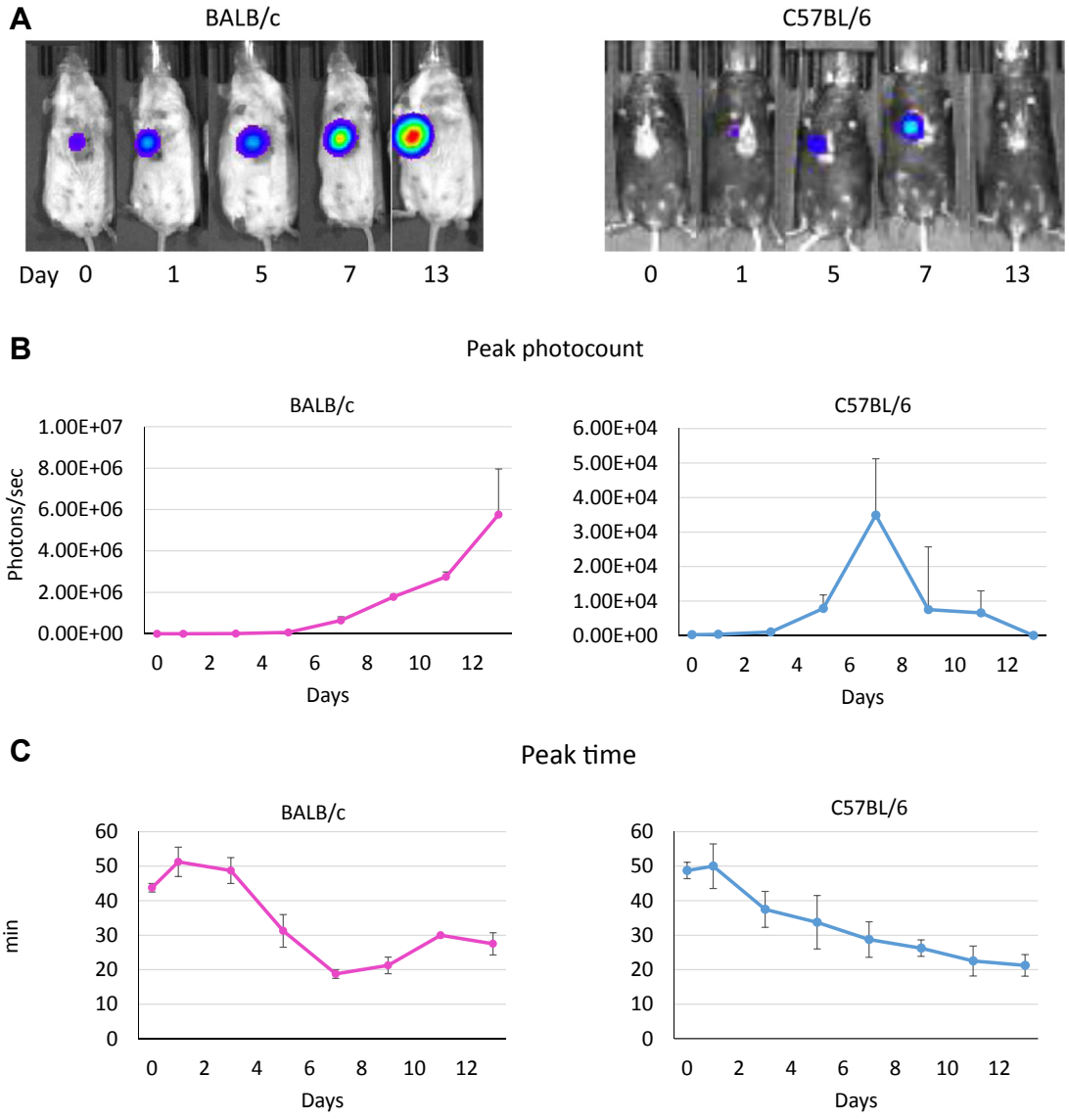


**Fig. 4 – 4T1-*luc2* breast cancer growth after orthotopic inoculation into the mammary pads of BALB/c or C57BL/6 mice. BALB/c or C57BL/6 mice were orthotopically inoculated with $1 \times 10^4$ 4T1-luc2 cells under direct vision, and tumor growth was evaluated by bioluminescence every other day. (A) Representative bioluminescence images of 4T1-*luc2* tumors after inoculation in BALB/c or C57BL/6 mice that showed tumor growth during observation period. (B) Tumor burden determined by photon counts was measured every other day ($n = 4$, mean ± standard error of the mean). (C) The time required to reach a peak photocount continued to decline in C57BL/6 mice, whereas it increased by day 10 in BALB/c mice. (Color version of figure is available online.)**

presumably reflective of perfusion of the tumor. Time to reach a peak photocount declined by day 7 in both BALB/c and C57BL/6 mice, after which it continued to decline in C57BL/6 tumor by day 13, whereas it increased after day 10 in BALB/c mice, most likely reflecting the growth of the tumor.

There were no significant differences in tumor weights at days 3 and 7 between tumors in BALB/c and C57BL/6, but a significant difference was observed by day 9 ($P = 0.0132$; Fig. 5A). Histologic analysis showed that cancer cells were surrounded by inflammatory cells on day 9 in the C57BL/6 mice and were destroyed by day 15 in the C57BL/6 mice, whereas cancer cells without inflammatory infiltrate filled the tumor in BALB/c mice (Fig. 5B).

## Discussion

For the last 8 y, our laboratory has been studying murine cancer models that mimic human cancer progression to be used for preclinical trials.[6] Our conclusion to date is that no murine model perfectly mimics human cancer progression; thus, multiple models should be used for preclinical studies to supplement each other's weaknesses.[6,7] Given the essential role of immune cells and inflammation in cancer progression, the preclinical results obtained using immune-deficient mice can be misleading and may be contributing to the low success rate of anticancer drug development.[6] Our prior work has

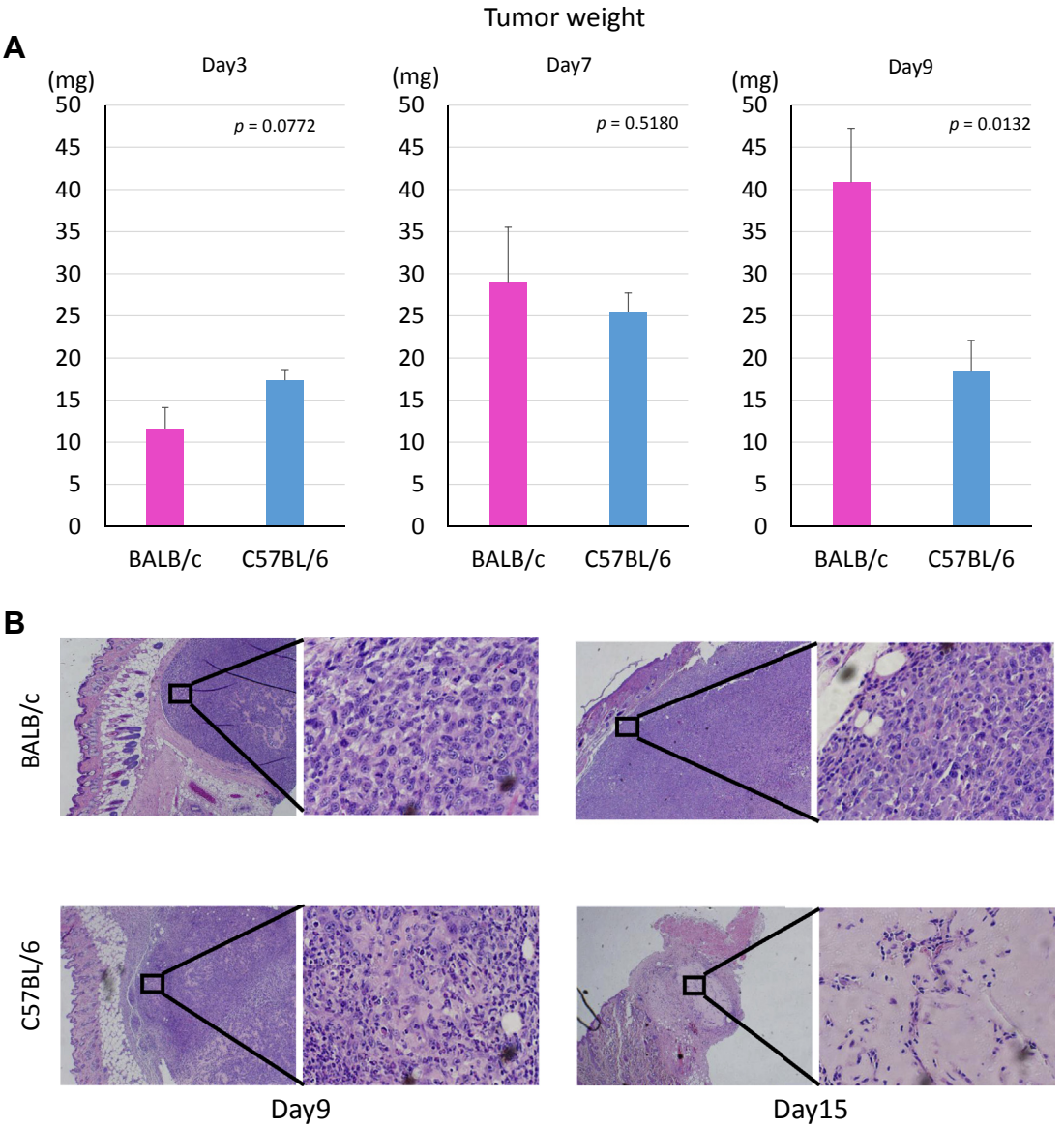


**Fig. 5 – Tumor weights and histologic analyses of 4T1-*luc2* tumors in BALB/c and C57BL/6 mice. (A) Tumors were harvested and weighed on days 3, 7, and 9 ($n = 8$, each). There were no significant differences in tumor weights on days 3 and 7 between tumors in BALB/c and C57BL/6. In contrast, a significant difference was observed on day 9. (B) Hematoxylin and eosin staining of 4T1-*luc2* tumors in BALB/c and C57BL/6 mice. Cancer cells were surrounded by inflammatory cells on day 9, and cancer cells were not seen on day 15 in the tumor site of C57BL/6 mice. (Color version of figure is available online.)**

shown that inoculation of syngeneic mouse cancer cells orthotopically into the mammary fat pads of immune intact mice under direct vision provides us with the most stable results that mimic human cancer progression.[13,16] This was also shown in a murine model of colon cancer, where cell suspension in Matrigel was found to be efficacious.[17] Together with previous reports that cell suspension in Matrigel facilitates the establishment of tumors in xenograft models,[18] our preliminary work led us to the present study to improve our breast cancer model using Matrigel. Compared with cells suspended in PBS, cells suspended in Matrigel developed tumors more efficiently and were more representative of primary breast tumors. We also identified the appropriate amount of Matrigel to be injected without spillage into the #2 and #4 mammary fat pads and found that the take rate correlated with the cell number inoculated. To our knowledge, this is the first to report this type of improved model using Matrigel for luciferase-tagged syngeneic breast cancer cell inoculation in the mammary fat pad under direct vision.

To test whether our improved model is suitable for preclinical evaluation of immunotherapy, we decided to investigate 4T1-*luc2* cell growth in a model invoking immune rejection, namely implantation of murine cancer cells into immune intact allogeneic mice. BALB/c-derived 4T1-*luc2* cells continued to proliferate in C57BL/6 mice for 1 wk before being eliminated, most likely reflecting the time to develop a primary immune response. Of note, the peak photon counts quantified by bioluminescence in immune-compatible BALB/c mice were approximately 12-fold and 240-fold higher compared with those in C57BL/6 mice on day 3 and day 7, respectively. Strikingly, there were no significant differences in tumor size between BALB/c and C57BL/6 mice on day 3 and day 7. Histologic analyses revealed that there were numerous infiltrating lymphocytes in the 4T1 tumors implanted in C57BL/6 mice, whereas predominantly, cancer cells were seen in BALB/c mice on day 9, suggesting that the tumor size in the C57BL/6 mice was maintained in part by tumor-infiltrating immune cells in the process of eliminating the cancer. Indeed, on day 15, no viable cancer cells were detected in the mammary pad of C57BL/6 mice. We also measured the time to reach the peak photon counts quantified by bioluminescence after intraperitoneal injection of D-luciferin, which is reflective of diffusion of the substrate into cancer cells. In agreement with a previous report,[19] the time to peak is prolonged after day 7 in BALB/c tumors after the enlargement of the tumor, whereas the time to peak continued to shorten in C57BL/6 tumor due to the tumor shrinkage.

One of the challenges of immunotherapy research is the method to evaluate the response to treatment. Commonly, the effect of systemic chemotherapy is evaluated by Response Evaluation Criteria in Solid Tumors (RECIST) criteria, which relies on tumor size reduction.[20] In contrast with chemotherapy's immediate and direct cytotoxic and tumor shrinkage effect, immunotherapy stimulates the patient's immune system to mount an antitumor response, which includes infiltration of immune-related cells into the tumor. This often results in a paradoxical transient increase in tumor size, which can mislead the physician to perceive this as treatment failure and result in premature termination of an effective immunotherapy. This is also the case in preclinical animal studies where viable cancer cells and not the size of the tumors need to be monitored. This paradox was observed in the present study as well, when the cancer cell number monitored by bioluminescence was significantly lower in the C57BL/6 immune rejection model when compared with BALB/c model, while the measured tumor sizes were not different. This further highlights the benefits of our luciferase-tagged syngeneic cell inoculation model, which could be used to assess immunotherapy for breast cancer, such as adoptive immunotherapy, cancer vaccines, or immune checkpoint inhibitors.

## Conclusions

In conclusion, we have established an improved murine orthotopic model using Matrigel, in combination with bioluminescence technology, which may be useful for preclinical studies of immunotherapy.

## Acknowledgment

This work was supported by NIH grant R01CA160688 and Susan G. Komen Foundation Investigator Initiated Research grant (IIR12222224) to K.T., and Department of Defense BCRP Program Award (W81XWH-14-1-0086) to S.S.

Authors' contributions: E.K., S.C.D., and K.P.T. conceptualized and performed experiments described in the article. E.K., S.S., G.Q.P., and H.D.B. prepared the article. K.T. provided supervision of experiments and preparation of the article.

## Disclosure

There are no potential conflicts of interest to disclose.

## REFERENCES

1. Mick R, Chen TT. Statistical challenges in the design of late-stage cancer immunotherapy studies. *Cancer Immunol Res*. 2015;3:1292–1298.
2. Topalian SL, Hodi FS, Brahmer JR, et al. Safety, activity, and immune correlates of anti-PD-1 antibody in cancer. *N Engl J Med*. 2012;366:2443–2454.
3. Hamid O, Robert C, Daud A, et al. Safety and tumor responses with lambrolizumab (anti-PD-1) in melanoma. *N Engl J Med*. 2013;369:134–144.
4. Brahmer JR, Tykodi SS, Chow LQ, et al. Safety and activity of anti-PD-L1 antibody in patients with advanced cancer. *N Engl J Med*. 2012;366:2455–2465.
5. Couzin-Frankel J. Breakthrough of the year 2013. Cancer immunotherapy. *Science*. 2013;342:1432–1433.
6. Rashid OM, Takabe K. Animal models for exploring the pharmacokinetics of breast cancer therapies. *Expert Opin Drug Metab Toxicol*. 2015;11:221–230.
7. Rashid OM, Takabe K. Does removal of the primary tumor in metastatic breast cancer improve survival? *J Womens Health (Larchmt)*. 2014;23:184–188.
8. Hait NC, Avni D, Yamada A, et al. The phosphorylated prodrug FTY720 is a histone deacetylase inhibitor that

reactivates ERalpha expression and enhances hormonal therapy for breast cancer. *Oncogenesis*. 2015;4:e156.
9. Liang J, Nagahashi M, Kim EY, et al. Sphingosine-1-phosphate links persistent STAT3 activation, chronic intestinal inflammation, and development of colitis-associated cancer. *Cancer Cell*. 2013;23:107–120.
10. Whittle JR, Lewis MT, Lindeman GJ, Visvader JE. Patient-derived xenograft models of breast cancer and their predictive power. *Breast Cancer Res*. 2015;17:17.
11. Lawson DA, Bhakta NR, Kessenbrock K, et al. Single-cell analysis reveals a stem-cell program in human metastatic breast cancer cells. *Nature*. 2015;526:131–135.
12. Aparicio S, Hidalgo M, Kung AL. Examining the utility of patient-derived xenograft mouse models. *Nat Rev Cancer*. 2015;15:311–316.
13. Rashid OM, Nagahashi M, Ramachandran S, et al. An improved syngeneic orthotopic murine model of human breast cancer progression. *Breast Cancer Res Treat*. 2014;147:501–512.
14. Rashid OM, Nagahashi M, Ramachandran S, et al. Resection of the primary tumor improves survival in metastatic breast cancer by reducing overall tumor burden. *Surgery*. 2013;153:771–778.
15. Nagahashi M, Ramachandran S, Kim EY, et al. Sphingosine-1-phosphate produced by sphingosine kinase 1 promotes breast cancer progression by stimulating angiogenesis and lymphangiogenesis. *Cancer Res*. 2012;72:726–735.
16. Rashid OM, Nagahashi M, Ramachandran S, et al. Is tail vein injection a relevant breast cancer lung metastasis model? *J Thorac Dis*. 2013;5:385–392.
17. Terracina KP, Aoyagi T, Huang WC, et al. Development of a metastatic murine colon cancer model. *J Surg Res*. 2015;199:106–114.
18. Mullen P. The use of Matrigel to facilitate the establishment of human cancer cell lines as xenografts. *Methods Mol Med*. 2004;88:287–292.
19. Cui K, Xu X, Zhao H, Wong ST. A quantitative study of factors affecting in vivo bioluminescence imaging. *Luminescence*. 2008;23:292–295.
20. Eisenhauer EA, Therasse P, Bogaerts J, et al. New response evaluation criteria in solid tumours: revised RECIST guideline (version 1.1). *Eur J Cancer*. 2009;45:228–247.

LETTER

doi:10.1038/nature20792

# Genome-wide *in vivo* screen identifies novel host regulators of metastatic colonization

Louise van der Weyden[1], Mark J. Arends[2], Andrew D. Campbell[3], Tobias Bald[4,5], Hannah Wardle-Jones[1], Nicola Griggs[1], Martin Del Castillo Velasco-Herrera[1], Thomas Tüting[4], Owen J. Sansom[3], Natasha A. Karp[1], Simon Clare[1], Diane Gleeson[1], Edward Ryder[1], Antonella Galli[1], Elizabeth Tuck[1], Emma L. Cambridge[1], Thierry Voet[1,6], Iain C. Macaulay[1], Kim Wong[1], Sanger Mouse Genetics Project†, Sarah Spiegel[7], Anneliese O. Speak[1]* & David J. Adams[1]*

**Metastasis is the leading cause of death for cancer patients. This multi-stage process requires tumour cells to survive in the circulation, extravasate at distant sites, then proliferate; it involves contributions from both the tumour cell and tumour microenvironment ('host', which includes stromal cells and the immune system[1]). Studies suggest the early steps of the metastatic process are relatively efficient, with the post-extravasation regulation of tumour growth ('colonization') being critical in determining metastatic outcome[2]. Here we show the results of screening 810 mutant mouse lines using an *in vivo* assay to identify microenvironmental regulators of metastatic colonization. We identify 23 genes that, when disrupted in mouse, modify the ability of tumour cells to establish metastatic foci, with 19 of these genes not previously demonstrated to play a role in host control of metastasis. The largest reduction in pulmonary metastasis was observed in sphingosine-1-phosphate (S1P) transporter spinster homologue 2 (*Spns2*)-deficient mice. We demonstrate a novel outcome of S1P-mediated regulation of lymphocyte trafficking, whereby deletion of *Spns2*, either globally or in a lymphatic endothelial-specific manner, creates a circulating lymphopenia and a higher percentage of effector T cells and natural killer (NK) cells present in the lung. This allows for potent tumour cell killing, and an overall decreased metastatic burden.**

To identify microenvironmental genes that regulate metastatic colonization, we performed an 'experimental metastasis assay' involving intravenous injection of B16-F10 mouse metastatic melanoma cells, used previously in the development of checkpoint inhibitors such as CTLA4 and PD-1 (refs 3, 4), and the assessment of pulmonary colonization (Fig. 1a). The 810 mutant mouse lines we assayed were randomly selected and cover a diverse range of molecular functions (Extended Data Fig. 1a and Supplementary Table 1). Using a stringent two-stage selection process, we identified 23 mutant lines showing significantly decreased or increased numbers of pulmonary melanoma foci, defined as a ratio of $\leq 0.6$ or $\geq 1.6$ and $P \leq 0.0175$ (Mann–Whitney test) for mutant mice versus wild types assayed concurrently (in the initial cohort assayed (Fig. 1a)), and $P < 0.01$ in an integrative data analysis performed on three or more additional cohorts (Supplementary Table 2 and Methods). Since these strains were extensively phenotyped[5], we were able to determine that alterations of immune-related phenotypic traits featured prominently in these 23 mutant lines (Fig. 1b), highlighting the key role of the immune system in microenvironmental regulation of metastasis.

Of the eight genes identified as suppressors of pulmonary metastases, two were members of the interferon regulatory family (IRF), important for immune function; loss of *Irf1* or *Irf7* increased pulmonary metastasis (as well as extra-pulmonary metastases in $Irf1^{tm1a/tm1a}$ mice), probably related to defects in their type-I interferon (IFN)-dependent response[6,7]. In contrast, *Irf5*-deficient mice, with their largely intact type-I IFN response[8], showed no altered pulmonary metastasis phenotype (Extended Data Fig. 1b–f). Similarly, the increased metastasis seen in the p110 catalytic subunit of phosphoinositide 3-kinase (*Pik3cg*)-deficient mice may be related to the critical function of this gene in multiple aspects of T cell, NK cell and neutrophil function[9,10], and the increased metastasis seen in immunoglobulin heavy chain 6 (*Ighm*)-deficient mice is probably due to their multiple immune system abnormalities[11]. In contrast, very little is known about the other four genes we identified as microenvironmental suppressors of metastasis, namely *Abhd17a*, *Dph6*, *Slc9a3r2* and *Rnf10*, which represent novel factors for further studies. Of the 15 mutant mouse lines we identified as having decreased pulmonary melanoma colonies, only four have been previously described as having roles in regulating metastasis: *Entpd1 (Cd39)*, *Nbeal2*, *Cybb* and *Hsp90aa1*, contributing to regulatory T-cell control of NK cells[12], platelet α-granule function[13], generation of phagocyte-derived oxygen radicals[14] and the chaperoning of client proteins involved in tumour progression[15], respectively.

We focused on the S1P transporter *Spns2*, as $Spns2^{tm1a/tm1a}$ mice showed the greatest suppression in the number of pulmonary metastatic melanoma foci, with $Spns2^{tm1a/+}$ mice showing an intermediate phenotype (Fig. 2a). Further, $Spns2^{tm1a/tm1a}$ mice showed reduced numbers of foci in the lungs after tail vein administration of lung CMT-167, colorectal MC-38 or breast EO771.LMB cancer cells (Fig. 2b), and decreased spontaneous pulmonary metastasis (both in number and size of metastatic foci) after subcutaneous administration of HCmel12–mCherry melanoma cells (Fig. 2c and Extended Data Fig. 2a). In contrast, there was no difference in the growth rate of the primary tumour between wild-type and $Spns2^{tm1a/tm1a}$ mice, either for HCmel12–mCherry or B16-BL6 melanoma cells, and no difference in the spontaneous incidence of cancer in aged wild-type and $Spns2^{tm1a/tm1a}$ mice (Extended Data Fig. 2b–d). Tail vein administration of transformed melanocyte WT31 cells (Fig. 2d) and intra-splenic administration of B16-F10 cells (Fig. 2e) resulted in a reduced number of foci in the livers of $Spns2^{tm1a/tm1a}$ mice, suggesting that resistance to metastatic colonization is not pulmonary-restricted.

S1P is a bioactive lipid mediator that plays important roles in diverse cellular functions such as cell proliferation, differentiation, migration and tumorigenesis[16]. Previous studies have shown that SPNS2 functions as a cell-surface S1P transporter that allows intracellular S1P to be secreted into the blood and lymph[17–19]. In agreement with

[1]Wellcome Trust Sanger Institute, Wellcome Genome Campus, Cambridge CB10 1SA, UK. [2]University of Edinburgh Division of Pathology, Edinburgh Cancer Research UK Cancer Centre, Institute of Genetics & Molecular Medicine, Edinburgh EH4 2XR, UK. [3]Cancer Research UK Beatson Institute, Glasgow G61 1BD, UK. [4]Department of Dermatology, University Hospital Magdeburg, Magdeburg 39120, Germany. [5]Department of Immunology in Cancer and Infection Laboratory, QIMR Berghofer Medical Research Institute, Herston 4006, Australia. [6]Department of Human Genetics, University of Leuven (KU Leuven), Leuven, 3000, Belgium. [7]Department of Biochemistry and Molecular Biology, Virginia Commonwealth University School of Medicine, Richmond, Virginia 23298-0614, USA.

*These authors contributed equally to this work.

†Lists of participants and their affiliations appear in the Supplementary Information.

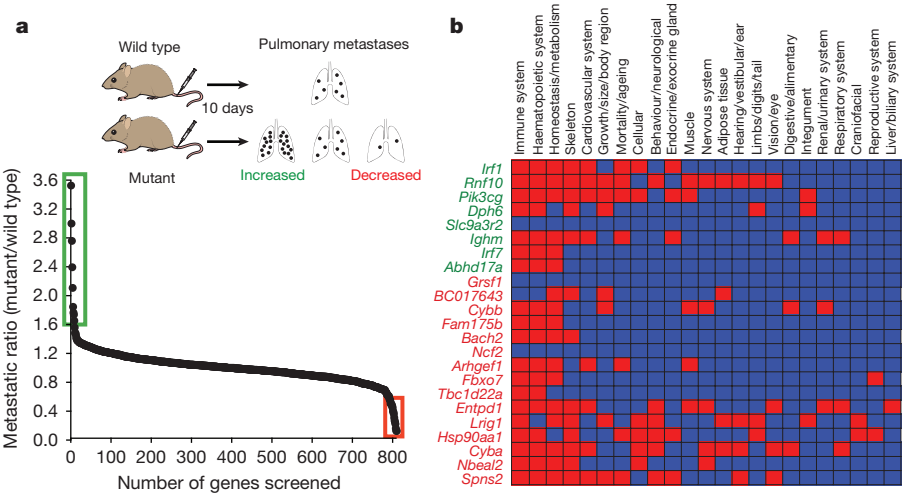


**Figure 1 | Identification of microenvironmental regulators of metastatic colonization of the lung. a**, Experimental model (schematic) and results from stage 1 of the screen: experimental metastasis assay performed on 810 mutant mouse lines (detailed in the Extended Methods). Those lines with a metastatic ratio of $\leq$0.6 (red box) or $\geq$1.6 (green box) and Mann–Whitney test $P \leq 0.0175$ were taken forward to stage 2 as detailed in Methods. **b**, Top-level mammalian phenotype ontology terms for the 23 statistically significant genes following an integrative data analysis of experimental metastasis assay results from three or more additional cohorts (green is increased metastasis and red is decreased). In the heatmap, red boxes indicate a phenodeviant call, and blue no phenotype annotated (either no phenotype detected or not assayed) as detailed in Methods.

previous studies[17,19], S1P was decreased in serum and increased in lungs of *Spns2*$^{tm1a/tm1a}$ mice (Extended Data Fig. 3a, b). Although extracellular S1P is a key regulator of endothelial barrier homeostasis[20], vascular permeability/extravasation of Evans Blue dye in *Spns2*$^{tm1a/tm1a}$ mice was the same as in controls (Extended Data Fig. 3c), as was the arrival of B16-F10 cells in the lung 90 min after tail vein administration (Extended Data Fig. 3d). However, a significant increase in the number of pulmonary B16-F10 cells showing evidence of apoptosis was observed after 12 h (Extended Data Fig. 3e), suggesting that the lungs of *Spns2*$^{tm1a/tm1a}$ mice represent a hostile environment for tumour cell engraftment. RNA sequencing (RNA-seq) analysis comparing viable B16-F10 cells isolated from lungs 24 h after their administration identified nine differentially expressed (upregulated) genes (Supplementary Table 3); six of these genes (*Pla2g16*, *Epsti1*, *Traf1*, *Glipr2*, *Marcksl1* and *Ccl5*) are known to be involved in pro-metastatic phenotypes of tumour cells, and H2-Q7-positive B16 cells have been shown to be targeted by both NK and cytotoxic T cells[21]. Thus, the transcriptional profile of B16-F10 cells from *Spns2*$^{tm1a/tm1a}$ lungs suggests they are upregulating genes to facilitate their survival in a hostile environment, while at the same time provoking activation of the immune system.

One of the most notable effects of S1P is the regulation of lymphocyte trafficking[22]. SPNS2 has been reported to function as an S1P transporter in endothelial cells but not in erythrocytes or platelets[17]. In agreement with others[17–19,23], *Spns2*$^{tm1a/tm1a}$ mice have a profound reduction in circulating T and B cells, with all other leukocyte (including NK cells) and blood cell lineages unaffected (Extended Data Fig. 4a–c). In the lung, the percentage of T cells was significantly reduced with a small reduction in the B cell percentage and increased NK cells (Fig. 3a), with similar phenotypes observed in the liver (Extended Data Fig. 4d). Consistent with *Spns2* expression in endothelial cells[17], bone marrow chimaeras showed a lymphocyte and metastatic colonization phenotype identical to the genotype of the host (Fig. 3b and Extended Data Fig. 4e, f), confirming that non-haematopoietic stroma regulates these observations. Expression of *Spns2* by endothelial cells is required for the maintenance of an S1P gradient in the lymph that is critical for regulating lymphocyte circulation[18]. In agreement with this, we showed that mice with lymphatic endothelial cell (LEC)-specific deletion of *Spns2* (*Spns2*$^{tm1c/tm1c}$; *Lyve1*$^{cre/+}$ mice) did not have altered serum or lung S1P levels (Extended Data Fig. 5a, b), yet displayed lymphopenia in the blood (Fig. 3c), lungs (Fig. 3d) and other tissues examined (Extended Data Fig. 5c). Critically, this resulted in a decreased number of pulmonary metastasis in *Spns2*$^{tm1c/tm1c}$; *Lyve1*$^{cre/+}$ mice administered either B16-F10 or MC-38 cells (Fig. 3e and Extended Data Fig. 5d).

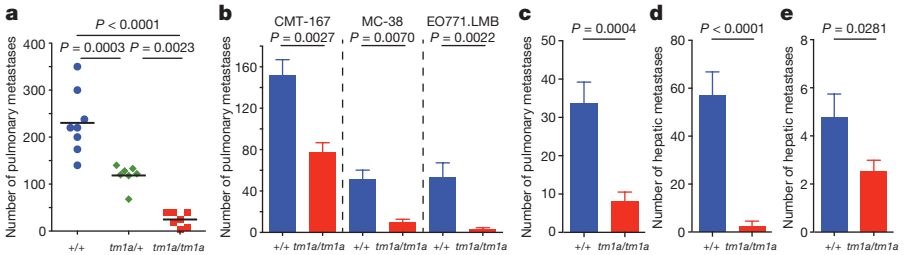


**Figure 2 | Ability of *Spns2*-deficient mice to regulate metastatic colonization. a**, Experimental metastasis assay using B16-F10 cells in +/+ (blue), *tm1a*/+ (green) or *tm1a/tm1a* (red) male mice. **b**, Experimental metastasis assay using CMT-167 (+/+, $n = 8$; *tm1a/tm1a*, $n = 6$ female mice), MC-38 (+/+, $n = 10$; *tm1a/tm1a*, $n = 5$ male mice) and EO771.LMB cells (+/+, $n = 12$; *tm1a/tm1a*, $n = 5$ female mice). **c**, Spontaneous metastasis assay using HCmel12–mCherry melanoma cells in male mice ($n = 10$ per genotype). **d**, Experimental metastasis assay using WT31 transformed melanocytes in +/+($n = 18$) and *tm1a/tm1a* ($n = 6$) male mice. **e**, Intra-splenic administration of B16-F10 cells in +/+ ($n = 16$) and *tm1a/tm1a* ($n = 15$) female mice. Shown are representative data from two (**b**, CMT-167) or three independent experiments (**a**, **b** (MC-38 and EO771.LMB), **d**) or cumulative results of two independent experiments (**c**, **e**) with mean ± s.e.m. (**b**–**e**) or symbols representing individual mice with horizontal bar at the mean (**a**). *P* values are indicated from one-way analysis of variance (ANOVA) with Šídák's multiple comparisons adjusting for multiple testing (**a**), Mann–Whitney test (**b**–**d**) or one-tailed unpaired *t*-test (**e**).

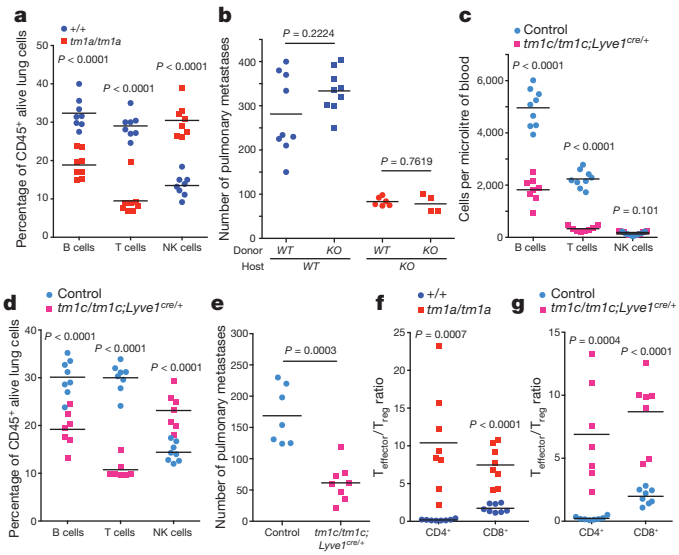


**Figure 3 | Characterization of the lymphocyte composition and phenotype in *Spns2*-deficient mice. a**, The percentage of lymphocyte subsets in the lungs of +/+ and *tm1a/tm1a* female mice. **b**, Number of metastases in B16-F10-dosed male bone marrow chimaeras (genotypes: +/+ (WT) and *tm1a/tm1a* (KO)). **c**, Numbers of lymphocytes in the blood of control and *tm1c/tm1c; Lyve1*$^{cre/+}$ male mice. **d**, The percentage of lymphocyte subsets in the lungs of control and *tm1c/tm1c; Lyve1*$^{cre/+}$ male mice. **e**, Experimental metastasis assay using B16-F10 cells in control and *tm1c/tm1c; Lyve1*$^{cre/+}$ female mice. **f**, **g**, Effector:regulatory T-cell ratio in the lungs of +/+ and *tm1a/tm1a* female mice or control and *tm1c/tm1c; Lyve1*$^{cre/+}$ male mice. Shown are representative data from two (**b**) or three independent experiments (**a**, **c**–**g**) with symbols representing individual mice with horizontal bar at the mean. *P* values are indicated from two-tailed unpaired *t*-test adjusted by the Holm–Šídák method with $\alpha$ set to 5% (**a**, **c**–**d**, **f**, **g**) or Mann–Whitney test (**b**, **e**).

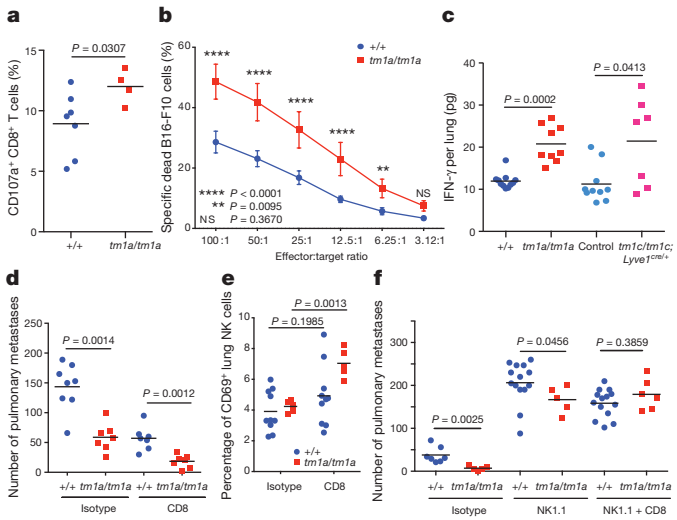


**Figure 4 | Lymphocyte regulation of metastatic colonization in *Spns2*-deficient mice. a**, Degranulation assay on pulmonary leukocytes from B16-F10-stimulated +/+ and *tm1a/tm1a* female mice in response to *in vitro* re-stimulation with B16-F10. **b**, Cytotoxicity assay on pulmonary leukocytes from B16-F10-stimulated +/+ and *tm1a/tm1a* female mice ($n = 8$ per genotype). **c**, Measurement of IFN-γ in lungs of B16-F10-stimulated +/+ and *tm1a/tm1a* female mice, and control and *tm1c/tm1c; Lyve1*$^{cre/+}$ male mice. **d**, Experimental metastasis assay using B16-F10 cells in +/+ and *tm1a/tm1a* female mice treated with either isotype or anti-CD8 antibody. **e**, The proportion of activated (CD69$^+$) NK cells present in the lungs of +/+ and *tm1a/tm1a* female mice dosed with isotype or anti-CD8 antibody. **f**, Experimental metastasis assay using B16-F10 cells in +/+ and *tm1a/tm1a* male mice treated with isotype, anti-NK1.1 or anti-NK1.1 and CD8 antibody. Shown are representative data from three independent experiments, with symbols representing individual mice with horizontal bar at the mean (**a**, **c**–**f**) or mean ± s.e.m. (**b**). *P* values are indicated from two-tailed unpaired *t*-test with Welch's correction (**a**, **c**, **e**), two-way repeated measures ANOVA with Šídák's multiple comparisons test for each effector:target ratio (**b**) or Mann–Whitney test (**d**, **f**).

We next set out to establish the contribution of SPNS2 to the pulmonary immune microenvironment. S1P–S1PR1 signalling is essential for the recirculation of naive T cells; however, memory T cells downregulate S1PR1 expression and rely on chemokine receptors for trafficking[24]. In contrast, NK cell trafficking in response to S1P requires S1PR5 not S1PR1 (ref. 25). In agreement with this differential requirement of S1P for trafficking, *Spns2*$^{tm1a/tm1a}$ mice showed a significantly higher percentage of anti-tumoural effector memory T cells (CD44$^{hi}$CD62L$^{lo}$) relative to immune suppressive regulatory T cells (CD4$^+$CD25$^+$), thus providing an enhanced effector:regulatory T cell ratio (Fig. 3f and Extended Data Fig. 6a, b), with the same observed in *Spns2*$^{tm1c/tm1c}$; *Lyve1*$^{cre/+}$ mice (Fig. 3g and Extended Data Fig. 6c, d). An increased proportion of activated T cells (KLRG1$^+$, CD69$^+$ and CXCR3$^+$) were also observed in the lungs of *Spns2*$^{tm1a/tm1a}$ and *Spns2*$^{tm1c/tm1c}$; *Lyve1*$^{cre/+}$ mice (Extended Data Fig. 6e, f), with a similar phenotype seen in the liver (Extended Data Fig. 7).

Based on this activated phenotype, we performed *ex vivo* re-stimulation assays, where T cells were isolated from the lungs of *Spns2*$^{tm1a/tm1a}$ and control mice 5 days after *in vivo* activation with B16-F10 cells. Using pharmacological stimulation, both CD4$^+$ and CD8$^+$ T cells from *Spns2*$^{tm1a/tm1a}$ mice showed an enhanced degranulation response (cell surface expression of CD107a/LAMP1), and increased intracellular interferon-γ (IFN-γ) relative to control mice (Extended Data Fig. 8a, b). Interestingly, only CD8$^+$ T cells demonstrated enhanced degranulation when co-cultured with B16-F10 cells *ex vivo* suggestive of the presence of an improved antigen-specific response towards B16-F10 (Fig. 4a). This functionally resulted in enhanced B16-F10 target cell killing in an *ex vivo* cytotoxicity assay (Fig. 4b), and increased IFN-γ in lung lysates from B16-F10-stimulated *Spns2*$^{tm1a/tm1a}$ and *Spns2*$^{tm1c/tm1c}$; *Lyve1*$^{cre/+}$ mice (Fig. 4c). Similarly, increased IFN-γ was also observed in lung lysates from MC-38-stimulated *Spns2*$^{tm1a/tm1a}$ mice (Extended Data Fig. 8c) indicating that this is not a B16-F10 restricted phenomenon. Although there was a significant increase in the relative proportion of NK cells in the lung, no difference in NK cell function could be observed *ex vivo* in *Spns2*$^{tm1a/tm1a}$ mice (Extended Data Fig. 8a, b), in agreement with normal NK cell KLRG1, CD69 and CXCR3 expression in both *Spns2*$^{tm1a/tm1a}$ and *Spns2*$^{tm1c/tm1c}$; *Lyve1*$^{Cre/+}$ mice (Extended Data Fig. 8d, e).

To determine whether the beneficial effects of *Spns2* in regulating metastatic colonization could be mediated by CD8$^+$ T cells, we performed *in vivo* depletion experiments using anti-CD8 antibodies. However, paradoxically, depletion of CD8$^+$ T cells (or all T and B cells, such as in *Rag1* knockout mice) has previously been shown to decrease B16-F10 pulmonary metastasis (but not primary tumour growth); this phenomenon has been explained by the 'pro-tumoural' phenotype of CD8$^+$ T cells before tumour cell exposure versus the 'anti-tumoural' effect of antigen-specific CD8$^+$ T cells[26]. Indeed, we replicated this finding observing decreased pulmonary B16-F10 metastases in CD8$^+$ T-cell-depleted wild-type mice (Fig. 4d; and *Rag2* knockout mice, Extended Data Fig. 9); however, a genotype-specific effect was still observed in *Spns2*$^{tm1a/tm1a}$ mice, suggesting the involvement of additional cell types in the regulation of metastatic colonization. Given that we observed compensatory NK cell activation (CD69$^+$) in the lungs of CD8$^+$ T-cell-depleted *Spns2*$^{tm1a/tm1a}$ mice (Fig. 4e), we hypothesized NK cells could be responsible for the significantly reduced metastasis count compared with wild types. To explore this observation further, we performed NK cell depletion, resulting in increased B16-F10 metastases as reported previously[26]; however, *Spns2*$^{tm1a/tm1a}$ mice still showed a significantly reduced number of metastatic foci compared with

wild types (Fig. 4f), in agreement with the enhanced $CD8^+$ response to B16-F10 cells observed *ex vivo* (Fig. 4a). To demonstrate the dual cellular identity responsible for protection in *Spns2*$^{tm1a/tm1a}$ we co-depleted NK and $CD8^+$ cells *in vivo* restoring the number of metastatic foci observed in *Spns2*$^{tm1a/tm1a}$ mice to those of wild-type (Fig. 4f). Thus, we demonstrate that both $CD8^+$ T cells and NK cells can contribute to the reduced pulmonary metastatic burden observed in *Spns2*$^{tm1a/tm1a}$ mice. An alteration of lymphatic endothelial cell function or lung sphingolipid levels in *Spns2*-deficient mice may also contribute to the reduced pulmonary metastatic burden we observe.

Finally, we sought to manipulate the S1P axis pharmacologically by inhibiting S1P lyase, which degrades S1P, using 4′-deoxypyridoxine (DOP), a compound previously shown to increase lymphoid tissue S1P levels and induce a circulating lymphopenia[22]. DOP treatment phenocopied the immune and pulmonary metastasis phenotype of *Spns2*$^{tm1a/tm1a}$ mice (Extended Data Fig. 10), further validating the importance of the S1P axis in control of pulmonary metastatic burden. Importantly modulation of SPNS2 could be a more favourable approach than the S1P-blocking antibody Sphingomab[27,28] or the prodrug FTY720 (ref. 24) (which is phosphorylated *in vivo* to a functional antagonist of S1PR1) as these interventions increase regulatory T cell activity, suppress proliferation of effector T cells[29,30] and increase vascular permeability[18]. Furthermore, as lymphatic endothelial cell-specific deletion of *Spns2* is sufficient to regulate lymphocyte circulation to allow a higher percentage of effector T cells and NK cells in the lung (and liver) and more tumour cell killing, targeting SPNS2 is potentially a more promising option for regulating metastatic colonization than existing S1P pathway modulators.

**Online Content** Methods, along with any additional Extended Data display items and Source Data, are available in the online version of the paper; references unique to these sections appear only in the online paper.

**Received 11 September 2015; accepted 15 November 2016.**
**Published online 4 January 2017.**

1. Quail, D. F. & Joyce, J. A. Microenvironmental regulation of tumor progression and metastasis. *Nature Med.* **19,** 1423–1437 (2013).
2. Chambers, A. F. *et al.* Critical steps in hematogenous metastasis: an overview. *Surg. Oncol. Clin. N. Am.* **10,** 243–255 (2001).
3. Blank, C. *et al.* PD-L1/B7H-1 inhibits the effector phase of tumor rejection by T cell receptor (TCR) transgenic $CD8^+$ T cells. *Cancer Res.* **64,** 1140–1145 (2004).
4. van Elsas, A., Hurwitz, A. A. & Allison, J. P. Combination immunotherapy of B16 melanoma using anti-cytotoxic T lymphocyte-associated antigen 4 (CTLA-4) and granulocyte/macrophage colony-stimulating factor (GM-CSF)-producing vaccines induces rejection of subcutaneous and metastatic tumors accompanied by autoimmune depigmentation. *J. Exp. Med.* **190,** 355–366 (1999).
5. White, J. K. *et al.* Genome-wide generation and systematic phenotyping of knockout mice reveals new roles for many genes. *Cell* **154,** 452–464 (2013).
6. Ogasawara, K. *et al.* Requirement for IRF-1 in the microenvironment supporting development of natural killer cells. *Nature* **391,** 700–703 (1998).
7. Honda, K. *et al.* IRF-7 is the master regulator of type-I interferon-dependent immune responses. *Nature* **434,** 772–777 (2005).
8. Purtha, W. E., Swiecki, M., Colonna, M., Diamond, M. S. & Bhattacharya, D. Spontaneous mutation of the *Dock2* gene in *Irf5*$^{-/-}$ mice complicates interpretation of type I interferon production and antibody responses. *Proc. Natl Acad. Sci. USA* **109,** E898–E904 (2012).
9. Sasaki, T. *et al.* Function of PI3Kγ in thymocyte development, T cell activation, and neutrophil migration. *Science* **287,** 1040–1046 (2000).
10. Tassi, I. *et al.* p110γ and p110δ phosphoinositide 3-kinase signaling pathways synergize to control development and functions of murine NK cells. *Immunity* **27,** 214–227 (2007).
11. Kitamura, D., Roes, J., Kühn, R. & Rajewsky, K. A B cell-deficient mouse by targeted disruption of the membrane exon of the immunoglobulin μ chain gene. *Nature* **350,** 423–426 (1991).
12. Sun, X. *et al.* CD39/ENTPD1 expression by $CD4^+Foxp3^+$ regulatory T cells promotes hepatic metastatic tumor growth in mice. *Gastroenterology* **139,** 1030–1040 (2010).
13. Guerrero, J. A. *et al.* Gray platelet syndrome: proinflammatory megakaryocytes and α-granule loss cause myelofibrosis and confer metastasis resistance in mice. *Blood* **124,** 3624–3635 (2014).
14. Okada, F. *et al.* The role of nicotinamide adenine dinucleotide phosphate oxidase-derived reactive oxygen species in the acquisition of metastatic ability of tumor cells. *Am. J. Pathol.* **169,** 294–302 (2006).
15. Kang, B. H. *et al.* Targeted inhibition of mitochondrial Hsp90 suppresses localised and metastatic prostate cancer growth in a genetic mouse model of disease. *Br. J. Cancer* **104,** 629–634 (2011).
16. Takabe, K. & Spiegel, S. Export of sphingosine-1-phosphate and cancer progression. *J. Lipid Res.* **55,** 1839–1846 (2014).
17. Fukuhara, S. *et al.* The sphingosine-1-phosphate transporter Spns2 expressed on endothelial cells regulates lymphocyte trafficking in mice. *J. Clin. Invest.* **122,** 1416–1426 (2012).
18. Mendoza, A. *et al.* The transporter Spns2 is required for secretion of lymph but not plasma sphingosine-1-phosphate. *Cell Reports* **2,** 1104–1110 (2012).
19. Nagahashi, M. *et al.* Spns2, a transporter of phosphorylated sphingoid bases, regulates their blood and lymph levels, and the lymphatic network. *FASEB J.* **27,** 1001–1011 (2013).
20. Wilkerson, B. A. & Argraves, K. M. The role of sphingosine-1-phosphate in endothelial barrier function. *Biochim. Biophys. Acta* **1841,** 1403–1412 (2014).
21. Chiang, E. Y., Henson, M. & Stroynowski, I. Correction of defects responsible for impaired Qa-2 class Ib MHC expression on melanoma cells protects mice from tumor growth. *J. Immunol.* **170,** 4515–4523 (2003).
22. Schwab, S. R. *et al.* Lymphocyte sequestration through S1P lyase inhibition and disruption of S1P gradients. *Science* **309,** 1735–1739 (2005).
23. Nijnik, A. *et al.* The role of sphingosine-1-phosphate transporter Spns2 in immune system function. *J. Immunol.* **189,** 102–111 (2012).
24. Garris, C. S., Blaho, V. A., Hla, T. & Han, M. H. Sphingosine-1-phosphate receptor 1 signalling in T cells: trafficking and beyond. *Immunology* **142,** 347–353 (2014).
25. Walzer, T. *et al.* Natural killer cell trafficking *in vivo* requires a dedicated sphingosine 1-phosphate receptor. *Nature Immunol.* **8,** 1337–1344 (2007).
26. Cuff, S., Dolton, G., Matthews, R. J. & Gallimore, A. Antigen specificity determines the pro- or antitumoral nature of $CD8^+$ T cells. *J. Immunol.* **184,** 607–614 (2010).
27. Ponnusamy, S. *et al.* Communication between host organism and cancer cells is transduced by systemic sphingosine kinase 1/sphingosine 1-phosphate signalling to regulate tumour metastasis. *EMBO Mol. Med.* **4,** 761–775 (2012).
28. Visentin, B. *et al.* Validation of an anti-sphingosine-1-phosphate antibody as a potential therapeutic in reducing growth, invasion, and angiogenesis in multiple tumor lineages. *Cancer Cell* **9,** 225–238 (2006).
29. Liu, G., Yang, K., Burns, S., Shrestha, S. & Chi, H. The S1P(1)-mTOR axis directs the reciprocal differentiation of T(H)1 and T(reg) cells. *Nature Immunol.* **11,** 1047–1056 (2010).
30. Liu, Y. *et al.* The sphingosine-1-phosphate receptor agonist FTY720 and its phosphorylated form affect the function of $CD4^+CD25^+$ T cells *in vitro*. *Int. J. Mol. Med.* **30,** 211–219 (2012).

**Supplementary Information** is available in the online version of the paper.

**Acknowledgements** This work was supported by grants from Cancer Research UK (D.J.A. and O.J.S.), the Wellcome Trust (WT098051), Combat Cancer (D.J.A.), the European Research Council (311301 COLONCAN to O.J.S. and A.D.C.), National Institutes of Health U54HG004028 (N.A.K.), and Department of Defense BCRP Program Award W81XWH-14-1-0086 (S.S.). T.T. was funded by project A27N in the SFB854, and T.B. was funded in part by an EMBO Long-Term Fellowship (ALTF 945-2015) and the European Commission (Marie Curie Action LTFCOFUND2013, GA-2013-609409). We thank J. Allegood for sphingolipid analyses and acknowledge the VCU Lipidomics Core, which is supported in part by funding from the National Institutes of Health–National Cancer Institute (NIH–NCI) Cancer Center Support Grant P30CA016059, V. Iyer (Wellcome Trust Sanger Institute) for bioinformatics analysis, and members of the Wellcome Trust Sanger Institute Research Support Facility for their care of the mice.

**Author Contributions** L.v.d.W. devised and implemented the pulmonary metastasis screen, performing all the primary screen, confirmation and characterization studies. M.J.A. analysed the histopathological sections. A.D.C. and O.J.S. performed and analysed the intrasplenic B16-F10 assays. T.B. and T.T. performed and analysed the spontaneous metastasis assay. H.W.-J. and N.G. managed mouse breeding and were responsible for issuing phenotyping cohorts. M.D.C.V.-H., T.V., I.C.M. and K.W. performed the RNA-seq analysis. D.G. and E.R. genotyped the mice and performed gene expression analysis. S.C., A.G., E.T. and E.L.C. performed additional phenotypic characterization. The Sanger Mouse Genetics Project generated and phenotyped the mice as part of a primary phenotyping pipeline. S.S. oversaw the lipidomic analysis and provided input to the project and the manuscript. A.O.S. devised, performed and analysed the immunophenotyping assays. L.v.d.W., A.O.S. and D.J.A. led the project. L.v.d.W., A.O.S. and D.J.A. wrote the manuscript with contributions from all authors.

**Author Information** Reprints and permissions information is available at www.nature.com/reprints. The authors declare no competing financial interests. Readers are welcome to comment on the online version of the paper. Correspondence and requests for materials should be addressed to L.v.d.W. (lvdw@sanger.ac.uk) or D.J.A. (da1@sanger.ac.uk).

**Reviewer Information** *Nature* thanks C. Ghajar and the other anonymous reviewer(s) for their contribution to the peer review of this work.

## METHODS

**Mice.** The generation and genotyping of *Spns2*$^{tm1a(KOMP)Wtsi}$ (referred to as *tm1a/tm1a*)[23], *Lyve1*$^{tm1.1(EGFP/cre)Cys/J}$ (referred to as *Lyve1*$^{cre}$) mice[31] and *Rag2*$^{tm1Fwa}$ mice[32] have been described previously. *Spns2*$^{tm1c(KOMP)Wtsi}$ (referred to as *tm1c/tm1c*) mice were generated from crossing *Spns2*$^{tm1a(KOMP)Wtsi}$ mice with Flp-deleter mice[33] and crossed to *Lyve1*$^{cre}$ mice to generate experimental mice (*tm1c/tm1c*; *Lyve1*$^{cre/+}$) with littermates used as controls (*tm1c/+*; *Lyve1*$^{+/+}$ and *tm1c/tm1c*; *Lyve1*$^{+/+}$; referred to as 'controls'). The care and use of all mice in this study were in accordance with the UK Animals in Science Regulation Unit's Code of Practice for the Housing and Care of Animals Bred, Supplied or Used for Scientific Purposes, the Animals (Scientific Procedures) Act 1986 Amendment Regulations 2012, and all procedures were performed under a UK Home Office Project licence, which was reviewed and approved by the Sanger Institute's Animal Welfare and Ethical Review Body (unless otherwise stated). Housing and husbandry conditions were as described previously[34], with the exceptions that a cage density of one to six mice per cage was used and mice were maintained on Mouse Breeders Diet (Laboratory Diets, 5021-3) throughout the study. Unless specified otherwise, all mice were used at 6–12 weeks of age.

**General experimental design.** For most experiments, random allocation to treatment group was achieved through the process of Mendelian inheritance, with age- and sex-matched mice being selected across different litters and matings (to minimize potential litter and/or cage effects). The two exceptions were the NK cell depletion study and bone marrow chimaera study: in these studies, Mendelian inheritance was used to randomize assignment of animals to a genotype group; then, within this block, alternate allocation was used to assign treatment. Unless specified otherwise, the researcher was not blinded to the identity of the genotype and/or treatment of a mouse during any procedures because these were written on the cage card. Pilot experiments were performed to determine sample size with adequate statistical power for all studies except the high throughput screen where this this was not possible owing to the scale of breeding that would be required. For each procedure, exclusion criteria used are listed where applicable in the materials and methods. If no exclusion criteria are detailed, all data were included. The manuscript was prepared to meet ARRIVE reporting guidelines[35].

**Cell lines.** The mouse melanoma B16-F10 cell line was purchased from ATCC (CRL-6475) and the highly metastatic mouse melanoma B16-BL6 cell line was purchased from the University of Texas, MD Anderson Cancer Center and authenticated by whole genome and transcriptome sequencing. The mouse lung carcinoma CMT-167 cell line was purchased from Sigma-Aldrich (10032302) and the other cell lines were obtained from the laboratories that generated them. Specifically, the metastatic mouse colorectal MC-38 cell line[36] was a gift from L. Borsig (University of Zurich, Switzerland), the metastatic mouse mammary cancer EO771.LMB cell line[37] was a gift from R. L. Anderson (Peter MacCallum Cancer Centre, Australia), the metastatic HCmel12–mCherry melanoma cell line[38] was a gift from T. Tuting (University Hospital Magdeburg, Germany) and the transformed mouse melanocyte WT31 cell line (*Tyr::Nras*$^{Q61K/°}$; *INK4a*$^{-/-}$)[39] was a gift from O. Sansom (Beatson Institute for Cancer Research, Scotland). None of the cell lines used appears in the International Cell Line Authentication Committee database. All cells (apart from WT31 cells) were maintained in DMEM with 10% (v/v) fetal calf serum and 2 mM glutamine, 100 U/mL penicillin/streptomycin (with the addition of 20 mM HEPES for EO771.LMB cells) at 37 °C, 5% $CO_2$. WT31 cells were maintained in RPMI with 10% (v/v) fetal calf serum and 2 mM glutamine, 100 U/mL penicillin/streptomycin at 37 °C, 5% $CO_2$. All cell lines were screened for the presence of mycoplasma and mouse pathogens (at Charles River Laboratories, USA) before culturing and never cultured for more than five passages. The B16-F10–mCherry cells, stably expressing mCherry, were generated by co-transfection of B16-F10 cells with 4.5 μg of PB-CAGG-LUC-2A–mCherry–PURO-PB plasmid (a gift from D. Ryan, Wellcome Trust Sanger Institute) and 0.5 μg of PBase-expressing plasmid using Fugene HD (Promega) according to the manufacturer's recommendations. After selection in 5 μg/mL puromycin (Gibco BRL) for 10 days, cell sorting was performed (MoFlo XDP, Beckman Coulter) to select for those cells expressing high levels of mCherry and was maintained in 5 μg/mL puromycin.

**Experimental metastasis assay.** B16-F10 ($4 \times 10^5$), CMT-167 ($1 \times 10^5$), MC-38 ($4 \times 10^5$), EO771.LMB ($4 \times 10^5$) or WT31 ($2.5 \times 10^6$) cells resuspended in 0.1 mL phosphate buffered saline (PBS) were injected into the tail vein of 6- to 12-week-old sex-matched syngeneic control and mutant mice. After 10 days (or 30 days if WT31 cells were used) the mice were killed, their lungs removed (or livers removed if WT31 cells were used) and the number of metastatic foci counted macroscopically (for B16-F10 and WT31 cells) or microscopically from formalin-fixed haematoxylin and eosin-stained sections by a pathologist (for CMT-167, MC-38 and EO771.LMB cells; the pathologist was blinded to the genotypes of the samples). For intrasplenic injections of B16-F10 melanoma cells, the mice were anaesthetized under isofluorane gas and a laparotomy performed to expose the spleen. B16-F10 cells ($1 \times 10^4$) resuspended in 0.03 mL PBS were injected into the tail of the spleen, after which surgical incisions were sutured and surgical clips applied. Animals were monitored throughout recovery with dietary support and analgesia (Rimadyl 100 μg/mL *ad libitum*) provided, as approved by the Glasgow University Ethics Committee. After 14 days, the mice were killed, their livers removed and the number of metastatic foci counted macroscopically.

**Metastatic colonization screen.** The experimental metastasis assay (detailed above) was performed by administering $4 \times 10^5$ B16-F10 cells to age- and sex-matched wild-type and mutant mice. The mice were 6–12 weeks old (typically 6–8 weeks) at time of dosing and dosing cohorts typically consisted of 12–24 control mice with 3–5 different mutant alleles being screened (3–8 mutant mice per allele). To ensure consistency, preparation of the cells, administration into the tail vein and counting of pulmonary metastatic foci were performed by the same individual. To ensure a high level of accuracy, a two-stage process was implemented, with final calls only being made after data had been collected from multiple independent cohorts (the data from all mice were included in the analysis except for when the full 0.1 mL of cell suspension were not successfully administered because of difficulties at the time of injection). The first stage was a high-throughput process to identify lines of potential interest for the second stage; in this stage, mutant lines with a 'metastatic ratio' (mean number of metastatic foci in the mutant cohort divided by mean number of metastatic foci in the wild-type cohort) $\leq 0.6$ or $\geq 1.6$ and $P \leq 0.0175$ in the Mann–Whitney test (a subsequent analysis estimated a false discovery rate of 15%) progressed to the second stage. In the second stage, at least three additional cohort(s) of mice (of both sexes) were independently studied and the data combined into an integrative data analysis (IDA) as detailed in the Statistics section.

**Bone-marrow chimaeras.** Wild-type (CD45.1 congenically marked syngeneic) and *tm1a/tm1a* mice were given 2 × 4.2 Gy whole-body irradiation followed by tail vein administration of $3 \times 10^6$ bone marrow cells from either wild-type (CD45.1 congenic) or *tm1a/tm1a* mice. Six weeks after transplantation, a tail vein blood sample was taken from the mice to assess the relative proportion of CD45.1 versus CD45.2 cells and the number of T and B lymphocytes present in the peripheral blood; 2 days later, an experimental metastasis assay was performed.

***In vivo* depletion studies.** Mice were given intraperitoneal doses of antibodies (anti-CD8 (clone YTS169.4), rat IgG2b isotype control (clone LTF-2), anti-NK1.1 (clone PK136), mouse IgG2a (clone C1.18.4)), 200 μg in 0.1 mL PBS on days −3, 0 and +5, with B16-F10 cells administered by tail vein on day 0 (CD8-depletion mice were dosed with $4 \times 10^5$ B16-F10 cells; NK and NK/CD8-depletion mice were dosed with $2 \times 10^5$ B16-F10 cells). Tail vein blood samples were collected from all mice on day +1 to confirm the depletion was effective. All antibodies were 'InVivoMAb' from BioXCell.

**S1P lyase inhibitor studies.** For S1P lyase inhibitor studies, the mice were either given glucose (10 g/L) or glucose plus 4′ deoxypyridoxine (DOP, 30 mg/L; Sigma) in their drinking water 1 week before any experimentation (with mice remaining on treatment for the duration of the experiment)[22].

**Primary tumour growth studies.** For examination of orthotopic tumour growth, wild-type and *tm1a/tm1a* male and female mice at 6–8 weeks of age were subcutaneously administered $2.5 \times 10^3$ B16-BL6 melanoma cells in the flank. The developing tumours were measured every second day and if they had reached (or were very close to) 2 $cm^2$ on the day of measurement the mice were immediately culled (no tumour was ever more than 2.4 $cm^2$), as approved by a Home Office Inspector under the authority of the Animals (Scientific Procedures) Act 1986.

**Spontaneous metastasis assay.** Wild-type and *tm1a/tm1a* mice were subcutaneously dosed with $2 \times 10^5$ HCmel12–mCherry melanoma cells and the resulting tumour growth was monitored by inspection and palpation. The size of the tumour was measured weekly using Vernier callipers and recorded as mean diameter. Mice were killed when progressively growing melanomas exceeded 20 mm in size and tissues collected for further analyses (in accordance with institutional and national guidelines for the care and use of laboratory animals with approval by the local government authorities (LANUV, NRW, Germany)). The number of macroscopically visible metastases present on the lung surface were counted by two independent investigators in a blinded fashion.

**Preparation of tissue cell suspensions.** Mice were perfused with 20 mL PBS by cardiac puncture and the tissues were disrupted in C tubes using program m_lung_01 with an gentleMACS (Miltenyi Biotec) in Hanks Balanced Salt solution (HBSS) containing calcium and magnesium. Liberase DL (Collagenase with low dispase content, Roche, Burgess Hill, UK) was added to a final concentration of 0.1 U/mL and incubated for 30 min at 37 °C. The tubes were then processed using program m_lung_02 and DNase (0.1 mg/mL) was added for a further 30 min at 37 °C. The resulting cell suspension was centrifuged at 400 *g* for 5 min, resuspended in 2 mL fluorescence-activated cell sorting (FACS) buffer (D-PBS without calcium and magnesium containing 2 mM EDTA, 0.5% fetal calf serum and 0.09% sodium azide), passed through a 30 μm cell strainer and analysed on the flow cytometer.

To determine the number or viability of melanoma cells present in the lungs of mice, the mice were dosed with either $1 \times 10^6$ B16-F10 cells labelled with 10 μM CFSE (Molecular Probes, Invitrogen) at 90 min before perfusion or $1 \times 10^6$ B16-F10–mCherry cells at 12 h before perfusion. In each case, the lung cell suspension was analysed on the flow cytometer. For lung/liver leukocyte analysis, the leukocytes were enriched from other cell types in the cell suspension on a Percoll discontinuous gradient (67.5%/44%) and washed three times with FACS buffer. Single cell suspensions from spleen and lymph nodes (pooled inguinal) were prepared using frosted end of microscope slides in FACS buffer. Red blood cells were lysed from spleen samples by the addition of 2 mL PharmLyse (BD Biosciences) for 90 s at room temperature then stopped by the addition of 10 mL FACS buffer. Both spleen and lymph node samples were passed through a 30 μm cell strainer before staining. 'Naive' mice were those that had not been administered B16-F10 cells and 'stimulated' mice were those that had been tail vein administered B16-F10 cells 3 or 5 days before analysis as indicated in the figure legend.

**FACS immunostaining.** Samples were blocked with 1 μg of Mouse BD FC Block (anti CD16/32, clone 2.4G2, BD Biosciences) for 10 min before addition of multicolour antibody cocktails using titrated amounts to give saturating binding (see Supplementary Table 4 for more details). After washing, cells were stained with a viability dye (Live/Dead Blue, Invitrogen, 1 in 1,000 dilution in PBS) for 10 min at room temperature, then washed before acquisition. For determination of apoptosis, lung preparations were prepared as above and were stained with Caspglow reagent (eBioscience UK) according to the manufacturer's instructions for 1 h at 37 °C. Cells were washed with Annexin binding buffer and stained with Annexin V-APC (both BD Biosciences) according to the manufacturer's instructions for 15 min at room temperature. Cells were washed with Annexin binding buffer and resuspended Annexin V binding buffer containing 1 μg/mL DAPI (Life Technologies) before acquisition. To determine absolute cell counts of leukocyte populations, whole blood was counted with a haematology analyser (Scil Vetabc) and the white blood cell count was used to derive the number cells per microlitre of blood, with the immune cell populations as percentage of leukocytes.

**Lung leukocyte cytotoxicity.** Leukocytes were prepared from perfused lungs 5 days after B16-F10 injection as described above. B16-F10 target cells were labelled with 1 μM CFSE (Molecular Probes, Invitrogen). Target cells and lung leukocytes were added to 96-well round-bottomed plates at effector to target ratios indicated for 4 hours at 37 °C in complete DMEM medium (prepared as described in 'Cell lines'). The cells were washed twice with ice-cold PBS then resuspended in 100 μL Live/Dead far red (Invitrogen, 1 in 1,000 dilution in PBS) for 10 min at room temperature. Cells were washed twice and resuspended in BD Cell Fix for 10 min at room temperature and washed twice with FACS buffer, before acquisition where 2,000 target cells were collected. Cytotoxicity was calculated according to the following equation: (percentage of dead target cells with effector cells) – (percentage of dead target cells with no effector cells added).

**Leukocyte degranulation and IFN-γ production.** Leukocytes were prepared from perfused lungs 5 days after B16-F10 injection as described above. Cells were stimulated with target cells (B16-F10 at effector to target ratio of 2.5:1) or phorbol myristate acetate (PMA) and ionomycin (100 ng/mL and 150 ng/mL, respectively both Sigma-Aldrich). Cells and stimulus were added to 96-well round-bottomed plates in the presence of anti-CD107a antibody and BD GolgiStop (monensin, final concentration 2 μM) in complete DMEM medium for 4 hours at 37 °C. The plates were washed twice with ice-cold FACS buffer before blocking then staining with anti-TCRβ, CD45, NK1.1 and CD8α antibodies. Cells were then stained with a fixable viability indicator (Live/Dead Blue, Invitrogen) before intracellular staining for IFN-γ according to standard methods and analysed by flow cytometry where a minimum of 50,000 $CD45^+$ alive leukocyte events were collected. CD107a and IFN-γ gates were set on unstimulated leukocyte samples and specific degranulation or intracellular IFN-γ staining was calculated by subtracting the leukocyte alone unstimulated values from the treated values.

**Flow cytometry.** All samples were analysed on an LSR II or LSRFortessa (both BD Biosciences) that were standardized using BD Cytometer Setup and Tracking Beads and software. Compensation was determined using Ultracomp eBeads (eBioscience) for all antibodies, and ArC amide binding beads (Invitrogen) for live/dead stains. Data acquisition was controlled with BD FACSDiva version 6.3 or version 8.0.1 software. For the analysis of B16-F10 apoptosis, a threshold was applied to the mCherry channel (561 nm laser 610/20 BP) to exclude 90% of the lung cells. For the analysis of cytotoxicity, a threshold was applied to the CFSE channel (488 nm laser 530/30 BP) to exclude 90% of the lung leukocytes. In both cases these were established using B16-F10 mCherry- or CFSE-labelled B16-F10 cells. In all other cases an FSC-A threshold was used to exclude debris. All samples were analysed using FlowJo 10.7 and were analysed genotype and/or treatment blind. For all phenotyping data, doublets were excluded using FSC-A versus FSC-H gates, sample acquisition issues (such as clumps and unstable event rate) were excluded using a time gate against a fluorescent parameter that was off the laser with the longest time delay, dead cells were excluded from all tissue analysis using a viability indicator and debris excluded with FSC-A versus SSC-A gates. A leukocyte gate was set with CD45 and SSC-A and all cell subsets are reported as the percentage of this parent gate. T cells were defined as $TCR\gamma\delta^-$ $CD3^+$ $NK1.1^-$ or $TCR\beta^+$ $NK1.1^-$ with $CD4^+$ and $CD8^+$ gates defined on this parent population, NK cells defined as $NK1.1^+$ $CD3^-$ or $TCR^-$, and B cells defined as $CD19^+$. T and NK cell phenotypes were determined using fluorescent minus one controls to establish gating. Data from a sample were excluded if there were insufficient events in the parent gate to allow analysis: for example, if there were fewer than 50,000 $CD45^+$ alive leukocytes in lung phenotyping data, these were excluded from the data set.

**Lung IFN-γ determination.** Five days after B16-F10 injection lungs were saline perfused and homogenized in Tris-buffered saline with 0.5% Triton X100 using M tubes and a gentleMACS (Miltenyi Biotec) with program protein_01. Samples were cleared by centrifugation for 10 min at 20,000 *g* at 4 °C. IFN-γ levels in the lung lysates were determined using a Ready Set Go ELISA kit (eBioscience, Hatfield, UK) according to the manufacturer's instructions.

**Transcriptome sequencing.** Wild-type and *tm1a/tm1a* mice tail vein dosed with $1 \times 10^6$ B16-F10–mCherry cells were killed after 24 h and lung cell suspensions prepared as described above. Using a cell sorter (MoFlo XDP), B16-F10–mCherry cells were identified after displaying in a bivariate plot of SSC-log versus mCherry by gating on high forward scatter versus side scatter to exclude some debris and dead cells and positively sorted. RNA was extracted from the sorted cells using the RNeasy Mini kit (Qiagen), according to the manufacturer's instructions, and used to generate cDNA with the Smart-seq2 protocol[40,41]. Multiplexed sequencing libraries were generated from amplified cDNA using Nextera XT (Illumina). The multiplexed mRNaseq libraries were pooled and sequenced across multiple lanes on the Illumina Hiseq 2000 (version 3). Paired-end 100 bp reads were aligned with STAR version 2.3.0 (ref. 42), allowing a minimum (50 bp) and maximum intron size (500,000 bp). STAR genome index files were generated using a GTF file corresponding to gene models from ENSEMBL version 74 and reference genome version GRCm38. Read counting was performed with htseq-count from the HTSeq package (version 0.5.4p5)[43]. The htseq-count software was run with the options 'intersection-nonempty' mode, non-stranded, minimum quality 10, and 'exon' was used as the feature type, with 'gene_id' as the GTF feature ID. The Bioconductor (version 3.1)[44] package DESeq2 (version 1.8.1)[45] was used for differential expression analysis. We used the local fit parameter for dispersion fitting and obtained the significance with the DESeq2 negative binomial Wald test function. Genes with adjusted to $P < 0.05$ after Benjamini–Hochberg correction and a $\log_2$(fold change) less than $-0.59$ or greater than 0.59 was considered significantly differentially expressed.

**Analysis of sphingolipids by LC-ESI-MS/MS.** Serum and saline perfused lung tissues were collected from the mice. After the addition of internal standards (0.5 nmol each; Avanti Polar Lipids, Alabaster, Alabama, USA) the lipids were extracted and sphingolipids were quantified by LC-ESI-MS/MS (4000 QTRAP, AB Sciex, Framingham, Massachusetts, USA) as described previously[46].

**Statistics.** Statistical tests were selected to be appropriate for the data properties (for example, normality or homogeneity of variance) and experimental design such that the assumptions of the test would be met. Where multiple testing occurred within a study, it was managed by controlling the family-wise error rate as detailed in the associated figure legend. Integrative data analysis (also called mega-analysis)[47] was completed using R (package nlme version 3.1), treating each experiment as a fixed effect. An iterative top-down modelling strategy was implemented starting with the most comprehensive model (either equations (1) or (2)) appropriate for the collection strategy implemented and ensuring the model only included terms where they could be independently assessed:

$$Y = \beta_0 + \beta_{1,\ \mathrm{Sex}} + \beta_{2,\ \mathrm{Experiment}} + \beta_{3,\ \mathrm{Genotype}} + \beta_{4,\ \mathrm{Sex*Genotype}} \quad (1)$$

$$Y = \beta_0 + \beta_{2,\ \mathrm{Experiment}} + \beta_{3,\ \mathrm{Genotype}} \quad (2)$$

The optimization process first selected a covariance structure for the residual, then the model was reduced by removing non-significant fixed effects, and finally the genotype effect was tested and model diagnostics visualized. For the hypothesis test of primary interest, the impact of genotype, the per-comparison error rate threshold *P* values were adjusted to account for the multiple comparisons to control the family-wise error rate to 5% using the Hochberg method[48].

**Bioinformatic analysis of molecular functions and phenotype.** Using the Mouse Genome Informatics (MGI) portal (http://www.informatics.jax.org), all 810 mutant lines screened were separated into unique symbols (to separate out microRNA clusters) and annotated with molecular function using the Gene Ontology (GO) batch query selecting the GO_Slim annotations. Phenotypic information was pulled from MGI as a batch query (MGI 6.06, release date

5 October 2016) and supplemented with annotations from the International Mouse Phenotyping Consortium (IMPC – release 4.3, 26 April 2016) portal (http://www.mousephenotype.org). The reported mammalian phenotype (mp) terms returned were collapsed to the top-level term for the generation of the heatmap. We were not able to discriminate between no phenotype detected and no phenotypic data present; thus both outcomes are represented with a blue cell with the presence of phenotypes indicated by the red cell.

**Data availability.** The data that support the findings of this study are available from the corresponding author upon reasonable request. The data for Extended Data Fig. 2c are available in the online version of this paper. The data for the results of the experimental metastasis assay from stage 1 of the screen and the integrative data analysis are available in the online version of this paper. All RNA-seq data are available under European Nucleotide Archive accession number ERP005660 and ArrayExpress accession number E-ERAD-287, with the results of the analysis shown in Supplementary Table 3.


31. Pham, T. H. *et al.* Lymphatic endothelial cell sphingosine kinase activity is required for lymphocyte egress and lymphatic patterning. *J. Exp. Med.* **207,** 17–27 (2010).
32. Shinkai, Y. *et al.* RAG-2-deficient mice lack mature lymphocytes owing to inability to initiate V(D)J rearrangement. *Cell* **68,** 855–867 (1992).
33. Kranz, A. *et al.* An improved Flp deleter mouse in C57Bl/6 based on Flpo recombinase. *Genesis* **48,** 512–520 (2010).
34. Karp, N. A. *et al.* Impact of temporal variation on design and analysis of mouse knockout phenotyping studies. *PLoS ONE* **9,** e111239 (2014).
35. Kilkenny, C., Browne, W. J., Cuthill, I. C., Emerson, M. & Altman, D. G. Improving bioscience research reporting: the ARRIVE guidelines for reporting animal research. *PLoS Biol.* **8,** e1000412 (2010).
36. Borsig, L., Wong, R., Hynes, R. O., Varki, N. M. & Varki, A. Synergistic effects of L- and P-selectin in facilitating tumor metastasis can involve non-mucin ligands and implicate leukocytes as enhancers of metastasis. *Proc. Natl Acad. Sci. USA* **99,** 2193–2198 (2002).
37. Johnstone, C. N. *et al.* Functional and molecular characterisation of EO771. LMB tumours, a new C57BL/6-mouse-derived model of spontaneously metastatic mammary cancer. *Dis. Model. Mech*. **8,** 237–251 (2015).
38. Bald, T. *et al.* Ultraviolet-radiation-induced inflammation promotes angiotropism and metastasis in melanoma. *Nature* **507,** 109–113 (2014).
39. Lindsay, C. R. *et al.* P-Rex1 is required for efficient melanoblast migration and melanoma metastasis. *Nature Commun*. **2,** 555 (2011).
40. Picelli, S. *et al.* Smart-seq2 for sensitive full-length transcriptome profiling in single cells. *Nature Methods* **10,** 1096–1098 (2013).
41. Picelli, S. *et al.* Full-length RNA-seq from single cells using Smart-seq2. *Nature Protocols* **9,** 171–181 (2014).
42. Dobin, A. *et al.* STAR: ultrafast universal RNA-seq aligner. *Bioinformatics* **29,** 15–21 (2013).
43. Anders, S., Pyl, P. T. & Huber, W. HTSeq—a Python framework to work with high-throughput sequencing data. *Bioinformatics* **31,** 166–169 (2015).
44. Gentleman, R. C. *et al.* Bioconductor: open software development for computational biology and bioinformatics. *Genome Biol.* **5,** R80 (2004).
45. Love, M. I., Huber, W. & Anders, S. Moderated estimation of fold change and dispersion for RNA-seq data with DESeq2. *Genome Biol.* **15,** 550 (2014).
46. Hait, N. C. *et al.* Regulation of histone acetylation in the nucleus by sphingosine-1-phosphate. *Science* **325,** 1254–1257 (2009).
47. Curran, P. J. & Hussong, A. M. Integrative data analysis: the simultaneous analysis of multiple data sets. *Psychol. Methods* **14,** 81–100 (2009).
48. Hochberg, Y. A sharper Bonferroni procedure for multiple tests of significance. *Biometrika* **75,** 800–802 (1988).

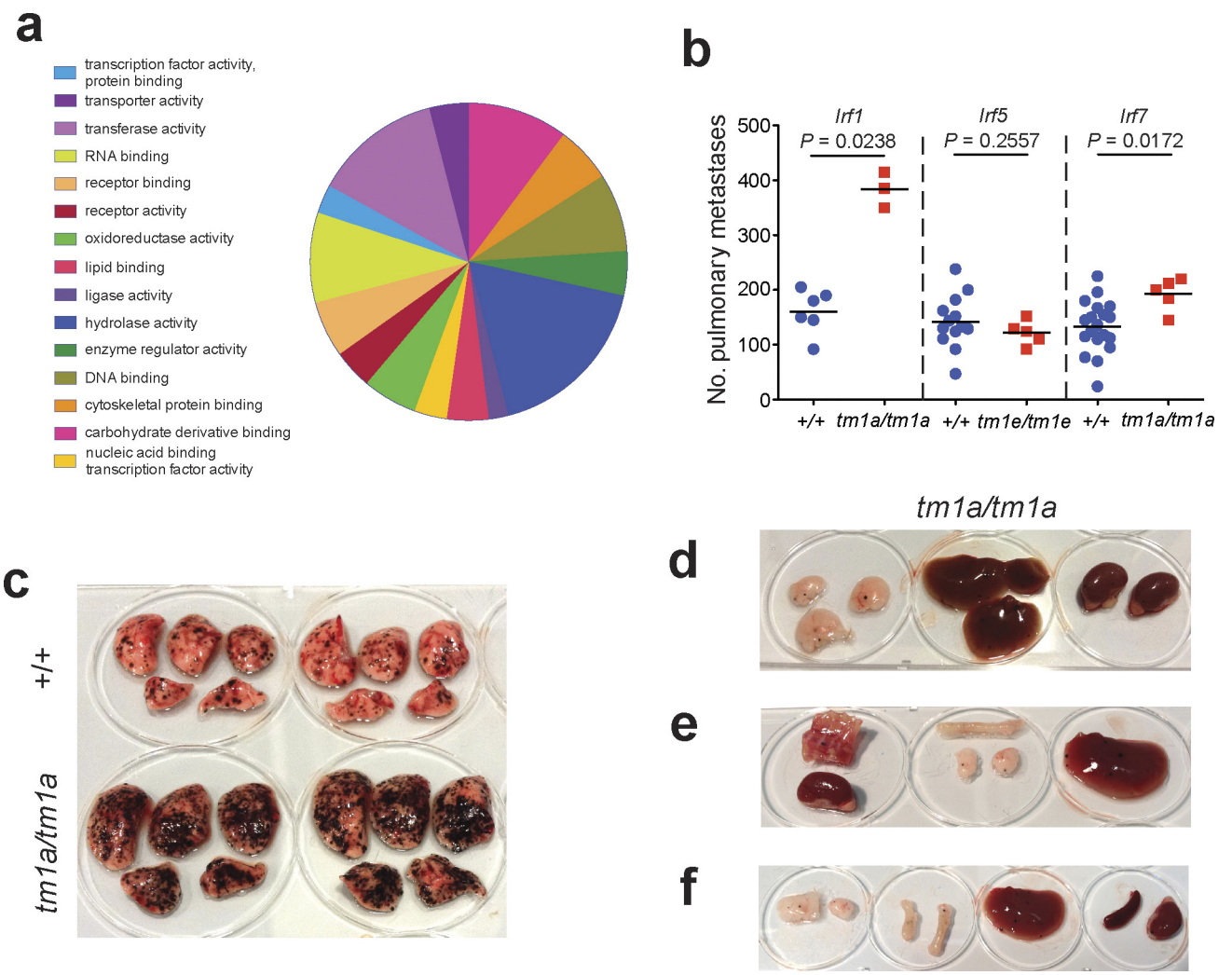


**Extended Data Figure 1 | Molecular function of 810 mutant mouse lines screened and phenotypic characterization members of the interferon regulatory factor (*Irf*) family. a**, Molecular function Gene Ontology annotation of the 810 mutant mouse lines screened as detailed in Methods. **b**, Experimental metastasis assay using B16-F10 cells in $Irf1^{tm1a/tm1a}$, $Irf5^{tm1e/tm1e}$, $Irf7^{tm1a/tm1a}$ and concurrent control female mice. Shown are representative data from two (*Irf5*), four (*Irf1*) or six (*Irf7*) independent experiments. Symbols represent individual mice with a horizontal bar at the mean. *P* values are from a Mann–Whitney test. **c–f**, Representative photographs showing B16-F10 metastatic colonies on the (**c**) lungs of +/+ and $Irf1^{tm1a/tm1a}$ mice and (**d–f**) the presence of extra-pulmonary metastases in $Irf1^{tm1a/tm1a}$ mice (tissues from three mice shown).

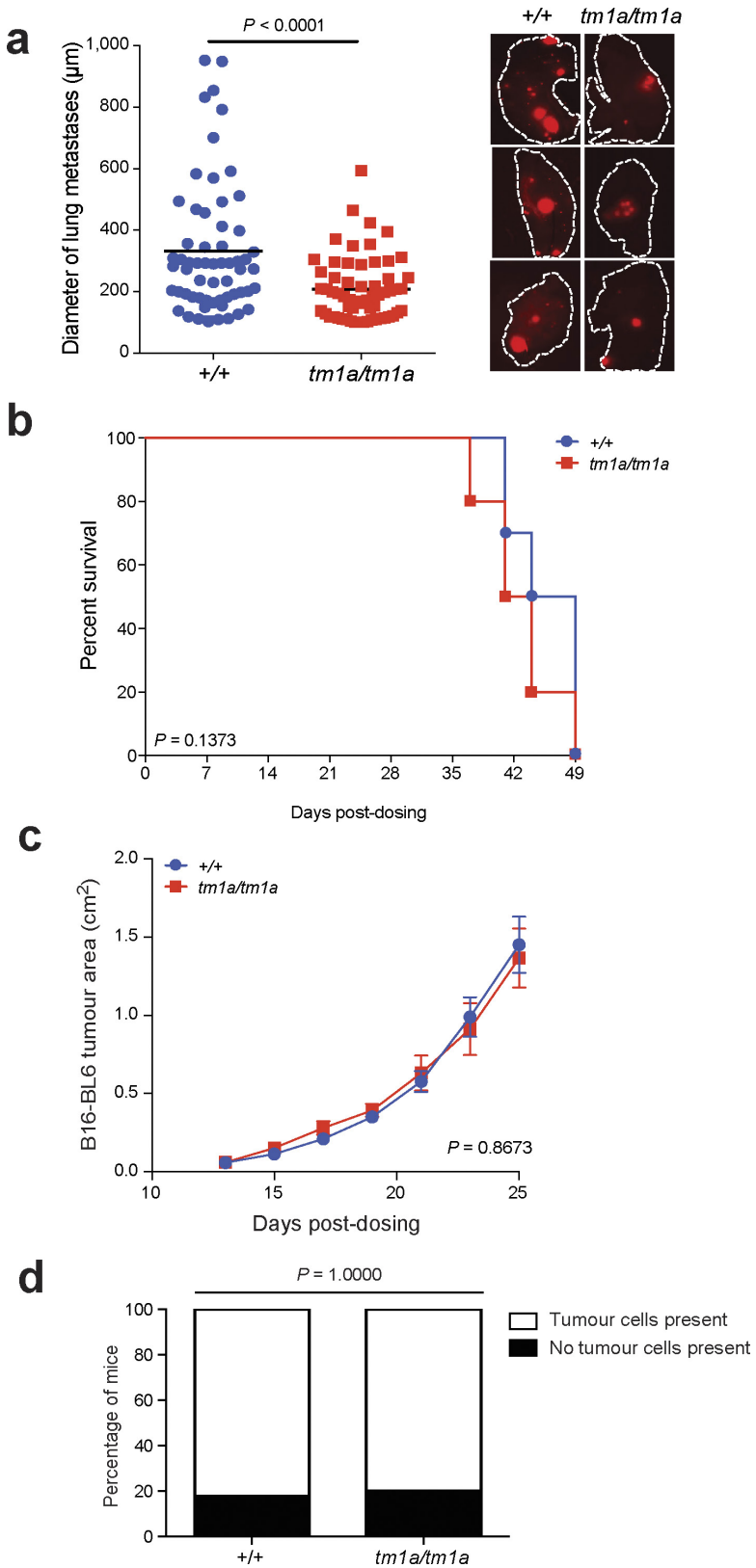


**Extended Data Figure 2 | Spontaneous pulmonary metastases and primary tumour growth in *Spns2* mice. a**, Size measurements of spontaneous pulmonary HCmel12–mCherry melanoma cell metastases of male mice with representative fluorescent images (lines indicate the edge of the lungs); $n = 10$ per genotype, horizontal bars represent mean (of 50 individual metastases counted per genotype) (one-way ANOVA with blocking factor of experiment, cumulative results of two independent experiments shown). **b**, Survival curve of +/+ and *tm1a/tm1a* male mice ($n = 10$ per genotype) in a spontaneous metastasis assay using HCmel12–mCherry cells (log-rank test (Mantel–Cox), cumulative results of two independent experiments shown). **c**, Growth of subcutaneously administered B16-BL6 cells in +/+ (four male, five female) and *tm1a/tm1a* (five male, one female) mice. Symbols represent mean ± s.e.m. with a two-tailed unpaired *t*-test with Welch's correction used to compare the area under the curve. **d**, Incidence of cancer in aged (>40 weeks) +/+ ($n = 15$; 4 males, 11 females) and *tm1a/tm1a* ($n = 18$; 5 males, 13 females) mice. Statistical analysis was performed using a Fisher's exact test.

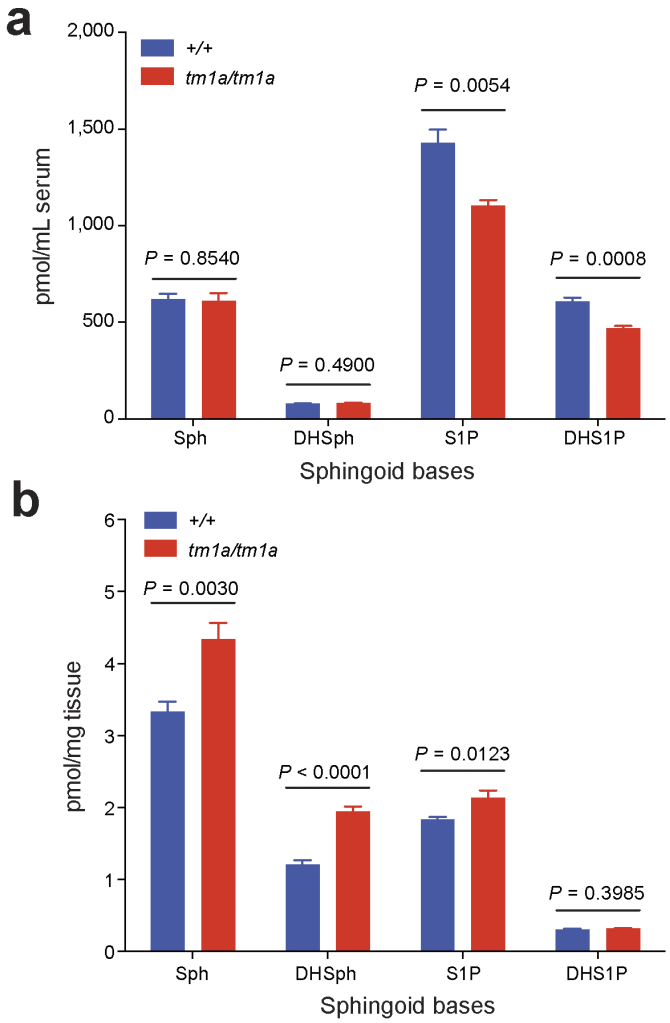


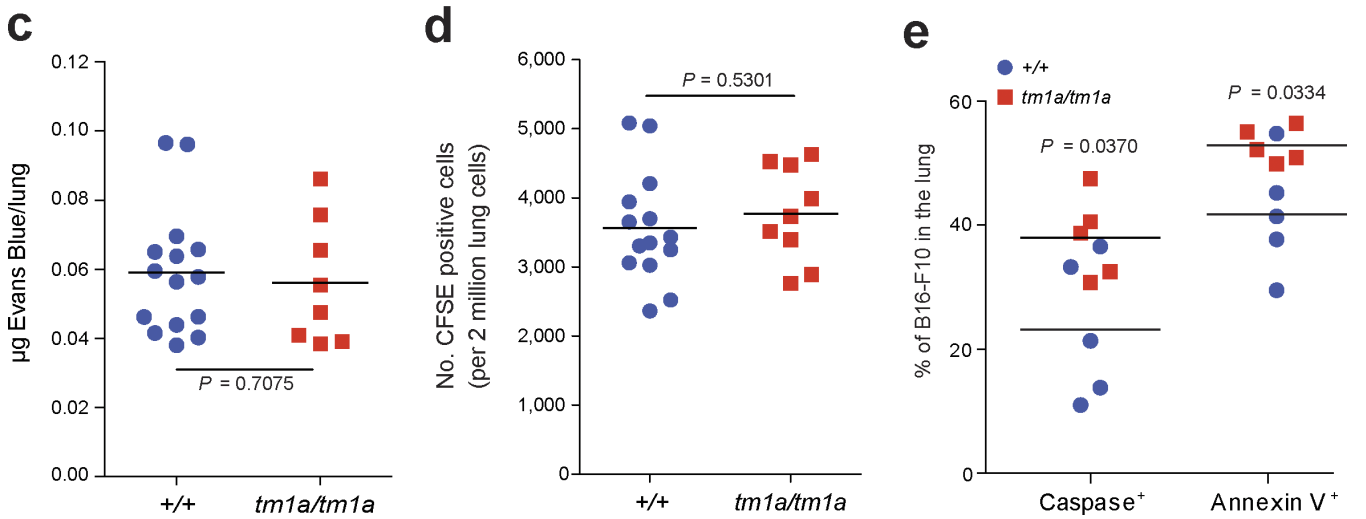


**Extended Data Figure 3 | Phenotyping of the serum and lungs of *Spns2* mice.** Sphingoid base levels in the (**a**) serum (+/+, $n = 5$; *tm1a/tm1a*, $n = 4$) and (**b**) lungs (+/+, $n = 6$; *tm1a/tm1a*, $n = 5$) of male mice; data are mean ± s.e.m., multiple two-tailed unpaired *t*-tests with *P* value adjusted by the Holm–Šídák method with $\alpha$ set to 5%. Sph, sphingosine; DHSph, dihydrosphingosine; S1P, sphingosine-1-phosphate; DHS1P, dihydrosphingosine-1-phosphate. **c**, Micrograms of extravasated Evans blue dye in the lungs of +/+ and *tm1a/tm1a* male mice. **d**, Number of CFSE-labelled B16-F10 cells present in the lungs of female mice 90 min after administration. **e**, Levels of apoptosis in B16-F10–mCherry cells 12 h after administration to male mice. Shown are representative data from three independent experiments, with symbols representing individual mice. *P* values are indicated from two-tailed unpaired *t*-test with Welch's correction (**c**–**e**).

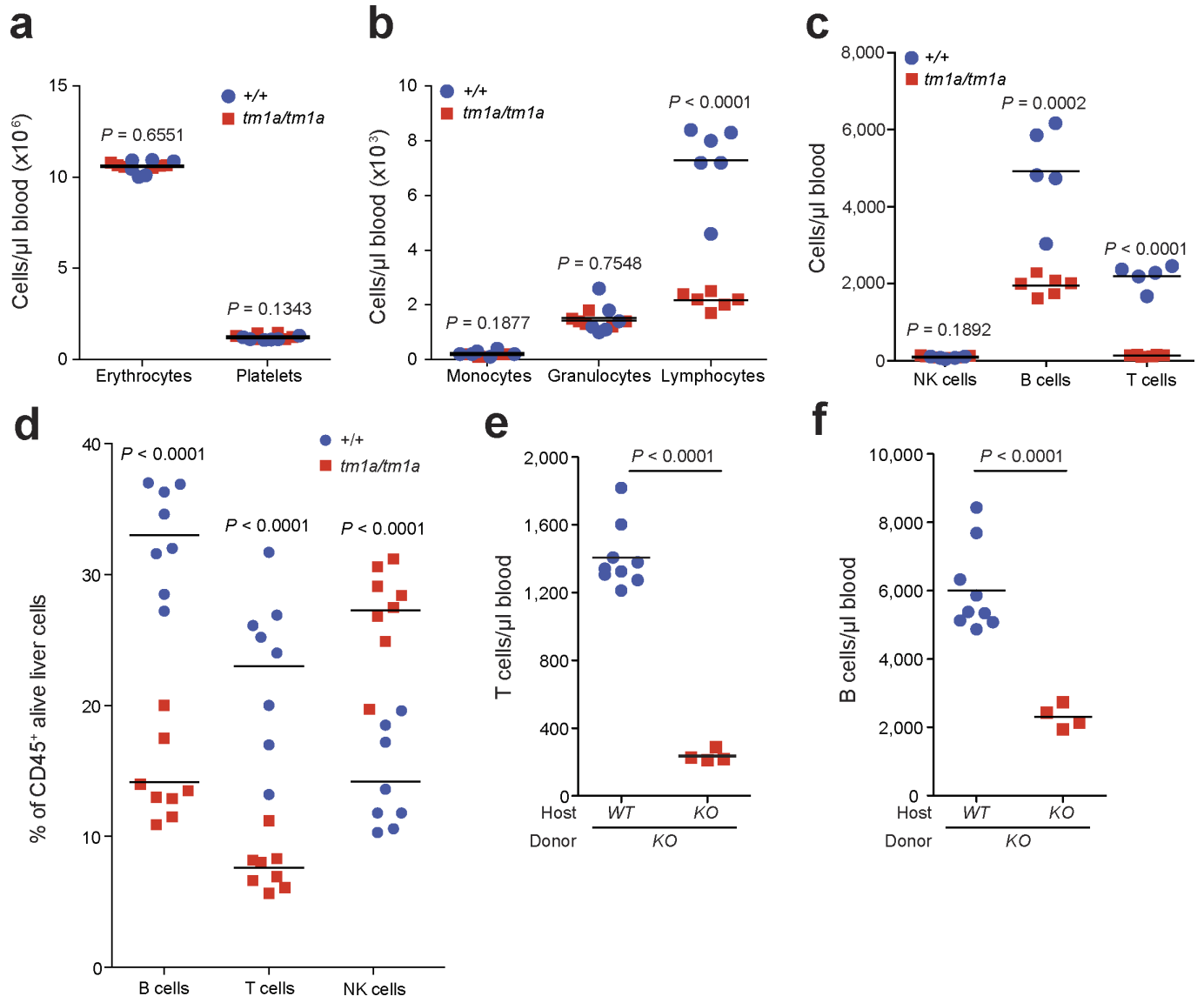


**Extended Data Figure 4 | Phenotypic characterization of the haematopoietic system of *Spns2* mice. a–c**, The numbers of erythrocytes and platelets, monocytes, granulocytes and lymphocyte subsets present in the blood of naive +/+ and *tm1a/tm1a* female mice (multiple two-tailed unpaired *t*-tests with *P* value adjusted by the Holm–Šídák method with $\alpha$ set to 5%; data shown are representative of three independent experiments). **d**, Analysis of lymphocyte subsets in the liver of naive +/+ and *tm1a/tm1a* female mice (multiple two-tailed unpaired *t*-tests with *P* value adjusted by the Holm–Šídák method with $\alpha$ set to 5%; data shown are representative of three independent experiments). **e**, **f**, T- and B-lymphocyte numbers in the blood of male naive (unstimulated) bone marrow chimaeras (unpaired two-tailed *t*-test with Welch's correction; data shown are representative of two independent experiments). Symbols represent individual mice; horizontal bars represent mean.

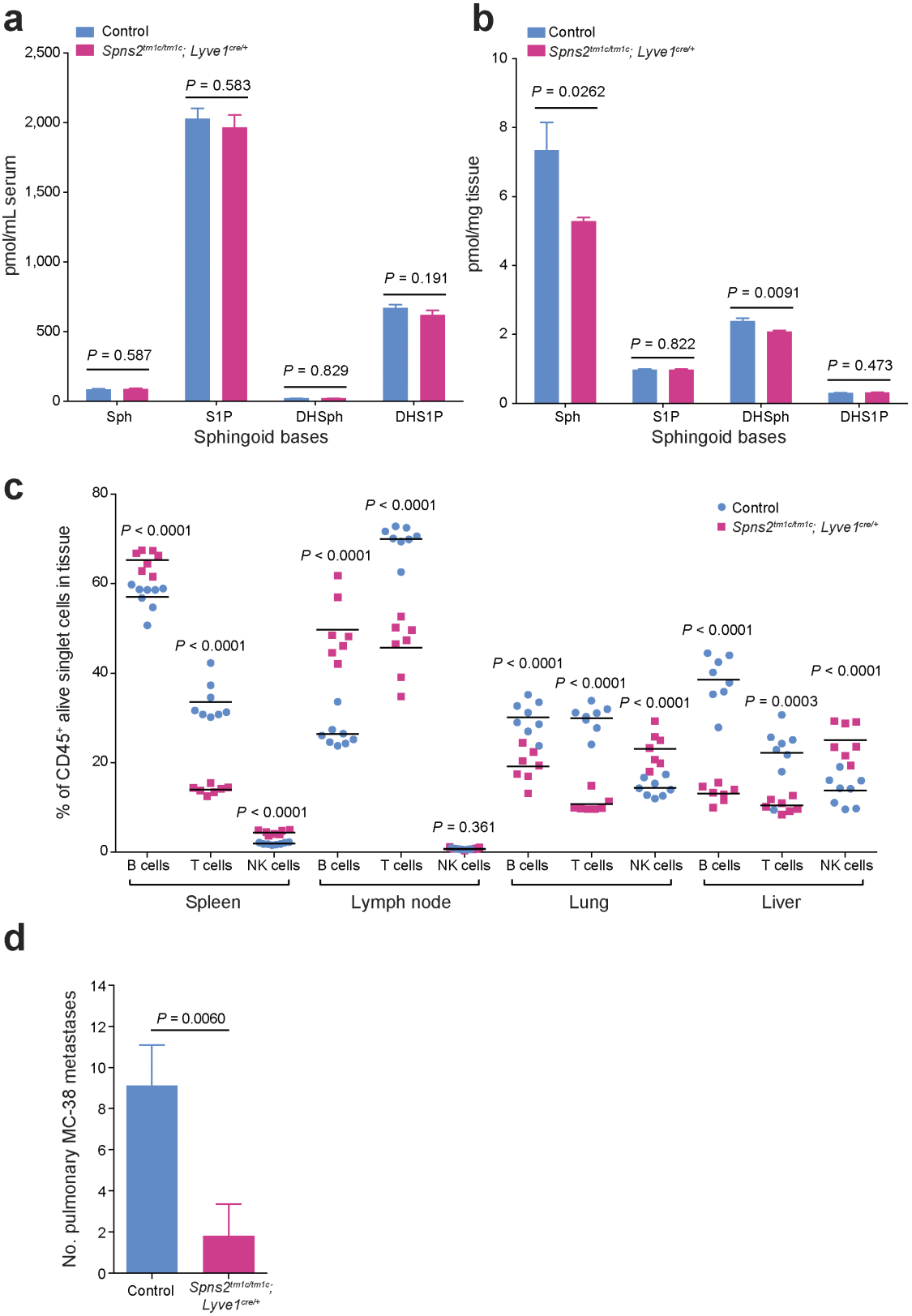


**Extended Data Figure 5 | Characterization of the phenotype of lymphatic endothelial cell *Spns2* deficient mice. a**, **b**, Sphingoid base levels in the (**a**) serum or (**b**) lung of control and *Spns2*$^{tm1c/tm1c}$; *Lyve1*$^{cre/+}$ male mice (data are mean ± s.e.m., control $n = 11$, *Spns2*$^{tm1c/tm1c}$; *Lyve1*$^{cre/+}$ $n = 10$, multiple two-tailed unpaired *t*-tests with *P* value adjusted by the Holm–Šídák method with $\alpha$ set to 5%). Sph, sphingosine; DH-Sph, dihydrosphingosine; S1P, sphingosine-1-phosphate; DH-S1P, dihydrosphingosine-1-phosphate. **c**, Lymphocyte subsets in the spleen, lymph node, lung and liver of +/+ and *tm1a/tm1a* male mice (symbols represent individual mice, horizontal bars represent mean, multiple two-tailed unpaired *t*-tests with *P* value adjusted by the Holm–Šídák method with $\alpha$ set to 5%; data shown are representative of three independent experiments). **d**, Experimental metastasis assay using MC-38 cells in control ($n = 9$) and *Spns2*$^{tm1c/tm1c}$; *Lyve1*$^{cre/+}$ ($n = 5$) in female mice. Data shown are mean ± s.e.m., Mann–Whitney test, representative of three independent experiments.

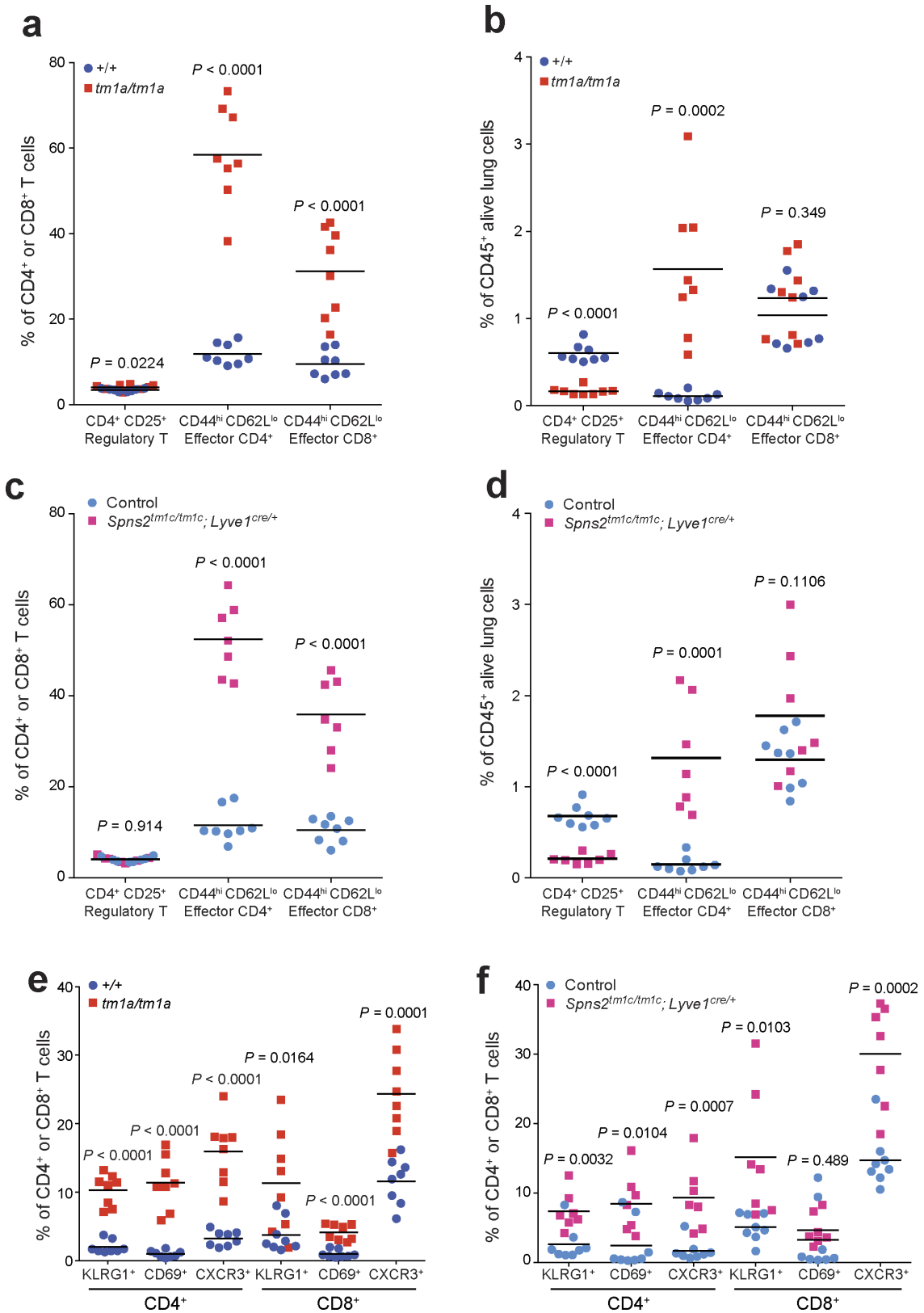


**Extended Data Figure 6 | T cell subsets in the lungs of *Spns2* mice.** The proportion of T cell subsets present in the lungs of naive +/+ and *tm1a/tm1a* female mice (**a**, **b**, **e**) and control and *Spns2*$^{tm1c/tm1c}$; *Lyve1*$^{cre/+}$ male mice (**c**, **d**, **f**). Data are shown as percentage of parent CD4$^+$ and CD8$^+$ T cells (**a**, **c**, **e**, **f**) or percentage of CD45$^+$ alive lung cells present (**b**, **d**). Symbols represent individual mice with horizontal bar at the mean. *P* values are indicated from two-tailed unpaired *t*-test adjusted by the Holm–Šídák method with $\alpha$ set to 5%. Data shown are representative of three independent experiments.

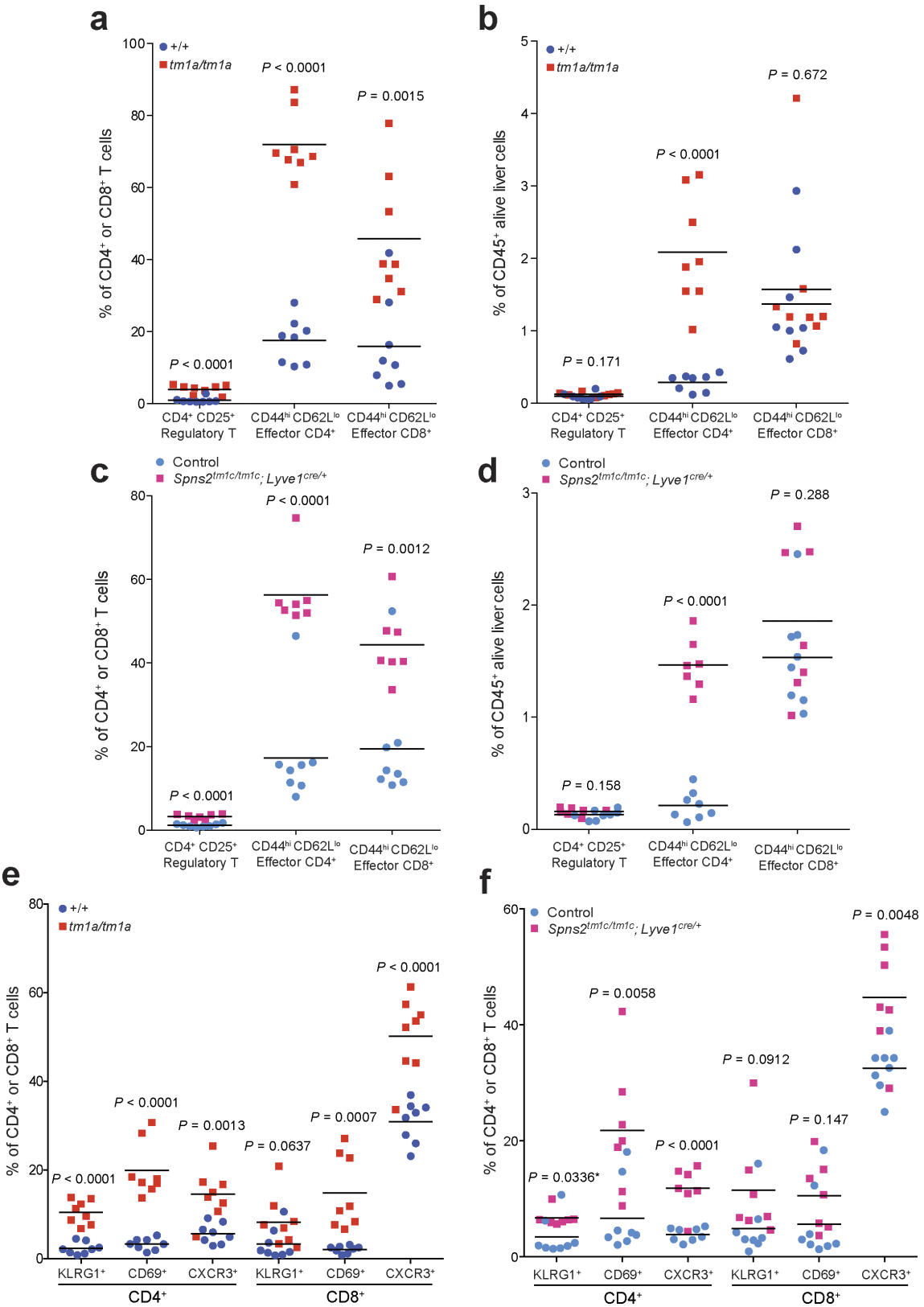


**Extended Data Figure 7 | T cell subsets in the liver of *Spns2* mice.** The proportion of T cell subsets present in the liver of naive +/+ versus *tm1a/tm1a* female mice and control versus *Spns2*$^{tm1c/tm1c}$; *Lyve1*$^{cre/+}$ male mice. Data are shown as percentage of parent CD4$^+$ and CD8$^+$ T cells (**a**, **c**, **e**, **f**) or percentage of CD45$^+$ alive liver cells present (**b**, **d**). Symbols represent individual mice; statistical analysis used multiple two-tailed unpaired *t*-tests with *P* value adjusted by the Holm–Šídák method with $\alpha$ set to 5%, with * indicating a *P* value not considered significant after correcting for multiple testing. Data shown are representative of three independent experiments.

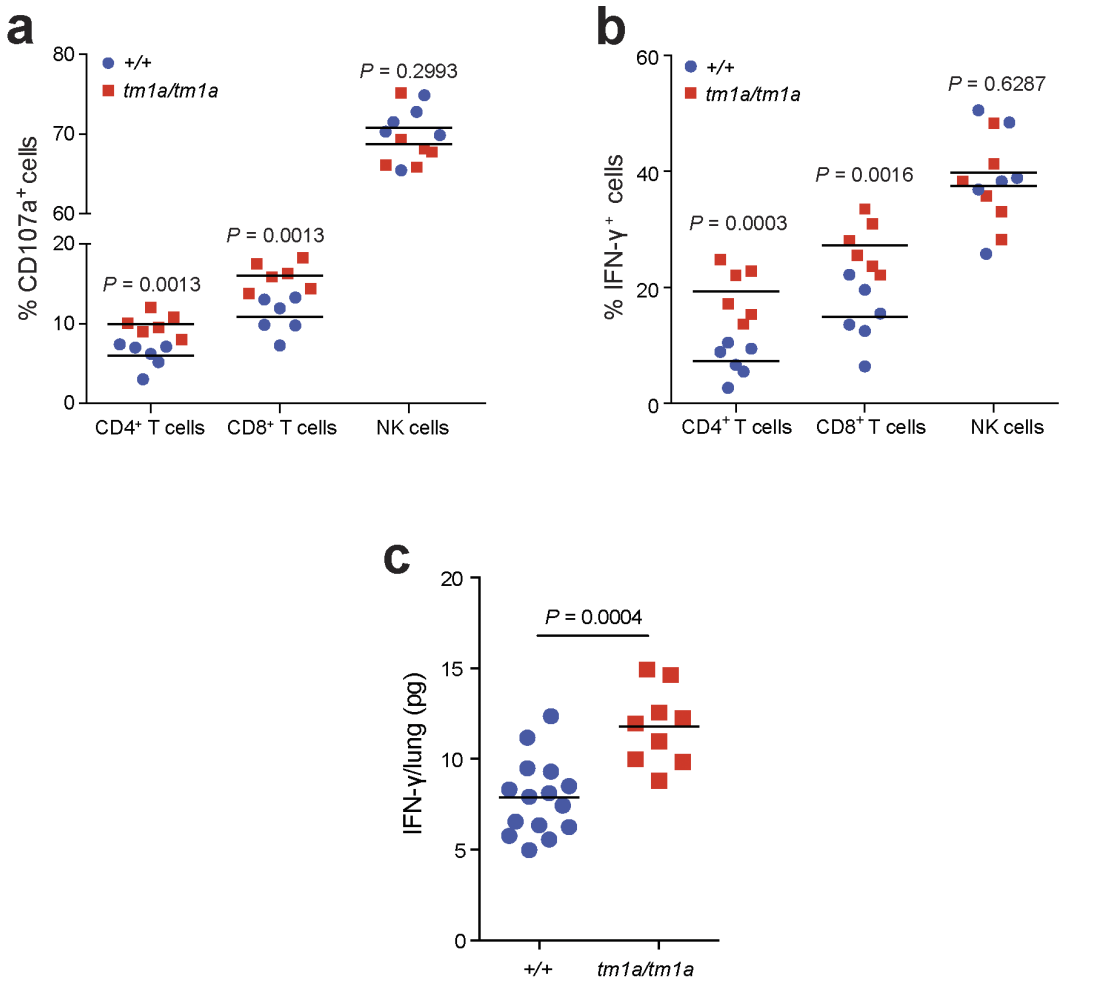


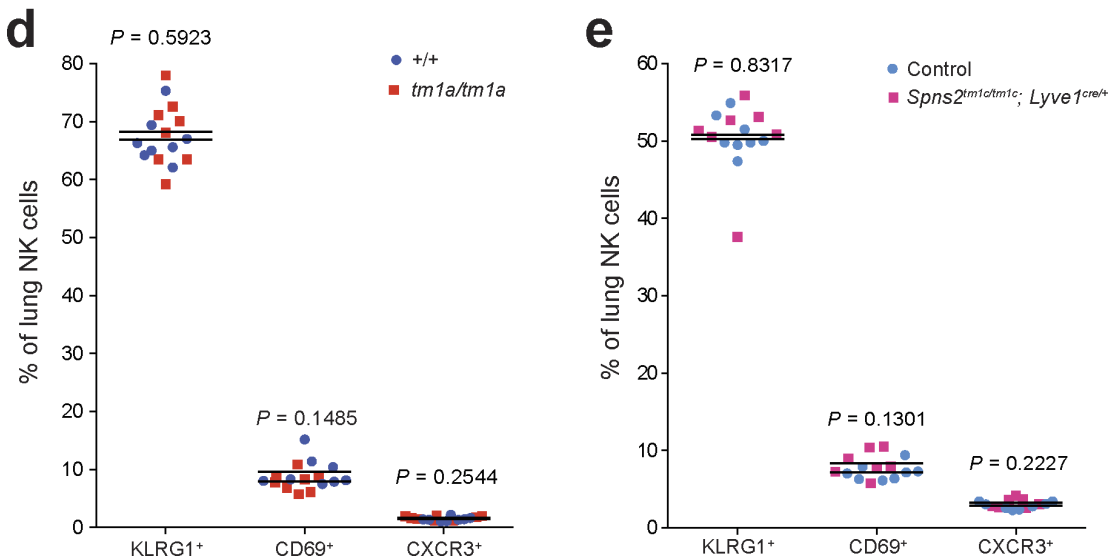


**Extended Data Figure 8 | Phenotyping of *Spns2* lungs. a**, **b**, *Ex vivo* re-stimulation (PMA/ionomycin) of pulmonary leukocytes from B16-F10-stimulated +/+ and *tm1a/tm1a* female mice (two-tailed unpaired *t*-test adjusted by the Holm–Šídák method with $\alpha$ set to 5%). **c**, Measurement of IFN-$\gamma$ in lungs of MC-38-stimulated +/+ and *tm1a/tm1a* male mice (two-tailed unpaired *t*-test with Welch's correction). **d**, **e**, The proportion of NK cell subsets present in the lungs of naive +/+ versus *tm1a/tm1a* female mice (**d**) and control versus *Spns2*$^{tm1c/tm1c}$; *Lyve1*$^{cre/+}$ male mice (**e**) (multiple two-tailed unpaired *t*-tests with *P* value adjusted by the Holm–Šídák method with $\alpha$ set to 5%). Symbols represent individual mice, horizontal bars represent mean; data shown are representative of three independent experiments.

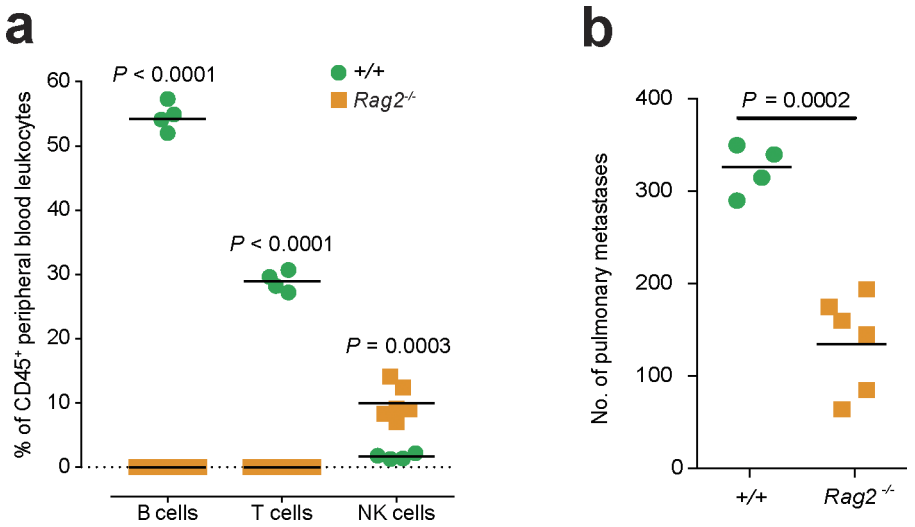


**Extended Data Figure 9 | Studies in T- and B-cell-deficient mice.** **a**, Measurement of lymphocyte subsets in the blood of +/+ and *Rag2*$^{-/-}$ mice (multiple two-tailed unpaired *t*-tests with *P* value adjusted by the Holm–Šídák method with $\alpha$ set to 5%). **b**, Experimental metastasis assay using B16-F10 cells in +/+ and *Rag2*$^{-/-}$ female mice (Mann–Whitney test). Symbols represent individual mice, horizontal bars represent mean; data shown are representative of three independent experiments.

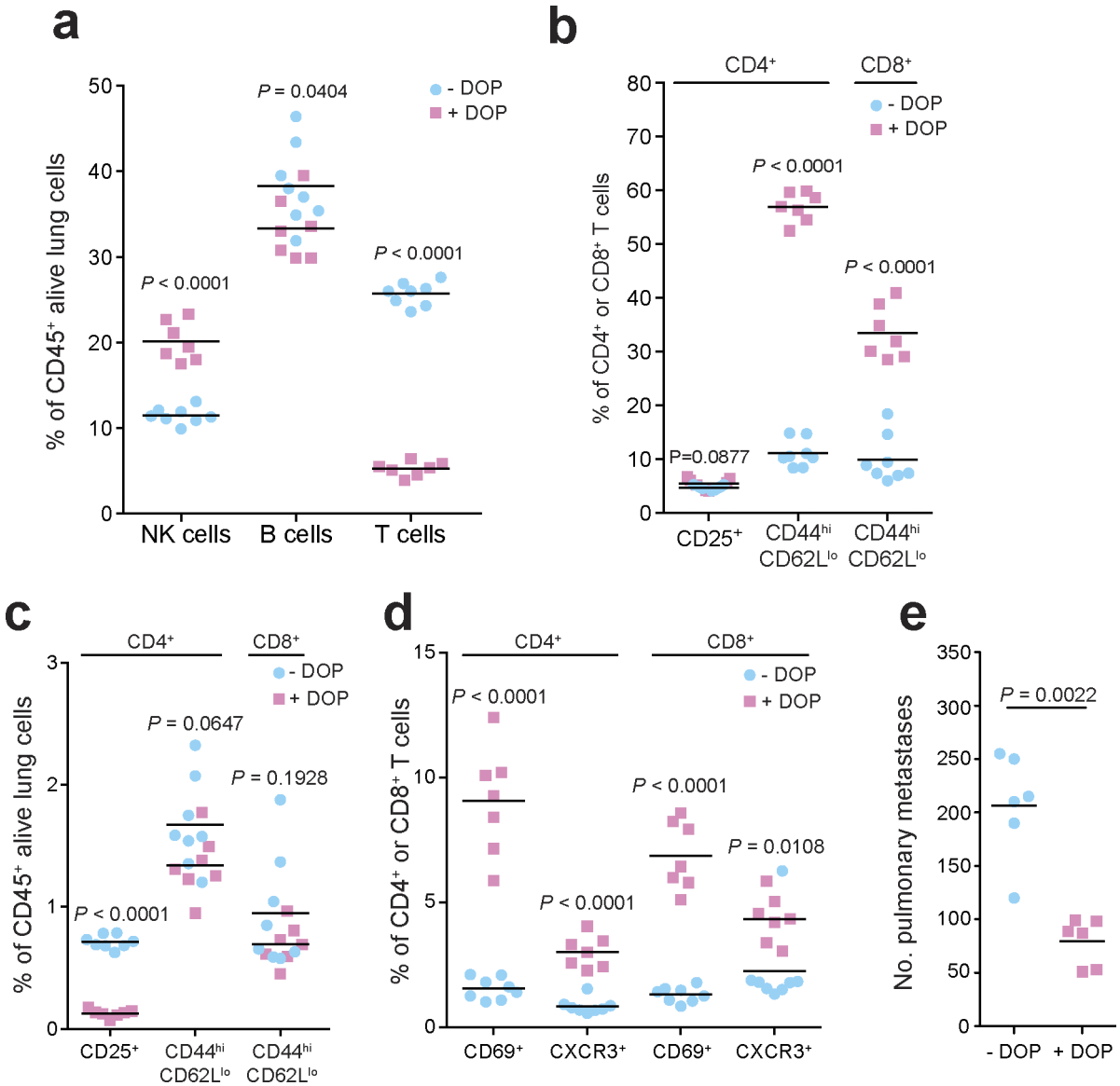


**Extended Data Figure 10 | Characterization of the leukocyte composition and phenotype in DOP-treated mice. a–d**, The number of leukocytes and T cell subsets present in the lungs of B16-F10-dosed glucose- or DOP-treated wild-type male mice presented as the percentages of viable $CD45^+$ lung leukocytes (**a**, **c**) or parent $CD4^+$ or $CD8^+$ T cells (**b**, **d**) (multiple unpaired *t*-tests with *P* value adjusted by the Holm–Šídák method with $\alpha$ set to 5%). **e**, Experimental metastasis assay in B16-F10 dosed glucose- or DOP-treated wild-type female mice (Mann–Whitney test). Symbols represent individual mice, horizontal bars represent mean; data shown are representative of two independent experiments.

# Sphingosine kinase 1 activation by estrogen receptor α36 contributes to tamoxifen resistance in breast cancer

**Melissa A. Maczis,* Michael Maceyka,* Michael R. Waters,* Jason Newton,* Manjulata Singh,* Madisyn F. Rigsby,* Tia H. Turner,† Mohammad A. Alzubi,† J. Chuck Harrell,† Sheldon Milstien,* and Sarah Spiegel[1],***

Department of Biochemistry and Molecular Biology* and Department of Pathology and the Massey Cancer Center,† Virginia Commonwealth University School of Medicine, Richmond, VA 23298

**Abstract** **In breast cancer, 17β-estradiol (E2) plays critical roles mainly by binding to its canonical receptor, estrogen receptor (ER) α66, and eliciting genomic effects. E2 also triggers rapid, nongenomic responses. E2 activates sphingosine kinase 1 (SphK1), increasing sphingosine-1-phosphate (S1P) that binds to its receptors, leading to important breast cancer signaling. However, the E2 receptor responsible for SphK1 activation has not yet been identified. Here, we demonstrate in triple-negative breast cancer cells, which lack the canonical ERα66 but express the novel splice variant ERα36, that ERα36 is the receptor responsible for E2-induced activation of SphK1 and formation and secretion of S1P and dihydro-S1P, the ligands for S1PRs. Tamoxifen, the first-line endocrine therapy for breast cancer, is an antagonist of ERα66, but an agonist of ERα36, and, like E2, activates SphK1 and markedly increases secretion of S1P. A major problem with tamoxifen therapy is development of acquired resistance. We found that tamoxifen resistance correlated with increased SphK1 and ERα36 expression in tamoxifen-resistant breast cancer cells, in patient-derived xenografts, and in endocrine-resistant breast cancer patients. Our data also indicate that targeting this ERα36 and SphK1 axis may be a therapeutic option to circumvent endocrine resistance and improve patient outcome.**—Maczis, M. A., M. Maceyka, M. R. Waters, J. Newton, M. Singh, M. F. Rigsby, T. H. Turner, M. A. Alzubi, J. C. Harrell, S. Milstien, and S. Spiegel. **Sphingosine kinase 1 activation by estrogen receptor α36 contributes to tamoxifen resistance in breast cancer.** ***J. Lipid Res.*** **2018.** 59: **2297–2307.**

**Supplementary key words** estradiol • estrogen receptor-α • splice variant • sphingosine-1-phosphate

Breast cancer is the most prevalent type of cancer in women, and 1 in 8 women in the United States will develop breast cancer over their lifetime. The estrogen receptor-α (ERα) and its ligand 17β-estradiol (E2) play important roles in cancer pathogenesis, progression, and metastasis. Patients with tumors that express the full-length ERα66 are termed ERα-positive and those lacking it as ERα-negative. Endocrine therapy, such as tamoxifen, is a first-line treatment of ERα-positive breast cancer (1, 2). Unfortunately, more than 50% of these patients will ultimately fail therapy due to acquired resistance. Moreover, triple-negative breast cancers (TNBCs) lacking ERα66, progesterone receptor (PR), and human epidermal growth factor receptor (EGFR) are aggressive cancers with high recurrence, metastatic, and mortality rates and limited treatment options, and they do not respond to hormonal therapy (3, 4). Understanding the mechanisms responsible for de novo and acquired hormonal therapy resistance may provide clues to better treatments.

E2 elicits most of its cellular effects by binding to ERα66 in the cytosol, followed by receptor dimerization and translocation to the nucleus, where it regulates expression of genes that are important for tumor growth and survival by binding to estrogen response elements on target genes (5, 6). These genomic responses are slow and take hours to days to induce effects. However, it has become apparent that E2 also exerts rapid, within minutes, nongenomic effects through membrane-associated receptors (7, 8). Most of the nongenomic responses of E2 have been linked to ERα36, a 36-kDa splice variant of ERα66 (9–15) that is mainly expressed on the plasma membranes of breast cancer cells, particularly in TNBC (15, 16). ERα36 has a novel noncoding exon as its first exon, which is spliced into exons 2–6 of the ERα66 gene, and also has a unique 27 amino acid domain (exon 9) that replaces the last 138 amino acids

*This work was supported by National Institutes of Health Grants F31 CA220798 (M.A.M.) and R01GM043880 (S.S.); and U.S. Department of Defense Breast Cancer Research Program Award W81XWH-14-1-0086 (S.S). The content is solely the responsibility of the authors and does not necessarily represent the official views of the National Institutes of Health. The authors declare no conflicts of interest.*

*Manuscript received 19 March 2018 and in revised form 4 October 2018.*

*Published, JLR Papers in Press, October 12, 2018*
*DOI https://doi.org/10.1194/jlr.M085191*



Abbreviations: E2, 17β-estradiol; E2-BSA, 17β-estradiol conjugated to BSA; EGFR, epidermal growth factor receptor; ERα, estrogen receptor α; PDX, patient-derived xenograft; PR, progesterone receptor; S1P, sphingosine-1-phosphate; S1PR, sphingosine-1-phosphate receptor; SphK, sphingosine kinase; TCGA, The Cancer Genome Atlas; TNBC, triple-negative breast cancer.

[1]To whom correspondence should be addressed.
e-mail: sarah.spiegel@vcuhealth.org

encoded by exons 7 and 8 of the ERα66 gene. Although tamoxifen is an antagonist of ERα66, it activates ERα36, which lacks both transcriptional activation domains of ERα66 (AF-1 and AF-2) and a large portion of the ligand-binding domain (16–18). It has been suggested that tamoxifen resistance is due to upregulation of ERα36 (18, 19). Moreover, recent studies correlated increased expression of ERα36 with advanced severity of breast cancer and endocrine therapy resistance, as well as increased distant metastasis and poor prognosis (17, 19, 20).

Abundant evidence indicates that sphingosine-1-phosphate (S1P), a pleiotropic bioactive sphingolipid metabolite formed by sphingosine kinase 1 (SphK1), is involved in breast cancer growth, progression, transformation, and metastasis (21–23). Overexpression of SphK1 in ERα-positive breast cancer cells promotes tumorigenesis and angiogenesis of xenografts (24). SphK1 is commonly upregulated in breast tumors and has been linked to worse prognosis and progression, possibly leading to resistance to certain anticancer therapies (25–29). There is an emerging idea that S1P may play an important role in the nongenomic responses mediated by E2 (30, 31). Several studies have shown that E2 treatment of MCF-7 breast cancer cells that express all ERα splice variants (ERα66, ERα46, and ERα36) rapidly activates SphK1, leading to formation and secretion of S1P (32–34). S1P in turn binds to S1P receptors (S1PRs) present on breast cancer cells, leading to downstream signaling pathways, including ERK1/2, Akt, protein kinase C, and even transactivation of EGFR, events important for breast cancer progression and metastasis (30, 31, 35–37). Therefore, it has been suggested that some of the nongenomic effects of E2 are mediated via the SphK1/S1P/S1PR axis. However, the E2 receptor responsible for SphK1 activation has not yet been identified. In this work, we have demonstrated that the novel ERα splice variant ERα36 is the major membrane surface receptor for E2 that rapidly activates SphK1 and subsequent S1P signaling and that hormone therapy resistance occurs through upregulation of ERα36 and SphK1.

## MATERIALS AND METHODS

### Materials

E2 (catalog no. 50282), E2-BSA (catalog no. E5630), tamoxifen (catalog no. T5648), and FA-free BSA (catalog no. A8806) were from MilliporeSigma (St. Louis, MO). ERα36-neutralizing Ab was from Alpha Diagnostic (San Diego, CA). HALT protease and phosphatase inhibitor (catalog no. 78440) was from ThermoFisher (Waltham, MA). The SphK1-specific inhibitor SK1-I (catalog no. BML-EI411) was from Enzo Life Sciences (Farmingdale, NY). RPMI 1640 phenol red-free medium and DMEM phenol red-free medium were from Gibco, and FBS (catalog no. ES-009-B) was from MilliporeSigma.

### Cell culture

HCC38 and MDA-MB-231 human breast cancer cells were from American Type Culture Collection (Manassas, VA). HCC38 cells were cultured in phenol red-free RPMI 1640 containing 10% FBS and penicillin/streptomycin. MDA-MB-231 cells were cultured in phenol red-free DMEM supplemented with 10% FBS, 1% L-glutamine, and antibiotics. MCF-7/S0.5 (catalog no. SCC100) and MCF-7/TAMR-7 (catalog no. SCC101) cells were from MilliporeSigma. MCF-7/S0.5 and MCF-7/TAMR were grown in DMEM/F12 medium without phenol red, containing 10% FBS, 2.5 mM L-glutamine, and 6 ng/ml insulin. MCF-7/TAMR cell medium also contained 1 nM tamoxifen.

In some experiments, cells were transfected with ON-TARGET plus siRNAs specific for the unique 27 amino acid sequence at the N terminus of ERα36 (#1 UCUCACAUGUAGAAGCAAAUU; #3 GCAAAGAAGAGAAUCCUGAUU) or control siRNA (Dharmacon, Lafayette, CO), according to the manufacturer's protocol.

### Patient-derived xenografts

Patient-derived xenograft (PDX) lines were obtained from Washington University in St. Louis (WHIM2 and WHIM30) (38), the University of Utah (HCI lines) (39), and the University of Colorado (UCD18 and UCD52) (40). They were implanted in the fourth mammary fat pads of nonobese diabetic severe combined immunodeficient γ (NSG) mice until tumors reached a size of ~10 × 10 mm. Tumor pieces were flash frozen, and protein extracts were prepared in RIPA buffer.

### SphK1 translocation and activity assays

To determine translocation of SphK1 to membranes, cells were lysed, and membrane fractions were prepared by 100,000 *g* centrifugation as described (41). SphK1 activity was determined with sphingosine (50 μM) and ATP (1 mM) containing $MgCl_2$ (10 mM) in the presence of 0.25% Triton X-100, which inhibits SphK2, as described previously (42). SphK2 activity was determined similarly when sphingosine was added as a complex with 4 mg/ml BSA in the presence of 1 M KCl, which inhibits SphK1 activity (42). S1P formation was measured by LC-ESI-MS/MS. Activity is expressed as pmol of S1P formed per min/mg protein.

### Treatment with E2 and measurement of phosphorylated sphingoid bases by LC/ESI/MS/MS

Cells cultured in 6-well tissue culture plates ($10^5$/well) were washed twice with 1 ml of PBS and starved in 0.5 ml of serum-free medium containing 1% FA-free BSA for 2 h. Cells were then treated with vehicle or E2 (100 nM) in 0.5 ml of the same serum-free medium containing 1% FA-free BSA for the indicated times. After treatments, plates were placed on ice, and the medium was removed and added to prechilled 13 × 100 mm borosilicate tubes containing 1 ml of ice-cold LC/MS grade methanol. Cells were washed two times with prechilled PBS and 300 μl of ice cold-PBS containing 1:100 HALT protease, and phosphatase inhibitor was added. Cells were scraped, and suspensions (200 μl) were added to 13 × 100 mm borosilicate tube containing 0.5 ml of ice-cold LC/MS grade methanol. An aliquot of the remaining 100 μl cell suspension was used for protein quantification with the Bio-Rad Protein Assay. Sphingolipids were measured by LC/ESI/MS/MS (Sciex 5500 QTRAP; ABSciex, Farmingham, MA). Cellular sphingolipid levels were expressed as pmol per milligram of protein and secreted as pmol per milliliter of medium.

### Confocal microscopy

Immunofluorescent localization was performed essentially as described previously (43). Briefly, MDA-MB-231 cells were seeded onto glass coverslips in 6-well dishes and transfected with V5-SphK1 using Lipofectamine Plus. After treatment with E2, cells were washed twice with room temperature PBS and then fixed with 3.7% paraformaldehyde with 0.1% Triton X-100 for 10 min.

Fixative was quenched by extensive washing with 10 mM glycine-PBS, and cells permeabilized for 3 min with 0.5% Triton X-100. After washing, coverslips were incubated for 20 min with mouse anti-V5 Ab (1:100; ThermoFisher) in 1% IgG-free BSA in glycine-PBS, washed three times, and then incubated with Alexa 488-labeled anti-mouse Ab (1:400; ThermoFisher). Coverslips were washed and mounted with 10 mM *n*-propylgallate in 100% glycerol and visualized with a Zeiss LSM 700 confocal microscope (Carl Zeiss, Oberkochen, Germany).

### Western blotting

Cells were washed with ice-cold PBS and scraped into lysis buffer containing 20 mM Tris-HCl (pH 7.4), 1 mM EDTA, 150 mM NaCl, 1% Triton X-100, 1 mM β-mercaptoethanol, 1 mM $Na_3VO_4$, and 1:100 HALT protease and phosphatase inhibitor. Lysates were sonicated three times for 10 s each and centrifuged at 10,000 *g* for 10 min. Protein was measured by the Bio-Rad protein assay, and equal amounts were separated by SDS-PAGE and blotted onto nitrocellulose. Membranes were incubated overnight at 4°C with the following specific primary Abs: p-SphK1 (Ser225) (1:1,000; ECM Bioscience, catalog no. SP1641), SphK1 (1:1,000; Sigma, catalog no. HPA0229829), ERα36 (1:1,000; Cell Application, catalog no. CY1109), GAPDH (1:3,000; Cell Signaling, catalog no. 2218L), tubulin (1:3,000, Cell Signaling, catalog no. 2146S), p-Akt (S473) (1:1,000; Cell Signaling, catalog no. 9271S), Akt (1:1,000; Cell Signaling, catalog no. 9272S), ERα (H222) (1:500; Santa Cruz, catalog no. sc-53492), transferrin receptor (1:1,000; Cell Signaling, catalog no. 3113S), ABCC1 (1:2,000; Cell Signaling, catalog no. 72202S), ABCG2 (1:3,000; Cell Signaling, catalog no. 42078), and Spns2 (1:3,000; Sigma-Aldrich, catalog no. SAB2104271). Immunopositive bands were visualized by ECL after 2 h incubations at room temperature with secondary Abs conjugated with HRP (1:10,000) and Super-Signal West Pico chemiluminescent substrate (ThermoFisher). Blots were stripped and reprobed with anti-tubulin or anti-GAPDH as loading controls. Optical densities of bands associated with proteins of interest were quantified with NIH ImageJ and normalized to the optical densities of their respective loading control bands.

### Cell proliferation

Cell proliferation was determined with WST-8 [2-(2-methoxy-4-nitrophenyl)-3-(4-nitrophenyl)-5-(2,4-disulfophenyl)-2H-tetrazolium and monosodium salt] or with Alamar blue as previously described (44).

### Statistical analysis

Statistical analyses were performed using an unpaired two-tailed Student's *t*-test for comparison of two groups or ANOVA with Bonferroni post hoc analyses for multiple groups (GraphPad Prism; GraphPad, San Diego, CA). All experiments were repeated independently at least three times, and representative data are shown. A value of $P < 0.05$ was considered significant.

## RESULTS

### SphK1 is activated by E2 to produce S1P in cells only expressing ERα splice variant ERα36

Previous studies have shown that E2 stimulates formation and secretion of S1P in a SphK1-dependent manner in MCF-7 breast cancer cells (32–34). However, the E2 receptor involved in the activation of SphK1 has not been identified. Because MCF-7 cells express ERα66, ERα46, ERα36, a classical G protein-coupled E2 receptor GPER1, and a low level of ERβ, we sought to examine the effects of E2 on SphK1 activation and formation of S1P in TNBC cells that lack both ERα66 and ERα46 and only express ERα36 and GPER1, such as MDA-MB-231 cells (45). Similar to previous studies with MCF-7 cells (32–34), SphK1 was rapidly activated by E2 in MDA-MB-231 cells, although little to no increased SphK2 activity was detected (**Fig. 1A**). Multiple studies have demonstrated that SphK1 is translocated to the plasma membrane upon its activation (46–48). Consistent with these studies, Western blotting with anti-SphK1 confirmed that SphK1 is translocated to MDA-MB-231 cell membranes within 3 min after E2 treatment (Fig. 1B). Moreover, confocal immunofluorescence microscopy revealed that E2 also induced rapid translocation of epitope-tagged SphK1 from the cytosol to the plasma membrane in MDA-MB-231 cells within 3–5 min (Fig. 1C). There was also a significant increase in cellular and secreted S1P within 3 min that remained elevated for at least 9 min and declined thereafter (Fig. 1D).

Similar results were observed in ERα-negative HCC38 breast cancer cells that express only ERα36 and GPER1 (**Fig. 2**). Moreover, E2 also increased phosphorylation of SphK1 on serine 225 (Fig. 2A), which is known to enhance its enzymatic activity (47). This rapid increase in phosphorylated SphK1 was evident within 1 min and remained elevated for at least 30 min (Fig. 2A). In agreement, E2 induced rapid increases of cellular S1P and secreted S1P, reaching a maximum at 6 min and declining thereafter (Fig. 2B). This decline is partly due to rapid degradation of S1P to sphingosine (Fig. 2C) by lipid phosphate phosphatases known to be present on the outer leaflet of the plasma membrane (49). Moreover, there were no changes in expression of known S1P transporters (31, 50), including ABCC1, ABCG2, and Spns2 (Fig. 2D).

To further substantiate that these effects were mediated through a plasma membrane receptor, cells were treated with E2 conjugated to BSA (E2-BSA) that does not cross the plasma membrane and reach intracellular receptors, yet elicits many of the same effects as E2 (16). E2-BSA not only stimulated nongenomic pathways, such as Akt activation, in agreement with previous reports (13, 16, 51), but it also stimulated SphK1, as shown by immunoblotting with a phospho-specific Ab that recognizes activated SphK1, albeit to a lesser extent than E2 (**Fig. 3A**, B). Moreover, like E2, E2-BSA also induced secretion of S1P (Fig. 3C). Taken together, these results indicate that E2 activates SphK1 by a plasma membrane receptor in TNBC cells.

### Role of ERα36 in E2-mediated formation and secretion of S1P

Because previous studies have implicated ERα36, which is present on the plasma membrane, in nongenomic effects of E2, we focused our attention on its involvement (10–14). As a first approach, cells were treated with a rabbit Ab for human ERα36 raised against the unique peptide

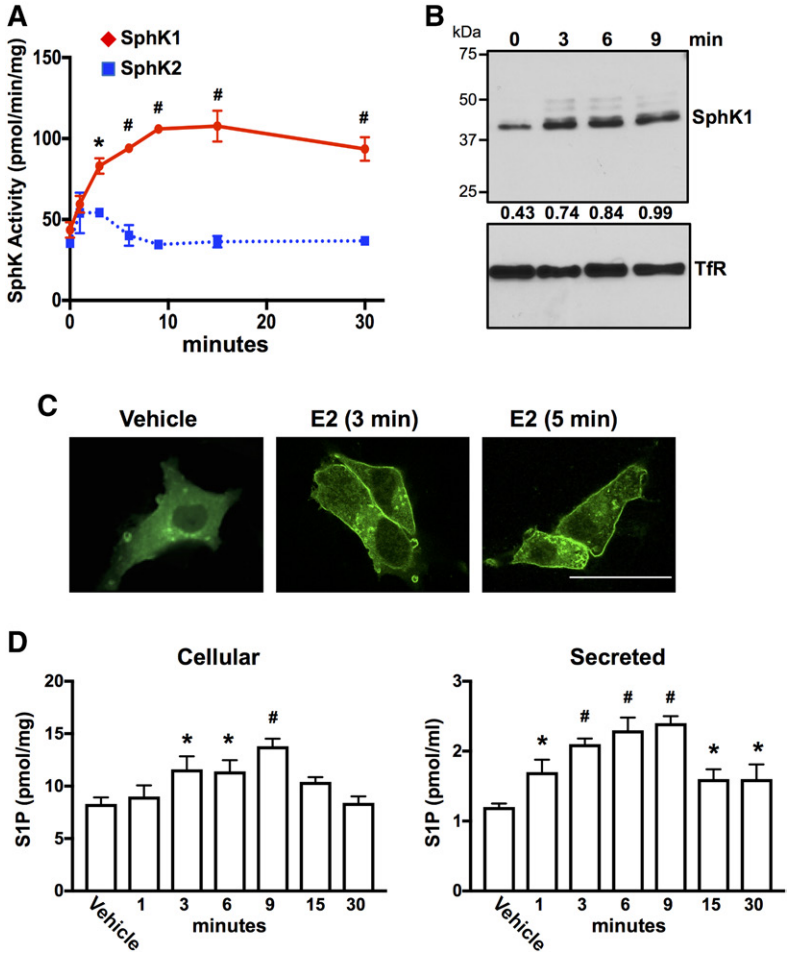


**Fig. 1.** E2 activates SphK1 and increases production and secretion of S1P in triple-negative MDA-MB-231 breast cancer cells. A, B, D: Serum-starved MDA-MB-231 cells were treated without (vehicle) or with E2 (100 nM) for the indicated time. A: SphK1 and SphK2 enzymatic activities in lysates were determined with isoenzyme-specific assays. * $P \leq 0.05$; # $P < 0.001$ (compared with 0 time). B: Equal amounts of membrane proteins were separated by SDS-PAGE and immunoblotted with anti-SphK1 Ab. Blots were stripped and reprobed with antitransferrin receptor (TfR) Ab as loading control. Proteins were quantified by densitometry, and numbers indicate relative optical density of SphK1 normalized to TfR. Similar results were obtained in two additional experiments. C: MDA-MB-231 cells were transfected with V5-SphK1, serum-starved, and stimulated with vehicle or with E2 for 3 or 5 min. Cells were stained with anti-V5 Ab (green) and visualized by confocal microscopy. Scale bar, 25 μm. D: Cellular S1P and S1P released into the medium during 30 min secretion assay were measured by LC/ESI/MS/MS. Data are mean ± SD. * $P \leq 0.05$; # $P < 0.001$ (compared with vehicle).

sequence of ERα36 that blocks ERα36 downstream signaling (16). Neutralizing ERα36 with this Ab that does not cross-react with other ERα family members markedly blocked activation of SphK1 by E2 (**Fig. 4A**). This Ab also greatly reduced activation of Akt induced by E2 (Fig. 4A), consistent with previous reports (13, 16, 51–53). Treatment with anti-ERα36 also almost completely suppressed E2-induced formation and secretion of S1P (Fig. 4B) and dihydro-S1P (Fig. 4C).

To confirm the role of ERα36 in activation of the SphK1 by E2, ERα36 was downregulated with two siRNAs specific for the unique 27 amino acid sequence at the N terminus of ERα36. siERα36 #3 that markedly reduced ERα36 levels in MCF-7 cells without reducing levels of ERα66 and ERα46 present in this breast cancer cell line that expresses all three ERα splice variants was selected for further studies (**Fig. 5A**). This siRNA significantly reduced ERα36 expression in MDA-MB-231 cells detected with either an anti-ERα Ab that recognizes all three splice variants or with anti-ERα36-specific Ab (Fig. 5B). Downregulation of ERα36 in MDA-MB-231 cells abrogated E2-mediated SphK1 activation and stimulation of Akt, a downstream signaling pathway (Fig. 5B). In both MDA-MB-231 and MCF-7 cells, knockdown of ERα36 significantly reduced secretion of S1P and dihydro-S1P (**Fig. 6A**, B). These results suggest that ERα36, a plasma membrane E2 receptor, plays a role in the rapid, nongenomic E2 activation of SphK1 and subsequent S1P signaling.

### Role of ERα36 and SphK1 in acquired tamoxifen resistance

Tamoxifen, an antagonist of ERα66 and one of the first-line endocrine therapies for treatment of ERα-positive breast cancer (1, 2), was shown to be an agonist of ERα36 (9, 17). Therefore, we next examined the ability of tamoxifen to stimulate SphK1 and S1P secretion from ERα-negative MDA-MB-231 cells. Like E2, tamoxifen activated SphK1 and markedly increased secretion of S1P in a dose-dependent manner (**Fig. 7A**). A concentration of tamoxifen as low as 0.1 nM significantly increased secretion of S1P from MCF-7 cells expressing all three splice variants and from MDA-MB-231 cells. Maximum secretion of S1P and dihydro-S1P from both cell lines was observed at tamoxifen concentrations of 10–100 nM (Fig. 7A).

A major problem with tamoxifen therapy in breast cancer is development of acquired resistance. It has been suggested that tamoxifen resistance correlates not only with decreased expression of ERα66 but also with upregulation or activation of ERα36, leading to increased nongenomic signaling induced by tamoxifen (17, 54). To further substantiate that tamoxifen resistance may be due to increased expression of ERα36 and SphK1, we utilized tamoxifen-resistant

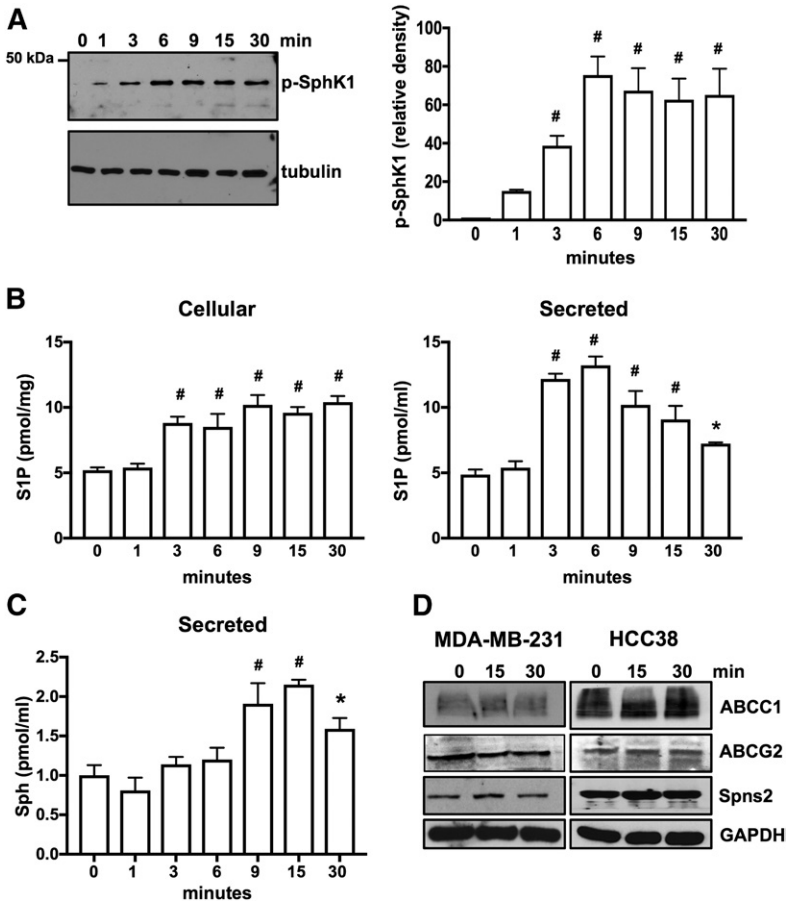


**Fig. 2.** E2 induces phosphorylation of SphK1 for production and secretion of S1P in HCC38 breast cancer cells that express only ERα36. A, B: Serum-starved HCC38 cells were treated with E2 (100 nM) for the indicated time. A: Proteins in cell lysates were separated by SDS-PAGE and immunoblotted with anti-phospho-SphK1 Ab. Blots were stripped and reprobed with antitubulin to show equal transfer and loading. Phospho-SphK1 was quantified by densitometry and data expressed as relative density of p-SphK1 normalized to tubulin. B, C: Cellular S1P and S1P released into the medium during 30 min secretion assays as well as sphingosine (Sph) were measured by LC/ESI/MS/MS. Data are mean ± SD. * $P \leq 0.05$; # $P < 0.001$ (compared with 0 time). D: Serum-starved MDA-MB-231 and HCC38 cells were treated with E2 (100 nM) for the indicated time, and cell lysate proteins were immunoblotted with the indicated Abs. Blots were stripped and reprobed with anti-GAPDH to show equal transfer and loading.

MCF-7 cells (MCF-7/TAMR-1), derived from the parental MCF-7/S0.5 cell line, which acquired resistance after long-term culturing in the presence of 1 μM tamoxifen. In both de novo tamoxifen-resistant MDA-MB-231 TNBC cells and acquired tamoxifen-resistant MCF-7/TAMR-1 cells, ERα36 was significantly upregulated compared with MCF-7 parental cells (Fig. 7B). Levels of SphK1 and particularly activated SphK1, determined with a phospho-specific Ab, were greatly elevated in tamoxifen-resistant cells (Fig. 7B). Growth of MCF-7 cells was significantly reduced by treatment

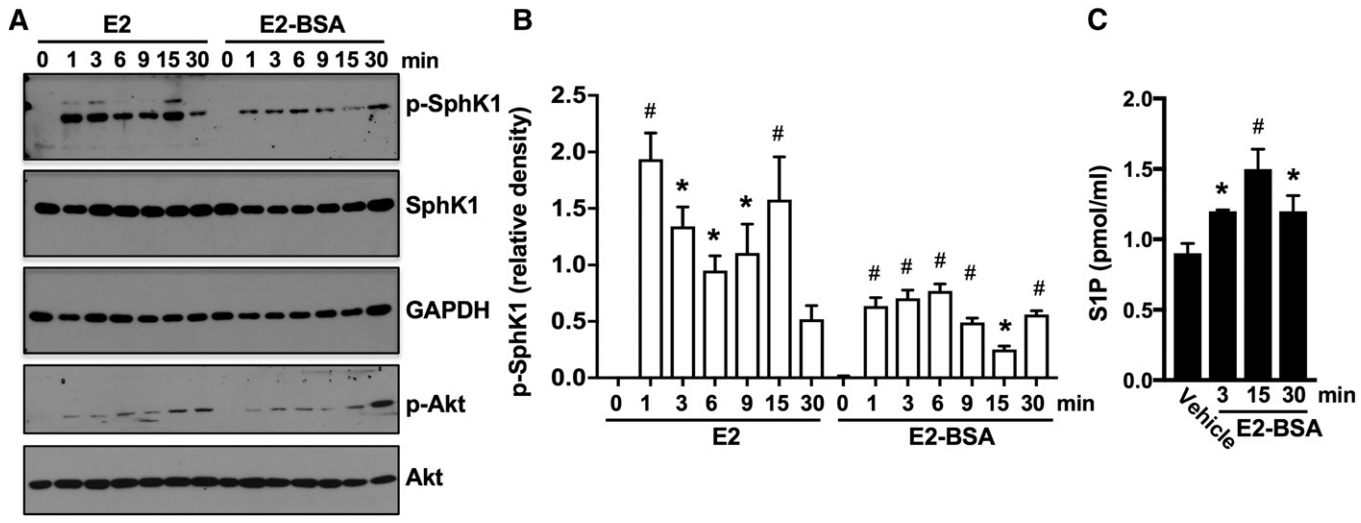


**Fig. 3.** Membrane-impermeable E2-BSA activates SphK1 and enhances secretion of S1P. A, B: MDA-MB-231 cells treated with E2 (100 nM) or with E2-BSA (100 nM) for the indicated times. A: Proteins in cell lysates were separated by SDS-PAGE and immunoblotted with the indicated Abs. B: Phospho-SphK1 was quantified by densitometry, and data are expressed as relative density of p-SphK1 normalized to SphK1. C: Cells from duplicate MDA-MB-231 cultures were treated without or with E2-BSA (100 nM) for the indicated times. S1P released into the medium during 30 min secretion assays was measured by LC/ESI/MS/MS. Data are mean ± SD. * $P \leq 0.05$; # $P < 0.001$ (compared with control).





JOURNAL OF LIPID RESEARCH ASBMB JLR

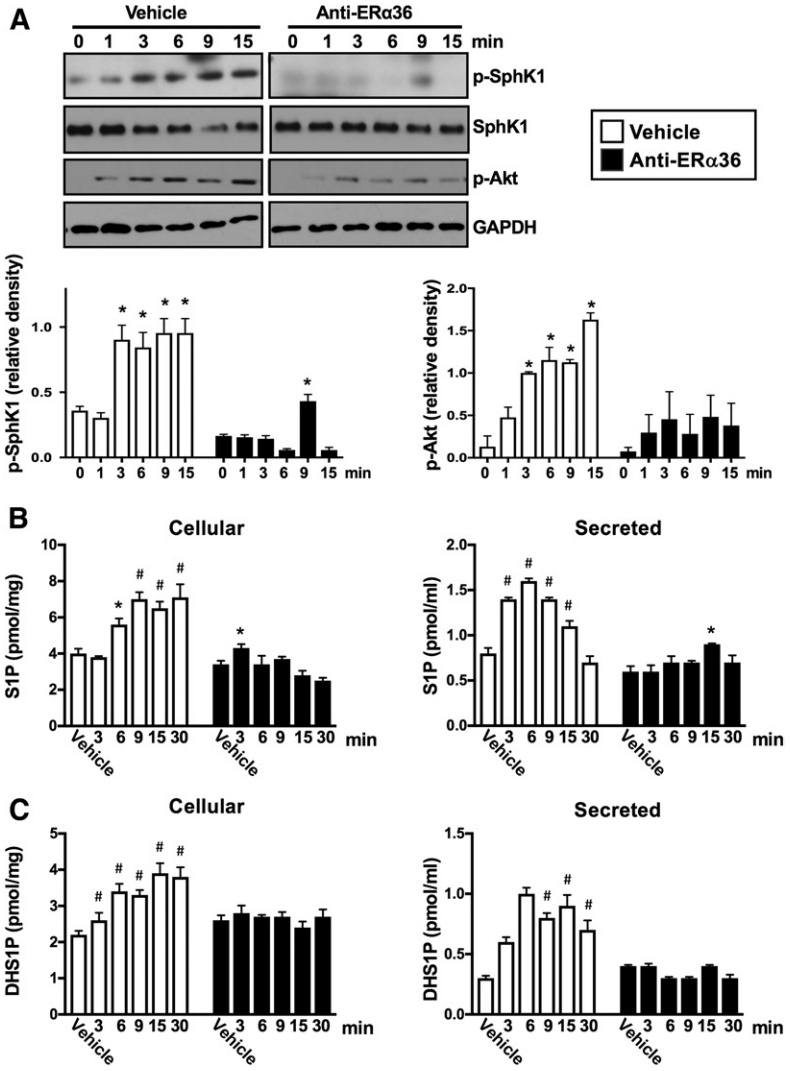


**Fig. 4.** ERα36 neutralizing Ab attenuates E2-induced SphK1 activation and S1P formation and secretion. MDA-MB-231 cells were pretreated without or with anti-ERα36 neutralizing Ab and then stimulated with vehicle or with E2 (100 nM) for the indicated times. A: Proteins in cell lysates were separated by SDS-PAGE and immunoblotted with the indicated Abs. p-SphK1 and p-Akt were quantified by densitometry, and data are expressed as relative densities normalized to GAPDH. Cellular S1P and S1P released into the medium (B) and cellular S1P and dihydro-S1P (DHS1P) (C) released into the medium during 30 min secretion assays were measured by LC/ESI/MS/MS. Data are mean ± SD. * $P \leq 0.05$; # $P < 0.001$ (compared with vehicle).

with tamoxifen or SK1-I, a specific SphK1 inhibitor that does not inhibit SphK2 (55), and was further decreased by their combination (Fig. 7C). As expected, tamoxifen was not toxic to MCF-7/TAMR-1 cells. Although treatment with SK1-I had a marginal effect on MCF-7/TAMR-1 cells, it markedly sensitized them to tamoxifen, and combination treatment significantly decreased viability by almost 80% (Fig. 7C). Similar to previous reports (19, 56), knockdown of ERα36 restored the sensitivity of MCF-7/TAMR-1 cells to the growth-inhibitory effects of tamoxifen (Fig. 7D). However, addition of exogenous S1P (100 nM) did not reverse it (Fig. 7D).

### Expression of SphK1 and ERα36 is increased in endocrine-resistant breast cancer patients

It has recently been noted that increased expression of ERα36 correlates with severity of breast cancer, metastasis and recurrence, and tamoxifen therapy resistance (17, 20). In addition, SphK1 is upregulated in drug- and endocrine-therapy-resistant breast cancers and correlates with poor prognosis (25, 26, 37). Consistent with these reports, immunoblotting of PDXs showed that ERα-positive tumors have low expression of ERα36 compared with ERα-negative tumors that have significantly higher ERα36 expression (**Fig. 8A**). Similarly, ERα-negative xenografts have significantly higher levels of SphK1 (Fig. 8A). Moreover, mining of The Cancer Genome Atlas (TCGA) breast tumor expression database indicated that TNBC patients have greater SphK1 expression compared with all other breast cancer patients (Fig. 8B). Furthermore, tumors from hormone therapy-resistant patients also have significantly higher SphK1 levels than patients that respond to hormone therapies, such as tamoxifen (Fig. 8C).

## DISCUSSION

E2 is traditionally considered to regulate complex functions by binding to its canonical receptor ERα66 and directing it to the nucleus, where it modulates gene expression (57). Although it has long been known that E2 also can elicit rapid, nongenomic signaling (58, 59), the identity of the receptor and the mechanisms involved has been a

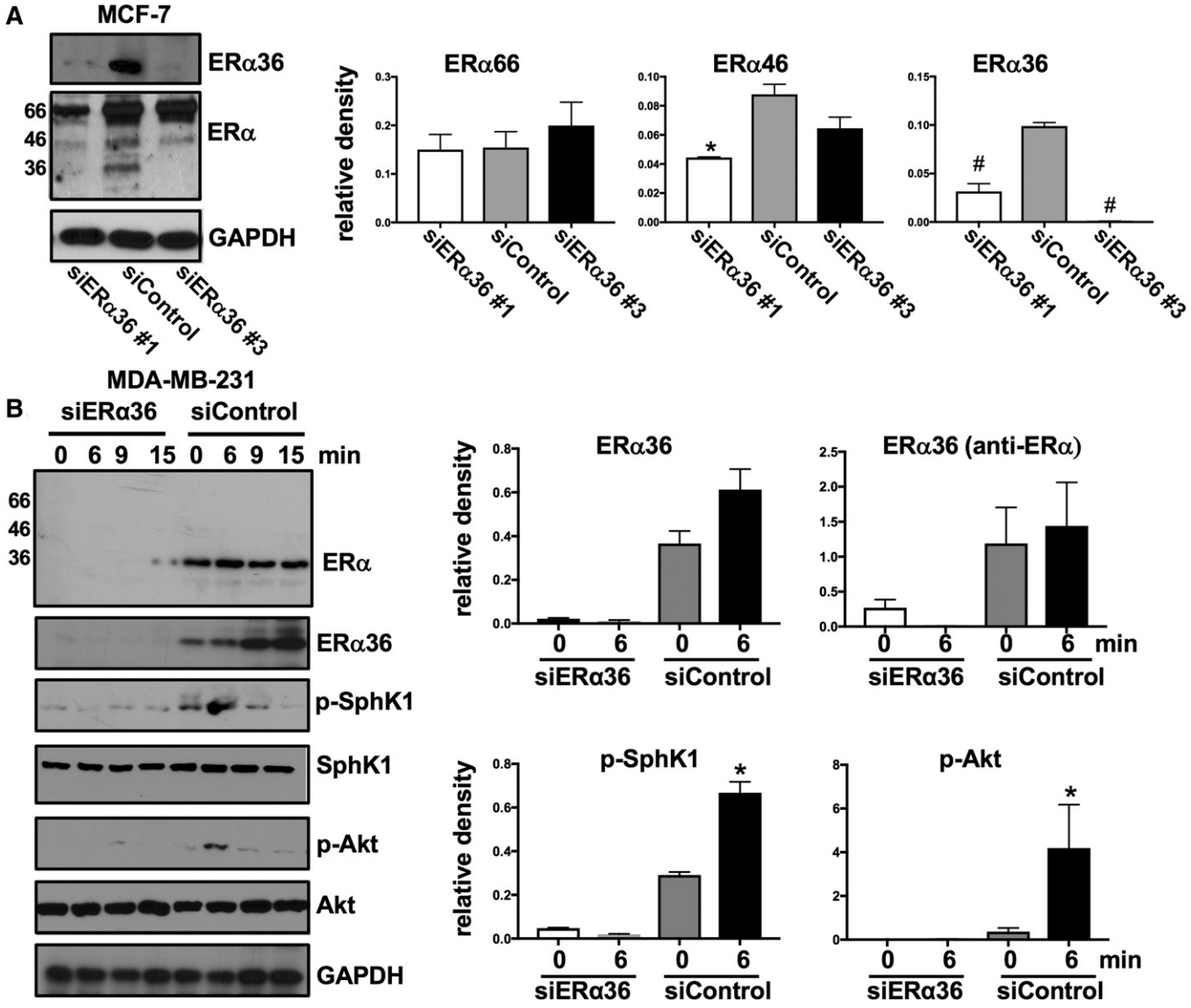


**Fig. 5.** Downregulation of ERα36 decreases E2-mediated SphK1 activation. A: MCF-7 cells were transfected with control siRNA or with the indicated siRNA targeted to ERα36. Proteins in cell lysates were separated by SDS-PAGE and immunoblotted with the indicated Abs. Protein bands of ERα66, ERα46, and ERα36 were quantified by densitometry and data are expressed as relative densities normalized to GAPDH. * $P \leq 0.05$; # $P < 0.001$ (compared with siControl). B: MDA-MB-231 cells transfected with control siRNA or with siRNA targeted to ERα36 (#3) were stimulated with vehicle or with E2 (100 nM) for the indicated times. Proteins in cell lysates were separated by SDS-PAGE and immunoblotted with the indicated Abs. ERα36, p-SphK1, and p-Akt were quantified by densitometry, and data are expressed as relative densities normalized to GAPDH, SphK1, and Akt, respectively. * $P \leq 0.05$; # $P < 0.001$ (compared with time 0).

matter of great debate. Several receptor candidates have been proposed to mediate these rapid effects of E2, including the canonical ERα receptors, ERα66 and ERα46, and the noncanonical ERα36, as well as GPER1 (7, 8). However, it is still controversial whether E2 is a physiological agonist of GPER1 and whether this receptor is even plasma membrane-associated, as some groups have shown that it is endoplasmic reticulum-associated (60, 61). Moreover, several studies have implicated the involvement of ERα36, but not GPER1, in nongenomic signaling of E2 (10–14, 16, 62).

Ample studies in TNBC cells have shown that this novel splice variant ERα36 enhances cell growth and survival in response to E2 (9, 11–15). Binding of E2 to ERα36 initiates diverse downstream signaling, including activation of phospholipase C, leading to production of diacylglycerol and inositol trisphosphate, calcium signaling, and protein kinase C activation, as well as activation of ERK1/2 and PI3K/Akt, all important survival pathways for breast cancer cells (10–15). However, the mechanism by which activation of ERα36 by E2 leads to these downstream signaling pathways is still unclear. In this work, we have uncovered this missing link. We have shown that nongenomic effects of E2 occur through binding of E2 to ERα36 and subsequent stimulation of SphK1, resulting in the formation and secretion of S1P and dihydro-S1P. Binding of these ligands to S1PRs leads to activation of downstream signaling pathways important for breast cancer progression,





JOURNAL OF LIPID RESEARCH ASBMB

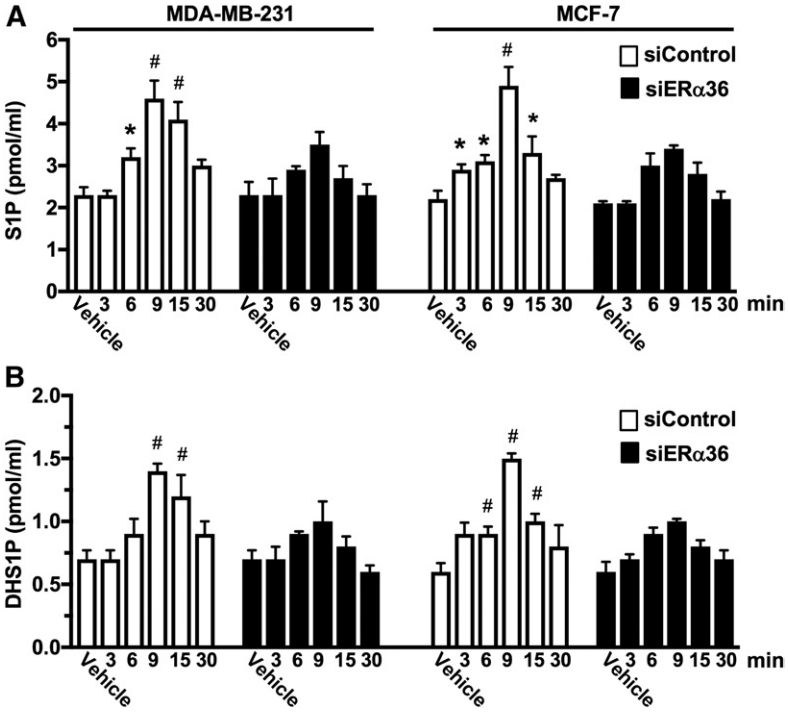


**Fig. 6.** Downregulation of ERα36 reduces S1P and dihydro-S1P secretion stimulated by E2. MDA-MB-231 cells and MCF-7 cells transfected with control siRNA or with siRNA targeted to ERα36 (#3) were stimulated with vehicle or with E2 (100 nM) for the indicated times. S1P (A) and dihydro-S1P (DHS1P) (B) released into the medium during 30 min secretion assays were measured by LC/ESI/MS/MS. Data are mean ± SD. * $P \leq 0.05$; # $P < 0.001$ (compared with vehicle).

metastasis, and hormone therapy resistance. In this regard, ligation of S1PR3 by S1P has been shown to lead to activation of Src and matrix metalloproteases, resulting in heparin-binding-EGF shedding and release that is necessary for transactivation of EGFR (22, 33, 35, 63). These signaling events explain how rapid increases in extracellular S1P and binding to S1PR3 after treatment with E2 can lead to long-lasting effects in cancer resistance to tamoxifen treatment.

We have now provided several lines of evidence that ERα36 is the E2 receptor responsible for activation of SphK1 by E2. First, in triple-negative MDA-MB-231 and ERα-negative HCC38 breast cancer cells that express only ERα36 and lack expression of ERα66 and ERα46, E2 activates SphK1, enhances its phosphorylation and translocation to the plasma membrane, and increases production and secretion of S1P. Second, in these cells, membrane-impermeable E2-BSA also activates SphK1 and enhances secretion of S1P. Third, ERα36-neutralizing Ab attenuates SphK1 activation and S1P formation and secretion following E2 stimulation. Finally, downregulation of ERα36 suppresses E2-mediated SphK1 activation and S1P and dihydro-S1P secretion. Interestingly, in MCF-7 breast cancer cells that are ERα-positive and express all three ERα splice variants, specific downregulation of ERα36 also significantly reduced the rapid secretion of S1P and dihydro-S1P induced by E2. This result suggests that, even in these cells, which have high expression levels of ERα66 and ERα46, low expression of ERα36 mediates the rapid, nongenomic activation of SphK1 and production of S1P and dihydro-S1P.

Despite extensive studies, endocrine resistance is still a major problem for adequate treatment of breast cancer, and 50% of patients that initially respond to tamoxifen treatment eventually acquire hormone-therapy resistance. Activation of ERα36 has also been associated with EGFR activation, and downregulation of ERα66 switches growth from E2-dependent to growth factor-dependent, suggesting that ERα36 is involved in hormone-therapy resistance (17, 54). Consistent with previous studies, we have shown that hormone-therapy resistance correlates with increased expression of ERα36 and SphK1 in tamoxifen-resistant breast cancer cell lines, as well as in PDXs from ERα-negative breast cancer patients. Similarly, data from TCGA show that tumors from ERα-negative as well as those from hormonal-resistant breast cancer patients have significantly higher expression of SphK1 compared with all other breast cancer patients. Our results support the notion that hormone-therapy resistance occurs through activation of ERα36, which in turn activates the SphK1/S1P axis important for growth, survival, switching breast cancer from E2-dependent to E2-independent progression, and resistance to hormonal therapies, such as tamoxifen. It should be noted that, although as was reported previously (19, 56), knockdown of ERα36 restored the sensitivity of tamoxifen-resistant cells to tamoxifen, addition of exogenous S1P did not rescue them. This could be due to degradation of exogenous S1P. Alternatively, intracellularly generated S1P rather than inside-out signaling via S1PR3 could contribute to cell growth and tamoxifen resistance, as both intracellular and secreted S1P are increased in response to activation of ERα36 by E2. These results are consistent with a previous study (64) and the notion that intracellular S1P might also contribute to cell growth and drug resistance (65–68). Moreover, in agreement with previous studies demonstrating that downregulation

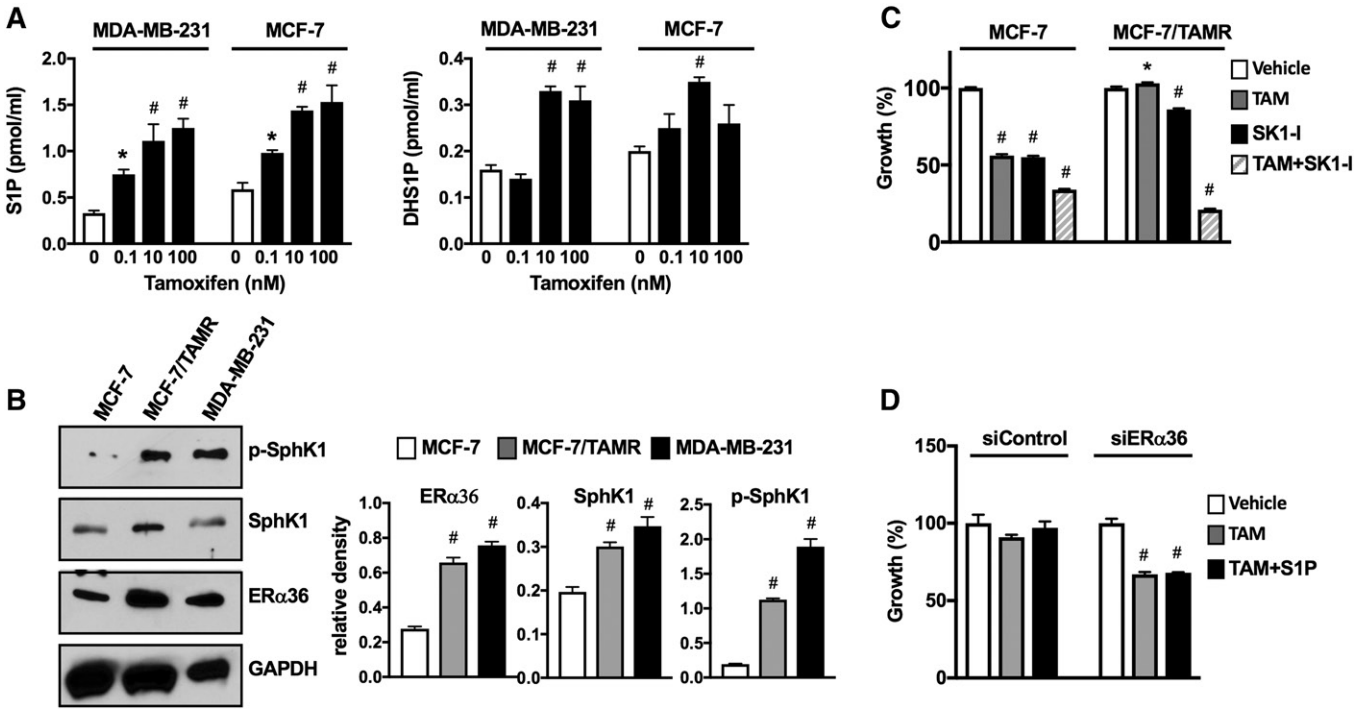


**Fig. 7.** Tamoxifen stimulates S1P production, and tamoxifen resistance is associated with increased ERα36 and SphK1 activation. A: MDA-MB-231 and MCF-7 cells were treated without or with the indicated concentrations of tamoxifen for 30 min. S1P and DHS1P released into the medium were measured by LC/ESI/MS/MS. Data are mean ± SD. * $P \leq 0.05$. B: Expression levels of SphK1, p-SphK1, and ERα36 were determined by immunoblot analysis in MDA-MB-231, MCF-7/TAMR-1, and parental MCF-7/S0.5 cells. Blots were stripped and reprobed with anti-GAPDH Ab to show equal loading and transfer. Indicated proteins were quantified by densitometry, and data are expressed as relative densities normalized to GAPDH. A, B: * $P \leq 0.05$, #$P < 0.001$ (compared to vehicle). C: MCF-7/TAMR-1 and MCF-7/S0.5 cells were treated with vehicle, tamoxifen (10 μM), SK1-I (15 μM), or both for 2 days, and cell growth was determined. D: MCF-7/TAMR-1 cells transfected with control siRNA or with siRNA targeted to ERα36 (#3) were treated with vehicle or tamoxifen (1 μM) in the absence or presence of S1P (100 nM) for 2 days, and cell growth was determined. C, D: Data are expressed as percent of vehicle-treated control and are mean ± SEM. * $P \leq 0.05$; # $P < 0.001$ (compared with vehicle).

of SphK1 sensitized tamoxifen-resistant breast cancer cell lines to tamoxifen (64), we demonstrated that a specific SphK1 inhibitor also greatly restored sensitivity to tamoxifen in resistant cells. Taken together, our findings indicate that ERα36 and the SphK1 axis may play an important role in nongenomic effects of E2 and development of de novo and acquired resistance to hormone therapy of breast cancer. Therefore, targeting this axis should be explored as a therapeutic option to circumvent endocrine resistance with potential improvement of clinical outcome.

The authors thank Dr. Jeremy Allegood for skillful sphingolipid analyses. The authors acknowledge the Virginia Commonwealth University Lipidomics and Microscopy Cores, which are supported in part by funding from the National Institutes of Health-National Cancer Institute Cancer Center Support Grant P30 CA016059.

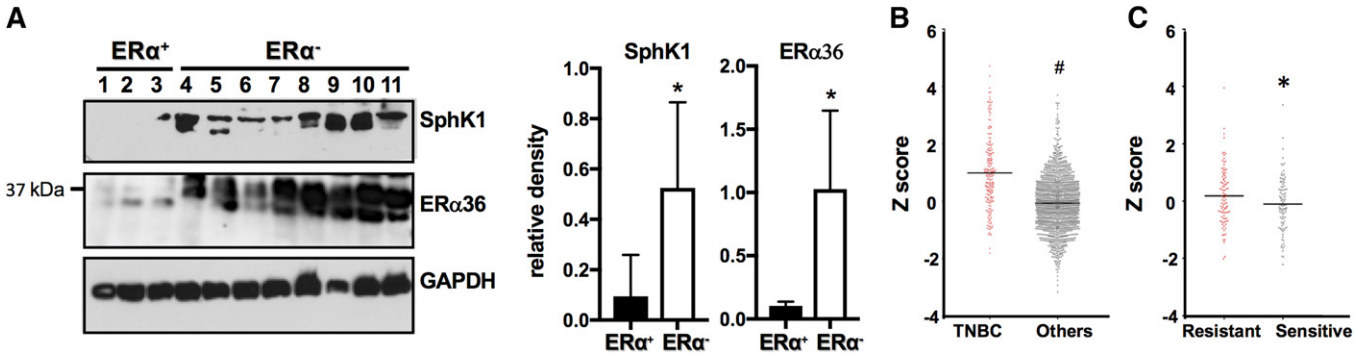


**Fig. 8.** Tamoxifen resistance correlates with increased SphK1 and ERα36 expression in breast cancer patients. A: Expression levels of SphK1 and ERα36 in the indicated PDXs derived from ERα-positive (1–3) and -negative (4–11) breast cancer patients were determined by immunoblot analysis and quantified by densitometry. Data are expressed as relative densities normalized to GAPDH. * $P \leq 0.05$. 1, HCI-03; 2, HCI-13; 3, HCI-11; 4, W2; 5, W30; 6, HCI-16; 7, HCI-10; 8, HCI-9; 9, HCI-1; 10, HCI-2; 11, UCD18. B, C: Breast cancer patient subtypes were from clinical expression information contained within TCGA datasets. B: SphK1 expression in TNBC versus other ERα-positive breast tumors. # $P = 0.0001$. C: Comparison of SphK1 expression in hormone therapy-sensitive and hormone therapy-resistant tumors. * $P = 0.04$.





JOURNAL OF LIPID RESEARCH ASBMB

## REFERENCES


1. Clarke, R., F. Leonessa, J. N. Welch, and T. C. Skaar. 2001. Cellular and molecular pharmacology of antiestrogen action and resistance. *Pharmacol. Rev.* **53:** 25–71.
2. McDonnell, D. P., and J. D. Norris. 2002. Connections and regulation of the human estrogen receptor. *Science.* **296:** 1642–1644.
3. Madaio, R. A., G. Spalletta, L. Cravello, M. Ceci, L. Repetto, and G. Naso. 2010. Overcoming endocrine resistance in breast cancer. *Curr. Cancer Drug Targets.* **10:** 519–528.
4. Bayraktar, S., and S. Gluck. 2013. Molecularly targeted therapies for metastatic triple-negative breast cancer. *Breast Cancer Res. Treat.* **138:** 21–35.
5. Klinge, C. M. 2001. Estrogen receptor interaction with estrogen response elements. *Nucleic Acids Res.* **29:** 2905–2919.
6. Mangelsdorf, D. J., C. Thummel, M. Beato, P. Herrlich, G. Schutz, K. Umesono, B. Blumberg, P. Kastner, M. Mark, P. Chambon, et al. 1995. The nuclear receptor superfamily: the second decade. *Cell.* **83:** 835–839.
7. Poulard, C., I. Treilleux, E. Lavergne, K. Bouchekioua-Bouzaghou, S. Goddard-Leon, S. Chabaud, O. Tredan, L. Corbo, and M. Le Romancer. 2012. Activation of rapid oestrogen signalling in aggressive human breast cancers. *EMBO Mol. Med.* **4:** 1200–1213.
8. Levin, E. R., and S. R. Hammes. 2016. Nuclear receptors outside the nucleus: extranuclear signalling by steroid receptors. *Nat. Rev. Mol. Cell Biol.* **17:** 783–797.
9. Wang, Z., X. Zhang, P. Shen, B. W. Loggie, Y. Chang, and T. F. Deuel. 2006. A variant of estrogen receptor-{alpha}, hER-{alpha}36: transduction of estrogen- and antiestrogen-dependent membrane-initiated mitogenic signaling. *Proc. Natl. Acad. Sci. USA.* **103:** 9063–9068.
10. Li, L., Q. Wang, X. Lv, L. Sha, H. Qin, L. Wang, and L. Li. 2015. Expression and localization of estrogen receptor in human breast cancer and its clinical significance. *Cell Biochem. Biophys.* **71:** 63–68.
11. Chamard-Jovenin, C., A. C. Jung, A. Chesnel, J. Abecassis, S. Flament, S. Ledrappier, C. Macabre, T. Boukhobza, and H. Dumond. 2015. From ERalpha66 to ERalpha36: a generic method for validating a prognosis marker of breast tumor progression. *BMC Syst. Biol.* **9:** 28.
12. Pelekanou, V., G. Notas, M. Kampa, E. Tsentelierou, J. Radojicic, G. Leclercq, E. Castanas, and E. N. Stathopoulos. 2012. ERalpha36, a new variant of the ERalpha is expressed in triple negative breast carcinomas and has a specific transcriptomic signature in breast cancer cell lines. *Steroids.* **77:** 928–934.
13. Chaudhri, R. A., R. Olivares-Navarrete, N. Cuenca, A. Hadadi, B. D. Boyan, and Z. Schwartz. 2012. Membrane estrogen signaling enhances tumorigenesis and metastatic potential of breast cancer cells via estrogen receptor-alpha36 (ERalpha36). *J. Biol. Chem.* **287:** 7169–7181.
14. Gu, Y., T. Chen, E. Lopez, W. Wu, X. Wang, J. Cao, and L. Teng. 2014. The therapeutic target of estrogen receptor-alpha36 in estrogen-dependent tumors. *J. Transl. Med.* **12:** 16.
15. Omarjee, S., J. Jacquemetton, C. Poulard, N. Rochel, A. Dejaegere, Y. Chebaro, I. Treilleux, E. Marangoni, L. Corbo, and M. L. Romancer. 2017. The molecular mechanisms underlying the ERalpha-36-mediated signaling in breast cancer. *Oncogene.* **36:** 2503–2514.
16. Chaudhri, R. A., A. Hadadi, K. S. Lobachev, Z. Schwartz, and B. D. Boyan. 2014. Estrogen receptor-alpha 36 mediates the anti-apoptotic effect of estradiol in triple negative breast cancer cells via a membrane-associated mechanism. *Biochim. Biophys. Acta.* **1843:** 2796–2806.
17. Su, X., X. Xu, G. Li, B. Lin, J. Cao, and L. Teng. 2014. ER-alpha36: a novel biomarker and potential therapeutic target in breast cancer. *Onco Targets Ther.* **7:** 1525–1533.
18. Wang, Z. Y., and L. Yin. 2015. Estrogen receptor alpha-36 (ER-alpha36): a new player in human breast cancer. *Mol. Cell. Endocrinol.* **418:** 193–206.
19. Gu, W., N. Dong, P. Wang, C. Shi, J. Yang, and J. Wang. 2017. Tamoxifen resistance and metastasis of human breast cancer cells were mediated by the membrane-associated estrogen receptor ER-alpha36 signaling in vitro. *Cell Biol. Toxicol.* **33:** 183–195.
20. Fahlén, M., H. Zhang, L. Löfgren, B. Masironi, E. Von Schoultz, B. O. Von Schoultz, and L. Sahlin. 2016. Expression of estrogen receptors in relation to hormone levels and the Nottingham prognostic index. *Anticancer Res.* **36:** 2839–2847.
21. Pyne, N. J., and S. Pyne. 2010. Sphingosine 1-phosphate and cancer. *Nat. Rev. Cancer.* **10:** 489–503.
22. Maczis, M., S. Milstien, and S. Spiegel. 2016. Sphingosine-1-phosphate and estrogen signaling in breast cancer. *Adv. Biol. Regul.* **60:** 160–165.
23. Geffken, K., and S. Spiegel. 2018. Sphingosine kinase 1 in breast cancer. *Adv. Biol. Regul.* **67:** 59–65.
24. Nava, V. E., J. P. Hobson, S. Murthy, S. Milstien, and S. Spiegel. 2002. Sphingosine kinase type 1 promotes estrogen-dependent tumorigenesis of breast cancer MCF-7 cells. *Exp. Cell Res.* **281:** 115–127.
25. Ruckhäberle, E., A. Rody, K. Engels, R. Gaetje, G. von Minckwitz, S. Schiffmann, S. Grösch, G. Geisslinger, U. Holtrich, T. Karn, et al. 2008. Microarray analysis of altered sphingolipid metabolism reveals prognostic significance of sphingosine kinase 1 in breast cancer. *Breast Cancer Res. Treat.* **112:** 41–52.
26. Watson, C., J. S. Long, C. Orange, C. L. Tannahill, E. Mallon, L. M. McGlynn, S. Pyne, N. J. Pyne, and J. Edwards. 2010. High expression of sphingosine 1-phosphate receptors, S1P1 and S1P3, sphingosine kinase 1, and extracellular signal-regulated kinase-1/2 is associated with development of tamoxifen resistance in estrogen receptor-positive breast cancer patients. *Am. J. Pathol.* **177:** 2205–2215.
27. Ohotski, J., J. Edwards, B. Elsberger, C. Watson, C. Orange, E. Mallon, S. Pyne, and N. J. Pyne. 2013. Identification of novel functional and spatial associations between sphingosine kinase 1, sphingosine 1-phosphate receptors and other signaling proteins that affect prognostic outcome in estrogen receptor-positive breast cancer. *Int. J. Cancer.* **132:** 605–616.
28. Gao, Y., F. Gao, K. Chen, M. L. Tian, and D. L. Zhao. 2015. Sphingosine kinase 1 as an anticancer therapeutic target. *Drug Des. Devel. Ther.* **9:** 3239–3245.
29. Datta, A., S. Y. Loo, B. Huang, L. Wong, S. S. Tan, T. Z. Tan, S. C. Lee, J. P. Thiery, Y. C. Lim, W. P. Yong, et al. 2014. SPHK1 regulates proliferation and survival responses in triple-negative breast cancer. *Oncotarget.* **5:** 5920–5933.
30. Sukocheva, O., and C. Wadham. 2014. Role of sphingolipids in oestrogen signalling in breast cancer cells: an update. *J. Endocrinol.* **220:** R25–R35.
31. Takabe, K., and S. Spiegel. 2014. Export of sphingosine-1-phosphate and cancer progression. *J. Lipid Res.* **55:** 1839–1846.
32. Sukocheva, O. A., L. Wang, N. Albanese, S. M. Pitson, M. A. Vadas, and P. Xia. 2003. Sphingosine kinase transmits estrogen signaling in human breast cancer cells. *Mol. Endocrinol.* **17:** 2002–2012.
33. Sukocheva, O., C. Wadham, A. Holmes, N. Albanese, E. Verrier, F. Feng, A. Bernal, C. K. Derian, A. Ullrich, M. A. Vadas, et al. 2006. Estrogen transactivates EGFR via the sphingosine 1-phosphate receptor Edg-3: the role of sphingosine kinase-1. *J. Cell Biol.* **173:** 301–310.
34. Takabe, K., R. H. Kim, J. C. Allegood, P. Mitra, S. Ramachandran, M. Nagahashi, K. B. Harikumar, N. C. Hait, S. Milstien, and S. Spiegel. 2010. Estradiol induces export of sphingosine 1-phosphate from breast cancer cells via ABCC1 and ABCG2. *J. Biol. Chem.* **285:** 10477–10486.
35. Sukocheva, O., C. Wadham, and P. Xia. 2013. Estrogen defines the dynamics and destination of transactivated EGF receptor in breast cancer cells: role of S1P(3) receptor and Cdc42. *Exp. Cell Res.* **319:** 455–465.
36. Truman, J. P., M. Garcia-Barros, L. M. Obeid, and Y. A. Hannun. 2014. Evolving concepts in cancer therapy through targeting sphingolipid metabolism. *Biochim. Biophys. Acta.* **1841:** 1174–1188.
37. Pyne, N. J., J. Ohotski, R. Bittman, and S. Pyne. 2014. The role of sphingosine 1-phosphate in inflammation and cancer. *Adv. Biol. Regul.* **54:** 121–129.
38. Huang, K. L., S. Li, P. Mertins, S. Cao, H. P. Gunawardena, K. V. Ruggles, D. R. Mani, K. R. Clauser, M. Tanioka, J. Usary, et al. 2017. Proteogenomic integration reveals therapeutic targets in breast cancer xenografts. *Nat. Commun.* **8:** 14864.
39. DeRose, Y. S., G. Wang, Y. C. Lin, P. S. Bernard, S. S. Buys, M. T. Ebbert, R. Factor, C. Matsen, B. A. Milash, E. Nelson, et al. 2011. Tumor grafts derived from women with breast cancer authentically reflect tumor pathology, growth, metastasis and disease outcomes. *Nat. Med.* **17:** 1514–1520.
40. Kabos, P., J. Finlay-Schultz, C. Li, E. Kline, C. Finlayson, J. Wisell, C. A. Manuel, S. M. Edgerton, J. C. Harrell, A. Elias, et al. 2012. Patient-derived luminal breast cancer xenografts retain hormone receptor heterogeneity and help define unique estrogen-dependent gene signatures. *Breast Cancer Res. Treat.* **135:** 415–432.
41. Sarkar, S., M. Maceyka, N. C. Hait, S. W. Paugh, H. Sankala, S. Milstien, and S. Spiegel. 2005. Sphingosine kinase 1 is required for

migration, proliferation and survival of MCF-7 human breast cancer cells. *FEBS Lett.* **579:** 5313–5317.
42. Liu, H., M. Sugiura, V. E. Nava, L. C. Edsall, K. Kono, S. Poulton, S. Milstien, T. Kohama, and S. Spiegel. 2000. Molecular cloning and functional characterization of a novel mammalian sphingosine kinase type 2 isoform. *J. Biol. Chem.* **275:** 19513–19520.
43. Kim, E. Y., J. L. Sturgill, N. C. Hait, D. Avni, E. C. Valencia, M. Maceyka, S. Lima, J. Allegood, W. C. Huang, S. Zhang, et al. 2014. Role of sphingosine kinase 1 and sphingosine-1-phosphate in CD40 signaling and IgE class switching. *FASEB J.* **28:** 4347–4358.
44. Hait, N. C., D. Avni, A. Yamada, M. Nagahashi, T. Aoyagi, H. Aoki, C. I. Dumur, Z. Zelenko, E. J. Gallagher, D. Leroith, et al. 2015. The phosphorylated prodrug FTY720 is a histone deacetylase inhibitor that reactivates ERalpha expression and enhances hormonal therapy for breast cancer. *Oncogenesis.* **4:** e156.
45. Chaudhri, R. A., N. Schwartz, K. Elbaradie, Z. Schwartz, and B. D. Boyan. 2014. Role of ERalpha36 in membrane-associated signaling by estrogen. *Steroids.* **81:** 74–80.
46. Johnson, K. R., K. P. Becker, M. M. Facchinetti, Y. A. Hannun, and L. M. Obeid. 2002. PKC-dependent activation of sphingosine kinase 1 and translocation to the plasma membrane. Extracellular release of sphingosine-1-phosphate induced by phorbol 12-myristate 13-acetate. *J. Biol. Chem.* **277:** 35257–35262.
47. Pitson, S. M., P. A. Moretti, J. R. Zebol, H. E. Lynn, P. Xia, M. A. Vadas, and B. W. Wattenberg. 2003. Activation of sphingosine kinase 1 by ERK1/2-mediated phosphorylation. *EMBO J.* **22:** 5491–5500.
48. Jarman, K. E., P. A. Moretti, J. R. Zebol, and S. M. Pitson. 2010. Translocation of sphingosine kinase 1 to the plasma membrane is mediated by calcium- and integrin-binding protein 1. *J. Biol. Chem.* **285:** 483–492.
49. Brindley, D. N., and C. Pilquil. 2009. Lipid phosphate phosphatases and signaling. *J. Lipid Res.* **50(Suppl):** S225–S230.
50. Nishi, T., N. Kobayashi, Y. Hisano, A. Kawahara, and A. Yamaguchi. 2014. Molecular and physiological functions of sphingosine 1-phosphate transporters. *Biochim. Biophys. Acta.* **1841:** 759–765.
51. Tong, J. S., Q. H. Zhang, Z. B. Wang, S. Li, C. R. Yang, X. Q. Fu, Y. Hou, Z. Y. Wang, J. Sheng, and Q. Y. Sun. 2010. ER-alpha36, a novel variant of ER-alpha, mediates estrogen-stimulated proliferation of endometrial carcinoma cells via the PKCdelta/ERK pathway. *PLoS One.* **5:** e15408.
52. Lin, S. L., L. Y. Yan, X. T. Zhang, J. Yuan, M. Li, J. Qiao, Z. Y. Wang, and Q. Y. Sun. 2010. ER-alpha36, a variant of ER-alpha, promotes tamoxifen agonist action in endometrial cancer cells via the MAPK/ERK and PI3K/Akt pathways. *PLoS One.* **5:** e9013.
53. Wang, H. B., T. Li, D. Z. Ma, and H. Zhi. 2018. ERalpha36 gene silencing promotes tau protein phosphorylation, inhibits cell proliferation, and induces apoptosis in human neuroblastoma SH-SY5Y cells. *FASEB J.* **22:** fj201701386.
54. Zhang, X. T., L. G. Kang, L. Ding, S. Vranic, Z. Gatalica, and Z. Y. Wang. 2011. A positive feedback loop of ER-alpha36/EGFR promotes malignant growth of ER-negative breast cancer cells. *Oncogene.* **30:** 770–780.
55. Paugh, S. W., B. S. Paugh, M. Rahmani, D. Kapitonov, J. A. Almenara, T. Kordula, S. Milstien, J. K. Adams, R. E. Zipkin, S. Grant, et al. 2008. A selective sphingosine kinase 1 inhibitor integrates multiple molecular therapeutic targets in human leukemia. *Blood.* **112:** 1382–1391.
56. Zhang, X., and Z. Y. Wang. 2013. Estrogen receptor-alpha variant, ER-alpha36, is involved in tamoxifen resistance and estrogen hypersensitivity. *Endocrinology.* **154:** 1990–1998.
57. Jensen, E. V., E. R. Desombre, T. Kawashima, T. Suzuki, K. Kyser, and P. W. Jungblut. 1967. Estrogen-binding substances of target tissues. *Science.* **158:** 529–530.
58. Szego, C. M., and J. S. Davis. 1967. Adenosine 3′,5′-monophosphate in rat uterus: acute elevation by estrogen. *Proc. Natl. Acad. Sci. USA.* **58:** 1711–1718.
59. Björnström, L., and M. Sjöberg. 2005. Mechanisms of estrogen receptor signaling: convergence of genomic and nongenomic actions on target genes. *Mol. Endocrinol.* **19:** 833–842.
60. Otto, C., B. Rohde-Schulz, G. Schwarz, I. Fuchs, M. Klewer, D. Brittain, G. Langer, B. Bader, K. Prelle, R. Nubbemeyer, et al. 2008. G protein-coupled receptor 30 localizes to the endoplasmic reticulum and is not activated by estradiol. *Endocrinology.* **149:** 4846–4856.
61. Revankar, C. M., D. F. Cimino, L. A. Sklar, J. B. Arterburn, and E. R. Prossnitz. 2005. A transmembrane intracellular estrogen receptor mediates rapid cell signaling. *Science.* **307:** 1625–1630.
62. Kang, L., X. Zhang, Y. Xie, Y. Tu, D. Wang, Z. Liu, and Z. Y. Wang. 2010. Involvement of estrogen receptor variant ER-alpha36, not GPR30, in nongenomic estrogen signaling. *Mol. Endocrinol.* **24:** 709–721.
63. Sukocheva, O., C. Wadham, and P. Xia. 2009. Role of sphingolipids in the cytoplasmic signaling of estrogens. *Steroids.* **74:** 562–567.
64. Sukocheva, O., L. Wang, E. Verrier, M. A. Vadas, and P. Xia. 2009. Restoring endocrine response in breast cancer cells by inhibition of the sphingosine kinase-1 signaling pathway. *Endocrinology.* **150:** 4484–4492.
65. Olivera, A., H. M. Rosenfeldt, M. Bektas, F. Wang, I. Ishii, J. Chun, S. Milstien, and S. Spiegel. 2003. Sphingosine kinase type 1 Induces G12/13-mediated stress fiber formation yet promotes growth and survival independent of G protein coupled receptors. *J. Biol. Chem.* **278:** 46452–46460.
66. Usatyuk, P. V., D. He, V. Bindokas, I. A. Gorshkova, E. V. Berdyshev, J. G. Garcia, and V. Natarajan. 2011. Photolysis of caged sphingosine-1-phosphate induces barrier enhancement and intracellular activation of lung endothelial cell signaling pathways. *Am. J. Physiol. Lung Cell. Mol. Physiol.* **300:** L840–L850.
67. Alvarez, S. E., K. B. Harikumar, N. C. Hait, J. Allegood, G. M. Strub, E. Y. Kim, M. Maceyka, H. Jiang, C. Luo, T. Kordula, et al. 2010. Sphingosine-1-phosphate is a missing cofactor for the E3 ubiquitin ligase TRAF2. *Nature.* **465:** 1084–1088.
68. Rashad, S., K. Niizuma, D. Saigusa, X. Han, M. Sato-Maeda, R. Saito, A. Uruno, M. Fujimura, S. Ikawa, M. Yamamoto, et al. 2018. Intracellular S1P levels dictate fate of different regions of the hippocampus following transient global cerebral ischemia. *Neuroscience.* **384:** 188–202.

Contents lists available at ScienceDirect

Advances in Biological Regulation

journal homepage: www.elsevier.com

# Sphingosine-1-phosphate signaling: A novel target for simultaneous adjuvant treatment of triple negative breast cancer and chemotherapy-induced neuropathic pain

Sandeep K. Singh, Sarah Spiegel *

*Department of Biochemistry and Molecular Biology, Virginia Commonwealth University School of Medicine and the Massey Cancer Center, Richmond, VA, USA*

ARTICLE INFO

*Keywords:*
Sphingosine-1-phosphate
Sphingosine kinase
Estradiol
Breast cancer
FTY720/Fingolimod
Neuropathic pain

ABSTRACT

Triple-negative breast cancer (TNBC) is very aggressive with high metastatic and mortality rates and unfortunately, except for chemotherapy, there are few therapeutic options. The bioactive sphingolipid metabolite sphingosine-1-phosphate (S1P) regulates numerous processes important for cancer progression, metastasis, and neuropathic pain. The pro-drug FTY720 (fingolimod, Gilenya) used to treat multiple sclerosis is phosphorylated in the body to a S1P mimic that binds to S1PRs, except S1PR2, and also acts as a functional antagonist of S1PR1. This review highlights current findings showing that FTY720 has multiple anti-cancer activities and simultaneously prevents formation and actions of S1P. Moreover, in mouse breast cancer models, treatment with FTY720 reduces tumor growth, metastasis, and enhances sensitivity of advanced and hormonal refractory breast cancer and TNBC to conventional therapies. We discuss recent studies demonstrating that neuropathic pain induced by the chemotherapeutic bortezomib is also greatly reduced by administration of clinically relevant doses of FTY720, likely by targeting S1PR1 on astrocytes. FTY720 also shows promising anticancer potential in pre-clinical studies and is FDA approved, thus we suggest in this review that further studies are needed to pave the way for fast-tracking approval of FTY720/fingolimod for enhancing chemotherapy effectiveness and reduction of painful neuropathies.

## 1. Therapeutic options for treatment of triple negative breast cancer

Breast cancer is the most commonly diagnosed cancer in women and is increasing in incidence and resistance to treatment. Since breast cancer is heterogeneous, identification of molecular markers, gene expression profiles, and patterns of genomic alteration are used to determine appropriate therapies and predict clinical outcomes. Approximately 70% of breast cancers are estrogen receptor (ER) and progesterone receptor (PR) positive and 10–15% overexpress human epidermal receptor 2 (HER2). However, 15–20% of breast cancers are ER, PR, and HER2 negative, known as triple negative breast cancer (TNBC). TNBC are the most aggressive type

*Abbreviations*: ER, estrogen receptor; E2, estradiol; HER2, human epidermal growth factor receptor 2; SphK, sphingosine kinase; S1P, sphingosine-1-phosphate; S1PR, S1P receptor; TNBC, triple-negative breast cancer; CCI, chronic constriction injury; CIPN, chemotherapy induced neuropathic pain; DHSC, dorsal horn of the spinal cord; DRG, dorsal root ganglia; GFAP, glial fibrillary acidic protein; STAT3, signal transducer and activator of transcription-3.

* Corresponding author.
*E-mail address:* sarah.spiegel@vcuhealth.org (S. Spiegel)

https://doi.org/10.1016/j.jbior.2019.100670
Received 5 October 2019; Received in revised form 10 October 2019; Accepted 12 October 2019
Available online xxx
2212-4926/

and metastasize to other organs leading to overall worse prognosis. Several decades of research have increased understanding of the mechanisms of breast cancer growth and have led to many effective therapies, including hormonal and chemotherapy. ER positive breast cancer responds best to tamoxifen hormonal therapy without many side effects. HER2 positive breast cancer can be effectively treated with Trastuzumab (Herceptin), a monoclonal antibody against HER2. However, TNBC do not respond to traditional hormonal and antibody therapies, leaving chemotherapy as a primary treatment option (Bayraktar and Gluck, 2013; Geffken and Spiegel, 2018). Typical treatment of TNBC involves a combination of surgery, radiation therapy, and chemotherapy. Although chemotherapy has substantially improved survival rate of TNBC patients, these cause side effects, including hair loss, nausea, and more significantly, peripheral neuropathy, referred to as chemotherapy-induced peripheral neuropathy (CIPN). CIPN is characterized by pain sensations, including tingling or hot or cold sensations in hands and feet due to the loss of sensory nerves. CIPN reduces the quality of life of cancer survivors and can interfere with effective anticancer treatment (Farquhar-Smith, 2011; Pachman et al., 2011). There are no preventive or curative interventions for CIPN. Dose reduction or treatment termination is often the only recourse for CIPN, as traditional analgesics are ineffective or have their own serious unwanted side effects (Farquhar-Smith, 2011; Pachman et al., 2011). Moreover, the current symptomatic therapies, antidepressants and morphine, have not shown consistent effectiveness in most patients and also have potential for drug abuse (Farquhar-Smith, 2011). Moreover, TNBC patients can develop resistance to many chemotherapies. Therefore, deeper understanding of the molecular mechanisms of TNBC progression and CIPN is needed to aid in development of novel therapeutics to not only treat TNBC but also reduce CIPN. (see Fig. 1)

In the past two decades, many avenues of research have implicated the pleiotropic bioactive sphingolipid, sphingosine-1-phosphate (S1P) and its receptor S1PR1, in the growth and metastasis of breast cancer due to their impacts on both cancer cells and tumor microenvironment (Hait et al., 2015; Maczis et al., 2016, 2018; Nagahashi et al., 2012, 2014, 2018; Nava et al., 2002; Pyne et al., 2014, 2016, 2018; Yamada et al., 2018). More recently, it is becoming clear that increased S1P signaling through S1PR1 is involved in neuropathic pain (Chen et al., 2019; Grenald et al., 2017; Stockstill et al., 2018). In this review, we summarize recent research advances in the role of the S1P/S1PR1 signaling axis in breast cancer progression, metastasis, and in neuropathic pain. We also discuss pre-clinical studies demonstrating the utility of targeting the S1P/S1PR1 axis with FTY720 to mitigate TNBC progression, metastasis, and CIPN.

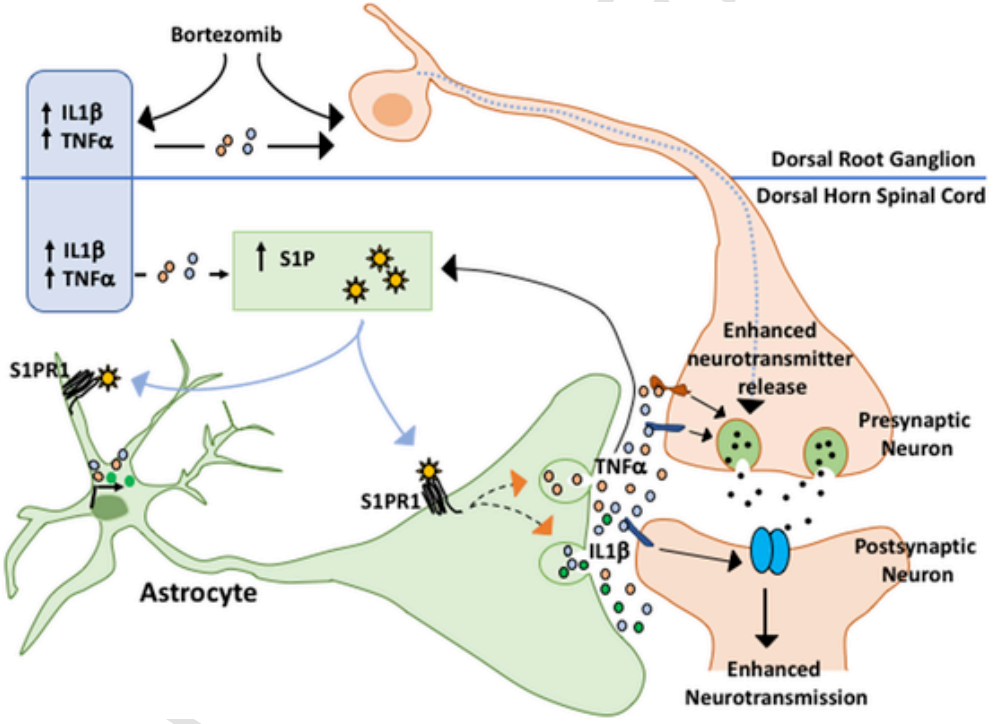


**Fig. 1. Scheme illustrating the proposed role of the SphK/S1P/S1PR1 signaling axis in astrocytes in CIPN**. An emerging concept proposed in this review is that neuroinflammation is one of the major mechanisms underlying CIPN (Robinson et al., 2014). Chemotherapies such as bortezomib increase the proinflammatory cytokines, TNFα, IL1β, and IL6 in plasma that gain access to the CNS (Scholz and Woolf, 2007; Wang et al., 2012). These cytokines can act directly to enhance neuronal excitability and also activate glial cells to enhance formation of S1P (Maceyka and Spiegel, 2014). S1P binds to S1PR1 on astrocytes to further increase these pro-inflammatory cytokines. It is suggested that interfering with S1P formation and S1PR1 functions and this feed-forward amplification loop with FTY720 may be a new approach to suppress CIPN and also synergize with the anti-cancer effects of chemotherapies. Modified from (Stockstill et al., 2018).

## 2. Biology and metabolism of sphingosine-1-phosphate

Sphingolipids are crucial component of cellular membranes in eukaryotic cells. Their metabolism generates metabolites such as ceramide, sphingosine, and S1P, with important biological functions (Coant and Hannun, 2019; Ebenezer et al., 2017; Hannun and Obeid, 2008; Wang and Bieberich, 2018). S1P is generated from sphingosine, the backbone of all sphingolipids, catalyzed by two sphingosine kinases (SphK1 and SphK2). SphK1 is activated by numerous stimuli, including growth factors, hormones, and cytokines, leading to its translocation to the plasma membrane where its substrate sphingosine resides (Gao et al., 2015; Maceyka et al., 2012; Maceyka and Spiegel, 2014; Maczis et al., 2016). S1P is exported out from the cells by several transporters, including spinster 2 (Spns2), and more promiscuous ATP-binding cassette transporters, ABCA1, ABCC1, and ABCG2. S1P then acts in an autocrine or paracrine manner by binding to five G-protein coupled cell surface receptors called S1PR1-5. Activation of S1PRs regulates many physiological functions involved in breast cancer progression and metastasis, such as cell growth, migration, angiogenesis, and immune cell trafficking (Maceyka and Spiegel, 2014; Ogretmen, 2018). Upregulation and activation of SphK1 has been linked to breast cancer progression and poor prognosis (Maczis et al., 2016; Ruckhaberle et al., 2008). Much less is known about the roles and activation of SphK2 that also resides in intracellular compartments including mitochondria (Strub et al., 2011) and the nucleus (Hait et al., 2009). Nevertheless, it has been suggested that S1P also has important intracellular actions in these two organelles, for instance, to regulate mitochondrial respiration and in epigenetic regulation of gene expression, respectively. Like other potent mediators, levels of S1P are tightly regulated and it is rapidly degraded, either by dephosphorylation back to sphingosine by phosphatases, or irreversibly cleaved by S1P lyase (Aguilar and Saba, 2012; Hannun and Obeid, 2008; Maceyka and Spiegel, 2014).

## 3. S1P signaling as a therapeutic target in breast cancer

S1P levels and expression of SphK1 are increased in TNBC and positively correlate with metastasis, poor prognosis, and worse disease-free survival (Maczis et al., 2016; Ruckhaberle et al., 2008). SphK1 signaling promotes metastasis in TNBC and targeting SPHK1 or its downstream target NF-κB with inhibitors suppressed aggressive mammary tumor growth and spontaneous lung metastasis in orthotopic syngeneic TNBC mouse models (Acharya et al., 2019). Expression levels of S1PR1 and S1PR3 are also increased in TNBC (Watson et al., 2010). Enhanced S1PR1 signaling has been shown to persistently activate the master transcription factors NF-κB and STAT3 in many types of cancer, including breast (Deng et al., 2012; Lee et al., 2010; Liang et al., 2013; Nagahashi et al., 2014). STAT3 hyperactivation has been linked to tumor growth and metastasis owing to its multi-pronged, pro-tumorigenic roles in cancer cell survival, invasion and metastasis, and in immune system modulation. Interestingly, activated STAT3 transcriptionally upregulates S1PR1 leading to an amplification loop where S1P/S1PR1 signaling activates the IL6/STAT3 axis that in turn upregulates S1PR1 (Deng et al., 2012; Lee et al., 2010; Liang et al., 2013; Nagahashi et al., 2014). Moreover, IL6 upregulates SphK1, the enzyme that produces S1P. Taken together, S1P/S1PR1/IL6/STAT3 signaling acts as a feed-forward loop, enabling tumor growth, metastasis, and resistance to chemotherapy (Nagahashi et al., 2014).

Obesity, which is now endemic and a known risk factor for breast cancer increases aggressiveness and metastasis of TNBC, and has been associated with worse prognosis (Neuhouser et al., 2015; Niraula et al., 2012; Pierobon and Frankenfeld, 2013). Moreover, S1P levels in serum from obese breast cancer patients are higher compared to those of non-obese patients. Similarly, placing mice on a high fat diet (HFD) accelerated the progression of breast tumors and increased triple-negative breast tumors in a spontaneous breast cancer mouse model (Neuhouser et al., 2015; Niraula et al., 2012; Pierobon and Frankenfeld, 2013). In these mice, S1P levels were increased in the serum, mammary fad pad, tumors, and in tumor interstitial fluid (Nagahashi et al., 2016). In addition, these tumors have increased expression of both SphK1 and S1PR1 (Nagahashi et al., 2018). Moreover, it was also reported that S1P produced in lung pre-metastatic niches by tumor-induced SphK1 increased macrophage recruitment and induced IL6 and signaling pathways important for metastatic colonization. Importantly, in tumor-bearing mice, FTY720 treatment reduced expression of SphK1, the enzyme that produces S1P, as well as S1PR1 expression. pro-inflammatory cytokines, macrophage infiltration, S1P-mediated signaling, and pulmonary metastasis, thereby prolonging survival (Nagahashi et al., 2018). While these observations establish a critical role for circulating S1P produced by tumors and the SphK1/S1P/S1PR1 axis in TNBC progression, inflammation, formation of lung metastatic niches, and metastasis, they also provide important insight into additional mechanisms of action of FTY720 on cancer progression due to reduction of S1P via suppression of SphK1 expression.

ERα-negative breast cancer is resistant to hormonal therapies, such as tamoxifen. Recently, FTY720 treatment of ER negative breast cancer cells was shown to reactivate expression of silenced ERα and sensitize the cells to tamoxifen. Interestingly, FTY720-P accumulated in the nucleus of these TNBC and acted as class I histone deacetylase (HDAC) inhibitor that enhanced histone acetylation and activated a set of genes including ERα (Hait et al., 2015). This explains why FTY720 sensitized TNBC towards tamoxifen treatment. Notably, HFD accelerated the onset of tumors and increased triple-negative spontaneous breast tumors and HDAC activity in MMTV-PyMT transgenic mice and FTY720 administration reversed the defect in expression of ERα, histone acetylation and HDAC activity in these tumors (Hait et al., 2015).

Recently, we demonstrated that TNBC cells do not express the canonical estrogen receptor, ERα66, but express the novel splice variant ERα36, and that estradiol (E2)/ERα36 signaling induced activation of SphK1 and formation and secretion of S1P (Maczis et al., 2018). Tamoxifen, the first-line endocrine therapy for breast cancer, is an antagonist of ERα66, but an agonist of ERα36, and, like E2, activates SphK1 and increases secretion of S1P. A major problem with tamoxifen therapy is development of acquired resistance. Our study also showed that tamoxifen resistance correlated with increased SphK1 and ERα36 expression in tamoxifen-resis-

tant breast cancer cells, in patient-derived xenografts, and in endocrine-resistant breast cancer patients. These results also support the idea that targeting the SphK1 axis with FTT720 may be a therapeutic option to circumvent endocrine resistance and improve survival and quality of life of TNBC patients.

Doxorubicin is commonly used chemotherapy for breast cancer; however, its effects can be limiting due to cardiotoxicity and drug resistance. In a recent study, it was found that combination therapy of FTY720 with low dose doxorubicin synergistically reduced TNBC growth *in vivo* (Katsuta et al., 2017). Interestingly, while doxorubicin treatment induced expression of SphK1, S1PR1, STAT3 and IL6 in TNBC tumors in mice, and a combination of FTY720 with doxorubicin blocked this increase (Katsuta et al., 2017). Similarly, FTY720 enhanced suppression of basal-like breast cancer growth by the EGFR kinase inhibitor gefitinib (Martin et al., 2017) and prevented resistance to afatinib, an ERBB1/2/4 inhibitor (Booth et al., 2018). These reports suggest that FTY720 enhances the efficacy of chemotherapeutics by suppressing S1P signaling. A recent study described development of a nanoparticle drug that combines docetaxel and FTY720 for enhanced anticancer effects in TNBC, targeted tumor delivery, and reduced systemic toxicity, without affecting lymphocyte trafficking (Alshaker et al., 2017).

Taken together, these reports suggest that FTY720 treatment has multiple anti-cancer activities: 1) the unphosphorylated FTY720 is a potent activator of PP2A, a heterotrimeric serine/threonine phosphatase that counteracts the activity of many kinase-driven signaling pathways, such as AKT (Perrotti and Neviani, 2013; Saddoughi et al., 2013). Because reduced PP2A activity is a common event in breast cancer, it might explain the increased sensitivity of TNBC to FTY720 (Baldacchino et al., 2014; McDermott et al., 2014; Rincon et al., 2015); 2) FTY720 itself also inhibits and induces proteasomal degradation of SphK1 (Lim et al., 2011), which is upregulated in breast cancer (Pyne and Pyne, 2010; Ruckhaberle et al., 2008); 3) the most well accepted action of FTY720-P is functional antagonism of S1PR1. Therefore, it can suppress tumor growth by targeting the S1P/S1PR1 signaling axis. This interferes with a feed-forward amplification loop for persistent NF-κB and STAT3 activation in the breast tumor microenvironment critical for malignant progression (Lee et al., 2010; Liang et al., 2013; Nagahashi et al., 2018; Priceman et al., 2014); 4) FTY720-P is also a potent inhibitor of class I HDACs (Hait et al., 2015) and acts similarly to other HDAC inhibitors to reactivate ERα expression sensitizing TNBC to tamoxifen therapy and other chemotherapies.

## 4. S1P/S1PR1 axis in chemotherapy-induced peripheral neuropathic pain

Commonly used chemotherapies for TNBC that prolong survival, including paclitaxel, carboplatin, and bortezomib, induce neurotoxic side effects that include painful peripheral neuropathy (CIPN). The exact cellular and molecular mechanisms of CIPN are currently not clear but depend on the type of chemotherapy. It is believed that the majority of chemotherapy drugs primarily affect peripheral sensory nerves, whose primary functions include sensation to touch, cold, hot, and allodynia. The bipolar sensory neurons receive sensory signals from skin by their dendrites and relay these signals to the dorsal horn of spinal cord (DHSC) via their axons. DHSC neurons relay sensory signals to the brain for further processing and appropriate action. The cell bodies of these sensory neurons are located as a bundle called dorsal root ganglia (DRG). Chemotherapy has direct effects on sensory neurons causing their hypersensitization, which then leads to activation of immune cells and glial cells in the DRG (Robinson et al., 2014). Within days, this hyperactivation induces neuroinflammation in both DRG and DHSC. Neuroinflammation underlying CIPN is characterized by activation of astrocytes and microglia leading to increased pro-inflammatory cytokines including, IL1β, IL6, and TNFα. Hypersensitivity and neuroinflammatory cytokines enhance neuronal synaptic connectivity and post-synaptic currents in DHSC and DRG neurons leading to neuropathic pain (Aiyer et al., 2018; Zhou et al., 2011).

Increased activity of sphingolipid enzymes involved in S1P metabolism, such as SPT, sphingomyelinase, and SphK1, was observed in the DHSC at the peak of mechanical hypersensitivity caused by paclitaxel in rats (Janes et al., 2014). S1PR1 receptor activation was found to be important for development of CIPN since administration of the specific antagonists of S1PR1, including W146, CYM5442, or the functional antagonist FTY720, completely rescued chemotherapy-induced mechano-allodynia. Inhibition of SphK1 with the specific inhibitor SK-I also reversed increased levels of S1P in DHSC and mitigated paclitaxel-induced neuropathic pain. In contrast, administration of the S1PR1-specific agonist SEW2871 led to the spontaneous development of neuropathic pain behavior in rats and was reversed by pre-application of S1PR1 antagonists. This provides the rationale that S1PR1 antagonism, but not agonism, attenuates and reverses CIPN, although further studies are needed to fully support this mechanism. Mechanistically, paclitaxel-induced neuropathic pain was associated with increased S1P and engagement of S1PR1 leading to increased NF-κB and activation of MAPKs (ERK1/2 and p38) with subsequent proinflammatory cytokine production and neuroinflammation in the spinal cord (Janes et al., 2014). This was the first study that identified the S1P/S1PR1 axis as a potential therapeutic target in CIPN and suggested that further studies are needed to understand the role of S1PR1 in CIPN.

Another chemotherapy drug bortezomib, with the known side effect of neuropathic pain-syndrome, caused mechano-hypersensitivity and increased levels of ceramide, dihydroceramide, S1P, dihydro-S1P and sphingosine in the DHSC in mice (Stockstill et al., 2018). Moreover, bortezomib-induced neuropathic pain was dependent on *de novo* synthesis of sphingolipids as it was blocked by myriocin, an inhibitor of serine palmitoyltransferase. Antagonism of S1PR1 by FTY720 or NIBR-14, or its downregulation by siRNA, rescued neuropathic pain behavior induced by bortezomib (Stockstill et al., 2018). As with the paclitaxel studies (Janes et al., 2014), S1PR1 antagonists blocked increased neuroinflammation and synaptic currents induced by bortezomib, further support for an important role of S1PR1 in CIPN. Because S1PR1 is highly expressed in astrocytes relative to neurons, oligodendrocytes, and microglia (Zhang et al., 2014), and astrocyte S1PR1 has been linked to neuroinflammatory diseases, such as multiple sclerosis (Choi et al., 2011), the contribution of astrocyte-specific S1PR1 to the development of CIPN was investigated (Stockstill et al., 2018). Mice with a specific deletion of S1PR1 in astrocytes ($S1PR1^{\Delta AST}$) did not develop bortezomib-induced neuropathic pain (Stockstill et al.,

2018). These data, which resemble those obtained with S1PR1 antagonists and siRNA, further suggest that activation S1PR1 signaling in astrocytes is necessary for both bortezomib-induced neuropathic pain and the analgesic effects of FTY720.

Bortezomib-induced dysregulation of sphingolipid metabolism was accompanied by neuroinflammation, astrocyte activation, and concomitant increases in the pro-inflammatory cytokines TNFα and IL-1β, together with decreased anti-inflammatory cytokines IL-10 and IL-4 (Stockstill et al., 2018). Intriguingly, FTY720 treatment suppressed these responses. Based on these results, it was suggested that bortezomib increases the proinflammatory cytokines TNFα and IL-1β in plasma that gain access to the CNS (Scholz and Woolf, 2007; Wang et al., 2012). These cytokines can act directly to enhance neuronal excitability and also activate glial cells to enhance formation of S1P (Maceyka and Spiegel, 2014). S1P binds to S1PR1 on astrocytes to further increase these pro-inflammatory cytokines and the latter event can be suppressed by FTY720 administration. Consistent with this idea, activation of S1PR1 with an intrathecal injection of the selective S1PR1 agonist SEW2871 led to the development of mechano-allodynia in wild-type mice but not in mice with astrocyte-specific deletion of *S1pr1*. Mechanohypersensitivity was likely due to activation of the inflammasome leading to caspase 1 cleavage and increased IL-1β in the dorsal horn of the spinal cord (Doyle et al., 2019). The functional S1PR1 antagonist FTY720 blocked inflammasome activation and IL-1β production further supporting a role for astrocytic S1PR1 in pain development.

## 5. S1P/S1PR1 axis in cancer-induced bone pain

Many types of cancer, including breast cancer, prostate cancer, and lung cancer, which frequently metastasize to bone, result in cancer-induced bone pain (CIBP) (Portenoy and Lesage, 1999). CIBP occurs in about 30–50% of all cancer patients for which there is also no therapy. CIBP results from a combination of tumor-associated peripheral skeletal, inflammatory, and neuropathic mechanisms (Lozano-Ondoua et al., 2013). In femoral arthrotomy and syngeneic tumor implantation in mice that induced CIBP, there was increased *de novo* sphingolipid biosynthesis and formation of S1P (Grenald et al., 2017). Moreover, Intrathecal or systemic administration of the competitive and functional S1PR1 antagonists, TASP0277308 and FTY720, in mice with CIBP attenuated pain behaviors and enhanced the level of the anti-inflammatory cytokine IL-10 in the lumbar spinal cord (Grenald et al., 2017). FTY720 did not alter bone metabolism. This study suggests that blocking the actions of the bioactive metabolite S1P in the lumbar spinal cord might also have beneficial effects for treatment of CIBP.

Many studies have shown that chemotherapy in cancer patients also causes cognitive impairment and memory dysfunction, known as chemo-brain (Hermelink, 2015). In this regard, it is interesting to note that active, phosphorylated FTY720, that inhibits HDACs, like other HDAC inhibitors enhances memory and learning in mice (Hait et al., 2014). This raises the thought that treatment with FTY720 could also suppress development of chemo-brain.

## 6. Concluding remarks: FTY720 as therapeutic agent for TNBC and CIPN

In this review, we have put forward the provocative idea that targeting the S1P/S1PR1 signaling axis by administration of FTY720 should be a multi-pronged approach to enhance chemotherapy efficacy for treatment of TNBC and suppress CIPN. FTY720 has several advantages as a potential new approach: i) it is orally bio-available; ii) it is already FDA approved; iii) it has good pharmacokinetics and a long half-life; iv) it has low toxicity and accumulates in the CNS; v) there is no evidence of tolerance or abuse; vi) it has the added benefit of synergizing with chemotherapeutics to reduce tumor growth and metastasis in pre-clinical studies; vii) and next generation S1PR1 targeting agents are already in clinical trials. Therefore, we suggest that there is scientific rationale for additional studies to examine S1PR1 targeted therapeutic agents for TNBC and CIPN. Such studies might pave the way for "fast track" support for rapid clinical translation to attain more effective, less toxic treatment regimens that will increase survival of cancer patients and improve their quality of life.

## Declaration of competing interest

The authors have no conflicts of interest to declare.

## Acknowledgements

This work was supported by grants from Department of Defense BCRP Program Award W81XWH-14-1-0086 (S. Spiegel).

## References

Acharya, S., Yao, J., Li, P., Zhang, C., Lowery, F.J., Zhang, Q., Guo, H., Qu, J., Yang, F., Wistuba, I.I., Piwnica-Worms, H., Sahin, A.A., Yu, D., 2019. Sphingosine kinase 1 signaling promotes metastasis of triple-negative breast cancer. Cancer Res. 79 (16), 4211–4226.

Aguilar, A., Saba, J.D., 2012. Truth and consequences of sphingosine-1-phosphate lyase. Adv. Biol. Regul. 52 (1), 17–30.

Aiyer, R., Mehta, N., Gungor, S., Gulati, A., 2018. A systematic review of NMDA receptor antagonists for treatment of neuropathic pain in clinical practice. Clin. J. Pain 34 (5), 450–467.

Alshaker, H., Wang, Q., Srivats, S., Chao, Y., Cooper, C., Pchejetski, D., 2017. New FTY720-docetaxel nanoparticle therapy overcomes FTY720-induced lymphopenia and inhibits metastatic breast tumour growth. Breast Canc. Res. Treat. 165 (3), 531–543.

Baldacchino, S., Saliba, C., Petroni, V., Fenech, A.G., Borg, N., Grech, G., 2014. Deregulation of the phosphatase, PP2A is a common event in breast cancer, predicting sensitivity to FTY720. EPMA J. 5 (1), 3.

Bayraktar, S., Gluck, S., 2013. Molecularly targeted therapies for metastatic triple-negative breast cancer. Breast Canc. Res. Treat. 138 (1), 21–35.

Booth, L., Roberts, J.L., Spiegel, S., Poklepovic, A., Dent, P., 2018. Fingolimod augments Pemetrexed killing of non-small cell lung cancer and overcomes resistance to ERBB inhibition. Cancer Biol. Ther. 1–11.

Chen, Z., Doyle, T.M., Luongo, L., Largent-Milnes, T.M., Giancotti, L.A., Kolar, G., Squillace, S., Boccella, S., Walker, J.K., Pendleton, A., Spiegel, S., Neumann, W.L., Vanderah, T.W., Salvemini, D., 2019. Sphingosine-1-phosphate receptor 1 activation in astrocytes contributes to neuropathic pain. Proc. Natl. Acad. Sci. U. S. A. 116 (21), 10557–10562.

Choi, J.W., Gardell, S.E., Herr, D.R., Rivera, R., Lee, C.W., Noguchi, K., Teo, S.T., Yung, Y.C., Lu, M., Kennedy, G., Chun, J., 2011. FTY720 (fingolimod) efficacy in an animal model of multiple sclerosis requires astrocyte sphingosine 1-phosphate receptor 1 (S1P1) modulation. Proc. Natl. Acad. Sci. U.S.A. 108 (2), 751–756.

Coant, N., Hannun, Y.A., 2019. Neutral ceramidase: advances in mechanisms, cell regulation, and roles in cancer. Adv. Biol. Regul. 71, 141–146.

Deng, J., Liu, Y., Lee, H., Herrmann, A., Zhang, W., Zhang, C., Shen, S., Priceman, S.J., Kujawski, M., Pal, S.K., Raubitschek, A., Hoon, D.S., Forman, S., Figlin, R.A., Liu, J., Jove, R., Yu, H., 2012. S1PR1-STAT3 signaling is crucial for myeloid cell colonization at future metastatic sites. Cancer Cell 21 (5), 642–654.

Doyle, T.M., Chen, Z., Durante, M., Salvemini, D., 2019. Activation of sphingosine-1-phosphate receptor 1 in the spinal cord produces mechanohypersensitivity through the activation of inflammasome and IL-1beta pathway. J. Pain 20 (8), 956–964.

Ebenezer, D.L., Fu, P., Suryadevara, V., Zhao, Y., Natarajan, V., 2017. Epigenetic regulation of pro-inflammatory cytokine secretion by sphingosine 1-phosphate (S1P) in acute lung injury: role of S1P lyase. Adv. Biol. Regul. 63, 156–166.

Farquhar-Smith, P., 2011. Chemotherapy-induced neuropathic pain. Curr. Opin. Support. Palliat. Care 5 (1), 1–7.

Gao, Y., Gao, F., Chen, K., Tian, M.L., Zhao, D.L., 2015. Sphingosine kinase 1 as an anticancer therapeutic target. Drug Des. Dev. Ther. 9, 3239–3245.

Geffken, K., Spiegel, S., 2018. Sphingosine kinase 1 in breast cancer. Adv. Biol. Regul. 67, 59–65.

Grenald, S.A., Doyle, T.M., Zhang, H., Slosky, L.M., Chen, Z., Largent-Milnes, T.M., Spiegel, S., Vanderah, T.W., Salvemini, D., 2017. Targeting the S1P/S1PR1 axis mitigates cancer-induced bone pain and neuroinflammation. Pain 158 (9), 1733–1742.

Hait, N.C., Allegood, J., Maceyka, M., Strub, G.M., Harikumar, K.B., Singh, S.K., Luo, C., Marmorstein, R., Kordula, T., Milstien, S., Spiegel, S., 2009. Regulation of histone acetylation in the nucleus by sphingosine-1-phosphate. Science 325 (5945), 1254–1257.

Hait, N.C., Avni, D., Yamada, A., Nagahashi, M., Aoyagi, T., Aoki, H., Dumur, C.I., Zelenko, Z., Gallagher, E.J., Leroith, D., Milstien, S., Takabe, K., Spiegel, S., 2015. The phosphorylated prodrug FTY720 is a histone deacetylase inhibitor that reactivates ERalpha expression and enhances hormonal therapy for breast cancer. Oncogenesis 4, e156.

Hait, N.C., Wise, L.E., Allegood, J.C., O'Brien, M., Avni, D., Reeves, T.M., Knapp, P.E., Lu, J., Luo, C., Miles, M.F., Milstien, S., Lichtman, A.H., Spiegel, S., 2014. Active, phosphorylated fingolimod inhibits histone deacetylases and facilitates fear extinction memory. Nat. Neurosci. 17 (7), 971–980.

Hannun, Y.A., Obeid, L.M., 2008. Principles of bioactive lipid signalling: lessons from sphingolipids. Nat. Rev. Mol. Cell Biol. 9 (2), 139–150.

Hermelink, K., 2015. Chemotherapy and cognitive function in breast cancer patients: the so-called chemo brain. J. Natl. Cancer Inst. Monogr. 2015 (51), 67–69.

Janes, K., Little, J.W., Li, C., Bryant, L., Chen, C., Chen, Z., Kamocki, K., Doyle, T., Snider, A., Esposito, E., Cuzzocrea, S., Bieberich, E., Obeid, L., Petrache, I., Nicol, G., Neumann, W.L., Salvemini, D., 2014. The development and maintenance of paclitaxel-induced neuropathic pain require activation of the sphingosine 1-phosphate receptor subtype 1. J. Biol. Chem. 289 (30), 21082–21097.

Katsuta, E., Yan, L., Nagahashi, M., Raza, A., Sturgill, J.L., Lyon, D.E., Rashid, O.M., Hait, N.C., Takabe, K., 2017. Doxorubicin effect is enhanced by sphingosine-1-phosphate signaling antagonist in breast cancer. J. Surg. Res. 219, 202–213.

Lee, H., Deng, J., Kujawski, M., Yang, C., Liu, Y., Herrmann, A., Kortylewski, M., Horne, D., Somlo, G., Forman, S., Jove, R., Yu, H., 2010. STAT3-induced S1PR1 expression is crucial for persistent STAT3 activation in tumors. Nat. Med. 16 (12), 1421–1428.

Liang, J., Nagahashi, M., Kim, E.Y., Harikumar, K.B., Yamada, A., Huang, W.C., Hait, N.C., Allegood, J.C., Price, M.M., Avni, D., Takabe, K., Kordula, T., Milstien, S., Spiegel, S., 2013. Sphingosine-1-phosphate links persistent STAT3 activation, chronic intestinal inflammation, and development of colitis-associated cancer. Cancer Cell 23 (1), 107–120.

Lim, K.G., Tonelli, F., Li, Z., Lu, X., Bittman, R., Pyne, S., Pyne, N.J., 2011. FTY720 analogues as sphingosine kinase 1 inhibitors: enzyme inhibition kinetics, allosterism, proteasomal degradation, and actin rearrangement in MCF-7 breast cancer cells. J. Biol. Chem. 286 (21), 18633–18640.

Lozano-Ondoua, A.N., Symons-Liguori, A.M., Vanderah, T.W., 2013. Cancer-induced bone pain: mechanisms and models. Neurosci. Lett. 557 Pt A, 52–59.

Maceyka, M., Harikumar, K.B., Milstien, S., Spiegel, S., 2012. Sphingosine-1-phosphate signaling and its role in disease. Trends Cell Biol. 22 (1), 50–60.

Maceyka, M., Spiegel, S., 2014. Sphingolipid metabolites in inflammatory disease. Nature 510 (7503), 58–67.

Maczis, M., Milstien, S., Spiegel, S., 2016. Sphingosine-1-phosphate and estrogen signaling in breast cancer. Adv. Biol. Regul. 60, 160–165.

Maczis, M.A., Maceyka, M., Waters, M.R., Newton, J., Singh, M., Rigsby, M.F., Turner, T.H., Alzubi, M.A., Harrell, J.C., Milstien, S., Spiegel, S., 2018. Sphingosine kinase 1 activation by estrogen receptor alpha36 contributes to tamoxifen resistance in breast cancer. J. Lipid Res. 59 (12), 2297–2307.

Martin, J.L., Julovi, S.M., Lin, M.Z., de Silva, H.C., Boyle, F.M., Baxter, R.C., 2017. Inhibition of basal-like breast cancer growth by FTY720 in combination with epidermal growth factor receptor kinase blockade. Breast Cancer Res. 19 (1), 90.

McDermott, M.S., Browne, B.C., Conlon, N.T., O'Brien, N.A., Slamon, D.J., Henry, M., Meleady, P., Clynes, M., Dowling, P., Crown, J., O'Donovan, N., 2014. PP2A inhibition overcomes acquired resistance to HER2 targeted therapy. Mol. Cancer 13, 157.

Nagahashi, M., Hait, N.C., Maceyka, M., Avni, D., Takabe, K., Milstien, S., Spiegel, S., 2014. Sphingosine-1-phosphate in chronic intestinal inflammation and cancer. Adv. Biol. Regul. 54C, 112–120.

Nagahashi, M., Ramachandran, S., Kim, E.Y., Allegood, J.C., Rashid, O.M., Yamada, A., Zhao, R., Milstien, S., Zhou, H., Spiegel, S., Takabe, K., 2012. Sphingosine-1-phosphate produced by sphingosine kinase 1 promotes breast cancer progression by stimulating angiogenesis and lymphangiogenesis. Cancer Res. 72 (3), 726–735.

Nagahashi, M., Yamada, A., Katsuta, E., Aoyagi, T., Huang, W.C., Terracina, K.P., Hait, N.C., Allegood, J.C., Tsuchida, J., Yuza, K., Nakajima, M., Abe, M., Sakimura, K., Milstien, S., Wakai, T., Spiegel, S., Takabe, K., 2018. Targeting the SphK1/S1P/S1PR1 Axis that links obesity, chronic inflammation, and breast cancer metastasis. Cancer Res. 78 (7), 1713–1725.

Nagahashi, M., Yamada, A., Miyazaki, H., Allegood, J.C., Tsuchida, J., Aoyagi, T., Huang, W.C., Terracina, K.P., Adams, B.J., Rashid, O.M., Milstien, S., Wakai, T., Spiegel, S., Takabe, K., 2016. Interstitial fluid sphingosine-1-phosphate in murine mammary gland and cancer and human breast tissue and cancer determined by novel methods. J. Mammary Gland Biol. Neoplasia 21 (1–2), 9–17.

Nava, V.E., Hobson, J.P., Murthy, S., Milstien, S., Spiegel, S., 2002. Sphingosine kinase type 1 promotes estrogen-dependent tumorigenesis of breast cancer MCF-7 cells. Exp. Cell Res. 281 (1), 115–127.

Neuhouser, M.L., Aragaki, A.K., Prentice, R.L., Manson, J.E., Chlebowski, R., Carty, C.L., Ochs-Balcom, H.M., Thomson, C.A., Caan, B.J., Tinker, L.F., Urrutia, R.P., Knudtson, J., Anderson, G.L., 2015. Overweight, obesity, and postmenopausal invasive breast cancer risk: a secondary analysis of the women's health initiative randomized clinical trials. JAMA Oncol. 1 (5), 611–621.

Niraula, S., Ocana, A., Ennis, M., Goodwin, P.J., 2012. Body size and breast cancer prognosis in relation to hormone receptor and menopausal status: a meta-analysis. Breast Canc. Res. Treat. 134 (2), 769–781.

Ogretmen, B., 2018. Sphingolipid metabolism in cancer signalling and therapy. Nat. Rev. Cancer 18, 33–50.

Pachman, D.R., Barton, D.L., Watson, J.C., Loprinzi, C.L., 2011. Chemotherapy-induced peripheral neuropathy: prevention and treatment. Clin. Pharmacol. Ther. 90 (3), 377–387.

Perrotti, D., Neviani, P., 2013. Protein phosphatase 2A: a target for anticancer therapy. Lancet Oncol. 14 (6), e229-238.

Pierobon, M., Frankenfeld, C.L., 2013. Obesity as a risk factor for triple-negative breast cancers: a systematic review and meta-analysis. Breast Canc. Res. Treat. 137 (1), 307–314.

Portenoy, R.K., Lesage, P., 1999. Management of cancer pain. Lancet 353 (9165), 1695–1700.

Priceman, S.J., Shen, S., Wang, L., Deng, J., Yue, C., Kujawski, M., Yu, H., 2014. S1PR1 is crucial for accumulation of regulatory T cells in tumors via STAT3. Cell Rep. 6 (6), 992–999.

Pyne, N.J., El Buri, A., Adams, D.R., Pyne, S., 2018. Sphingosine 1-phosphate and cancer. Adv. Biol. Regul. 68, 97–106.

Pyne, N.J., McNaughton, M., Boomkamp, S., MacRitchie, N., Evangelisti, C., Martelli, A.M., Jiang, H.R., Ubhi, S., Pyne, S., 2016. Role of sphingosine 1-phosphate receptors, sphingosine kinases and sphingosine in cancer and inflammation. Adv. Biol. Regul. 60, 151–159.

Pyne, N.J., Ohotski, J., Bittman, R., Pyne, S., 2014. The role of sphingosine 1-phosphate in inflammation and cancer. Adv. Biol. Regul. 54, 121–129.

Pyne, N.J., Pyne, S., 2010. Sphingosine 1-phosphate and cancer. Nat. Rev. Cancer 10 (7), 489–503.

Rincon, R., Cristobal, I., Zazo, S., Arpi, O., Menendez, S., Manso, R., Lluch, A., Eroles, P., Rovira, A., Albanell, J., Garcia-Foncillas, J., Madoz-Gurpide, J., Rojo, F., 2015. PP2A inhibition determines poor outcome and doxorubicin resistance in early breast cancer and its activation shows promising therapeutic effects. Oncotarget 6 (6), 4299–4314.

Robinson, C.R., Zhang, H., Dougherty, P.M., 2014. Astrocytes, but not microglia, are activated in oxaliplatin and bortezomib-induced peripheral neuropathy in the rat. Neuroscience 274, 308–317.

Ruckhaberle, E., Rody, A., Engels, K., Gaetje, R., von Minckwitz, G., Schiffmann, S., Grosch, S., Geisslinger, G., Holtrich, U., Karn, T., Kaufmann, M., 2008. Microarray analysis of altered sphingolipid metabolism reveals prognostic significance of sphingosine kinase 1 in breast cancer. Breast Canc. Res. Treat. 112 (1), 41–52.

Saddoughi, S.A., Gencer, S., Peterson, Y.K., Ward, K.E., Mukhopadhyay, A., Oaks, J., Bielawski, J., Szulc, Z.M., Thomas, R.J., Selvam, S.P., Senkal, C.E., Garrett-Mayer, E., De Palma, R.M., Fedarovich, D., Liu, A., Habib, A.A., Stahelin, R.V., Perrotti, D., Ogretmen, B., 2013. Sphingosine analogue drug FTY720 targets I2PP2A/SET and mediates lung tumour suppression via activation of PP2A-RIPK1-dependent necroptosis. EMBO Mol. Med. 5 (1), 105–121.

Scholz, J., Woolf, C.J., 2007. The neuropathic pain triad: neurons, immune cells and glia. Nat. Neurosci. 10 (11), 1361–1368.

Stockstill, K., Doyle, T.M., Yan, X., Chen, Z., Janes, K., Little, J.W., Braden, K., Lauro, F., Giancotti, L.A., Harada, C.M., Yadav, R., Xiao, W.H., Lionberger, J.M., Neumann, W.L., Bennett, G.J., Weng, H.R., Spiegel, S., Salvemini, D., 2018. Dysregulation of sphingolipid metabolism contributes to bortezomib-induced neuropathic pain. J. Exp. Med. 215 (5), 1301–1313.

Strub, G.M., Paillard, M., Liang, J., Gomez, L., Allegood, J.C., Hait, N.C., Maceyka, M., Price, M.M., Chen, Q., Simpson, D.C., Kordula, T., Milstien, S., Lesnefsky, E.J., Spiegel, S., 2011. Sphingosine-1-phosphate produced by sphingosine kinase 2 in mitochondria interacts with prohibitin 2 to regulate complex IV assembly and respiration. FASEB J. 25 (2), 600–612.

Wang, G., Bieberich, E., 2018. Sphingolipids in neurodegeneration (with focus on ceramide and S1P). Adv. Biol. Regul. 70, 51–64.

Wang, X.M., Lehky, T.J., Brell, J.M., Dorsey, S.G., 2012. Discovering cytokines as targets for chemotherapy-induced painful peripheral neuropathy. Cytokine 59 (1), 3–9.

Watson, C., Long, J.S., Orange, C., Tannahill, C.L., Mallon, E., McGlynn, L.M., Pyne, S., Pyne, N.J., Edwards, J., 2010. High expression of sphingosine 1-phosphate receptors, S1P1 and S1P3, sphingosine kinase 1, and extracellular signal-regulated kinase-1/2 is associated with development of tamoxifen resistance in estrogen receptor-positive breast cancer patients. Am. J. Pathol. 177 (5), 2205–2215.

Yamada, A., Nagahashi, M., Aoyagi, T., Huang, W.C., Lima, S., Hait, N.C., Maiti, A., Kida, K., Terracina, K.P., Miyazaki, H., Ishikawa, T., Endo, I., Waters, M.R., Qi, Q., Yan, L., Milstien, S., Spiegel, S., Takabe, K., 2018. ABCC1-Exported sphingosine-1-phosphate, produced by sphingosine kinase 1, shortens survival of mice and patients with breast cancer. Mol. Cancer Res. 16 (6), 1059–1070.

Zhang, Y., Chen, K., Sloan, S.A., Bennett, M.L., Scholze, A.R., O'Keeffe, S., Phatnani, H.P., Guarnieri, P., Caneda, C., Ruderisch, N., Deng, S., Liddelow, S.A., Zhang, C., Daneman, R., Maniatis, T., Barres, B.A., Wu, J.Q., 2014. An RNA-sequencing transcriptome and splicing database of glia, neurons, and vascular cells of the cerebral cortex. J. Neurosci. 34 (36), 11929–11947.

Zhou, H.Y., Chen, S.R., Pan, H.L., 2011. Targeting N-methyl-D-aspartate receptors for treatment of neuropathic pain. Expert Rev. Clin. Pharmacol. 4 (3), 379–388.